Phosphorylation-based control of cellular asymmetry and the cell cycle in *Caulobacter crescentus*

by

Yiyin Erin Chen

A.B. Biological Sciences
University of Chicago, Chicago, 2006

SUBMITTED TO THE DEPARTMENT OF BIOLOGY IN PARTIAL FULFILLMENT OF THE REQUIREMENTS FOR THE DEGREE OF

DOCTOR OF PHILOSOPHY IN BIOLOGY
AT THE
MASSACHUSETTS INSTITUTE OF TECHNOLOGY

SEPTEMBER 2011

Signature of Author _____

Yiyin Erin Chen
Department of Biology
June 15, 2011

Certified by: _____

Michael T. Laub
Assistant Professor of Biology
Thesis supervisor

Accepted by: _____

Robert T. Sauer
Salvador E. Luria Professor of Biology

Phosphorylation-based control of cellular asymmetry and the cell cycle in *Caulobacter crescentus*

by

Y. Erin Chen

Submitted to the Department of Biology
on June 15, 2011 in partial fulfillment of the requirements for the degree of
Doctor of Philosophy in Biology at the Massachusetts Institute of Technology

ABSTRACT

Asymmetric cell division allows for better environmental adaptation and organismal complexity. Cells often divide by binary fission to form two identical daughter cells with similar developmental fates. However, a cell can also divide asymmetrically to form two daughter cells with different developmental fates. This process makes possible diverse behaviors such as differing life cycles respondent to environmental stimuli and specialization of cellular functions to generate organ systems. How cells divide asymmetrically and how they enforce the differential fates of daughter cells remain unsolved, fundamental problems in biology.

In this work, I use the model organism *Caulobacter crescentus* to investigate how intracellular asymmetry within the mother cell is translated into the formation of two developmentally distinct daughter cells. *Caulobacter* is an alpha-proteobacterium that always divides asymmetrically to generate two daughter cells that are morphologically distinct and have different replicative capacities. I show that kinase and phosphatase activities at opposite poles of the cell generate a spatial gradient in the phosphorylation level of an essential cell cycle regulator called CtrA. This spatial gradient of CtrA phosphorylation enforces replicative asymmetry and couples it to the asymmetric morphogenesis of the daughter cells. I then investigate how CtrA's control of replicative asymmetry relates to the control of replication periodicity. I show that the activity of an essential replication initiator DnaA dictates the timing of replication initiation and oscillates independently of CtrA activity. The genetic separability of the spatial and temporal controls of replication in *Caulobacter* suggests that DnaA comprises an ancient and phylogenetically widespread control module for replication in almost all bacteria while CtrA developed later in α-proteobacteria and was recruited to enforce replicative asymmetry in daughter cells. This work provides a foundation for understanding cellular asymmetry and evolution of the cell cycle in bacteria.

Thesis Supervisor: Michael T. Laub
Title: Assistant Professor of Biology

ACKNOWLEDGEMENTS

This work would not have been possible without many wonderful people. For their camaraderie and scientific guidance, I am most grateful to the following people:

My advisor, Mike Laub, for being an awesome mentor. Thanks for always supporting me, being available to answer questions and to shoot around ideas, and letting me explore my ideas. You have helped me grow as a scientist in so many ways, by helping me develop my thinking, refine my experimental abilities, collaborate with others, and become a better writer. I am extremely honored to have worked with you.

My thesis committee members, Angelika Amon and Steve Bell, for giving so much thought to my project and for being a pleasure to work with. You have been wonderful role models.

David Rudner for serving on my thesis defense committee.

All the members of the Laub lab for having entered my life day in and day out, for forming a close and vibrant community, for contributing to my scientific development, and for making science fun, especially Christos and Kristina, who have worked closely with me, challenged me scientifically, and helped me grow intellectually. A special thank you to Kristina: you have been a great baymate and we've shared a lot of laughs! Emily for being a fun addition to Room 2 and for sharing your two-component expertise. Barrett for filling in the gaps while I was off at medical school and for teaching me the proper way to do everything. Emanuele for jumpstarting my very first Laub lab project. Kasia for being a loyal partner in crime for the fun stuff. Christos, Emma, and Kasia for starting on this adventure in the Laub lab with me and making it enjoyable.

My computational collaborators, Carolina Tropini and KC Huang, for making our work a success. Thank you KC and the rest of the Huang lab for your hospitality at Stanford and for spending so much time working with me on FRAP. I had a blast and learned so much.

My MSTP compatriots for all the food adventures, trips out of Boston, lab breaks, and good times in med school. Special thanks to Cameron, Mark, Vincent, and Fan. My friends outside of Boston, Jen, HSK, and Shayla, for sharing laughs and stories and for always visiting me and reminding me that there's also life outside of lab.

My family for their encouragement and love.

Finally, most of all, Phil for your love and support, for making everyone laugh at lab, for keeping me on track, and for lighting up my days in and out of lab.

TABLE OF CONTENTS

LIST OF FIGURES AND TABLES

Chapter One: Introduction

Chapter Two: Dynamics of two phosphorelays controlling cell cycle progression in *Caulobacter crescentus*

Chapter Three: A spatial gradient of protein phosphorylation underlies replicative asymmetry in a bacterium

Chapter Four: Modularity of the bacterial cell cycle enables independent spatial and temporal control of DNA replication

Chapter Five: Discussion and future directions

Chapter 1

Introduction

Introduction

Biological systems evolve toward increasing complexity to improve adaptability and to diversify cellular functions. In metazoans, a single totipotent embryonic cell divides repeatedly to generate increasingly specialized cells to form a complex pattern of organ systems. We are all the result of this tightly regulated process. Not only are we capable of engaging with our environment and with each other in complex, unpredictable ways, but we are also equipped to repeat the entire developmental process from single cell to fully formed person. A key process in generating this complexity is asymmetric cell division. Although cell division is often a simple binary fission that creates two identical cells, there are many cases in which cell division produces daughter cells with different fates. How cells divide asymmetrically and enforce the differential fates of daughter cells remain unsolved problems in biology.

There are two general ways to produce daughter cells with different fates [6]. A mother cell might divide to form two identical daughters that become distinct through later events, such as signaling with each other or with neighboring cells. Alternatively, a mother cell might first become polarized intracellularly, such that upon division, the two daughters inherit different fate-determining factors and are immediately distinct. This latter process is termed asymmetric cell division. Even during the development of the nematode *Caenorhabditis elegans*, a relatively simple animal, 807 of the 949 nongonadal cell divisions are asymmetric [7, 8], underscoring the importance of this process to development.

Although prokaryotes do not have a complex body plan, bacteria nonetheless lead richly asymmetric lives and often form multi-cellular structures, such as biofilms and fruiting bodies [9, 10]. Some bacteria decorate themselves with asymmetrically placed structures such as chemoreceptors, flagella, and pili, and some divide asymmetrically to adapt to environmental stresses, as in the case of *Bacillus subtilis* sporulation. To better understand the phenomenon of asymmetric cell division, I have pursued two questions using the alpha-proteobacterium *Caulobacter crescentus* as a model organism. One, how is intracellular asymmetry within the mother cell translated into the formation of two developmentally distinct daughter cells? And two, how does the cell couple asymmetric morphogenesis during the cell cycle to other essential events, such as DNA replication?

Generation of organismal asymmetry

The mechanisms for breaking cellular symmetry fall into two broad categories; the cell can either generate polarity *de novo* from a random internal cue or it can harness an existing asymmetric landmark or extrinsic signal. I will refer to these two methods as "random" and "deterministic" symmetry breaking. Below I describe examples of each and then the general mechanisms by which an initial asymmetry is ultimately translated into different daughter cell fates.

One example of random asymmetry formation is the placement of bud sites in the budding yeast *Saccharomyces cerevisiae*. *S. cerevisiae* cells can alternate between diploid and haploid growing states (Fig. 1.1). In vegetative nutrient-rich conditions, both haploid and diploid cells simply divide by mitosis [11]. However, under conditions of high stress, such as nutrient deprivation, haploid cells will die, whereas diploid cells can enter meiosis and produce four stress-resistant haploid spores [12]. When living conditions

improve, these haploid spores can then germinate and reenter the mitotic cell cycle. Alternatively, two haploid cells can mate to form a diploid cell. Haploid cells can be of two different mating types: a or α. Only haploid cells of opposite mating types can mate to form diploid cells, which then undergo mitotic cycles until environmental conditions provoke sporulation.

Both haploid and diploid *S. cerevisiae* cells divide through a special mitotic process called budding in which a mother cell buds off a daughter cell. Each cell division is thus asymmetric, yielding a larger mother cell and a smaller daughter cell, which have two major differences in cell fate (Fig. 1.1). Since the daughter cell is smaller, it must grow before it can initiate replication, while the mother cell can initiate replication soon after division. Mother and daughter cells also differ in their ability to switch mating type. Upon budding, mother and daughter cells start off with the same mating type; however, the mother cell can switch mating types but the daughter cannot. This ensures that mother and daughter cells will have opposite mating types such that an isolated spore can always form diploid cells through mating between descendants.

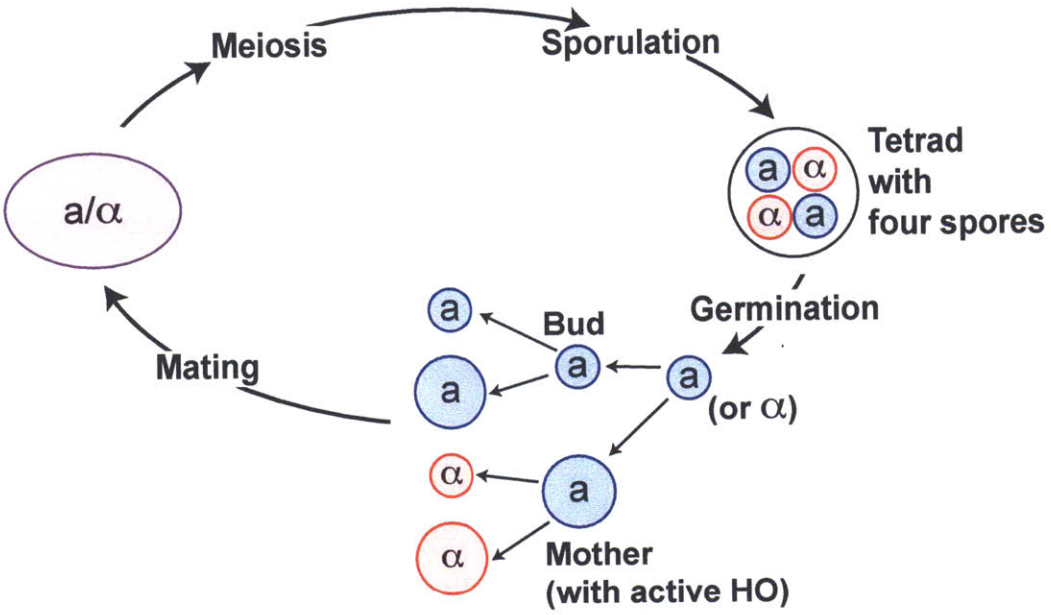

Figure 1.1. Life cycle of budding yeast. Each spore within the tetrad can bud to produce a smaller daughter cell and a larger mother cell. The mother cell has active HO and can switch mating types. The two mating types 'a' and 'α' are shown in blue and red, respectively. Haploid cells of opposite mating type can mate to produce a zygote (purple) that can undergo meiosis and sporulate to form a tetrad with four spores. Figure adapted from [3].

Mitosis in budding yeast thus consists of two major symmetry-breaking processes. One is determining the bud site and polarizing the cytoskeleton asymmetrically toward the bud site. The second is using this polarized cytoskeleton to partition fate-determining components asymmetrically between mother and daughter cells. The second process will be discussed in the next section. Below, we first focus on how bud site determination can be an example of random *de novo* generation of asymmetry.

Typically, asymmetrically localized determinants will persist at the site of a previous bud, called a bud scar, and these determinants inform the placement of new bud sites [13, 14]. In the absence of bud scars, however, *S. cerevisiae* can still form asymmetric buds, using the Rho GTPase Cdc42 [15]. Although Cdc42 appears randomly and uniformly distributed around the cell periphery, it can stochastically accumulate at a random

location on the cell surface, which will ultimately become the future bud site as follows (Fig. 1.2). In its active GTP-bound form, Cdc42-GTP stimulates actin nucleation, thus polarizing the actin network. The polarized actin cables transport more Cdc42-GTP to the future bud site, which stimulates further actin nucleation [16, 17]. The process whereby Cdc42 and the actin cytoskeleton positively feedback on each other enhances polarization in a single direction. After bud site determination, the polarized actin cytoskeleton is used for delivering vesicles from the mother cell to the daughter cell [18]. Therefore, the process of bud site determination not only initiates asymmetric bud formation but also sets up a system for asymmetrically distributing cytoplasmic components between the bud and mother cell.

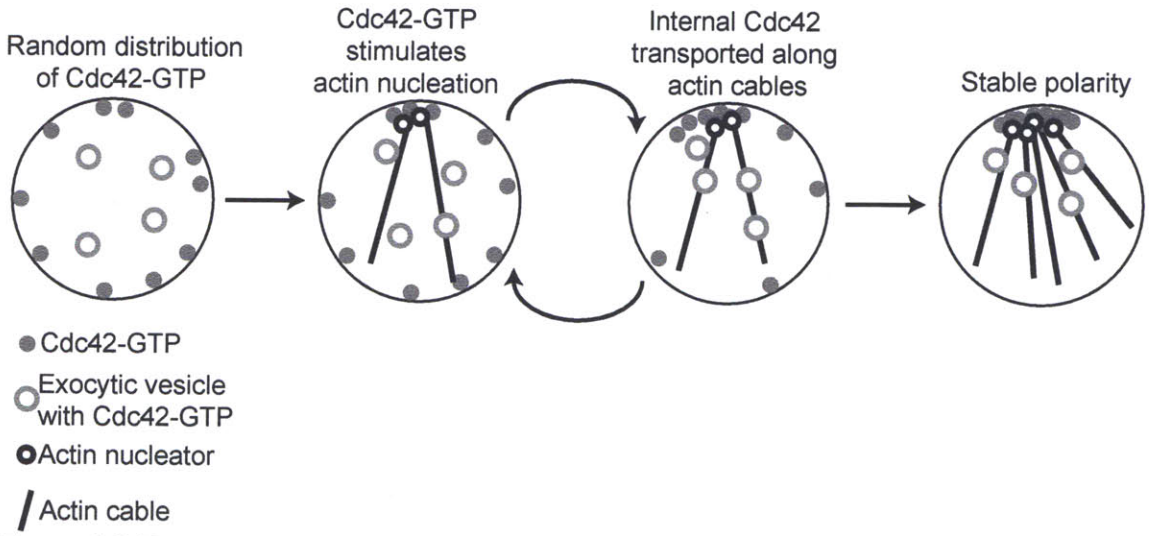

Figure 1.2. De novo symmetry breaking through actin-dependent positive feedback. Initial stochastic accumulation of Cdc42-GTP triggers actin nucleation. This leads to transport of internal Cdc42 to the polarizing site, leading to further nucleation of actin cables. Figure adapted from [2].

As with budding yeast, the first cell division for a newly fertilized *C. elegans* embryo is asymmetric, yielding a larger anterior cell called AB and a smaller posterior cell called P_1 [5, 19-21]. These sister cells undergo different patterns of cell division and ultimately generate different tissue types. AB undergoes a series of synchronous cleavages,

producing equally-sized daughter cells that go on to generate ectoderm [22]. By contrast, P_1 descendants undergo multiple asymmetric divisions and ultimately produce mesoderm, endoderm, the gonad, and some ectoderm [22].

Unlike budding yeast, the asymmetry of the *C. elegans* embryo cannot be determined randomly. Instead, it is defined deterministically using the site of sperm entry, which delineates the posterior pole [21]. Upon fertilization, a network of actin and myosin on the cell cortex of the embryo drives surface contractions uniformly around the cortex [23]. At the same time, the Rho GTPase-activating protein CYK-4 is transferred from the sperm to the zygote. CYK-4 then locally inactivates Rho, resulting in actomyosin relaxation around the posterior pole but continued actomyosin contractions in the anterior (Fig. 1.3). These asymmetrically placed actomyosin contractions profoundly reorganize the embryonic cytoplasm [23]. Yolk granules near the surface move away from the posterior and toward the anterior in a process called cortical flow. By contrast, yolk granules deeper within the embryo move posteriorly in a process called cytoplasmic flow. Cortical flow transports important polarity determinants, such as PAR-3, PAR-6 and the protein kinase PKC-3, to the anterior hemisphere of the embryo [23, 24]. Other determinants, such as PAR-1 and PAR-2 remain in the posterior. Negative crosstalk between PAR-3, PAR-6, and PKC-3 in the anterior and PAR-1 and PAR-2 in the posterior reinforce their separate spatial distributions, forming distinct anterior and posterior domains of the embryo. During this maintenance phase, the myosin network also breaks down to form smaller puncta (Fig. 1.3). Later, during the domain correction phase, the boundary between the anterior and posterior domains of the embryo that are defined by the PAR proteins aligns with the cleavage furrow; this is thought to be

mediated in part by the larger myosin puncta that form in the anterior and in the nascent contractile ring to be used for cytokinesis (Fig. 1.3) [4].

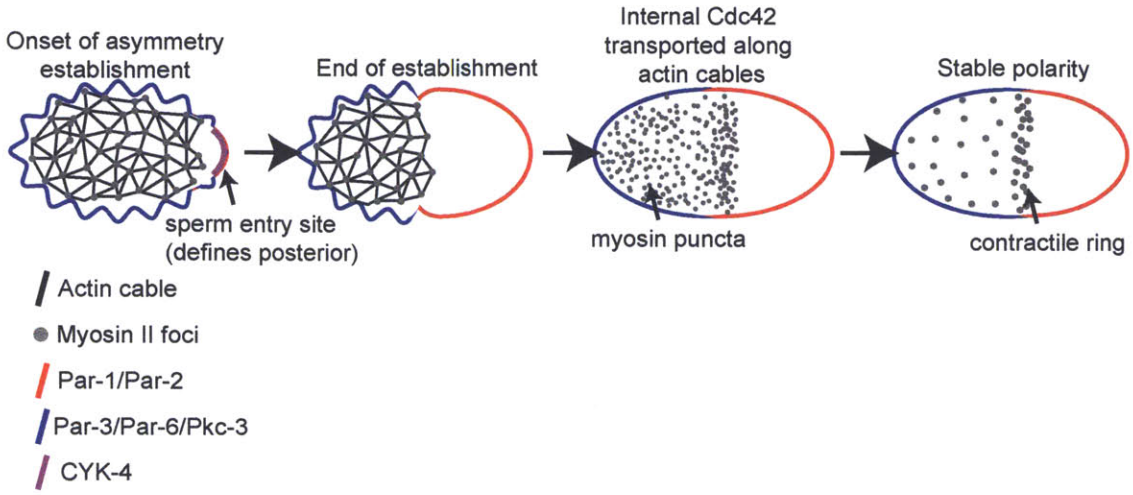

Figure 1.3. Symmetry breaking based on an external cue. CYK-4 (purple) at site of sperm entry locally inhibits actomyosin contraction (black lines and grey dots). This causes PAR-3, PAR-6, and PKC-3 (blue) to move towards the anterior while PAR-1 and PAR-2 (red) are released from inhibition in the posterior. At the end of asymmetry establishment, cortical ruffling induced by actomyosin contractions are restricted to the anterior half of the cell and two domains of different PAR proteins have been set up. Later the myosin network breaks down to form puncta and a contractile ring. Figure adapted from [4] and [5]

Establishment of anterior and posterior PAR protein domains then drives the next step toward asymmetric cell division: the asymmetric segregation of cytoplasmic components [25]. Although the mechanism by which each of the PAR proteins effect downstream functions is not completely understood, the best studied involves PAR-1. PAR-1 is critical for localizing germ plasm to the posterior end of the embryo. The germ plasm contains proteins and RNA-rich organelles called P granules that are essential for germline development in descendants of the posterior P_1 cell. Germ plasm components start out uniformly distributed throughout the oocyte but then segregate to the posterior only after the establishment of PAR domains. PAR-1 localizes germ plasm components through two redundant intermediates, MEX-5 and MEX-6, which localize to the anterior of the cell in a PAR-1 dependent manner [26]. MEX-5 and MEX-6 likely promote

degradation of germ plasm components in the anterior of the cell while PAR-1 by an unknown mechanism protects them from degradation in the posterior [27, 28]. In sum, the example of deterministic asymmetry formation in the *C. elegans* embryo demonstrates how an external signal (CYK-4) initiates the asymmetric partitioning of PAR proteins and how the PAR proteins then convert a transient stimulus (sperm entry) into a stable asymmetry by harnessing basic cellular functions like actomyosin contractions and protein degradation.

Translation of cellular asymmetry into distinct daughter cell fates

In both the random and deterministic examples of asymmetry, once polarity has been established, the cell must translate this polarity into an asymmetric cell division and different daughter cell fates. In eukaryotes, this often involves two key steps: (1) signaling from a pole to the cytoskeleton to asymmetrically organize transport and then (2) exploiting this directional transport to asymmetrically distribute components with effector functions [29]. We already saw briefly how these two steps contribute to asymmetric cell division in the *C. elegans* embryo. What are some other examples of the mechanisms used to differentiate sister cells?

Asymmetric fate determination ultimately results from the differential localization and inheritance of proteins by daughter cells. There are three major ways to achieve this asymmetric distribution of proteins [21]. One way is to localize mRNA, which can lead to either translational repression or translation of a specific product in the target daughter cell. Well-studied examples of this mechanism are the asymmetry in mating type switching in budding yeast [30] and body plan specification in *Drosophila* embryogenesis [31]. A second way is to localize the protein itself, which can then be

inherited asymmetrically by daughter cells. This mechanism drives neural development in *Drosophila melanogaster* [19]. A third mechanism is differential protein stability, which occurs in *C. elegans* embryos, where an E3 ligase causes degradation of germline specification proteins in daughters that are fated to be somatic cells [32]. Below, I will discuss the paradigmatic examples of differential mRNA localization in budding yeast and protein localization in *Drosophila* neural progenitors.

In budding yeast, localization of an mRNA specifically to the bud is responsible for inhibiting daughter cells from switching mating type. As discussed in the previous section, budding yeast divide asymmetrically into a larger mother cell and a smaller daughter cell that have different mating type switching abilities (Fig. 1.1). Mating type switching results from mother-specific expression of the *HO* endonuclease, which initiates a genomic rearrangement of the MAT locus. Using information copied from one of two silent mating-type cassettes on either side of the MAT locus, this rearrangement can convert an 'a' cell to an 'α' or vice-versa (reviewed in [33]). A screen for mutants in which daughter cells anomalously switch their mating type uncovered a gene called *ash1* [34]. Ash1p is a transcriptional repressor that silences *HO* expression in daughter cells. Therefore, the control of mating type switching centers on the asymmetric localization of Ash1p to daughter cells.

How is Ash1p localization controlled? In a budding cell, Cdc42 polarizes the actin cytoskeleton toward the bud, as discussed in the previous section. These polarized actin filaments are used to transport *ASH1* mRNA into the bud. In order to be transported, *ASH1* mRNA must first be packaged in an mRNP called the 'locasome'. Four 'zipcode' sequences within the *ASH1* mRNA are recognized by the protein She2p, which

complexes with an adaptor protein She3p and a type V myosin Myo4p to make up the core locasome (Fig. 1.4). During transport, Ash1p translation is repressed by two proteins that bind the *ASH1* mRNA, Puf6p and Khd1p [35-37]. The arrival of the locasome at the bud tip causes Khd1p, a cytoplasmic protein, to come close to the membrane, where it is phosphorylated by a membrane-bound kinase Yck1p. Phosphorylation reduces Khd1p affinity to RNA and thus unmasks *ASH1* mRNA, relieving its translational repression [38]. At this time, *ASH1* translation begins and newly produced Ash1p translocates into the daughter cell nucleus, where it silences the *HO* locus. By contrast, the mother cell does not express Ash1p and therefore is able to express HO and switch mating type.

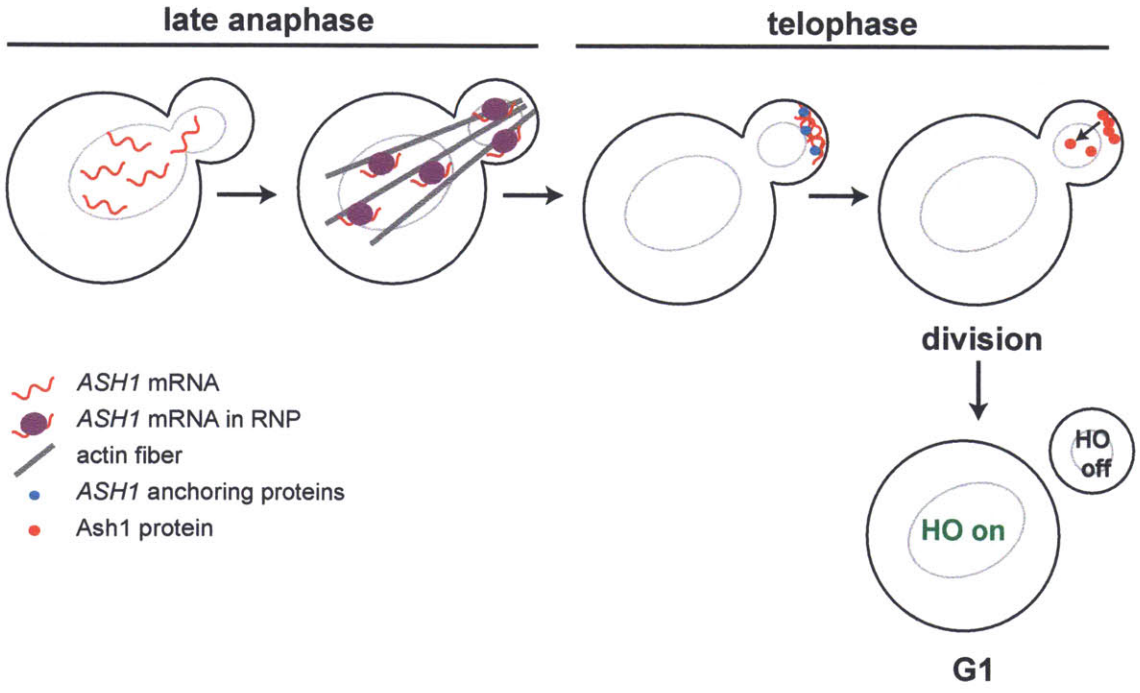

Figure 1.4. Asymmetrically localized Ash1p silences *HO* transcription in the daughter cell. In late anaphase, *ASH1* mRNA (red) is packaged into a locasome (purple, RNP) that represses *ASH1* translation. The RNP is transported along actin cables to the distal tip of the bud. In telophase, *ASH1* translation occurs and Ash1 protein (red) enters the nucleus, where it represses HO in the daughter cell. Figure adapted from [3]

Another classic model of asymmetric cell division is neural development in *Drosophila*; in this case, asymmetry is largely controlled at the level of protein and not mRNA. The *Drosophila* peripheral nervous system (PNS) consists of neurons that innervate sensory organs. These sensory organs can be mechano- or chemosensory and have external sensory structures in the cuticle such as bristles or campaniform sensilla that sense exoskeleton bending. Other than the eye, each external sensory organ develops from a single progenitor cell, called the sensory organ precursor (SOP) cell, which produces four cells that form the final organ [39]. The SOP cell divides asymmetrically to generate an anterior pIIb and a posterior pIIa cell (Fig. 1.5). pIIb descendents form the internal structure of the sensory organ while pIIa descendents generate its external structures [19, 40].

Localization of the Numb protein to the anterior of the SOP cell drives the asymmetry in cell fate upon division [41, 42]. In Numb-deficient mutants, the first SOP division produces two IIa cells, whereas if Numb is overexpressed, this division produces two IIb cells (Fig. 1.5). Numb is a plasma membrane-associated cytoplasmic protein that determines cell fate by antagonizing Notch signaling [43-45]. Although Notch and its associated signaling proteins are expressed in both pIIb and pIIa cells, signaling only occurs from pIIb toward pIIa. That is, pIIb secretes the Delta ligand that activates signaling from the Notch receptor only on pIIa cells. As a result, expression of *tramtrack* (*ttk*), which encodes a zinc-finger transcription factor, is activated in pIIa but not in pIIb cells; this results in transcriptional programs that differ between pIIa and pIIb cells.

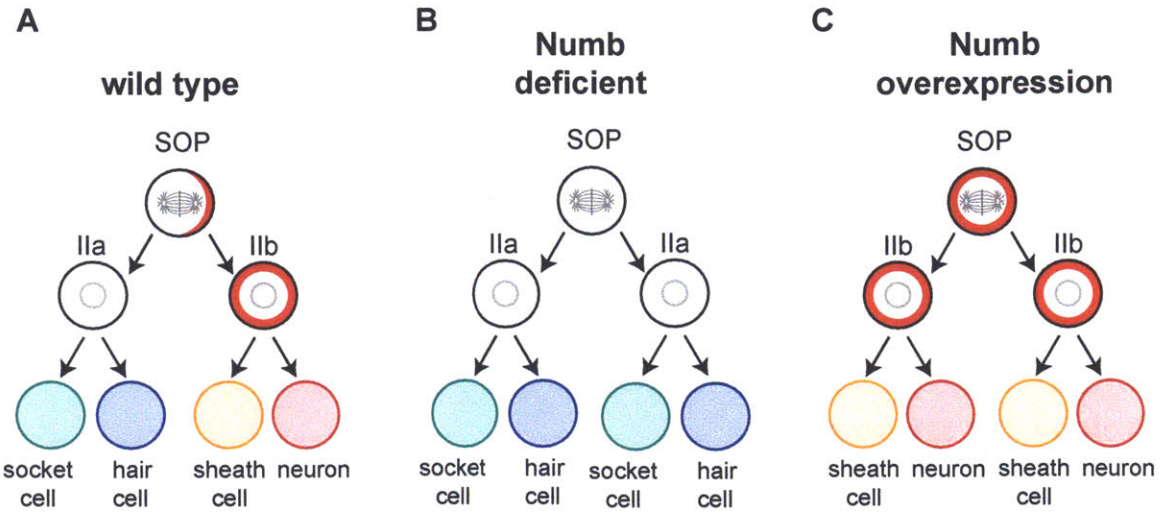

Figure 1.5. Asymmetrically localized Numb determines cell fate in the Drosophila peripheral nervous system. (A) In wild type cells, the sensory organ precursor (SOP) localizes Numb protein (red) anteriorly such that it is specifically inherited by the IIb cell. (B) In a Numb-deficient mutant, the SOP cell divides to form two IIa cells. (C) When Numb is overexpressed, the SOP cell divides to form two IIb cells.

How does Numb get localized specifically to the anterior? Just as the PAR proteins determine asymmetry in the *C. elegans* zygote, homologs of those same PAR proteins play a critical role here. Numb localizes opposite a complex containing Par3, Par6, and atypical protein kinase C (aPKC) in SOP cells undergoing division [41]. Recently, it was shown that the mitotic kinase Aurora A (AurA) directly phosphorylates Par6, a regulator of aPKC, and activates aPKC [46]. Activated aPKC phosphorylates another protein Lgl, causing its release from the cell cortex, which permits Par3 to complex with Par6 and aPKC. Par3 is a specificity factor that allows aPKC to phosphorylate Numb, which causes the release of Numb from the posterior cortex, leaving Numb at the anterior [47, 48]. How Par3, Par6, and aPKC specifically localize to the posterior cortex is not known.

In addition to Numb, signaling between pIIb and pIIa cells is also regulated by the E3 ubiquitin ligase Neur. Like Numb, Neur localizes to the anterior cortex of SOP cells

during mitosis and is therefore inherited only by pIIb daughter cells. It has been suggested that Neur ubiquitinates Delta and promotes its endocytosis into pIIb, which exposes Notch receptors on pIIa to an activating extracellular cleavage. Therefore, asymmetric cell fate determination in *Drosophila* PNS development involves asymmetric partitioning of fate determinants, such as Numb, as well as signaling between daughter cells via the Notch pathway to further specify cell fate.

Prokaryotic asymmetry

Unlike eukaryotic cells, bacterial cells typically do not have membrane-enclosed organelles or cytoskeletal components that transport fate determinants. Prokaryotic cells are also at least one order of magnitude smaller than eukaryotic cells. Despite these challenges, prokaryotes display a wide array of asymmetric phenomena, from structural features such as flagella and chemoreceptors to complex behaviors such as sporulation or dimorphic life cycles. This begs the question, how do prokaryotes generate, maintain, and utilize cellular asymmetry?

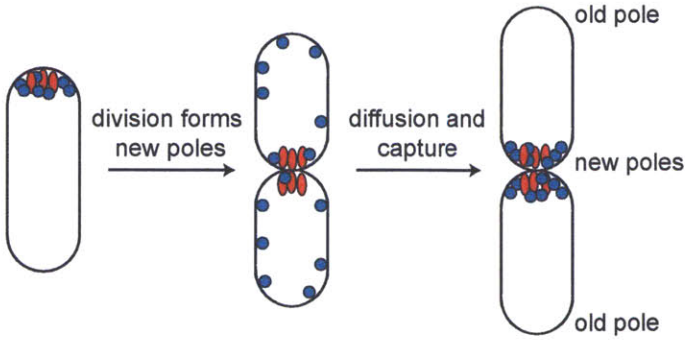

Figure 1.6. Cell division has inherent polar asymmetry. If certain proteins localize to the division septum, they will be inherited by both daughter cells and will mark the newly formed pole. Such a landmark protein (red) can also serve to capture other proteins (blue) and localize them specifically to the new pole. Therefore, even morphologically symmetric bacteria have an inherent polarity generated by each cell division.

One efficient and prevalent way to break symmetry in prokaryotes is to use the intrinsically asymmetrical process of cell division. With every division, the pole that arises from the division site is the "new" pole and can contain landmark proteins that differ from those at the "old" pole, which is inherited from the mother cell (Fig. 1.6). How the initial process of localizing proteins to the old or new pole will be discussed later. Below, I first discuss strategies for how cells take advantage of such polar localization, once established, and convert it into an asymmetry in cell fate.

Sporulation of *Bacillus subtilis* is a well-studied asymmetric division event that offers multiple examples for how an initial cell polarity can be converted into a difference in daughter cell fates [49]. *B. subtilis* is a rod-shaped Gram-positive bacterium commonly found in soil. In rich medium, *B. subtilis* divide by binary fission approximately every 30 minutes. Upon stress, however, it can develop a tough, dormant endospore that can tolerate extreme environmental conditions. This process of sporulation is a carefully orchestrated differentiation process that takes about 8 to 10 hours.

Sporulation begins when a threshold concentration of phosphorylated Spo0A is reached and only after one round of DNA replication has been completed [50]. This defines stage 0. During stage I, the replication origins of the two chromosomes are tethered to opposite poles (Fig. 1.7A). In stage II, an asymmetrical septum forms to divide the cell into a larger mother cell and a smaller forespore. This septum traps the origin-proximal region of one of the chromosomes, and the rest of this chromosome is actively pumped into the forespore over 10-20 minutes. In stage III, the mother cell engulfs the forespore. In stages IV through VII, the forespore differentiates into a dense spore that is resistant to many physical and chemical stresses, and finally, the mother cell lyses. When living conditions

improve, specific nutrients can trigger germination of the spore and re-entry into the vegetative life cycle.

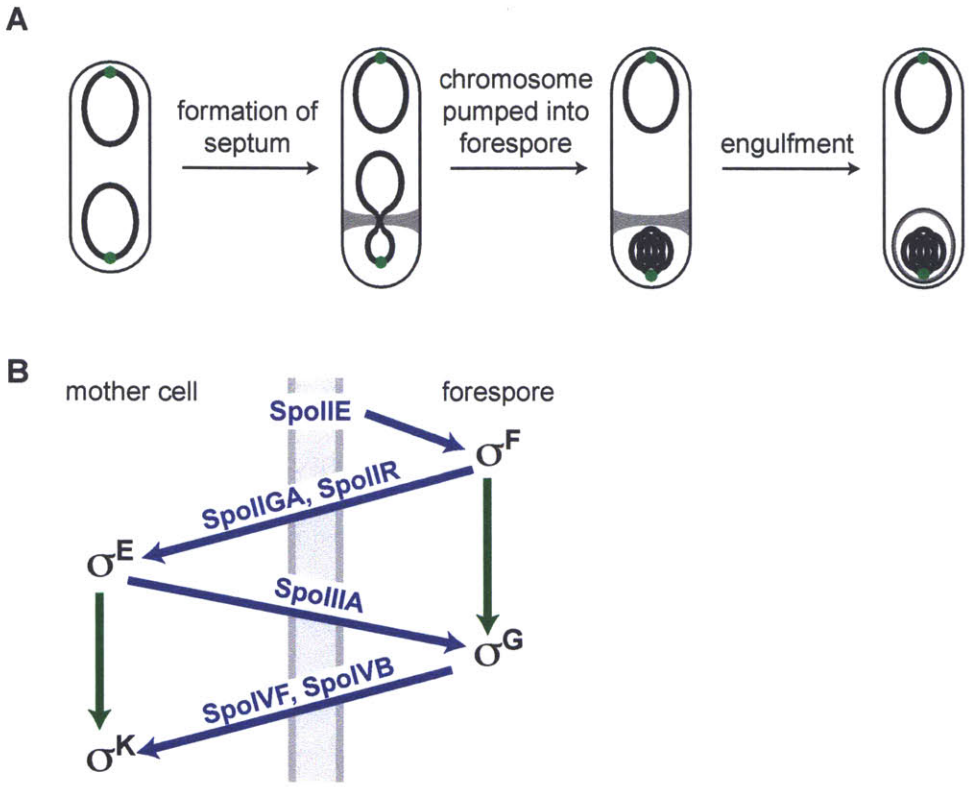

Figure 1.7. Sporulation in *Bacillus*. (A) After the cell commits to sporulation, it forms an asymmetrical septum. This septum captures an origin-proximal region of one chromosome (origins are shown as green dots) within the forespore. The chromosome is then pumped into the forespore, which is engulfed by the mother cell. (B) Sporulation is driven by four sigma factors, each requiring transcriptional activation (green arrow) from a previous step as well as posttranslational activation (blue arrow) from the other cell. Figure adapted from [1]

Sequential activation of five sigma factors (σ^H, σ^F, σ^E, σ^G, and σ^K) drives sporulation by directing the expression of distinct subsets of genes (Fig. 1.7B). Therefore, the controls at each step in sporulation are primarily directed toward regulating sigma factor activation. σ^F and σ^G are forespore-specific while σ^E and σ^K are mother cell-specific sigma factors. σ^G is only synthesized via σ^F-mediated transcription and σ^K is synthesized via σ^E-mediated transcription (Fig. 1.7B). Each of these sigma factors is inactive when synthesized and requires an activating signal that is made by the sister cell, thus forming

a developmental ratchet that requires crosstalk between the mother cell and forespore at each stage of differentiation [1]. For example, σ^E activity requires an activating proteolytic cleavage by SpoIIGA. SpoIIGA needs to be activated by SpoIIR, a protein secreted by the forespore that is transcribed only after σ^F activation [51]. σ^E then directs the next stage of differentiation by mediating the expression of an activating signal required by σ^G.

During the process of sporulation, the first asymmetrically activated sigma factor is σ^F, which defines the forespore's commitment to a different fate than the mother cell. σ^F activity is regulated by three proteins: the anti-sigma factor SpoIIAB, the anti-anti-sigma factor SpoIIAA, and a phosphatase SpoIIE (Fig. 1.8). SpoIIAB complexes with ATP and σ^F to prevent σ^F from binding to RNA polymerase. At the same time, SpoIIAB is a kinase that phosphorylates SpoIIAA at a conserved serine; this inhibitory phosphorylation prevents SpoIIAA from releasing SpoIIAB's inhibition of σ^F [52]. After formation of the asymmetrical septum, however, SpoIIE dephosphorylates SpoIIAA and enables it to bind SpoIIAB. This sequesters SpoIIAB away from σ^F and allows σ^F to bind RNA polymerase and activate forespore-specific gene expression.

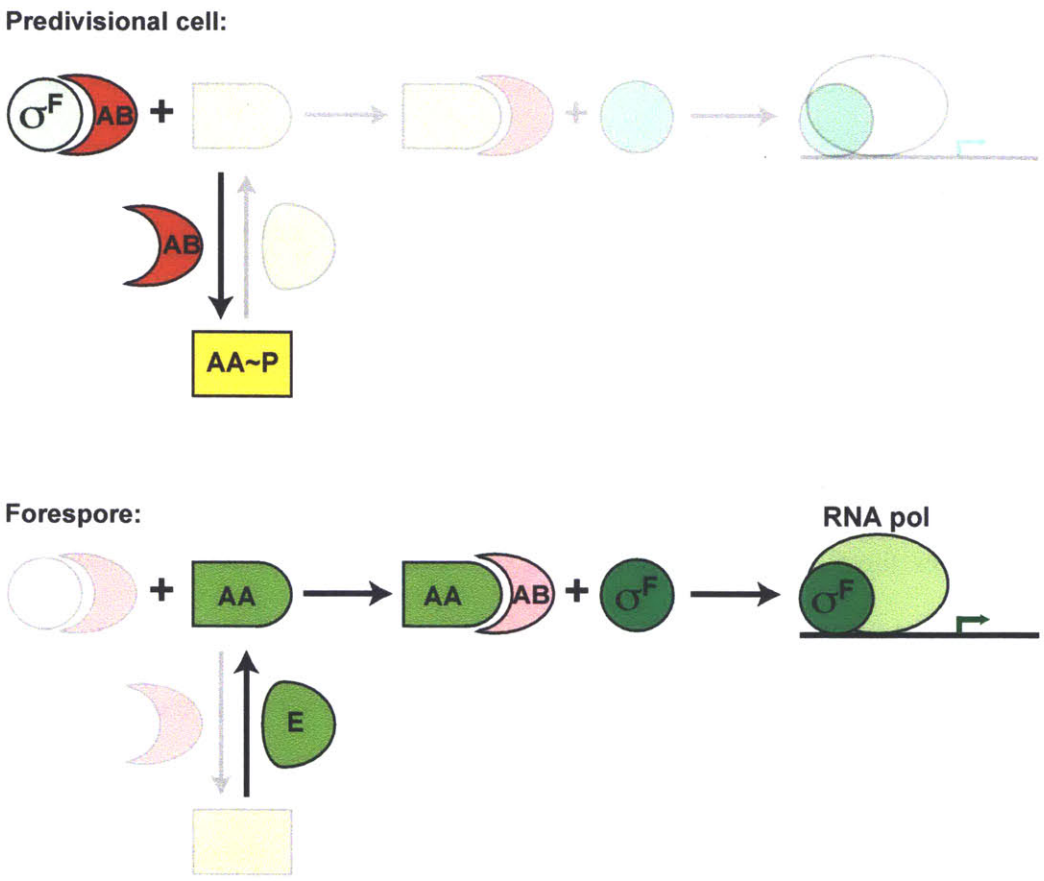

Figure 1.8. Regulation of σ^F. In the predivisional cell, the anti-sigma factor SpoIIAB (red, AB) binds σ^F and keeps it inactive. SpoIIAB also inactivates SpoIIAA by phosphorylating it to SpoIIAA~P (yellow, AA~P). In the forespore, SpoIIE (green, E) concentration increases. SpoIIE dephosphorylates SpoIIAA (green, AA), allowing SpoIIAA to sequester SpoIIAB away from σ^F. This allows σ^F to bind RNA polymerase and activate forespore-specific gene expression.

The asymmetry in SpoIIE activity is essential for activating σ^F in the forespore. However, SpoIIE, along with SpoIIAA, SpoIIAB, and σ^F, is found in both the mother cell and the forespore, so how is this asymmetry achieved? SpoIIE has three domains: a hydrophobic N-terminal domain responsible for membrane binding, a central domain involved in SpoIIE oligomerization and interaction with the cell division protein FtsZ, and a C-terminal protein phosphatase domain for SpoIIAA dephosphorylation. First, SpoIIE localizes to the FtsZ ring [53] where it contributes to asymmetric septal morphogenesis [54, 55]. Then, SpoIIE lines both sides of the septum and partitions equally to the mother

cell and forespore. Because the forespore has a much smaller volume, the SpoIIE to SpoIIAB ratio is increased by about 10-fold, sufficient to shift the equilibrium toward SpoIIAA dephosphorylation and the release of σ^F from SpoIIAB binding [56]. In sum, the major contributor to the asymmetry in SpoIIE activity is the difference in volume between forespore and mother cell that creates a difference in SpoIIE concentration.

In addition to a volume-dependent increase in SpoIIE activity in the forespore, another mechanism contributes to forespore-specific σ^F activation by decreasing SpoIIAB levels in the forespore. During the first step of sporulation, the septum forms over one of the two chromosomes, placing the origin-proximal one-third of the chromosome within the forespore and the rest of the chromosome outside (Fig. 1.7A). Therefore, during the 10-20 minutes it takes to pump the rest of the chromosome into the forespore, origin-distal genes, such as *spoIIAB*, are excluded [57, 58]. Since the SpoIIAB protein is constantly degraded by ClpCP and the *spoIIAB* gene is excluded from the forespore based on its chromosome location, SpoIIAB degradation exceeds SpoIIAB synthesis in the forespore. As a result, SpoIIAB proteins levels drop after formation of the septum, further decreasing its ability to block σ^F activity [59, 60]. Interestingly, in a strain lacking both of the genes essential to σ^F activation, *spoIIE* and *spoIIAA*, the ability to sporulate could be restored by moving the gene encoding σ^F to the origin-proximal region [61]. These data support the idea that a transient asymmetry in chromosome position, and therefore gene content, is significant enough to drive an asymmetry in protein content.

B. subtilis sporulation thus relies on an intrinsically asymmetric cell division as well as signaling between daughter cells. Formation of an asymmetrical division septum produces intrinsic differences between the forespore and mother cell—cell volume and

chromosome content—that result in forespore-specific σ^F activation. The mother cell and forespore must then engage in multiple rounds of signaling to activate a cascade of transcriptional regulators that drive further differentiation.

Caulobacter cell cycle as a model for studying cellular asymmetry

Another major model system for understanding the molecular basis of cellular asymmetry is the alpha-proteobacterium *Caulobacter crescentus*. Unlike *Bacillus subtilis*, every cell division for *Caulobacter crescentus* is asymmetric, yielding two morphologically different daughter cells: a motile swarmer cell with polarly localized flagellum and pili and an immotile stalked cell with a tubular extension of the cell envelope referred to as the stalk [62]. These two daughter cells also differ in their ability to initiate DNA replication [63]. A stalked cell can immediately initiate DNA replication while a swarmer cell must first differentiate into a stalked cell before it can initiate replication. The morphological transition from swarmer to stalked cell thus coincides with the G1 to S cell cycle transition. With each cell cycle, DNA replication occurs once and only once, resulting in distinguishable G1, S, and G2 phases.

Specific morphogenetic events, such as flagellar assembly or stalk development, always occur in coordination with cell cycle progression. Therefore, it was proposed early on that regulators of the cell cycle also cue the timing of morphologic events [64]. Indeed, chromosome replication is required for formation of the flagellum in the predivisional cell [65], suggesting that common factors control both the initiation of DNA replication and the transcription of early flagellar genes. Therefore, one might expect to find cell cycle regulators by screening for temperature-sensitive mutants that are defective in flagellar biogenesis at the permissive temperature and inviable at the higher restrictive

temperature due to a cell cycle defect. Genetic screens based on this logic resulted in the identification of two essential regulators of the *Caulobacter* cell cycle: the CtrA response regulator and the CckA histidine kinase [66, 67]. Temperature-sensitive mutants of CtrA ($ctrA^{ts}$) and CckA ($cckA^{ts}$) fail to form polar flagella, pili, and stalks at the permissive temperature; at the restrictive temperature, they fail to divide, become filamentous and accumulate multiple chromosomes, and eventually die [66, 67].

Subsequent analyses of CtrA demonstrated that it possesses two critical cell cycle activities, functioning as a transcription factor for nearly 100 genes as well as binding directly to the origin of replication to silence initiation (Fig. 1.9). DNA footprinting, expression profiling, and genome-wide ChIP-chip experiments have shown that CtrA binds to a conserved TTAA-N7-TTAA motif in approximately 55 promoters to control 95 genes, some organized into operons [68-70]. CtrA target genes include both morphogenetic genes important for flagellar synthesis, pili assembly, and chemotaxis, as well as essential cell cycle genes, such as the conserved cell division gene *ftsZ*. Microarray experiments comparing gene expression in wild type to $ctrA^{ts}$ showed that a third of all cell cycle-regulated genes are directly or indirectly under the control of CtrA [71]. In addition to acting as a global transcriptional regulator, CtrA also inhibits the initiation of DNA replication by directly binding to five sites within the origin of replication [72, 73]. These CtrA binding sites overlap with elements essential for the initiation of chromosome replication [74].

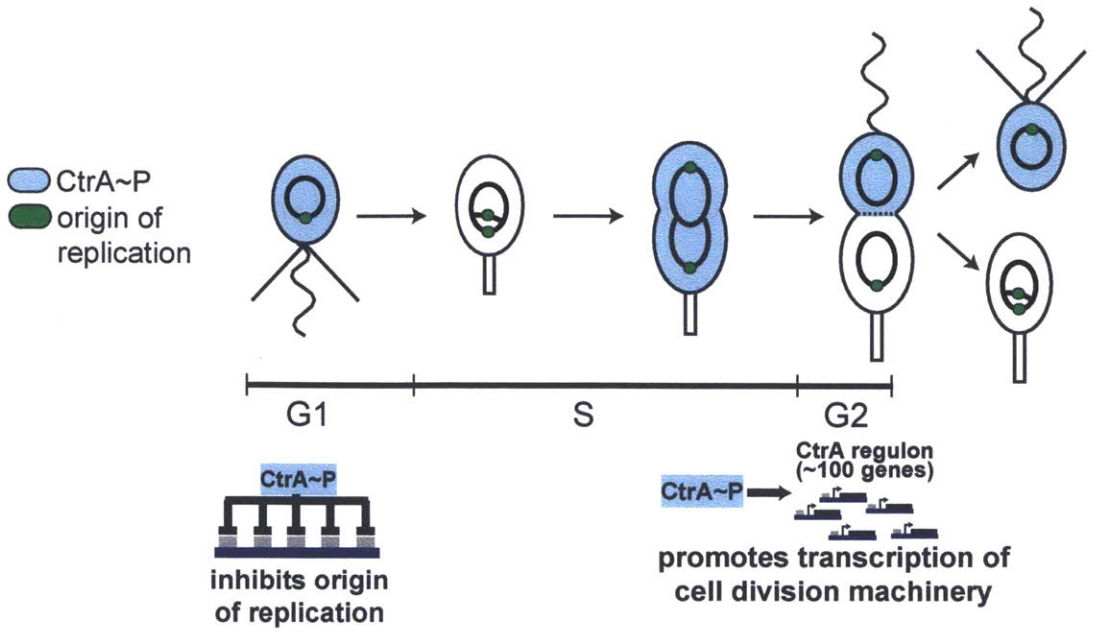

Figure 1.9. CtrA is the master regulator of Caulobacter cell cycle. In the G1 swarmer cell, CtrA is phosphorylated (CtrA~P, blue) and inhibits the origin of replication (green). During the G1-S transition, CtrA is cleared to allow for replication initiation, and the pili and flagellum are shed and replaced by the stalk. The stalk marks the stalked pole; the opposite pole is called the swarmer pole. In the predivisional cell, CtrA~P reaccumulates to directly regulate ~100 genes. Each division generates a swarmer daughter cell in G1 and a stalked daughter cell in S phase.

Progression through the *Caulobacter* cell cycle requires the periodic activation and inactivation of CtrA. Studies from several labs have shown that CtrA activity is controlled on at least three levels: transcription, proteolysis, and phosphorylation. Proteolysis and phosphorylation are the two primary mechanisms of control as the constitutive expression of *ctrA* does not lead to significant cell cycle or morphogenetic defects [75]. In G1 swarmer cells, CtrA is phosphorylated and abundant to inhibit the initiation of DNA replication. During the G1-S transition, two redundant mechanisms ensure clearance of CtrA activity: targeted proteolysis and dephosphorylation. Targeted CtrA proteolysis is mediated by the ClpXP protease complex and restricted to the G1-S transition [75, 76]. However, expression of a proteolysis-resistant allele of CtrA,

CtrAΔ3Ω, does not completely impede the cell cycle because CtrA can still be efficiently dephosphorylated and inactivated [75]. Similarly, the expression of a CtrA mutant (CtrAD51E) that partially mimics the phosphorylated state does not disrupt cell cycle progression because targeted proteolysis of CtrA still occurs. However, expression of a CtrA mutant that is both constitutively active and resistant to ClpXP-mediated proteolysis (CtrAD51EΔ3Ω) causes a dominant G1 arrest by preventing the initiation of DNA replication [75].

How does phosphorylation change CtrA activity? Phosphorylation enhances CtrA binding to its target DNA sequences [73, 77]. Binding of CtrA to a promoter can then either activate or repress a target gene. For CtrA-activated genes, the CtrA binding site is typically upstream of or near the -35 region, allowing CtrA to recruit RNA polymerase to the promoter. On the other hand, for CtrA-repressed genes, the site usually overlaps the -10 region; as a result, binding of CtrA at the promoter likely blocks RNA polymerase binding and thus represses gene expression. Consistently, peak expression of CtrA-repressed genes occurs at the beginning of S phase when CtrA activity is the lowest while that of CtrA-activated genes occurs in late predivisional cells when CtrA is maximally phosphorylated and active as a transcription factor [68, 71].

These experiments have led to the following model of how CtrA regulates cell cycle progression (Fig. 1.9). In G1, CtrA is phosphorylated and stabilized in daughter swarmer cells to inhibit DNA replication. CtrA also binds to a small protein SciP that prevents CtrA from activating target genes in this cell type [78]. During the G1-S transition, CtrA is both dephosphorylated and degraded to allow for DNA replication [75, 79, 80]. After replication, CtrA is again phosphorylated and stabilized in predivisional cells to activate

genes important for cell division and polar morphogenesis [66, 68]. Each division is asymmetric, generating a daughter swarmer cell with high CtrA activity and a daughter stalked cell that immediately clears CtrA. This difference in daughter cell levels of CtrA activity establishes their difference in replicative capacity. Therefore, how *Caulobacter* generates asymmetric cell fates is essentially a question of how CtrA activity is controlled in a spatially asymmetric manner.

Two-component signal transduction

CtrA is a member of the two-component signaling family of proteins. Before describing the regulatory network that governs CtrA activity, I will first introduce two-component signaling. Two-component systems are widespread in bacteria and archaea but are also found in yeast and plants [81, 82]. A two-component system typically consists of a homodimeric histidine kinase with an extracellular sensor domain that responds to specific signals. In response to a signal, the histidine kinase will typically autophosphorylate and then transfer the phosphoryl group to a cognate response regulator, which typically contains a DNA binding domain and becomes an active transcription factor upon phosphorylation [83].

All histidine kinases contain a dimerization and histidine phosphotransfer (DHp) domain and a C-terminal catalytic ATP binding (CA) domain. The CA domain binds ATP and catalyzes phosphorylation of a conserved histidine residue within the DHp domain in a process called autophosphorylation (Fig. 1.10). The phosphoryl group from the histidine is then transferred to an aspartate in the receiver domain of a cognate response regulator. In addition to a receiver domain, response regulators typically have an output domain, most commonly a DNA-binding domain. Phosphorylation usually changes the response

regulator's affinity for DNA, as is the case with CtrA, or its propensity to dimerize, thus modulating its transcription factor activity. Some response regulators without a DNA binding domain may contain enzymatic output domains, such as di-guanylate cyclase [84]. Some do not contain any additional output domain and rely on changes in conformation of the receiver domain to modulate changes in interactions with downstream interacting proteins. The final output of a two-component system depends on the level of response regulator phosphorylation, which results from a balance between phosphorylation and dephosphorylation. Frequently, the histidine kinase can catalyze the dephosphorylation of its cognate response regulator and this phosphatase activity can be regulated by upstream factors [85]. Alternatively, dedicated phosphatases can dephosphorylate the response regulator [86, 87]. As many as a hundred two-component systems can co-exist in a single cell without significant crosstalk [88].

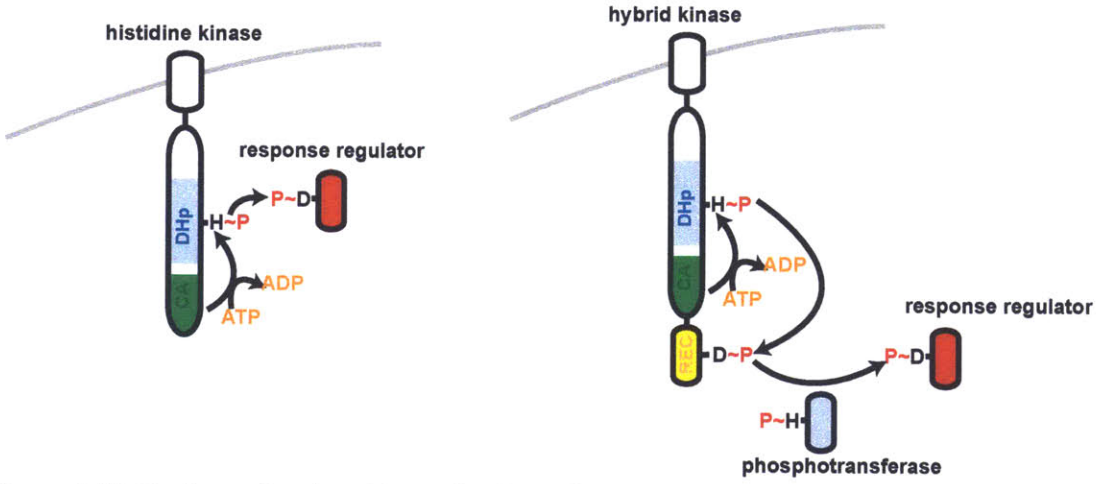

Figure 1.10. Prokaryotic signal transduction. The two-component system (left) consists of a histidine kinase with a transmembrane sensor domain and a response regulator. The histidine kinase uses its catalytic ATP binding (CA) domain to autophosphorylates the histidine in the dimerization and histidine phosphotransfer (DHp) domain, which then transfers the phosphoryl group to an exposed aspartate in the response regulator. A typical phosphorelay (right) consists of a hybrid kinase with an extra receiver domain (REC), which receives the phosphate from the DHp histidine and transfers it via a phosphotransferase to the response regulator.

A common variation of the two-component system is the phosphorelay. Phosphorelays typically begin with a hybrid histidine kinase that contains sensor, DHp, and CA domains, as well as a receiver domain similar to that found in response regulators (Fig. 1.10). The hybrid kinase autophosphorylates on the DHp histidine and then passes the phosphoryl group intramolecularly to the aspartate within the attached receiver domain. The phosphoryl group is then transferred to a histidine phosphotransferase and from there to the aspartate of a cognate, terminal response regulator. Therefore, a phosphorelay contains four phosphorylation steps, while a two-component system only has two. But similar to a two-component system, phosphotransfers only occur between a histidine and an aspartate, and never between two histidines or two aspartates. Although all phosphorelays contain four steps of phosphorylation, the molecular connectivity between each of the four steps may differ. In some cases, the hybrid kinase may be split into two parts: one part containing the sensor, DHp, and CA domains and another part containing the receiver domain [89]. In other cases, the hybrid kinase and histidine phosphotransferase may be fused into a single protein [87]. Since phosphorelays have more components than a two-component system, they can have additional points of control with additional regulatory proteins acting at various points along the phosphorelay [89].

Phosphorelay control of CtrA activity

CtrA activity is regulated by two phosphorelays, both initiating with the hybrid histidine kinase CckA and the histidine phosphotransferase ChpT (Fig. 1.11). A strain harboring a *cckA* loss-of-function allele ($cckA^{ts}$) displays a phenotype very similar to a $ctrA^{ts}$ strain, where cells accumulate chromosomes and are unable to divide. Additionally, comparative

microarray analysis of *ctrA*^{ts} and *cckA*^{ts} mutants at the restrictive temperature showed changes in the mRNA levels of an almost identical set of cell cycle-regulated genes [90]. *In vitro* and *in vivo* studies subsequently demonstrated that CckA transfers phosphate to the histidine phosphotransferase ChpT, which can then act as a phosphodonor for either CtrA or a single-domain response regulator called CpdR (Fig. 1.11) [79]. The phosphorylation of CtrA activates its DNA-binding and transcription factor activities, while phosphorylation of CpdR prevents it from triggering CtrA proteolysis [79]. When unphosphorylated, CpdR binds the ClpXP protease and localizes it to the new stalked cell pole during the G1-S transition; this localization of ClpXP is required for CtrA proteolysis. In a CpdR-deficient strain, CtrA remains abundant throughout the cell cycle and ClpX does not localize [80]. Collectively, these data suggest that CckA functions by driving CtrA phosphorylation and promoting its stability.

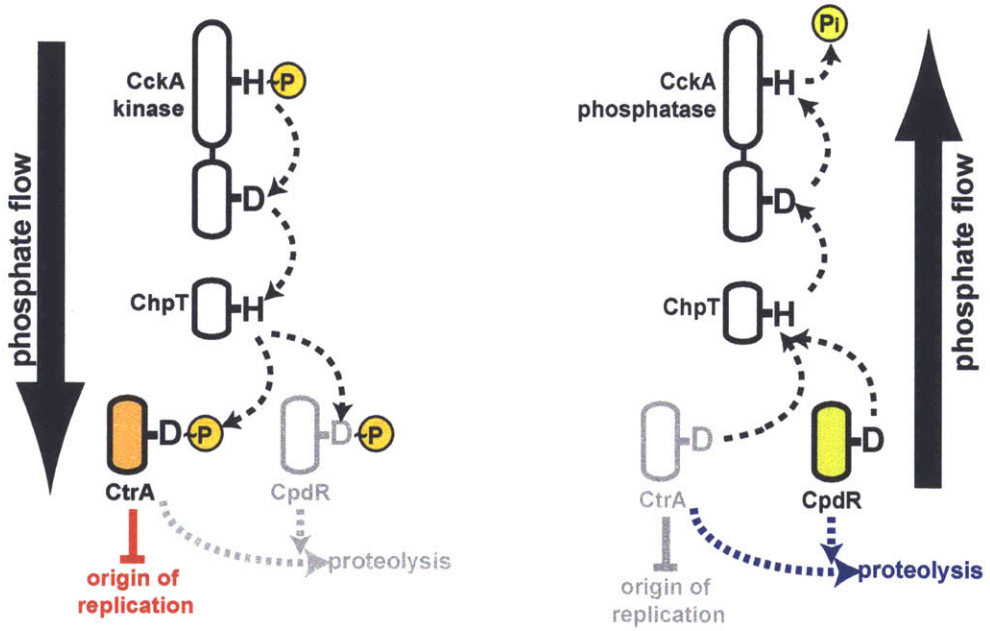

Figure 1.11: Phosphorelay control of CtrA activity. When activated as a kinase, CckA drives forward phosphate flow, resulting in the phosphorylation of both CtrA and CpdR. CtrA~P inhibits the origin of replication while CpdR~P is inactive. When activated as a phosphatase, CckA drives phosphate flow backward, dephosphorylating CtrA and CpdR.

Since CckA drives CtrA activation and accumulation, CckA kinase activity must be inhibited during the G1-S transition to permit replication initiation and S phase. Given that the phosphoryl groups on CtrA~P and CpdR~P are relatively stable *in vitro* [79], phosphatase activity is likely important to eliminate CtrA activity (and drive the dephosphorylation of CpdR) during the G1-S transition. For some phosphorelays, the hybrid kinase can act as a phosphatase to siphon phosphate away from the response regulator [91, 92]. For other phosphorelays, there are separate and dedicated phosphatases [93-95]. It was not known initially whether CckA could be a phosphatase *in vivo* or whether separate phosphatases exist for CtrA. In Chapter 2-3, I show that CckA can switch between kinase and phosphatase states and explore how CckA phosphatase activity contributes to establishing a spatial asymmetry of CtrA activity in predivisional cells.

Control of CckA activity by two-component signaling

CckA activity is controlled during the cell cycle by a circuit of two-component proteins that includes the essential single-domain response regulator DivK, which inhibits CckA kinase activity when phosphorylated. DivK phosphorylation is controlled by two antagonistic enzymes: the histidine kinase DivJ and the histidine kinase PleC, which acts predominantly as a DivK phosphatase *in vivo* [96, 97]. PleC was identified in a genetic screen for mutants with defects in polar morphogenesis; *pleC* null mutants can divide normally and assemble flagella but fail to turn on motility, shed the flagellum, or make stalks [98]. The idea that *pleC* might connect polar development to the cell cycle led to a genetic screen for mutations that suppressed the temperature-sensitive non-motile phenotype of a *pleC* mutant but also conferred a cold-sensitive cell division defect [99].

This screen yielded mutations in *divJ* and *divK*. *divJ* loss of function mutations lead to cells that are significantly elongated, suggestive of a cell division defect, and have long stalks that are often misplaced [100-102]. *divK* loss of function mutations cause abnormal stalk formation, cell filamentation, and a block in chromosome replication [99, 103, 104]. In addition to these genetic data, DivJ and PleC were shown to efficiently phosphorylate and dephosphorylate DivK *in vitro*, respectively [100, 103, 105]. Finally, it was shown that DivK~P levels are decreased *in vivo* in a *divJ* mutant but increased in a *pleC* mutant relative to wild type. These data suggested that *in vivo* DivJ activates DivK by phosphorylation but PleC inactivates DivK by dephosphorylation [97].

While the role of DivJ and PleC in the regulation of DivK phosphorylation became apparent, their role in regulating CtrA activity remained unclear. An important clue came from the G1 arrest observed in a conditional *divK* loss-of-function mutant; this suggested that without DivK, elevated CckA kinase activity may lead to a maintainance of CtrA phosphorylation and the constitutive silencing of DNA replication [79, 104]. Consistently, CckA phosphorylation is elevated in this *divK* mutant [79, 85].

Genetically, it is clear that DivK downregulates CckA kinase activity, but what is the mechanism of this inhibition? In contrast to the typical response regulator, DivK contains only a receiver domain [103, 106]. Other single domain response regulators either participate in protein-protein interactions or act as a phosphointermediate in a multicomponent phosphorelay [107]. Initial genetic evidence linked another protein, DivL, to DivK and CtrA regulation since *divL* was also isolated as a suppressor of the *pleC* motility phenotype, similar to *divJ* and *divK* [108]. DivL is an unorthodox kinase that was found to interact with DivK via yeast two-hybrid analysis [109]. A strain

carrying a temperature-sensitive loss of function allele of *divL* (*divL*^{ts}) exhibits cell filamentation, chromosome accumulation, and changes in CtrA-dependent gene expression similar to the *ctrA*^{ts} strain, suggesting that DivL positive regulates CtrA [85]. Epistasis experiments placed DivL between DivK and CckA, and *in vivo* phosphorylation assays showed that CckA~P levels significantly decreased in *divL*^{ts} cells grown at the restrictive temperature. Taken together, these data suggest that DivL promotes CckA activity and that phosphorylated DivK binds directly to DivL to prevent it from stimulating CckA kinase activity (Fig. 1.12). When DivL cannot stimulate CckA kinase activity, CckA most likely acts as a phosphatase, driving CtrA and CpdR dephosphorylation [110].

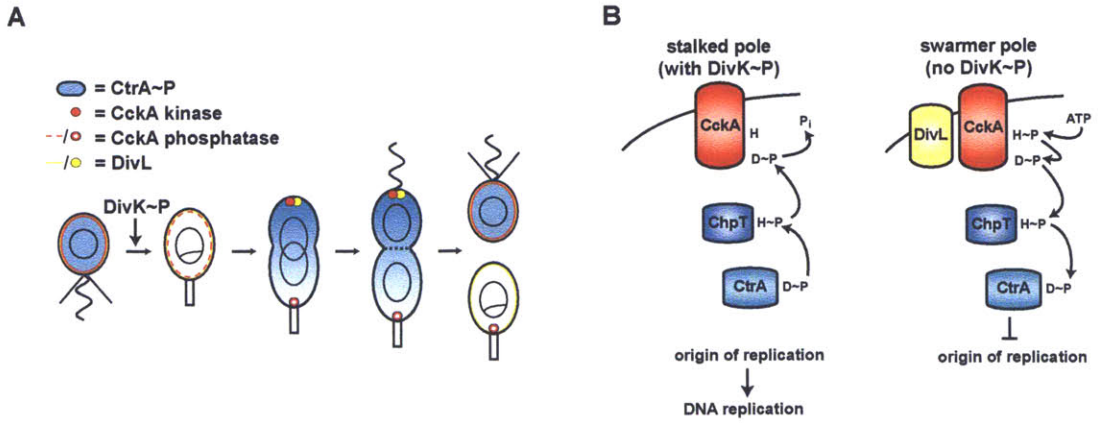

Figure 1.12. Regulation of CckA kinase activity by DivL. (A) Schematic of the cell cycle showing how CckA activity (red) and localization varies with the cell cycle. (B) Schematic of how DivK~P and DivL regulates CckA kinase and phosphatase activity at the stalked and swarmer poles of a predivisional cell and at the stalked pole of a stalked cell.

Dynamic localization of cell cycle kinases

One striking feature of *Caulobacter* cell cycle regulation is that the regulatory components dynamically localize to different cell poles in a cell cycle-dependent manner (Fig. 1.13). This dynamic localization may be a mechanism to regulate interactions

between different components in order to selectively drive either kinase or phosphatase activity of CckA. The membrane-bound CckA histidine kinase is dispersed in the G1 swarmer cell, but localizes to the new, swarmer pole in the early predivisional cell and then bipolarly in the late predivisional cell [79, 110, 111]. The swarmer pole localization of CckA is dependent on localization of DivL to the swarmer pole [85]. Upon division, CckA is again dispersed in the daughter swarmer cell but remains at the stalked pole in the daughter stalked cell while DivL becomes dispersed in both daughter cells. For DivL to stimulate CckA kinase activity, DivK must be unphosphorylated. Therefore, PleC localization at the swarmer pole mirrors DivL localization in the predivisional cell [102, 112]. PleC then remains at this pole during cell division, segregating to the daughter swarmer cell, where it maintains DivK in an unphosphorylated state until the G1-S transition. During the G1-S transition, PleC delocalizes and then re-localizes at the new swarmer pole after replication initiation.

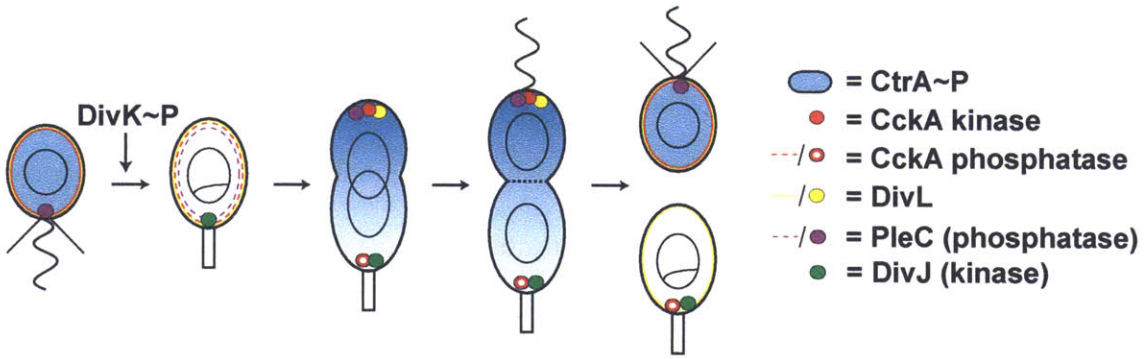

Figure 1.13. Dynamic localization of cell cycle kinases during the Caulobacter cell cycle. The histidine kinases PleC, DivJ, PleC, and CckA exhibit dynamic polar localization over the cell cycle. The G1-S transition requires an accumulation of phosphorylated DivK, indicated by the labeled arrow. DivK is a cytoplasmic protein that can exhibit polar foci on microscopy likely due to interactions with PleC, DivK, and DivK, but it does not stably localize at any cell pole.

In contrast to PleC, DivJ is absent in swarmer cells and is produced during the G1-S transition, when it becomes localized at the stalked pole, which replaces the old swarmer

pole (Fig. 1.13) [102]. DivJ then remains at the stalked pole for the remainder of the cell cycle. Consistent with the fact that DivJ and PleC have antagonistic enzymatic activities and localize to opposite poles of the predivisional cell, photobleaching and fluorescent resonance energy transfer (FRET) experiments have shown rapid diffusion of DivK between the cell poles, constantly turning over between the phosphorylated and unphosphorylated states [97]. After cytokinesis, the different poles of the cell along with DivJ and PleC activities become compartmentalized [113]. The stalked cell inherits DivJ, which drives DivK phosphorylation and ultimately the inactivation of CtrA, and the swarmer cell inherits PleC, which drives DivK dephosphorylation and maintains CtrA activity. In sum, spatial separation of DivJ and PleC ensure CckA kinase activity in predivisional cells as well as proper inheritance by daughter cells upon asymmetric cell division. Additionally, the colocalization of PleC, DivL, and CckA at the swarmer pole is essential to stimulate CckA kinase activity at the proper cell cycle stage.

The dynamic localization of DivJ, PleC, DivL, and CckA are important for their function; however, it is not known what mechanisms are responsible for localizing these crucial cell cycle kinases. To find proteins that organize polar complexes, the *Caulobacter* genome was screened for proteins with transmembrane regions and large coiled-coil protein interaction domains. One of the genes identified was subsequently shown to encode a birth scar protein called TipN [96, 114]. In stalked and early predivisional cells, TipN localizes to the new swarmer pole and then relocates to the division plane in late predivisional cells in order to be inherited at the new pole of both daughter cells upon division. The *tipN* knockout displays mislocalized flagella and PleC, suggesting that

swarmer pole factors use TipN as a localizing landmark. Additionally, *tipN* mutants display size inversion, with swarmer cells frequently larger than stalked cells [115].

In addition to TipN, PodJ, another coiled-coil rich protein, is also required for PleC localization [116, 117]. In *podJ* mutants, PleC is dispersed around the membrane with no polar localization. *podJ* mutants also display a phenotype similar to *pleC* mutants. Both strains lack pili and holdfast and cannot eject the flagellum; however, *pleC* mutants are stalkless and have paralyzed flagella while *podJ* mutants produce stalks and motile flagella [116-118]. As expected, PodJ localizes similarly to PleC, at the swarmer pole but how PodJ is targeted to the swarmer pole or inhibited from localizing at the stalked pole is unknown.

Consistent with the specific role of TipN as a new pole marker, old pole proteins such as DivJ do not have disturbed localization in the *tipN* mutant [115]. Instead, DivJ localization depends on SpmX, which has been shown to interact with DivJ in reciprocal coimmunoprecipitation experiments [119]. SpmX has a periplasmic muramidase domain and two transmembrane domains and has been suggested to interact with one of DivJ's five transmembrane domains. SpmX localization at the stalked pole depends on the muramidase domain, which is implicated in peptidoglycan binding; however, it is unclear what is different between stalked and swarmer pole peptidoglycans that would recruit SpmX specifically to the stalked pole.

Regulation of the *Caulobacter* cell cycle involves many asymmetrical localization events of multiple cascades of signaling proteins. The consequences of PleC, DivJ, CckA, and DivL localization on their activities and some of the landmark proteins required for their

localization are now more clearly understood. However, the mechanism by which landmark proteins, such as TipN, PodJ, and SpmX, then localize to the poles remains unclear.

Control of replication within the cell cycle

The *Caulobacter* cell cycle comprises both asymmetric morphogenesis and asymmetric replicative capacity in the daughter cells, necessitating tight coupling between the cell division cycle and replication. While the previous sections focused on CtrA, a negative regulator of DNA replication, *Caulobacter* also requires a positive regulator of replication, DnaA, which is a highly conserved protein present in almost all bacteria, with the exception of a few obligate endosymbionts [120]. DnaA is a member of the AAA+ family of ATPases with DnaA-ATP but not DnaA-ADP active to bind and help melt the origin of replication to promote initiation [121-123]. DnaA specifically interacts with 9-bp nonpalindromic sequences, called DnaA boxes, at the single origin of initiation, *oriC* [122, 124]. Based on a crystal structure of the major part of *Aquifex aeolicus* DnaA, DnaA-ATP monomers bound to DnaA boxes were suggested to oligomerize into a right-handed filament that wraps around the *oriC* region to promote local unwinding of an AT-rich region [125], resulting in helicase loading and replisome assembly.

In both eukaryotes and prokaryotes, replication control centers on the step of initiation. In prokaryotes, this might involve controlling the activity of DnaA and the availability of *oriC*. In *E. coli*, DnaA activity is tightly regulated, peaking immediately before DNA replication initiates and then dropping rapidly once replication commences (reviewed in [123]). Three mechanisms have been described in *E. coli* to prevent reinitiation from the newly replicated origins: inactivation of DnaA, titration of DnaA, and sequestration of

oriC. The inactivation of DnaA depends largely on a protein called Hda, which stimulates ATP hydrolysis by DnaA, thus converting active DnaA-ATP into inactive DnaA-ADP [126]. Titration of DnaA protein occurs by a cluster of high-affinity DnaA boxes (*datA*), which can bind over 300 DnaA molecules [127]. For reducing *oriC* accessibility, the SeqA protein preferably binds hemimethylated GATC sequences that are overrepresented within *oriC*. Since the newly replicated *oriC* regions are initially hemimethylated, SeqA binds to these regions and thus prevents DnaA from rebinding.

Although prokaryotic replication has been studied extensively, its coordination with the cell division cycle is not well understood. This is partly because in many prokaryotes, such as *E. coli*, multiple replication forks can progress simultaneously, yielding more than 2 chromosomes per cell during a normal cell cycle. This obscures the coordination between cell division and replication initiation since replication can initiate at multiple times with respect to division.

In *Caulobacter*, I now address both questions of how replication is coupled to the cell cycle and how asymmetric replicative fates are enforced with every division. A current model in *Caulobacter* suggests that CtrA and DnaA are connected through a transcriptional "ratchet", in which *dnaA* transcription is indirectly activated by CtrA and *ctrA* transcription is, in turn, indirectly activated by DnaA [128, 129]. This circuit, proposed to drive cell cycle progression, implies that the accumulation of DnaA depends on CtrA activity. However, cells lacking active CtrA accumulate multiple chromosomes [72], suggesting that CtrA is not required to promote DnaA activity. Moreover, cells constitutively transcribing *dnaA* or *ctrA* do not exhibit a severe cell cycle or replication phenotype [75, 130], suggesting that transcriptional changes do not drive cell cycle

progression. Additionally, although CtrA is often assumed to prevent re-replication in predivisional cell, cells harboring mutations in CtrA binding sites within the origin do not exhibit severe defects in DNA replication [131]. These incongruencies raise the question of whether, or to what extent, CtrA contributes to the temporal regulation of DNA replication.

Research Approach

In the subsequent chapters, I describe a series of experiments that investigate how the CtrA phosphorelay drives replicative asymmetry and how the control of replicative asymmetry relates to replication periodicity. Chapter 2 details the biochemical characterization of CckA point mutants that have altered kinase or phosphatase activities. I show that these mutants have effects *in vivo* that are consistent with their *in vitro* activities. I show that a kinase-only allele of CckA that has no phosphatase activity *in vitro* can complement a CckA deletion, suggesting that although CckA phosphatase activity contributes to CtrA regulation, its absence can be compensated by another unknown phosphatase for CtrA.

In Chapter 3, I explore the role of CckA's bifunctionality in establishing cellular asymmetry. I use a fluorescent repressor-operator system [132, 133] and fluorescence microscopy to observe replication events in individual living cells as they progress through the cell cycle. I show that steady-state gradients of CtrA activity can inhibit replication at the swarmer pole where CtrA~P is highest but not at the stalked pole where CtrA~P is lowest. This gradient of phosphorylated CtrA requires CckA kinase and phosphatase activities at opposite poles. Importantly, we can abolish replicative asymmetry by mutating the CtrA binding sites at the origin. This demonstrates that CtrA

exerts its effect on replication by direct binding to the origin and not indirectly through transcriptional activation of another factor. Our collaborators generated a reaction-diffusion model to explore the minimal requirements of maintaining such a phosphogradient and corroborated our experimental findings with theoretical predictions.

Chapter 4 describes a collaborative study investigating the separate roles of CtrA and DnaA in controlling replication and coordinating it with the cell cycle. Using the same fluorescent repressor-operator system, we examined the timing of replication initiation while genetically changing either CtrA or DnaA activity. We show that CtrA activity is necessary and sufficient to enforce replicative asymmetry in daughter cells. However, losing CtrA activity does not change the periodicity of replication in stalked cells, suggesting that DnaA comprises an autonomous oscillator that controls replication timing. In accordance, we found that changing DnaA activity positively or negatively profoundly impacted replication periodicity. We conclude that DnaA lies at the heart of a primordial cell cycle oscillator that continues to dictate replication timing in Caulobacter, as it does in most bacteria, while CtrA was co-opted later in evolution to enforce replicative asymmetry and to coordinate replication with cellular differentiation. The modularity of replication control in *Caulobacter* thus reflects its evolution and reveals its relationship to the cell cycles of other bacteria.

References

1. Stragier, P., and Losick, R. (1996). Molecular genetics of sporulation in Bacillus subtilis. Annu Rev Genet *30*, 297-241.

2. Slaughter, B.D., Smith, S.E., and Li, R. (2009). Symmetry breaking in the life cycle of the budding yeast. Cold Spring Harb Perspect Biol *1*, a003384.

3. Cosma, M.P. (2004). Daughter-specific repression of Saccharomyces cerevisiae HO: Ash1 is the commander. EMBO Rep *5*, 953-957.

4. Nance, J., and Zallen, J.A. (2011). Elaborating polarity: PAR proteins and the cytoskeleton. Development *138*, 799-809.

5. Munro, E., and Bowerman, B. (2009). Cellular symmetry breaking during Caenorhabditis elegans development. Cold Spring Harb Perspect Biol *1*, a003400.

6. Horvitz, H.R., and Herskowitz, I. (1992). Mechanisms of asymmetric cell division: two Bs or not two Bs, that is the question. Cell *68*, 237-255.

7. Kimble, J., and Hirsh, D. (1979). The postembryonic cell lineages of the hermaphrodite and male gonads in Caenorhabditis elegans. Dev Biol *70*, 396-417.

8. Sulston, J.E., and Horvitz, H.R. (1977). Post-embryonic cell lineages of the nematode, Caenorhabditis elegans. Dev Biol *56*, 110-156.

9. Vlamakis, H., Aguilar, C., Losick, R., and Kolter, R. (2008). Control of cell fate by the formation of an architecturally complex bacterial community. Genes Dev *22*, 945-953.

10. Kroos, L. (2007). The Bacillus and Myxococcus developmental networks and their transcriptional regulators. Annu Rev Genet *41*, 13-39.

11. Balasubramanian, M.K., Bi, E., and Glotzer, M. (2004). Comparative analysis of cytokinesis in budding yeast, fission yeast and animal cells. Curr Biol *14*, R806-818.

12. Neiman, A.M. (2005). Ascospore formation in the yeast Saccharomyces cerevisiae. Microbiol Mol Biol Rev *69*, 565-584.

13. Casamayor, A., and Snyder, M. (2002). Bud-site selection and cell polarity in budding yeast. Curr Opin Microbiol *5*, 179-186.

14. Freifelder, D. (1960). Bud position in Saccharomyces cerevisiae. Journal of bacteriology *80*, 567-568.

15. Adams, A.E., Johnson, D.I., Longnecker, R.M., Sloat, B.F., and Pringle, J.R. (1990). CDC42 and CDC43, two additional genes involved in budding and the establishment of cell polarity in the yeast Saccharomyces cerevisiae. J Cell Biol *111*, 131-142.

16. Moseley, J.B., and Goode, B.L. (2006). The yeast actin cytoskeleton: from cellular function to biochemical mechanism. Microbiol Mol Biol Rev *70*, 605-645.

17. Park, H.O., and Bi, E. (2007). Central roles of small GTPases in the development of cell polarity in yeast and beyond. Microbiol Mol Biol Rev *71*, 48-96.

18. Nelson, W.J. (2003). Mum, this bud's for you: where do you want it? Roles for Cdc42 in controlling bud site selection in Saccharomyces cerevisiae. Bioessays *25*, 833-836.

19. Betschinger, J., and Knoblich, J.A. (2004). Dare to be different: asymmetric cell division in Drosophila, C. elegans and vertebrates. Curr Biol *14*, R674-685.

20. Goldstein, B., and Hird, S.N. (1996). Specification of the anteroposterior axis in Caenorhabditis elegans. Development *122*, 1467-1474.

21. Gonczy, P. (2008). Mechanisms of asymmetric cell division: flies and worms pave the way. Nat Rev Mol Cell Biol *9*, 355-366.

22. Gonczy, P., and Rose, L.S. (2005). Asymmetric cell division and axis formation in the embryo. WormBook, 1-20.

23. Munro, E., Nance, J., and Priess, J.R. (2004). Cortical flows powered by asymmetrical contraction transport PAR proteins to establish and maintain anterior-posterior polarity in the early C. elegans embryo. Dev Cell *7*, 413-424.

24. Jenkins, N., Saam, J.R., and Mango, S.E. (2006). CYK-4/GAP provides a localized cue to initiate anteroposterior polarity upon fertilization. Science *313*, 1298-1301.

25. Pellettieri, J., and Seydoux, G. (2002). Anterior-posterior polarity in C. elegans and Drosophila--PARallels and differences. Science *298*, 1946-1950.

26. Schubert, C.M., Lin, R., de Vries, C.J., Plasterk, R.H., and Priess, J.R. (2000). MEX-5 and MEX-6 function to establish soma/germline asymmetry in early C. elegans embryos. Mol Cell *5*, 671-682.

27. Reese, K.J., Dunn, M.A., Waddle, J.A., and Seydoux, G. (2000). Asymmetric segregation of PIE-1 in C. elegans is mediated by two complementary mechanisms that act through separate PIE-1 protein domains. Mol Cell *6*, 445-455.

28. Hird, S.N., Paulsen, J.E., and Strome, S. (1996). Segregation of germ granules in living Caenorhabditis elegans embryos: cell-type-specific mechanisms for cytoplasmic localisation. Development *122*, 1303-1312.

29. Perez, P., and Rincon, S.A. (2010). Rho GTPases: regulation of cell polarity and growth in yeasts. Biochem J *426*, 243-253.

30. Darzacq, X., Powrie, E., Gu, W., Singer, R.H., and Zenklusen, D. (2003). RNA asymmetric distribution and daughter/mother differentiation in yeast. Curr Opin Microbiol *6*, 614-620.

31. Johnstone, O., and Lasko, P. (2001). Translational regulation and RNA localization in Drosophila oocytes and embryos. Annu Rev Genet *35*, 365-406.

32. DeRenzo, C., Reese, K.J., and Seydoux, G. (2003). Exclusion of germ plasm proteins from somatic lineages by cullin-dependent degradation. Nature *424*, 685-689.

33. Herskowitz, I. (1988). Life cycle of the budding yeast Saccharomyces cerevisiae. Microbiol Rev *52*, 536-553.

34. Sil, A., and Herskowitz, I. (1996). Identification of asymmetrically localized determinant, Ash1p, required for lineage-specific transcription of the yeast HO gene. Cell *84*, 711-722.

35. Chartrand, P., Meng, X.H., Huttelmaier, S., Donato, D., and Singer, R.H. (2002). Asymmetric sorting of ash1p in yeast results from inhibition of translation by localization elements in the mRNA. Mol Cell *10*, 1319-1330.

36. Irie, K., Tadauchi, T., Takizawa, P.A., Vale, R.D., Matsumoto, K., and Herskowitz, I. (2002). The Khd1 protein, which has three KH RNA-binding motifs, is required for proper localization of ASH1 mRNA in yeast. Embo J *21*, 1158-1167.

37. Gu, W., Deng, Y., Zenklusen, D., and Singer, R.H. (2004). A new yeast PUF family protein, Puf6p, represses ASH1 mRNA translation and is required for its localization. Genes Dev *18*, 1452-1465.

38. Paquin, N., Menade, M., Poirier, G., Donato, D., Drouet, E., and Chartrand, P. (2007). Local activation of yeast ASH1 mRNA translation through phosphorylation of Khd1p by the casein kinase Yck1p. Mol Cell *26*, 795-809.

39. Cayouette, M., and Raff, M. (2002). Asymmetric segregation of Numb: a mechanism for neural specification from Drosophila to mammals. Nat Neurosci *5*, 1265-1269.

40. Vervoort, M., Dambly-Chaudiere, C., and Ghysen, A. (1997). Cell fate determination in Drosophila. Curr Opin Neurobiol *7*, 21-28.

41. Rhyu, M.S., Jan, L.Y., and Jan, Y.N. (1994). Asymmetric distribution of numb protein during division of the sensory organ precursor cell confers distinct fates to daughter cells. Cell *76*, 477-491.

42. Uemura, T., Shepherd, S., Ackerman, L., Jan, L.Y., and Jan, Y.N. (1989). numb, a gene required in determination of cell fate during sensory organ formation in Drosophila embryos. Cell *58*, 349-360.

43. Frise, E., Knoblich, J.A., Younger-Shepherd, S., Jan, L.Y., and Jan, Y.N. (1996). The Drosophila Numb protein inhibits signaling of the Notch receptor during cell-cell

interaction in sensory organ lineage. Proceedings of the National Academy of Sciences of the United States of America *93*, 11925-11932.

44. Guo, M., Jan, L.Y., and Jan, Y.N. (1996). Control of daughter cell fates during asymmetric division: interaction of Numb and Notch. Neuron *17*, 27-41.

45. Spana, E.P., and Doe, C.Q. (1996). Numb antagonizes Notch signaling to specify sibling neuron cell fates. Neuron *17*, 21-26.

46. Wirtz-Peitz, F., Nishimura, T., and Knoblich, J.A. (2008). Linking cell cycle to asymmetric division: Aurora-A phosphorylates the Par complex to regulate Numb localization. Cell *135*, 161-173.

47. Smith, C.A., Lau, K.M., Rahmani, Z., Dho, S.E., Brothers, G., She, Y.M., Berry, D.M., Bonneil, E., Thibault, P., Schweisguth, F., et al. (2007). aPKC-mediated phosphorylation regulates asymmetric membrane localization of the cell fate determinant Numb. Embo J *26*, 468-480.

48. Nishimura, T., and Kaibuchi, K. (2007). Numb controls integrin endocytosis for directional cell migration with aPKC and PAR-3. Dev Cell *13*, 15-28.

49. Barak, I., and Wilkinson, A.J. (2005). Where asymmetry in gene expression originates. Molecular microbiology *57*, 611-620.

50. Veening, J.W., Murray, H., and Errington, J. (2009). A mechanism for cell cycle regulation of sporulation initiation in Bacillus subtilis. Genes Dev *23*, 1959-1970.

51. Hofmeister, A.E., Londono-Vallejo, A., Harry, E., Stragier, P., and Losick, R. (1995). Extracellular signal protein triggering the proteolytic activation of a developmental transcription factor in B. subtilis. Cell *83*, 219-226.

52. Min, K.T., Hilditch, C.M., Diederich, B., Errington, J., and Yudkin, M.D. (1993). Sigma F, the first compartment-specific transcription factor of B. subtilis, is regulated by an anti-sigma factor that is also a protein kinase. Cell *74*, 735-742.

53. Levin, P.A., Losick, R., Stragier, P., and Arigoni, F. (1997). Localization of the sporulation protein SpoIIE in Bacillus subtilis is dependent upon the cell division protein FtsZ. Molecular microbiology *25*, 839-846.

54. Khvorova, A., Zhang, L., Higgins, M.L., and Piggot, P.J. (1998). The spoIIE locus is involved in the Spo0A-dependent switch in the location of FtsZ rings in Bacillus subtilis. Journal of bacteriology *180*, 1256-1260.

55. Piggot, P.J. (1973). Mapping of asporogenous mutations of Bacillus subtilis: a minimum estimate of the number of sporeulation operons. Journal of bacteriology *114*, 1241-1253.

56. Clarkson, J., Campbell, I.D., and Yudkin, M.D. (2004). Efficient regulation of sigmaF, the first sporulation-specific sigma factor in B.subtilis. Journal of molecular biology *342*, 1187-1195.

57. Dworkin, J. (2003). Transient genetic asymmetry and cell fate in a bacterium. Trends Genet *19*, 107-112.

58. Wu, L.J., and Errington, J. (1998). Use of asymmetric cell division and spoIIIE mutants to probe chromosome orientation and organization in Bacillus subtilis. Molecular microbiology *27*, 777-786.

59. Dworkin, J., and Losick, R. (2001). Differential gene expression governed by chromosomal spatial asymmetry. Cell *107*, 339-346.

60. Pan, Q., Garsin, D.A., and Losick, R. (2001). Self-reinforcing activation of a cell-specific transcription factor by proteolysis of an anti-sigma factor in B. subtilis. Mol Cell *8*, 873-883.

61. Frandsen, N., Barak, I., Karmazyn-Campelli, C., and Stragier, P. (1999). Transient gene asymmetry during sporulation and establishment of cell specificity in Bacillus subtilis. Genes Dev *13*, 394-399.

62. Poindexter, J.S. (1964). Biological Properties and Classification of the Caulobacter Group. Bacteriol Rev *28*, 231-295.

63. Curtis, P.D., and Brun, Y.V. (2010). Getting in the loop: regulation of development in Caulobacter crescentus. Microbiol Mol Biol Rev *74*, 13-41.

64. Huguenel, E.D., and Newton, A. (1982). Localization of surface structures during procaryotic differentiation: role of cell division in Caulobacter crescentus. Differentiation *21*, 71-78.

65. Sheffery, M., and Newton, A. (1981). Regulation of periodic protein synthesis in the cell cycle: control of initiation and termination of flagellar gene expression. Cell *24*, 49-57.

66. Quon, K.C., Marczynski, G.T., and Shapiro, L. (1996). Cell cycle control by an essential bacterial two-component signal transduction protein. Cell *84*, 83-93.

67. Jacobs, C., Domian, I.J., Maddock, J.R., and Shapiro, L. (1999). Cell cycle-dependent polar localization of an essential bacterial histidine kinase that controls DNA replication and cell division. Cell *97*, 111-120.

68. Laub, M.T., Chen, S.L., Shapiro, L., and McAdams, H.H. (2002). Genes directly controlled by CtrA, a master regulator of the Caulobacter cell cycle. Proceedings of the National Academy of Sciences of the United States of America *99*, 4632-4637.

69. Mohr, C.D., MacKichan, J.K., and Shapiro, L. (1998). A membrane-associated protein, FliX, is required for an early step in Caulobacter flagellar assembly. Journal of bacteriology *180*, 2175-2185.

70. Ouimet, M.C., and Marczynski, G.T. (2000). Analysis of a cell-cycle promoter bound by a response regulator. Journal of molecular biology *302*, 761-775.

71. Laub, M.T., McAdams, H.H., Feldblyum, T., Fraser, C.M., and Shapiro, L. (2000). Global analysis of the genetic network controlling a bacterial cell cycle. Science *290*, 2144-2148.

72. Quon, K.C., Yang, B., Domian, I.J., Shapiro, L., and Marczynski, G.T. (1998). Negative control of bacterial DNA replication by a cell cycle regulatory protein that binds at the chromosome origin. Proceedings of the National Academy of Sciences of the United States of America *95*, 120-125.

73. Siam, R., and Marczynski, G.T. (2000). Cell cycle regulator phosphorylation stimulates two distinct modes of binding at a chromosome replication origin. Embo J *19*, 1138-1147.

74. Marczynski, G.T., Lentine, K., and Shapiro, L. (1995). A developmentally regulated chromosomal origin of replication uses essential transcription elements. Genes Dev *9*, 1543-1557.

75. Domian, I.J., Quon, K.C., and Shapiro, L. (1997). Cell type-specific phosphorylation and proteolysis of a transcriptional regulator controls the G1-to-S transition in a bacterial cell cycle. Cell *90*, 415-424.

76. Jenal, U., and Fuchs, T. (1998). An essential protease involved in bacterial cell-cycle control. Embo J *17*, 5658-5669.

77. Reisenauer, A., Quon, K., and Shapiro, L. (1999). The CtrA response regulator mediates temporal control of gene expression during the Caulobacter cell cycle. Journal of bacteriology *181*, 2430-2439.

78. Gora, K.G., Tsokos, C.G., Chen, Y.E., Srinivasan, B.S., Perchuk, B.S., and Laub, M.T. (2010). A cell-type-specific protein-protein interaction modulates transcriptional activity of a master regulator in Caulobacter crescentus. Mol Cell *39*, 455-467.

79. Biondi, E.G., Reisinger, S.J., Skerker, J.M., Arif, M., Perchuk, B.S., Ryan, K.R., and Laub, M.T. (2006). Regulation of the bacterial cell cycle by an integrated genetic circuit. Nature *444*, 899-904.

80. Iniesta, A.A., McGrath, P.T., Reisenauer, A., McAdams, H.H., and Shapiro, L. (2006). A phospho-signaling pathway controls the localization and activity of a protease complex critical for bacterial cell cycle progression. Proceedings of the National Academy of Sciences of the United States of America *103*, 10935-10940.

81. Thomason, P., and Kay, R. (2000). Eukaryotic signal transduction via histidine-aspartate phosphorelay. J Cell Sci *113 (Pt 18)*, 3141-3150.

82. Casino, P., Rubio, V., and Marina, A. (2010). The mechanism of signal transduction by two-component systems. Curr Opin Struct Biol *20*, 763-771.

83. Gao, R., and Stock, A.M. (2009). Biological insights from structures of two-component proteins. Annual review of microbiology *63*, 133-154.

84. Paul, R., Weiser, S., Amiot, N.C., Chan, C., Schirmer, T., Giese, B., and Jenal, U. (2004). Cell cycle-dependent dynamic localization of a bacterial response regulator with a novel di-guanylate cyclase output domain. Genes Dev *18*, 715-727.

85. Tsokos, C.G., Perchuk, B.S., and Laub, M.T. (2011). A Dynamic Complex of Signaling Proteins Uses Polar Localization to Regulate Cell-Fate Asymmetry in Caulobacter crescentus. Dev Cell *20*, 329-341.

86. Sonenshein, A.L. (2000). Control of sporulation initiation in Bacillus subtilis. Curr Opin Microbiol *3*, 561-566.

87. Wadhams, G.H., and Armitage, J.P. (2004). Making sense of it all: bacterial chemotaxis. Nat Rev Mol Cell Biol *5*, 1024-1037.

88. Skerker, J.M., Perchuk, B.S., Siryaporn, A., Lubin, E.A., Ashenberg, O., Goulian, M., and Laub, M.T. (2008). Rewiring the specificity of two-component signal transduction systems. Cell *133*, 1043-1054.

89. Piggot, P.J., and Hilbert, D.W. (2004). Sporulation of Bacillus subtilis. Curr Opin Microbiol *7*, 579-586.

90. Jacobs, C., Ausmees, N., Cordwell, S.J., Shapiro, L., and Laub, M.T. (2003). Functions of the CckA histidine kinase in Caulobacter cell cycle control. Molecular microbiology *47*, 1279-1290.

91. Freeman, J.A., and Bassler, B.L. (1999). Sequence and function of LuxU: a two-component phosphorelay protein that regulates quorum sensing in Vibrio harveyi. Journal of bacteriology *181*, 899-906.

92. Freeman, J.A., and Bassler, B.L. (1999). A genetic analysis of the function of LuxO, a two-component response regulator involved in quorum sensing in Vibrio harveyi. Molecular microbiology *31*, 665-677.

93. Ohlsen, K.L., Grimsley, J.K., and Hoch, J.A. (1994). Deactivation of the sporulation transcription factor Spo0A by the Spo0E protein phosphatase. Proceedings of the National Academy of Sciences of the United States of America *91*, 1756-1760.

94. Perego, M. (2001). A new family of aspartyl phosphate phosphatases targeting the sporulation transcription factor Spo0A of Bacillus subtilis. Molecular microbiology *42*, 133-143.

95. Perego, M., Hanstein, C., Welsh, K.M., Djavakhishvili, T., Glaser, P., and Hoch, J.A. (1994). Multiple protein-aspartate phosphatases provide a mechanism for the integration of diverse signals in the control of development in B. subtilis. Cell *79*, 1047-1055.

96. Lam, H., Matroule, J.Y., and Jacobs-Wagner, C. (2003). The asymmetric spatial distribution of bacterial signal transduction proteins coordinates cell cycle events. Dev Cell *5*, 149-159.

97. Matroule, J.Y., Lam, H., Burnette, D.T., and Jacobs-Wagner, C. (2004). Cytokinesis monitoring during development; rapid pole-to-pole shuttling of a signaling protein by localized kinase and phosphatase in Caulobacter. Cell *118*, 579-590.

98. Ely, B., Croft, R.H., and Gerardot, C.J. (1984). Genetic mapping of genes required for motility in Caulobacter crescentus. Genetics *108*, 523-532.

99. Sommer, J.M., and Newton, A. (1991). Pseudoreversion analysis indicates a direct role of cell division genes in polar morphogenesis and differentiation in Caulobacter crescentus. Genetics *129*, 623-630.

100. Ohta, N., Lane, T., Ninfa, E.G., Sommer, J.M., and Newton, A. (1992). A histidine protein kinase homologue required for regulation of bacterial cell division and differentiation. Proceedings of the National Academy of Sciences of the United States of America *89*, 10297-10301.

101. Sommer, J.M., and Newton, A. (1989). Turning off flagellum rotation requires the pleiotropic gene pleD: pleA, pleC, and pleD define two morphogenic pathways in Caulobacter crescentus. J Bacteriol *171*, 392-401.

102. Wheeler, R.T., and Shapiro, L. (1999). Differential localization of two histidine kinases controlling bacterial cell differentiation. Mol Cell *4*, 683-694.

103. Hecht, G.B., Lane, T., Ohta, N., Sommer, J.M., and Newton, A. (1995). An essential single domain response regulator required for normal cell division and differentiation in Caulobacter crescentus. Embo J *14*, 3915-3924.

104. Hung, D.Y., and Shapiro, L. (2002). A signal transduction protein cues proteolytic events critical to Caulobacter cell cycle progression. Proceedings of the National Academy of Sciences of the United States of America *99*, 13160-13165.

105. Wang, S.P., Sharma, P.L., Schoenlein, P.V., and Ely, B. (1993). A histidine protein kinase is involved in polar organelle development in Caulobacter crescentus. Proceedings of the National Academy of Sciences of the United States of America *90*, 630-634.

106. Guillet, V., Ohta, N., Cabantous, S., Newton, A., and Samama, J.P. (2002). Crystallographic and biochemical studies of DivK reveal novel features of an essential response regulator in Caulobacter crescentus. J Biol Chem *277*, 42003-42010.

107. Jenal, U., and Galperin, M.Y. (2009). Single domain response regulators: molecular switches with emerging roles in cell organization and dynamics. Curr Opin Microbiol *12*, 152-160.

108. Wu, J., Ohta, N., Zhao, J.L., and Newton, A. (1999). A novel bacterial tyrosine kinase essential for cell division and differentiation. Proceedings of the National Academy of Sciences of the United States of America *96*, 13068-13073.

109. Ohta, N., and Newton, A. (2003). The core dimerization domains of histidine kinases contain recognition specificity for the cognate response regulator. Journal of bacteriology *185*, 4424-4431.

110. Chen, Y.E., Tsokos, C.G., Biondi, E.G., Perchuk, B.S., and Laub, M.T. (2009). Dynamics of two Phosphorelays controlling cell cycle progression in Caulobacter crescentus. J Bacteriol *191*, 7417-7429.

111. Angelastro, P.S., Sliusarenko, O., and Jacobs-Wagner, C. (2010). Polar localization of the CckA histidine kinase and cell cycle periodicity of the essential master regulator CtrA in Caulobacter crescentus. J Bacteriol *192*, 539-552.

112. Deich, J., Judd, E.M., McAdams, H.H., and Moerner, W.E. (2004). Visualization of the movement of single histidine kinase molecules in live Caulobacter cells. Proceedings of the National Academy of Sciences of the United States of America *101*, 15921-15926.

113. Judd, E.M., Ryan, K.R., Moerner, W.E., Shapiro, L., and McAdams, H.H. (2003). Fluorescence bleaching reveals asymmetric compartment formation prior to cell division in Caulobacter. Proceedings of the National Academy of Sciences of the United States of America *100*, 8235-8240.

114. Huitema, E., Pritchard, S., Matteson, D., Radhakrishnan, S.K., and Viollier, P.H. (2006). Bacterial birth scar proteins mark future flagellum assembly site. Cell *124*, 1025-1037.

115. Lam, H., Schofield, W.B., and Jacobs-Wagner, C. (2006). A landmark protein essential for establishing and perpetuating the polarity of a bacterial cell. Cell *124*, 1011-1023.

116. Hinz, A.J., Larson, D.E., Smith, C.S., and Brun, Y.V. (2003). The Caulobacter crescentus polar organelle development protein PodJ is differentially localized and is required for polar targeting of the PleC development regulator. Molecular microbiology *47*, 929-941.

117. Viollier, P.H., Sternheim, N., and Shapiro, L. (2002). Identification of a localization factor for the polar positioning of bacterial structural and regulatory proteins. Proceedings of the National Academy of Sciences of the United States of America *99*, 13831-13836.

118. Crymes, W.B., Jr., Zhang, D., and Ely, B. (1999). Regulation of podJ expression during the Caulobacter crescentus cell cycle. Journal of bacteriology *181*, 3967-3973.

119. Radhakrishnan, S.K., Thanbichler, M., and Viollier, P.H. (2008). The dynamic interplay between a cell fate determinant and a lysozyme homolog drives the asymmetric division cycle of Caulobacter crescentus. Genes Dev *22*, 212-225.

120. Klasson, L., and Andersson, S.G. (2004). Evolution of minimal-gene-sets in host-dependent bacteria. Trends Microbiol *12*, 37-43.

121. Mott, M.L., and Berger, J.M. (2007). DNA replication initiation: mechanisms and regulation in bacteria. Nature reviews. Microbiology *5*, 343-354.

122. Kaguni, J.M. (2006). DnaA: controlling the initiation of bacterial DNA replication and more. Annual review of microbiology *60*, 351-375.

123. Katayama, T., Ozaki, S., Keyamura, K., and Fujimitsu, K. (2010). Regulation of the replication cycle: conserved and diverse regulatory systems for DnaA and oriC. Nature reviews. Microbiology *8*, 163-170.

124. Messer, W. (2002). The bacterial replication initiator DnaA. DnaA and oriC, the bacterial mode to initiate DNA replication. FEMS Microbiol Rev *26*, 355-374.

125. Erzberger, J.P., Mott, M.L., and Berger, J.M. (2006). Structural basis for ATP-dependent DnaA assembly and replication-origin remodeling. Nat Struct Mol Biol *13*, 676-683.

126. Kato, J., and Katayama, T. (2001). Hda, a novel DnaA-related protein, regulates the replication cycle in Escherichia coli. Embo J *20*, 4253-4262.

127. Kitagawa, R., Ozaki, T., Moriya, S., and Ogawa, T. (1998). Negative control of replication initiation by a novel chromosomal locus exhibiting exceptional affinity for Escherichia coli DnaA protein. Genes Dev *12*, 3032-3043.

128. Shen, X., Collier, J., Dill, D., Shapiro, L., Horowitz, M., and McAdams, H.H. (2008). Architecture and inherent robustness of a bacterial cell-cycle control system. Proceedings of the National Academy of Sciences of the United States of America *105*, 11340-11345.

129. Collier, J., McAdams, H.H., and Shapiro, L. (2007). A DNA methylation ratchet governs progression through a bacterial cell cycle. Proceedings of the National Academy of Sciences of the United States of America *104*, 17111-17116.

130. Collier, J., and Shapiro, L. (2009). Feedback control of DnaA-mediated replication initiation by replisome-associated HdaA protein in Caulobacter. Journal of bacteriology *191*, 5706-5716.

131. Bastedo, D.P., and Marczynski, G.T. (2009). CtrA response regulator binding to the Caulobacter chromosome replication origin is required during nutrient and antibiotic stress as well as during cell cycle progression. Molecular microbiology *72*, 139-154.

132. Robinett, C.C., Straight, A., Li, G., Willhelm, C., Sudlow, G., Murray, A., and Belmont, A.S. (1996). In vivo localization of DNA sequences and visualization of large-scale chromatin organization using lac operator/repressor recognition. J Cell Biol *135*, 1685-1700.

133. Lau, I.F., Filipe, S.R., Soballe, B., Okstad, O.A., Barre, F.X., and Sherratt, D.J. (2003). Spatial and temporal organization of replicating Escherichia coli chromosomes. Molecular microbiology *49*, 731-743.

Chapter 2

Dynamics of two phosphorelays controlling cell cycle progression in *Caulobacter crescentus*

This work was published as Y. Erin Chen, Christos G. Tsokos, Emanuele G. Biondi, Barrett S. Perchuk, and Michael T. Laub. 2009 J Bacteriol. Dec;191(24):7417-29.

Y.E.C. and M.T.L. designed the study, analyzed the data, and wrote the manuscript. Y.E.C. executed the experiments for all figures. C.T. and K.C.H. designed and performed the mathematical modeling. E.G.B. purified ChpT for antibody production. B.S.P. and C.G.T. assisted with strain construction. All authors discussed the results and commented on the manuscript.

Abstract

In *Caulobacter crescentus*, progression through the cell cycle is governed by the periodic activation and inactivation of the master regulator CtrA. Two phosphorelays, each initiating with the histidine kinase CckA, promote CtrA activation by driving its phosphorylation and by inactivating its proteolysis. Here, we examined whether the CckA phosphorelays also influence the down-regulation of CtrA. We demonstrate that CckA is bifunctional, capable of acting as either a kinase or phosphatase to drive the activation or inactivation, respectively, of CtrA. By identifying mutations that uncouple these two activities, we show that CckA's phosphatase activity is important for down-regulating CtrA prior to DNA replication initiation *in vivo*, but that other phosphatases may exist. Our results demonstrate that cell cycle transitions in *Caulobacter* require, and are likely driven by, the toggling of CckA between its kinase and phosphatase states. More generally, our results emphasize how the bifunctional nature of histidine kinases can help switch cells between mutually exclusive states.

Introduction

Caulobacter crescentus is a tractable model system for understanding the molecular mechanisms underlying cell cycle progression and the establishment of cellular asymmetry in bacteria. Each cell division for *Caulobacter* produces two morphologically different daughter cells, a swarmer cell and a stalked cell, which also differ in their ability to initiate DNA replication. A stalked cell can immediately initiate DNA replication following cell division, whereas a swarmer cell cannot initiate until after differentiating into a stalked cell. The swarmer-to-stalked cell transition thus coincides with a G1-S cell cycle transition. DNA replication occurs once-and-only-once per cell cycle, resulting in distinguishable G1, S, and G2 phases.

Progression through the *Caulobacter* cell cycle requires the precise temporal and spatial coordination of both morphological and cell cycle events. Previous genetic screens have uncovered numerous two-component signal transduction genes that help to regulate these events [1-8]. Two-component signaling pathways are typically comprised of a sensor histidine kinase that, upon activation, autophosphorylates and subsequently transfers its phosphoryl group to a cognate response regulator, which can then effect changes in cellular physiology [9]. One common variation of this signaling paradigm is called a phosphorelay [10]. Such pathways also initiate with the autophosphorylation of a histidine kinase and subsequent phosphotransfer to a response regulator, but these steps often occur intramolecularly within a hybrid histidine kinase. The phosphoryl group on the receiver domain of a hybrid kinase is then passed to a histidine phosphotransferase, which subsequently phosphorylates a soluble response regulator to effect an output response. Relative to canonical two-component pathways, phosphorelays provide

additional points of control and enable signal integration; they are often involved in regulating key cell fate decisions in processes such as sporulation, cell cycle transitions, and quorum sensing [10-12].

The master regulator of the *Caulobacter* cell cycle is CtrA, an essential response regulator that directly activates the expression of at least 70 genes [4, 13]. CtrA also regulates DNA replication by binding to and silencing the origin of replication [14]. Progression through the *Caulobacter* cell cycle thus requires the precise control of CtrA activity. CtrA must be abundant and active thoughout most of the cell cycle to drive gene expression and to silence the origin, but must be temporarily inactivated in stalked cells prior to S-phase to permit the initiation of DNA replication (also see Fig. 2.8).

CtrA is regulated on at least three levels: transcription, proteolysis, and phosphorylation [15, 16]. During G1, CtrA is phosphorylated and proteolytically stable. At the G1-S transition, CtrA is dephosphorylated and degraded, thereby freeing the origin of replication to fire. After DNA replication initiates, *ctrA* is transcribed and the newly synthesized CtrA is again phosphorylated and protected from proteolysis. Following septation of the predivisional cell, CtrA remains phosphorylated and stable in the swarmer cell, but is dephosphorylated and degraded in the stalked cell to permit DNA replication initiation. Cells that constitutively transcribe *ctrA* are viable and display only a mild phenotype indicating that regulated phosphorylation and proteolysis alone can ensure the periodicity of CtrA activity [16]. Cells producing nondegradable, constitutively-active CtrA arrest in G1 because CtrA activity cannot be eliminated [16].

The regulation of CtrA activity involves two phosphorelays. Each initiates with CckA, a hybrid histidine kinase, and ChpT, a histidine phosphotransferase. After receiving a phosphoryl group from CckA, ChpT can act as the phosphodonor for either CtrA or the single-domain response regulator CpdR [11]. Phosphorylation of CpdR prevents it from triggering CtrA proteolysis [11, 17]. Unphosphorylated CpdR triggers CtrA degradation, by somehow influencing the polar localization of the protease ClpXP [17], although why the protease must be localized is unclear.

The down-regulation of CtrA prior to DNA replication involves the dephosphorylation of CtrA and CpdR, such that CtrA is both dephosphorylated and, ultimately, degraded. These events coincide with the time in the cell cycle when CckA's kinase activity is lowest [18]. As the phosphoryl groups on CtrA~P and CpdR~P are relatively stable, at least *in vitro* [11], phosphatases are likely critical to eliminating CtrA activity prior to S-phase. For some phosphorelays, inactivation of the top-level kinase leads to a siphoning of phosphoryl groups from the terminal regulator back to the hybrid kinase's receiver domain. The bifunctional hybrid kinase then acts as a phosphatase, stimulating hydrolysis and loss of the phosphoryl group [12, 19]. For other phosphorelays there are separate and dedicated phosphatases [20-22].

Here, we demonstrate that CckA is bifunctional and can act as both a kinase and a phosphatase such that inactivation of CckA as a kinase stimulates the dephosphorylation of CtrA~P and CpdR~P. We provide evidence that CckA's phosphatase activity contributes to the down-regulation of CtrA *in vivo*, but that other phosphatases may exist. Our results indicate that the periodic toggling of CckA between kinase and phosphatase states is crucial to cell cycle progression in *Caulobacter*.

Results

CckA and ChpT are present throughout the cell cycle

CckA, unlike CtrA, is present throughout the cell cycle, but is only active at certain stages of the cell cycle [2, 18]. To test whether the abundance of ChpT is cell cycle-regulated and hence a possible means of controlling the timing of CtrA activity, we generated polyclonal antibodies for ChpT. Immunoblotting with crude sera revealed a single major band in wild-type lysates that was absent in lysates from a *chpT* depletion strain and that was the correct approximate size (Fig. 2.1). To examine the cell cycle abundance of ChpT, we synchronized a population of wild-type cells and isolated samples every 20 minutes. Immunoblotting of these samples demonstrated that ChpT was present throughout the cell cycle, in contrast to CtrA, which showed a characteristic cell cycle-dependence (Fig. 2.2). These results suggest that phosphate flux from CckA to CtrA is probably not regulated by changes in ChpT abundance.

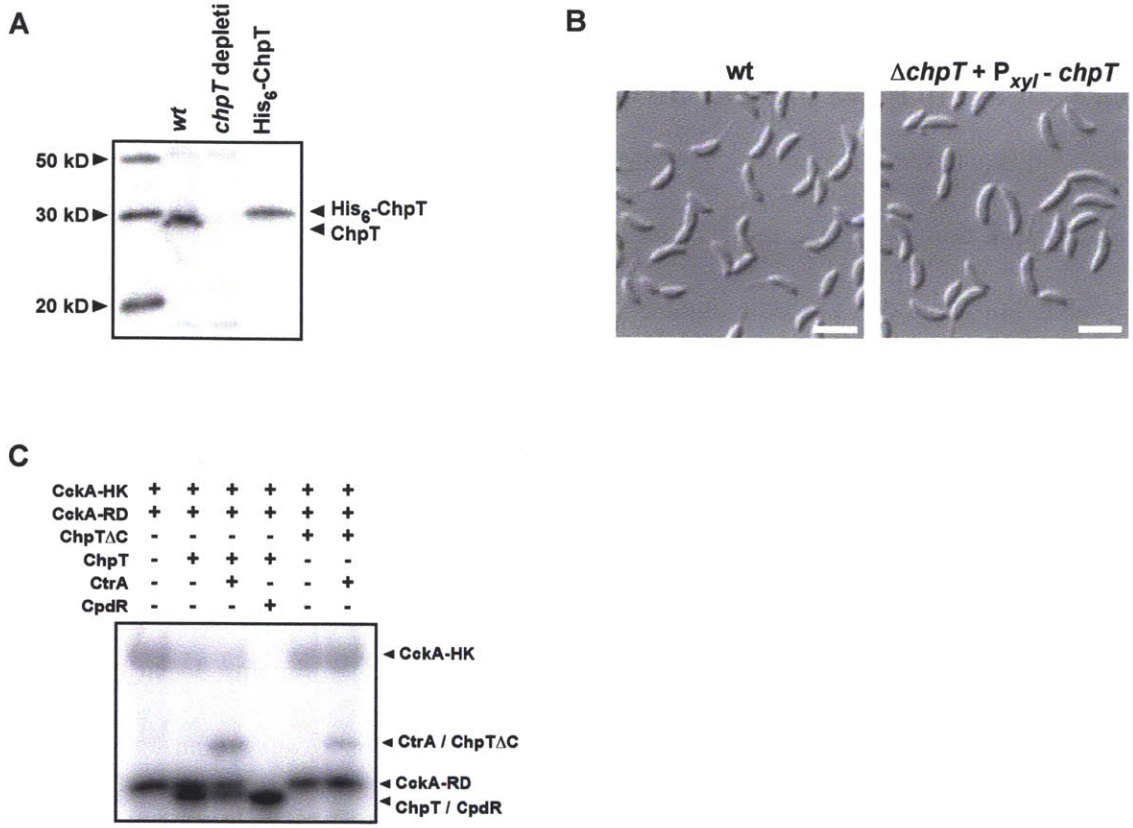

Figure 2.1. Analysis of ChpT protein size and cell cycle abundance. (A) Western blot of cell lysates from exponential phase cultures of wild type (CB15N) and the *chpT* depletion strain ML808 and of purified His_6-ChpT. (B) Cellular morphology of wild type and ML1054, a *chpT* deletion strain in which the shorter version of *chpT* (see text) is expressed from a medium-copy plasmid. (C) Phosphorelay reconstitutions using the purified components indicated by pluses and minuses. The components indicated were mixed together without ATP. Phosphotransfer reactions were started with the addition of ATP and then allowed to proceed for 30 minutes at 30 °C before being stopped. The position of each component is marked with an arrowhead on the right. CckA-HK contains a His_6-MBP tag, CtrA and ChpTDC contain thioredoxin-His6 tags, and CckA-RD, ChpT, and CpdR contain His_6 tags. ChpTDC is missing the last 126 amino acids, but retains the entire H-box region of the protein. Scale bar, 4 μm.

Figure 2.2. Cell cycle abundance of ChpT. Wild-type cells were synchronized and allowed to proceed through a single cell cycle with lysates collected every 20 minutes and used for immunoblotting with anti-CtrA or anti-ChpT serum. The cell cycle diagram above indicates the approximate cell cycle stage at each time point.

Our ChpT antiserum also recognized purified His_6-ChpT, although the molecular weight of this purified ChpT appeared slightly larger than that found in wild-type lysates (Fig. 2.1). This difference could not be accounted for by the epitope tag, suggesting that the translational start-site for *chpT* might have been erroneous in the original annotation of the *C. crescentus* genome [23]. The *chpT* open reading frame contains methionines at positions 19 and 29 (relative to the originally annotated protein), each of which could serve as the *bona fide* translational start site. Alignment of *chpT* orthologs from several α-proteobacteria indicated that the first 28 amino acids of *C. crescentus* ChpT were not conserved (Fig. 2.3). We were able to complement the lethality of a chromosomal deletion of *chpT* with a plasmid expressing a version of *chpT* lacking the first 28 codons of the original annotation (Fig. 2.1). This result strongly suggests that *C. crescentus chpT* encodes a protein of only 225 amino acids with a molecular weight of 23.4 kDa.

To verify that the smaller version of ChpT is capable of shuttling phosphate from CckA to CtrA and CpdR, we reconstituted the two cell cycle phosphorelays (CckA-ChpT-CtrA and CckA-ChpT-CpdR) using a purified version of the smaller ChpT, hereafter referred to simply as ChpT (Fig. 2.1). Indeed, this shorter version of ChpT was able to efficiently shuttle phosphate from the receiver domain of CckA to either CtrA or CpdR.

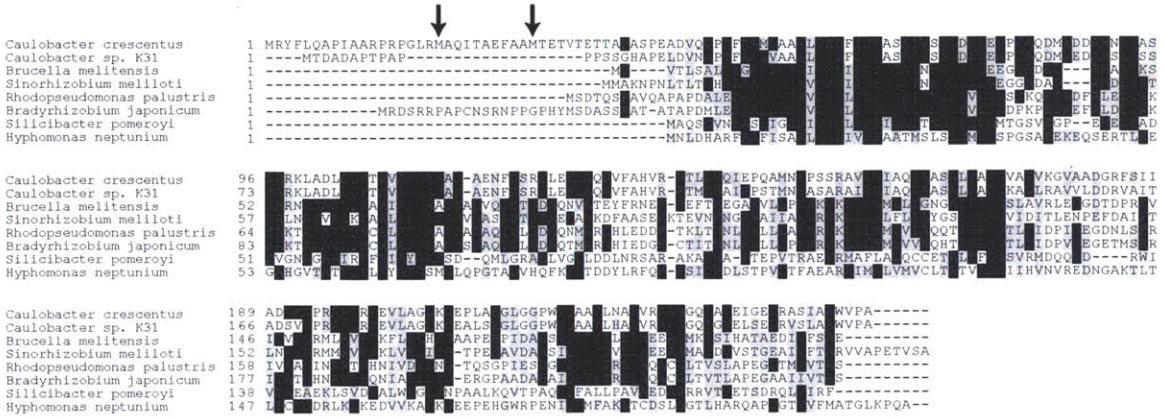

Figure 2.3. Multiple sequence alignment of ChpT orthologs. Orthologs of *C. crescentus* ChpT from seven α-proteobacterial species were aligned using ClustalW. Black and grey shading indicate high and medium levels of conservation, respectively. The arrows point to methionines that may act as the bona fide start site of *C. crescentus* ChpT.

Reconstitution of the CckA-based cell cycle phosphorelays

The reconstituted cell cycle phosphorelays shown in Figure 2.1 and those reported previously [11] involved a split version of CckA in which the histidine kinase (CckA-HK) and receiver domains (CckA-RD) were purified as separate polypeptides. Here, we wanted to examine the phosphotransfer behavior of a CckA construct containing both the kinase and receiver domains, as occurs *in vivo*. This construct, called CckA-HK-RD, lacking only the transmembrane domains, autophosphorylated and was an efficient phosphodonor for ChpT (Fig. 2.4A), which then transferred the phosphoryl group to

either CtrA or CpdR, as with the split version of CckA [11]. These data confirm that CckA initiates two phosphorelays, culminating in the phosphorylation of CtrA and CpdR.

Phosphorelays are often reversible, such that phosphoryl groups can flow either up or down the pathway according to the principles of mass-action equilibrium [12, 19, 24, 25]. In some cases, the histidine kinase involved can be bifunctional, acting to stimulate dephosphorylation of its cognate response regulator or, in the case of a hybrid kinase, its receiver domain. These bifunctional kinases can thus drive the rapid dephosphorylation of the terminal response regulator when they are not stimulated to autophosphorylate. To test whether CckA is bifunctional, we isolated radiolabeled, phosphorylated CtrA (CtrA~P) and CpdR (CpdR~P) by phosphorylating each regulator for extended periods of time with the heterologous kinases PhoR (a histidine kinase from *C. crescentus*) and EnvZ(T247R) (a histidine kinase from *E. coli* that does not harbor significant phosphatase activity), respectively. The phosphorylated response regulators were then purified away from unreacted, radiolabeled ATP. This purification step was not 100% efficient and each preparation of phosphorylated CtrA or CpdR retains some radiolabeled ATP that runs at a similar position as inorganic phosphate at the bottom of each gel in Fig. 2.4B-C.

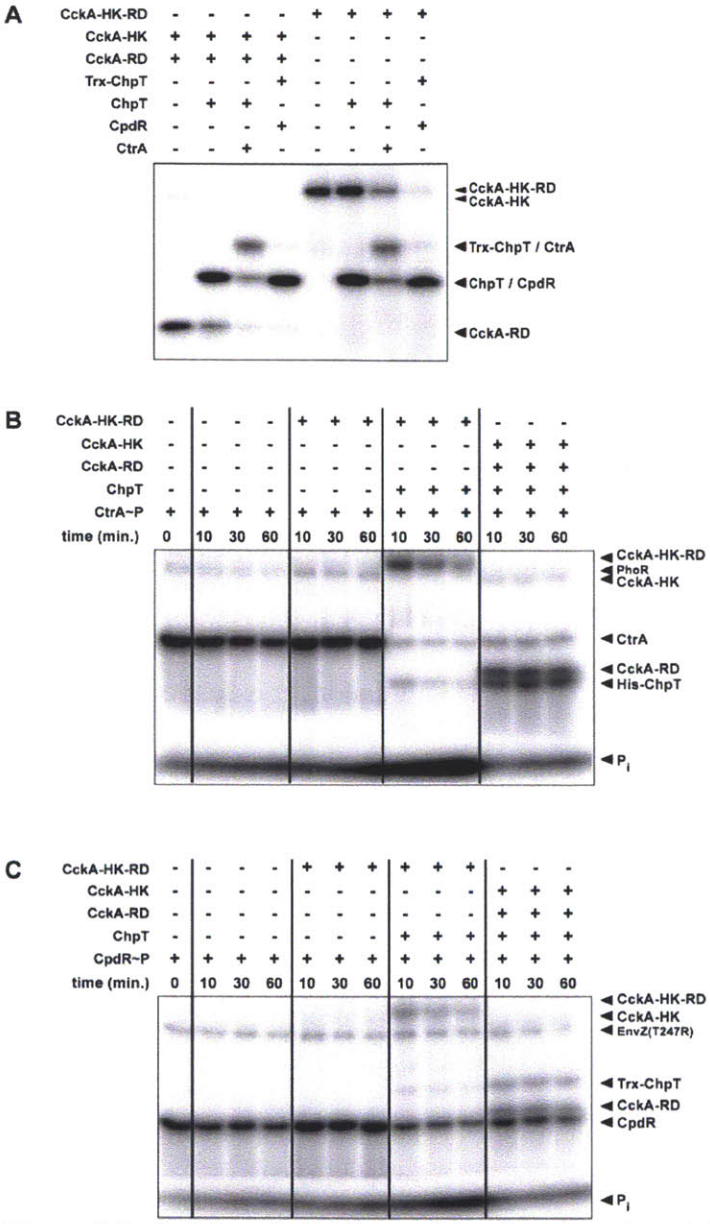

Figure 2.4. Full-length CckA can drive the phosphorylation and dephosphorylation of CtrA and CpdR. (A) Phosphorelay reconstitutions using the purified components indicated by pluses and minuses. The components indicated were mixed together without ATP. Phosphotransfer reactions were started with the addition of ATP and incubated for 30 minutes at 30 °C. The position of each phosphorylated component is marked with an arrowhead on the right. (B-C) Dephosphorylation of CtrA and CpdR. Purified CtrA~P (B) or CpdR~P (C) was incubated with the components indicated, but without ATP, to test for backtransfer and dephosphorylation to yield inorganic phosphate (Pi). Phosphatase reactions were started with the addition of CckA and, if indicated, ChpT. Each reaction was allowed to proceed for 0, 10, 30, or 60 minutes before being stopped. Note that the faint bands appearing in the first lane of panels (B) and (C) correspond to the components used to phosphorylate CtrA and CpdR (see Methods). In each panel, CckA-HK-RD and CckA-HK contain His_6-MBP tags, CckA-RD, Trx-ChpT, CpdR, and CtrA contain thioredoxin-His_6 tags, and ChpT contains a His_6 tag. Different tags for ChpT were used to optimize band separation.

Incubation of each regulator in buffer alone demonstrated that their aspartyl-phosphates are both relatively stable against autodephosphorylation *in vitro*, showing only a minor production of radiolabeled inorganic phosphate after 60 minutes; the band at the bottom of lanes 2-4 in Fig. 2.4B-C increases in intensity only marginally relative to lane 1. By contrast, incubation of CtrA~P with ChpT and CckA-HK-RD led to a significant depletion of radiolabel from CtrA~P within 10 minutes with nearly complete depletion in 60 minutes (Fig. 2.4B, lanes 8-10). The loss of radiolabel from CtrA~P also coincided with the appearance of radiolabeled inorganic phosphate, suggesting active dephosphorylation and not just partitioning of the phosphoryl groups among phosphorelay components. Incubation of CpdR~P with ChpT and CckA-HK-RD also led to a decrease in radiolabeled CpdR~P and an increase in inorganic phosphate (Fig. 2.4C, lanes 8-10), although not as much as with CtrA.

Notably, the dephosphorylation of CtrA and CpdR occurred at a much higher rate when the kinase and reciever domains of CckA were fused as a single polypeptide. Incubation of the radiolabeled response regulators with ChpT and the split version of CckA (CckA-HK and CckA-RD) did not lead to a significant production of inorganic phosphate (Fig. 2.4B-C, lanes 5-7). In these cases, phosphoryl groups did flow up the phoshorelay, as manifest by the appearance of radiolabeled ChpT and CckA-RD and the depletion of radiolabeled CtrA and CpdR. However, the levels of inorganic phosphate did not increase significantly indicating that CckA-RD must be tethered to CckA-HK for efficient dephosphorylation. Taken together, our data suggest that the cell cycle phosphorelays can run in reverse and that CckA is bifunctional such that it can stimulate the dephosphorylation of its own receiver domain. Together these two mechanisms,

phosphorelay reversal and the phosphatase activity of CckA on its own receiver domain, can indirectly drive the dephosphorylation of CtrA~P and CpdR~P.

Mutations that genetically separate kinase and phosphatase activities of CckA

To assess whether CckA and phosphorelay reversal contribute to the dephosphorylation of CtrA or CpdR *in vivo*, we sought to identify mutations in *cckA* that uncouple its kinase and phosphatase activities to yield CckA with kinase-only (K^+P^-) or phosphatase-only (K^-P^+) activity. To this end we generated ten mutant alleles of *cckA* based on mutations that render *E. coli* EnvZ either K^+P^- or K^-P^+ (Fig. 2.5A) [26-31]. We also made alanine mutations at the site of histidine autophosphorylation (H322) and at the site of aspartate phosphorylation in the receiver domain (D623), for a total of 12 mutations. We first introduced these mutations into our CckA-HK-RD construct and tested their abilities to autophosphorylate and phosphotransfer to ChpT *in vitro* (Fig. 2.5B). Four of the mutant kinases (harboring mutations G318T, G319E, and, V366P, and D623A) retained clear, detectable levels of autophosphorylation, and each construct could phosphotransfer to ChpT except for D623A. The mutations G318T and G319E each led to significantly higher levels of autophosphorylated CckA-HK-RD and higher levels of phosphorylated ChpT when compared to wild-type CckA-HK-RD. The V366P mutation, however, produced levels of CckA autophosphorylation and ChpT~P comparable to that seen with wild-type CckA-HK-RD.

Next, we tested whether any of the mutant kinase constructs that autophosphorylated could efficiently drive the dephosphorylation of CtrA~P via phosphorelay reversal and hydrolysis of phosphorylated CckA-RD (Fig. 2.5C). Each mutant construct that retained

kinase activity was added to ChpT and CtrA~P and then incubated for 30 minutes at 30°C. For the H322A, G318T, G319E, and V366P mutants, the radiolabeled phosphoryl groups flowed in reverse as seen by the appearance of radiolabeled bands corresponding to ChpT and CckA. For CckA(D623A) phosphoryl groups partitioned between CtrA and ChpT, but could not transfer back to CckA. CckA(D623A) lacks the aspartate phosphorylation site within the receiver domain and therefore cannot participate in phosphotransfer with ChpT. The dephosphorylation of CckA's receiver domain by its kinase domain was assessed by examining the production of inorganic phosphate and the coincident depletion of radiolabel from all other bands. The only mutant with phosphatase activity comparable to wild-type CckA was that harboring the substitution H322A.

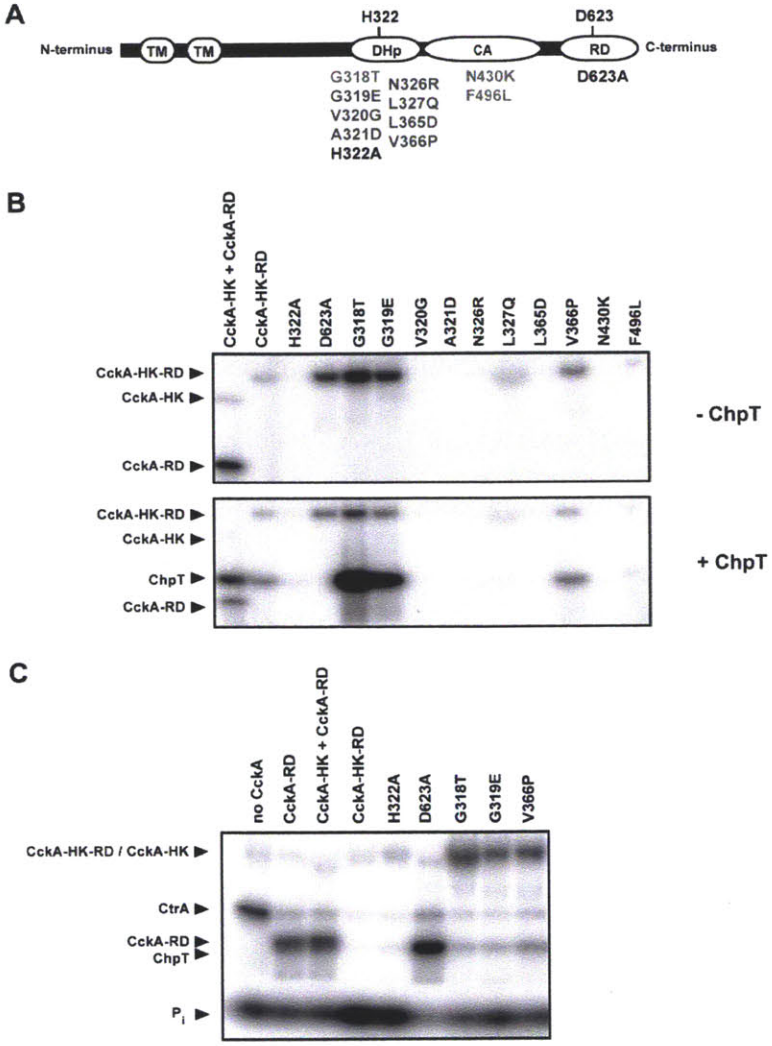

Figure 2.5. Identification of mutants that uncouple kinase and phosphatase activity in CckA. (A) Summary of CckA mutations tested. For mutations reported previously to produce K+P- (green) or K-P+ (blue) EnvZ, the same amino acid substitutions were introduced at the corresponding sites of CckA, based on an alignment of EnvZ and CckA sequences. Mutations are listed below the domain of CckA in which they were constructed. Domains include transmembrane (TM), dimerization and histidine phosphotransfer (DHp), catalytic and ATPase (CA), and receiver domain (RD). Phosphorylation sites (H322 and D623) are indicated above their respective locations. (B) Each mutant version of CckA-HK-RD was tested for autophosphorylation (top) and phosphotransfer to ChpT (bottom panel). Autophosphorylation reactions were started with the addition of ATP to preincubated mixtures of the indicated mutant CckA and reaction buffer. Reactions were incubated for 30 minutes at 30 °C. Phosphotransfer reactions were performed using autophosphorylated CckA. These reactions were started with the addition of ChpT and allowed to proceed for 30 minutes before being stopped. (C) Each mutant version of CckA-HK-RD was tested for dephosphorylation of CtrA~P. Purified CtrA~P was isolated and reactions were started with the addition of ChpT and mutant versions of CckA, and then allowed to proceed for 30 minutes at 30 °C. The positions of phosphorylated components in each panel are marked with arrowheads on the left.

These *in vitro* data indicate that the V366P mutation produces a version of CckA that retains kinase activity but lacks significant phosphatase activity (K^+P^-) while the H322A mutation produces a version lacking kinase but not phosphatase activity (K^-P^+). To better characterize these two mutants, we analyzed time courses of CtrA~P dephosphorylation (Fig. 2.6A-C). CckA-HK-RD and CckA-HK-RD(H322A) each showed a depletion of radiolabel from the phosphorelay components along with an increase in inorganic phosphate. By contrast, the constructs harboring D623A and V366P showed little to no depletion of phosphorelay components and no significant production of inorganic phosphate. These data support the characterization of V366P as a K^+P^- mutant of CckA with kinase activity comparable to wild-type CckA.

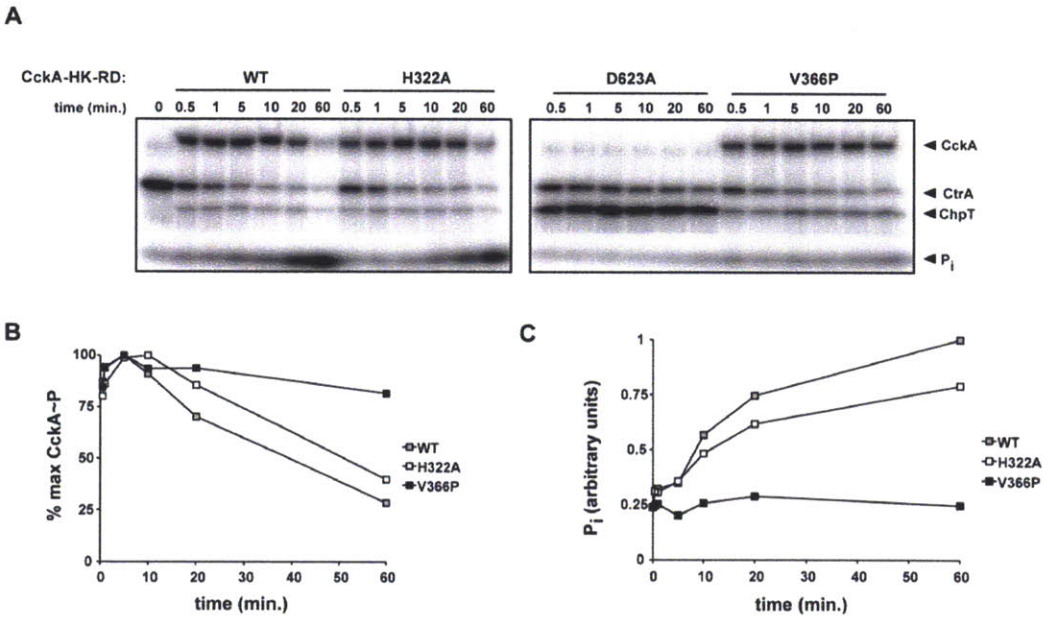

Figure 2.6. Biochemical characterization of CckA(V366P). (A) Time-course of CtrA dephosphorylation by CckA-HK-RD constructs. Point mutations are indicated above each time course. (B) Quantification of CckA-HK-RD band intensities in time-courses from panel A. The intensities for each construct were normalized to the percent maximum. (C) Quantification of inorganic phosphate band intensities in time-courses from panel A.

Phosphatase activity of CckA is important, but not essential, for dephosphorylation of CtrA and CpdR

To test whether the phosphatase activity of CckA is important for cell cycle progression and viability, we tested whether the mutant alleles of *cckA* we created could complement a *cckA* chromosomal deletion. For these experiments, we placed a full-length copy of each mutant allele of *cckA*, driven by the native *cckA* promoter, on the low-copy plasmid pMR20. Each plasmid was transformed into wild type, followed by transduction of a gentamicin-marked *cckA* deletion onto the chromosome. As expected, transduction of Δ*cckA* into a strain harboring the wild-type copy of *cckA* yielded thousands of colonies while transduction into a strain harboring an empty vector yielded none. Transduction of Δ*cckA* into a strain containing *cckA(D623A)* also produced no colonies, consistent with the notion that phosphorylation of the receiver domain is essential for viability. Unexpectedly, we recovered hundreds of colonies when transducing Δ*cckA* into a strain containing *cckA(H322A)*. However, sequencing of the plasmids in several of these colonies revealed that the mutation had reverted in each case, likely via recombination with the chromosomal copy of *cckA* prior to transduction. Reversion did not occur with the plasmid harboring *cckA(D623A)*, probably because the D623A mutation is toward the end of the *cckA* coding region and does not have sufficiently long regions of homology to efficiently drive recombination. Because we were unable to produce the CckA(H322A) + Δ*cckA* strain, we conclude that H322, like D623, is essential for CckA function.

As with H322A, transduction of Δ*cckA* into a strain expressing *cckA(G318T)* yielded abundant colonies, but plasmid sequencing from multiple colonies indicated reversion to wild-type CckA. *In vitro*, CckA(G318T) had shown significantly increased kinase

activity relative to wild-type CckA-HK-RD and no detectable phosphatase activity (see Fig. 2.5). The inability of *cckA(G318T)* to complement a *cckA* deletion suggests that an imbalance in CckA activities is lethal. We cannot, however, say whether the lethality results from a lack of phosphatase activity or excessive kinase activity, or both.

For the G319E and V366P mutants we successfully constructed and sequence-verified strains in which the chromosomal copy of *cckA* was deleted and the mutant allele of *cckA* was carried on a plasmid. The strain expressing *cckA(G319E)* grew more slowly than a strain expressing wild-type *cckA* and exhibited severe cellular filamentation (Fig. 2.7). These cells formed long, relatively straight filaments reminiscent of the morphology of a strain overproducing CtrA(D51E)Δ3Ω, a non-proteolyzable version of CtrA that mimics the phosphorylated state and induces a G1-arrest [16]. Indeed, the *cckA(G319E)* + Δ*cckA* strain showed a significant increase in cells with one chromosome (Fig. 2.7). Our *in vitro* studies showed that CckA(G319E) exhibits a substantial increase in autophosphorylation relative to wild-type CckA. Taken together, these data suggest that the G319E mutation renders CckA hyperactive as a kinase, resulting in constitutive phosphorylation of CtrA and CpdR and hence, a G1-arrest.

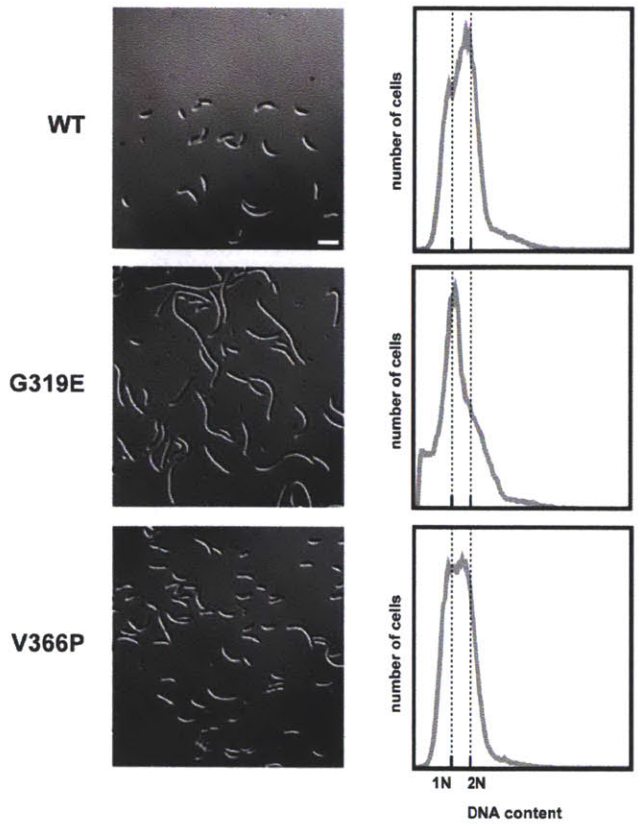

Figure 2.7. Complementation analysis of mutant alleles of *cckA*. Cellular morphology (left) and flow cytometry (right) analysis of strains in which the chromosomal copy of *cckA* was deleted and the *cckA* allele indicated on the far left was driven by the native cckA promoter on a low-copy plasmid. Scale bar, 4 μm.

The K^+P^- mutation V366P did not lead to a severe cell cycle phenotype (Fig. 2.7), suggesting that the phosphatase activity of CckA is either not strictly essential for viability or that V366P does not completely eliminate phosphatase activity *in vivo*. However, even if CckA phosphatase activity is not strictly essential, CckA could still be an important phosphatase *in vivo* for either CtrA or CpdR. To further test this possibility, we sought to examine whether the phenotype of a strain expressing *cckA(V366P)* as the only copy of *cckA* was exacerbated by the synthesis of CtrA(D51E) or CtrAΔ3Ω. For example, if CckA is a key phosphatase for CtrA, cells producing both CtrAΔ3Ω and a K^+P^- version of CckA may exhibit a G1-arrest phenotype, as with cells producing

CtrA(D51E)Δ3Ω. For these experiments, we transformed the pMR20-*cckA(V366P)* + Δ*cckA* strain with medium-copy plasmids carrying *ctrA*, *ctrA(D51E)*, *ctrAΔ3Ω*, or *ctrA(D51E)Δ3Ω* under the control of a xylose-inducible promoter. For comparison, we transformed the pMR20-*cckA* + Δ*cckA* strain with the same set of plasmids. Each strain was grown in the presence of xylose to mid-exponential phase and chromosome content measured by flow cytometry (Fig. 2.8). The strains synthesizing CtrA(D51E) or CtrAΔ3Ω each showed a small, but reproducible increase in G1-phased cells when combined with *cckA(V366P)* compared to *cckA*. No difference was seen between the strains synthesizing CtrA(D51E)Δ3Ω indicating that CckA(V366P) mediates its cell-cycle effect through the CckA-ChpT phosphorelays and not through other pathways. These data further suggest that CckA participates in the dephosphorylation of both CtrA~P and CpdR~P *in vivo*. However, the fact that CckA(V366P) does not yield a G1 arrest suggests that other phosphatases for CtrA and CpdR may exist. Or, as noted, the V366P mutation may be an imperfect K^+P^- allele that retains sufficient phosphatase activity *in vivo* to permit the dephosphorylation of CtrA~P and CpdR~P prior to DNA replication initiation.

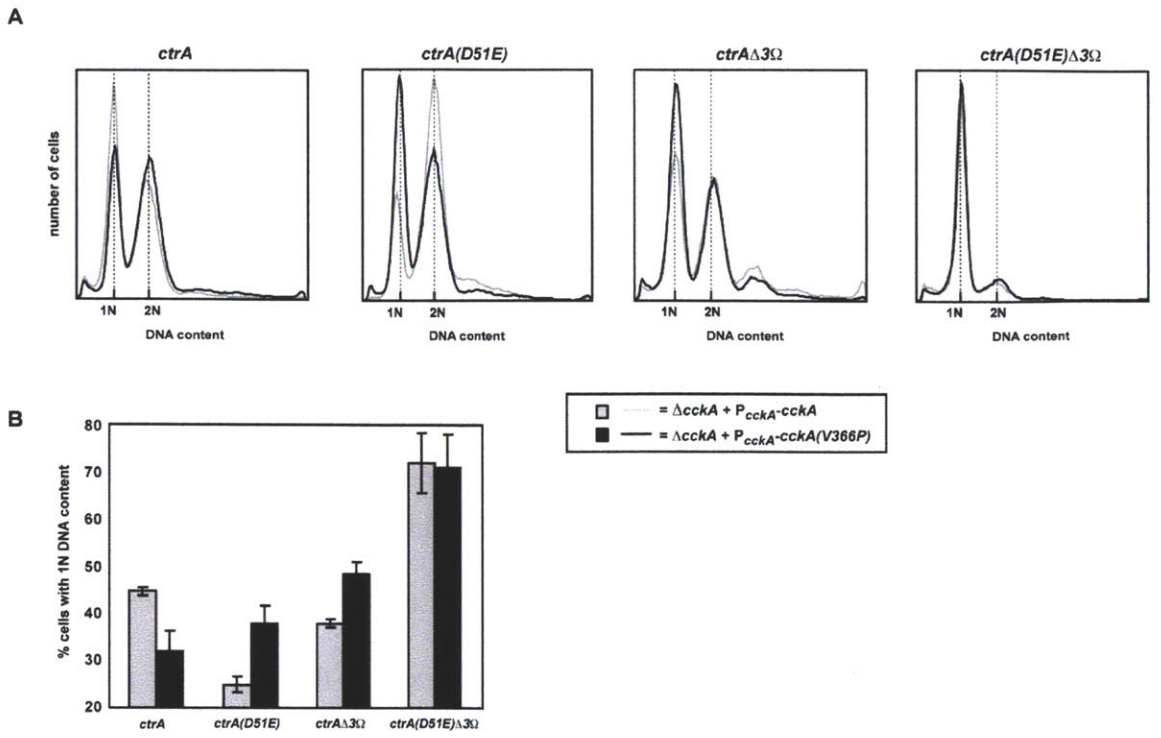

Figure 2.8. CckA contributes to, but is not essential for, the inactivation of CtrA and CpdR. Cells expressing various combinations of *cckA* and *ctrA* alleles were analyzed by flow cytometry to assess chromosomal content as a readout of CtrA activity. Each strain harbored a cckA chromosomal deletion and expressed either *cckA* (light grey) or *cckA(V366P)* (dark grey) from a low-copy plasmid using the native *cckA* promoter. Strains expressed the *ctrA* allele indicated above each panel from a medium-copy plasmid using the xylose-inducible promoter P_{xyl}. High levels of CtrA(D51E) partially mimics phosphorylated CtrA. CtrAΔ3Ω is a non-proteolyzable version of CtrA. All strains were grown in M2G to mid-exponential phase (OD600 ~ 0.2-0.4) in the presence of xylose for 8 hours, followed by the addition of rifampicin for 3 additional hours, and then analyzed by flow cytometry. (A) Representative flow cytometry profiles. (B) Quantification of the percentage of cells with one chromosome in the flow cytometry profiles. Error bars represent the standard error of the mean (n=3).

Overproducing CckA drives the dephosphorylation of CtrA~P and CpdR~P

To further test whether phosphorelay reversal and CckA phosphatase activity can drive the dephosphorylation of CtrA~P and CpdR~P *in vivo*, we examined the effect of overexpressing *cckA*. We hypothesized that overproducing CckA should siphon phosphoryl groups back through the phosphorelay driving the dephosphorylation of CtrA

and CpdR, leading to a decrease in CtrA activity. To test this prediction, we placed a full-length copy of *cckA* on the plasmid pJS14 under the control of a xylose-inducible promoter. After growth in xylose for 4 hours, this strain exhibited mild cellular filamentation and some accumulation of chromosomes, consistent with a downregulation of CtrA (Fig. 2.9A). Overproducing a version of CckA lacking its transmembrane domains, CckAΔTM, produced more severe filamentation and led to excessive accumulation of chromosomal DNA (Fig. 2.9A), consistent with an even more significant downregulation of CtrA. This cellular filamentation and accumulation of chromosomes depended on backtransfer to the CckA receiver domain as overproducing CckAΔTM(D623A) did not severely disrupt the cell cycle (Fig. 2.9A). However, backtransfer alone was insufficient and CtrA downregulation also depended on the phosphatase activity of CckA as overproducing the CckA receiver domain alone (CckA-RD) or a version of CckA lacking phosphatase activity, CckAΔTM(V366P), did not lead to cellular filamentation or chromosome accumulation (Fig. 2.9A).

The more severe phenotype of overproducing CckAΔTM relative to full-length CckA may indicate that CckA in the membrane can adopt either a kinase or phosphatase state while a cytoplasmic fragment functions primarily as a phosphatase. Consistent with this hypothesis, we found that overproducing a full-length version of CckA(H322A), which can only function as a phosphatase, produced a more severe phenotype than overproducing wild type full-length CckA (Fig. 2.9A); CckA(H322A) may also have a dominant negative effect by forming inactive heterodimers with the chromosomally-expressed CckA.

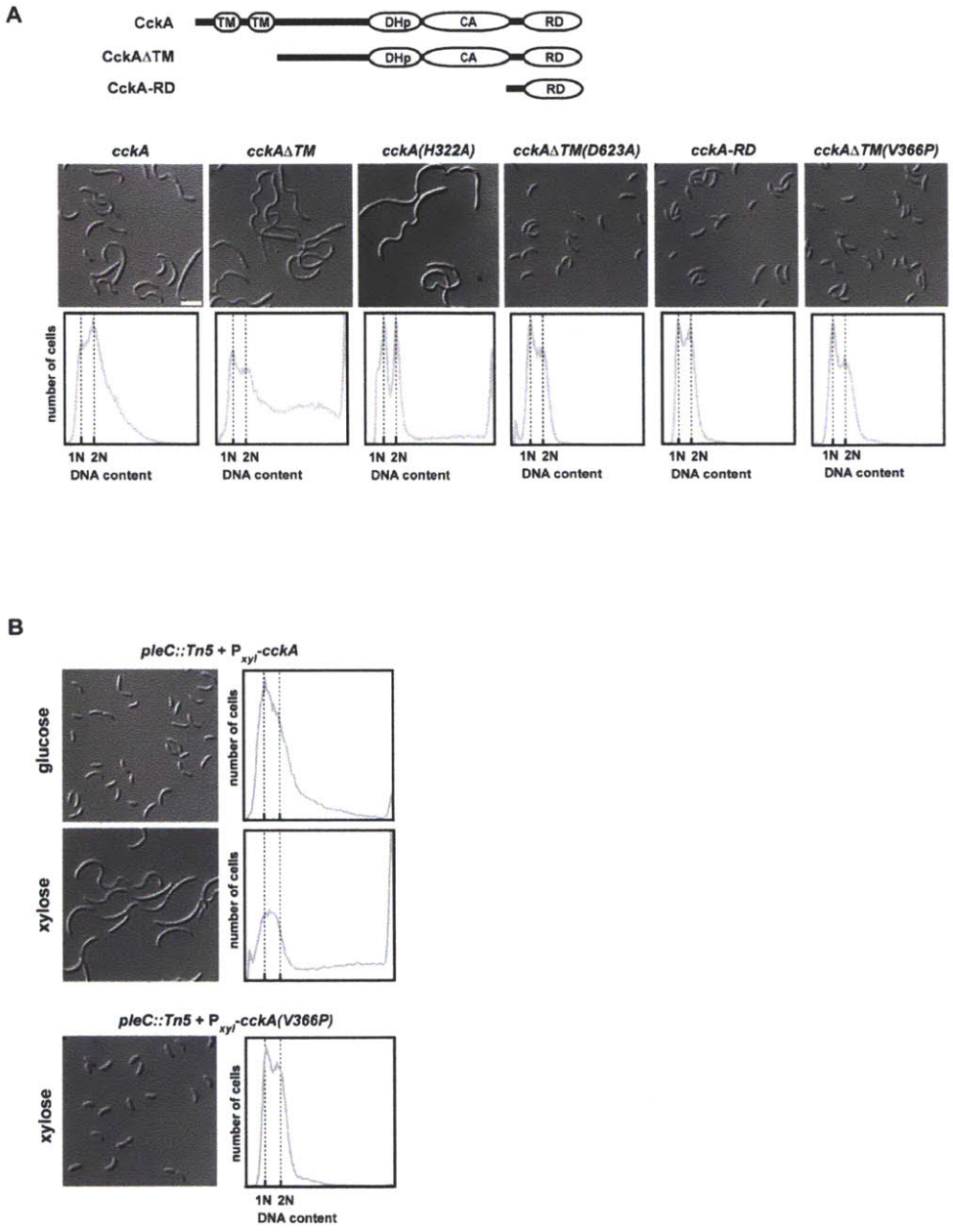

Figure 2.9. Overproducing CckA inactivates CtrA. (A) The effect of overproducing various CckA constructs was examined by light microscopy and flow cytometry. A diagram of the overexpression constructs used is shown at the top with abbreviations as in Fig. 2.5. Cells harbored the construct indicated above each pair of micrograph and flow cytometry profile. Each construct was expressed from a xylose-inducible promoter on a medium-copy plasmid. Cultures were grown to mid-exponential phase (OD600 ~ 0.2-0.4) in the presence of xylose for four hours and then fixed for microscopy and flow cytometry analysis. (B) Genetic interactions between *pleC* and *cckA*. Cells harbored a transposon insertion in *pleC* and carried a full-length copy of *cckA* or *cckA(V366P)* under the control of a xylose-inducible promoter. Note that in the flow cytometry profiles, the far right edge of the profile includes an integration of all cells that have chromosome accumulation beyond the range shown, if any. Scale bar, 4 μm.

Taken together, these data support a model in which the direction and flow of phosphoryl groups through the cell cycle phosphorelays *in vivo* is dictated by both mass-action equilibrium and the kinase/phosphatase balance of CckA. When CckA is stimulated to autophosphorylate, the net result is an accumulation of phosphoryl groups on CtrA and CpdR. Conversely, when CckA is not activated as an autokinase, phosphoryl groups can flow back to the CckA receiver domain where the kinase domain stimulates their hydrolysis.

As noted, overproducing a full-length version of CckA did not yield a severe cell cycle phenotype, in contrast to the case of overproducing CckAΔTM, indicating that full-length CckA may retain a balance of kinase and phosphatase activities. If so, the overexpression of full-length CckA should, in principle, be exacerbated by mutations in other genes that regulate the activity of CckA. Our previous studies indicated that the response regulator DivK is a negative regulator of CckA [11]. DivK phosphorylation is controlled by the reciprocal actions of a cognate histidine kinase, DivJ, and a cognate phosphatase, PleC [3, 6, 32]. We therefore tested the effect of overproducing full-length CckA in either a *divJ* or a *pleC* mutant background. While CckA overproduction did not have a strong effect in the *divJ* mutant (data not shown), it appeared to be strongly synthetic with the *pleC* mutant (Fig. 2.9B). CckA overproduction and the *pleC* mutation each yield a relatively mild phenotype on their own; however, the combination produced cells that were extremely filamentous and that accumulated multiple chromosomes, consistent with a significant drop in CtrA~P (Fig. 2.9B). This severe cell cycle phenotype was completely dependent on the phosphatase activity of CckA as overproducing full-length CckA(V366P) in a *pleC* mutant background had little to no effect on cells (Fig. 2.9B).

These results indicate that *cckA* likely lies genetically downstream of *pleC* and further support a model in which phosphorylated DivK downregulates CtrA by influencing the kinase/phosphatase balance of CckA.

Subcellular localization of CckA

In addition to changing from kinase to phosphatase during the cell cycle, CckA also dynamically changes its subcellular localization. CckA, which is present thoughout the cell cycle, was first reported to be polarly localized only in predivisional cells [2], with a second study indicating that CckA is also polarly localized in swarmer cells [11]. Here, to further characterize CckA's polar localization and identify the source of this difference we fused full-length *cckA* to *gfp* and integrated this construct on the chromosome as the only copy of *cckA*. The fusion used here includes the last two amino acids, both alanines, of CckA that had been removed in fusing *cckA* to *gfp* in both of the previous studies. By following a synchronous population of swarmer cells isolated from an exponential phase culture (Fig. 2.10), we found that CckA-GFP was delocalized in nearly all swarmer cells and remained delocalized upon differentiation into stalked cells. CckA-GFP then localized to the nascent swarmer pole in late stalked and early predivisional cells before localizing bipolarly in late predivisional cells. CckA-GFP was delocalized in daughter swarmer cells following cell division. In the daughter stalked cells the pattern was variable with CckA-GFP delocalized in some cells but retained at the stalked pole in most (>75%) cells, in contrast to both of the previous studies showing, at least in the small number of cells examined, that CckA-GFP is delocalized following cell division. Finally, we found that CckA-GFP localization in the initial synchronized population of swarmer cells was strongly dependent on the density of the culture used for synchronization. As

cells progressed through early exponential phase and into late exponential phase, an increasing percentage of swarmer cells showed polarly localized CckA (Fig. 2.11) indicating that the localization of CckA-GFP in swarmer cells is dependent on culture conditions but is not typically localized in early exponential phase. The overall pattern of subcellular localization observed here for CckA-GFP is in accord with that described by the Jacobs-Wagner group (personal communication). Also, we note that a similar pattern of CckA-GFP localization during synchronous cell cycle progression was seen with a strain expressing CckA-GFP from the low-copy plasmid pMR20 (data not shown). Whether the subcellular localization of CckA affects its activity as a kinase or phosphatase, or *vice versa*, is not yet clear and will likely require the identification of polar factors that directly influence CckA.

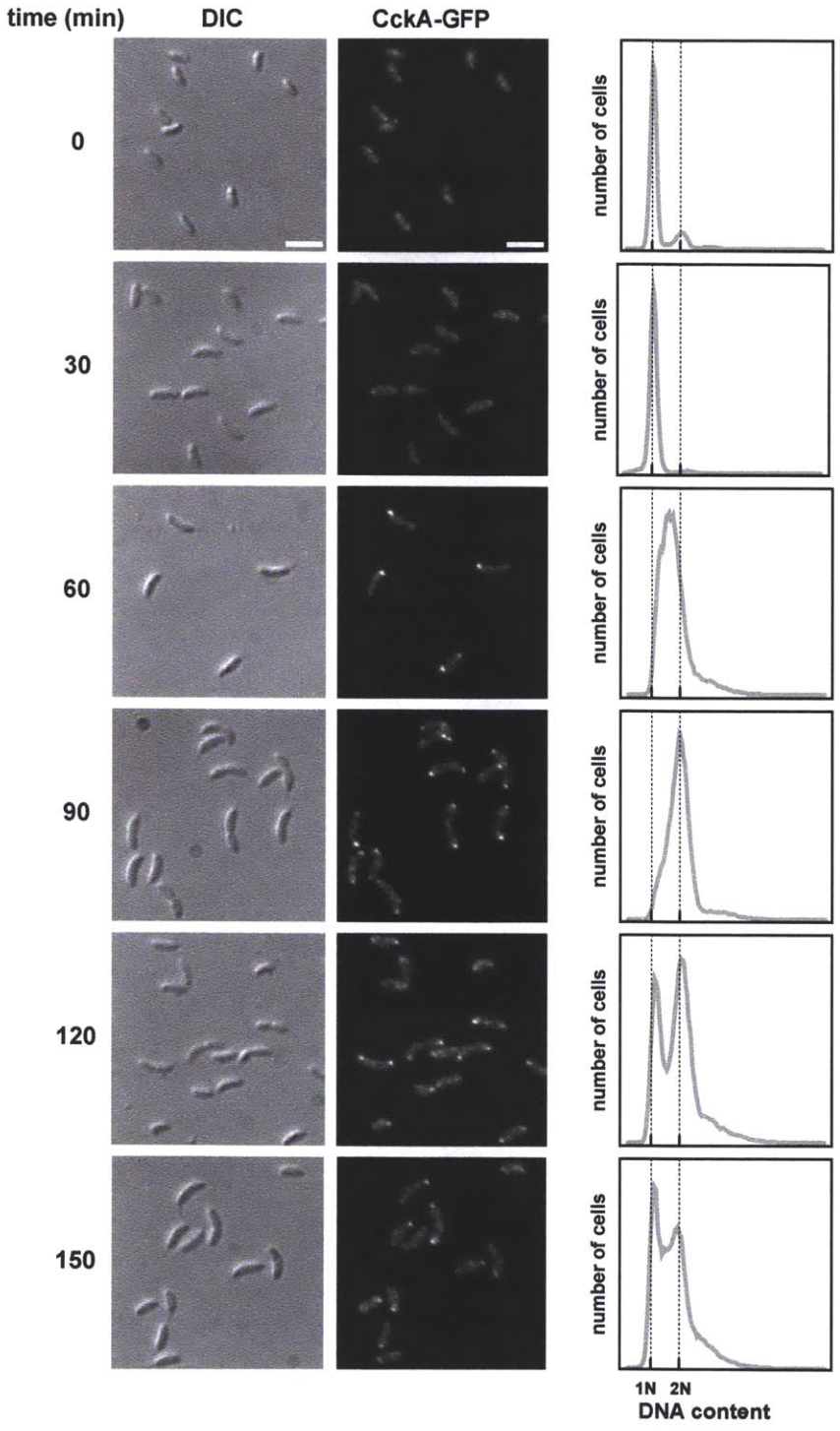

Figure 2.10. Figure S3. Subcellular localization of CckA. Swarmer cells from a culture of strain ML1681 grown to OD_{600} ~0.4 were synchronized and allowed to progress through the cell cycle. At the time points indicated, samples were taken for DIC (left) and epi-fluorescence (center) microscopy and for flow cytometry (right). Scale bar, 4 μm.

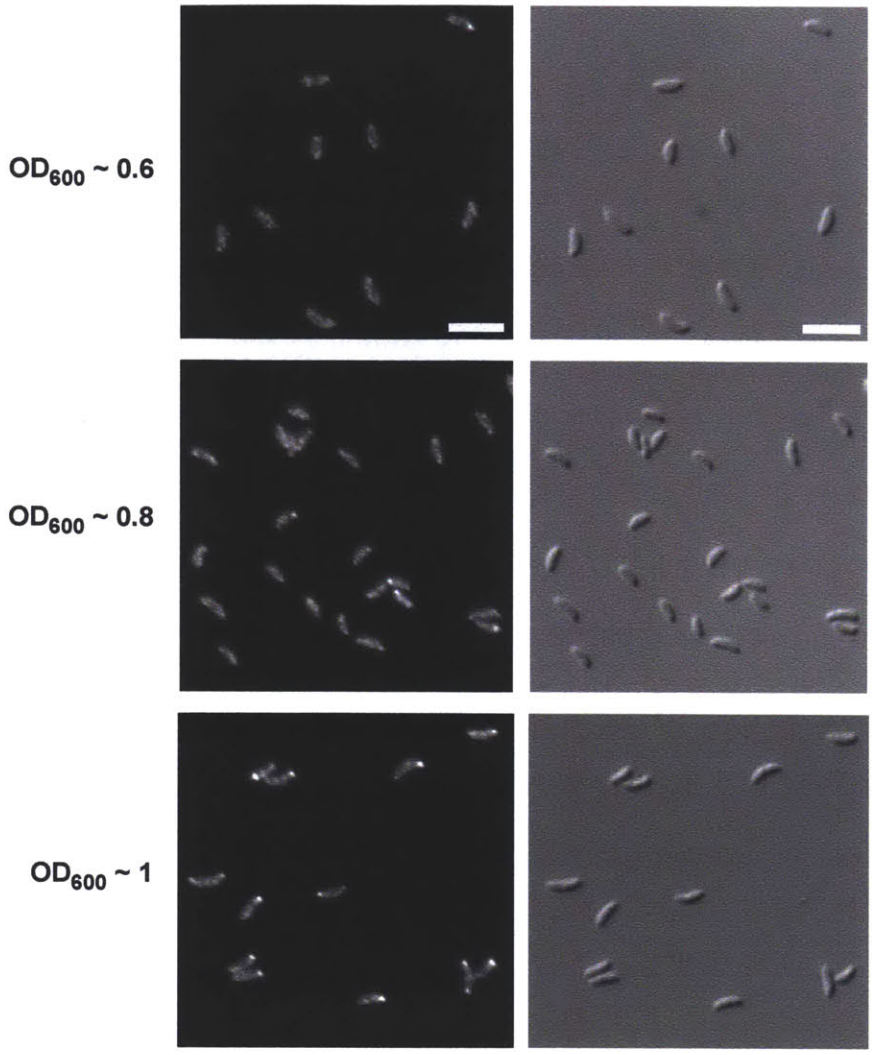

Figure 2.11. Culture density-dependence of CckA-GFP localization in swarmer cells. Increased polar localization of CckA in swarmer cells correlates with increasing cell density. Cells were grown in M2G, harvested at OD_{600} 0.6, 0.8, or 1.0, synchronized, and then released into fresh M2G at OD_{600} <0.2. Samples were taken for DIC (left) and epi-fluorescence (right) microscopy immediately after release into fresh M2G. Scale bar, 4 μm.

Discussion

The *Caulobacter* cell cycle is ultimately driven by the periodic rise and fall in activity of the master regulator CtrA (Fig. 2.12A). Our previous work identified two phosphorelays that collaborate to activate CtrA, by promoting its phosphorylation and proteolytic stabilization, the latter via CpdR phosphorylation. Conversely, the down-regulation of CtrA depends critically on the dephosphorylation of CtrA and CpdR, but the mechanisms involved have been unknown previously. Here, we demonstrated that CckA, when not active as a kinase, can stimulate the dephosphorylation of CtrA and CpdR to help drive the initiation of DNA replication. We showed that phosphoryl groups can be transferred from CtrA~P and CpdR~P back to the CckA receiver domain, via ChpT, where the bifunctional CckA can stimulate hydrolysis (Fig. 2.12B).

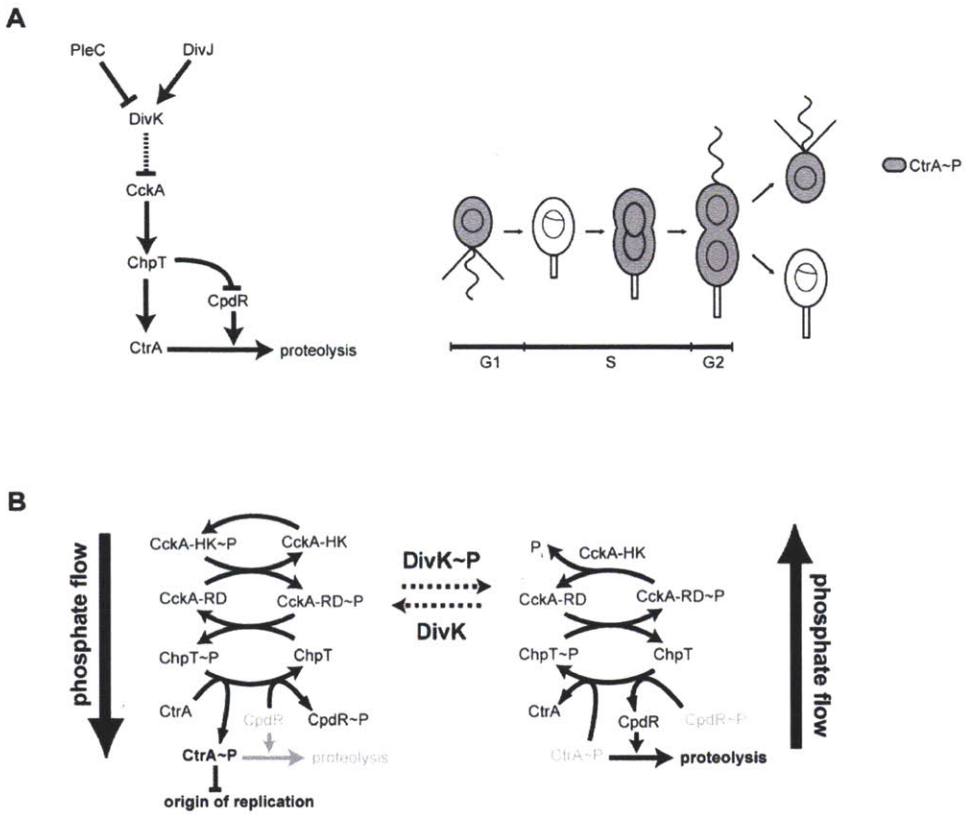

Figure 2.12. Regulation of the balance between CckA kinase and phosphatase activities controls cell cycle. (A) Summary of regulatory pathway controlling CtrA activity (left). Schematic of Caulobacter cell cycle indicating temporal pattern of CtrA activity (right). (B) Summary of cell cycle phosphorelays. Net phosphate flow depends on the activity of CckA. As a kinase, CckA drives the phosphorylation of CtrA and CpdR. As a phosphatase, CckA drives the dephosphorylation of CtrA and CpdR. Cell cycle transitions and changes in CtrA activity are thus driven by changes in the kinase/phosphatase balance of CckA. DivK influences CckA's switching between kinase and phosphatase states.

Like phosphorelays in other organisms [12, 19, 24, 25], the direction of flow through the cell cycle phosphorelays in *C. crescentus* appears to be dictated by mass-action. Hence, when CckA is not active as a kinase to drive CtrA and CpdR phosphorylation, the flow of phosphate can reverse. Overexpressing full-length *cckA*, however, resulted in a relatively minor cell cycle phenotype, likely because the CckA produced retains a balance of kinase and phosphatase activities. By contrast, overproducing a version of CckA lacking the transmembrane domains, CckAΔTM, led to a severe disruption of the cell cycle and

downregulation of CtrA activity as evidenced by chromosome accumulation. The more severe effect of overproducing CckAΔTM relative to full-length CckA may indicate that CckA must associate with other factors in the membrane to autophosphorylate. This downregulation requires both the reversed flow of phosphoryl groups and their active elimination by CckA phosphatase activity (Fig. 2.9A). The latter requirement is supported by the observation that overexpressing CckAΔTM(V366P) did not disrupt cell cycle progression. In wild type cells, CckA and ChpT are present at much lower levels (E.G.B, M.T.L, unpublished data) than CtrA, which is estimated to be present at ~20,000 molecules per cell [33]. Such stochiometries imply that redistribution alone could only ever deplete a small fraction of the phosphate on CtrA without CckA participating as a phosphatase.

Phosphorelay reversal and CckA phosphatase activity together constitute one mechanism for inactivating CtrA prior to S-phase. Using a K^+P^- mutant of CckA, V366P, we demonstrated that the phosphatase activity of CckA contributes to the down-regulation of CtrA and CpdR *in vivo*. However, cells producing CckA(V366P) are still viable and able to initiate DNA replication indicating that other phosphatases likely exist. If other phosphatases do exist, they may be difficult to identify owing to redundancy with CckA's phosphatase activity, either of which may be sufficient for survival. Moreover, aspartyl-phosphatases do not comprise a single, paralogous family and typically show little to no sequence homology with one another making their identification difficult [20-22, 34, 35]. Alternatively, no other phosphatases may exist if the phosphoryl groups on CtrA~P and CpdR~P are intrinsically labile, as with CheY and other response regulators [36-38]. However, our data suggest that the aspartyl-phosphates on CtrA and CpdR are relatively

stable (Fig. 2.4B-C) indicating that active dephosphorylation is probably necessary and tightly regulated. Finally, as noted earlier, CckA could be the only phosphatase if the V366P mutation does not completely eliminate phosphatase activity. Our *in vitro* studies did not indicate any significant phosphatase activity for CckA(V366P), but the *in vitro* conditions may not perfectly reflect *in vivo* conditions.

How does the V366P mutation produce a kinase-positive and phosphatase-negative version of CckA? Notably, valine-366 in CckA is predicted, based on alignment to EnvZ, to lie at the C-terminal end of α-helix-2 in the DHp domain near the linker that connects the DHp and CA domains. It is thus tempting to speculate that a proline at this position (V366P in CckA, which was based on the previously reported L288P in EnvZ [28]) may interfere with kinase/phosphatase balance by affecting domain-domain interactions. Recent structural studies of a full-length histidine kinase provided evidence that modulating DHp-CA domain interactions significantly influences the kinase/phosphatase balance of bifunctional histidine kinases [39]. It will be interesting to see whether mutations equivalent to V366P in CckA and L288P in EnvZ can produce K^+P^- versions of other bifunctional histidine kinases.

In sum our results indicate that CckA switches between a kinase state and a phosphatase state to help drive the changes in CtrA activity crucial for proper cell cycle progression. *In vivo* measurements of CckA phosphorylation indicated that CckA kinase activity is detectable in swarmer cells, drops to its lowest levels in stalked cells, and then accumulates again to maximal levels in predivisional cells [18]. CtrA and CpdR phosphorylation levels change in a similar fashion during the cell cycle [16-18],

consistent with a model in which changes in CckA's kinase activity are translated into changes in CtrA activity (Fig. 2.12A).

What then regulates CckA activity? The essential single-domain response regulator DivK plays a key role. A *divK*^{cs} mutant is unable to down-regulate CtrA and consequently arrests with a single chromosome [40], as seen with cells overproducing CtrA(D51E)Δ3Ω [16] or as seen here with cells overproducing CckA(G319E), a version of CckA with high kinase activity. While DivK could control CtrA phosphorylation and degradation independently, a simpler model is that DivK regulates CckA, either directly or indirectly switching CckA from the kinase to phosphatase state. Consistent with this model, CckA phosphorylation levels per cell were found to increase in a *divK*^{cs} mutant [11]. Although the increase was only four-fold, it should be noted that this measurement compared *divK*^{cs} to a mixed population of wild type which includes predivisional cells where CckA is most active. The *divK*^{cs} strain, however, is arrested at the G1-S transition when CckA kinase activity is normally at its lowest; in fact, the unabated activity of CckA as a kinase in the *divK*^{cs} strain may be responsible for its G1 arrest phenotype. We also found here that *cckA* overexpression exhibits a strong synthetic interaction with *pleC*, which encodes a key phosphatase of DivK. This synthetic interaction was dependent on CckA's ability to act as a phosphatase as overexpressing the phosphatase-deficient CckA(V366P) in a *pleC* mutant did not cause cellular filamentation or chromosomal accumulation (Fig. 2.9B). In a *pleC* mutant, DivK~P levels are elevated [32] and our results suggest that this increase may bias CckA toward the phosphatase state when overproduced, leading to the down-regulation of CtrA and a severe cell cycle phenotype (Fig. 2.9B). If DivK functioned independently of CckA to regulate CtrA, the

overexpression of *cckA* in a *pleC* background may have resulted in an additive, and consequently less severe, effect on the cell cycle.

DivK also affects CckA localization, with CckA-GFP present at the stalked pole but absent from the opposite pole in $divK^{cs}$ mutants [11]. However, this may be a secondary effect of DivK's effect on CckA activity and the consequent G1-arrest. Whether the localization of CckA influences its activity as a kinase or phosphatase, or *vice versa*, is not yet clear. CckA is most active as a kinase in predivisional cells when it is localized to the nascent swarmer pole and least active in stalked cells where it is either delocalized or only at the stalked pole. This may suggest that CckA receives an activation signal at the nascent swarmer pole or a repressing signal at the stalked pole. However, CckA also has moderate kinase activity in exponential phase swarmer cells when it is typically delocalized. A better understanding of the role of subcellular localization in modulating the kinase and phosphatase states of CckA will require the identification of factors that directly activate or repress CckA.

The model that DivK negatively regulates CckA is consistent with recent data suggesting that CpdR phosphorylation levels may increase after prolonged depletion of DivK [41]. This observation could indicate that DivK functions in a second pathway to specifically stimulate CpdR dephosphorylation. Alternatively, or perhaps in addition, the depletion of DivK may simply lead CckA to remain in a kinase rather than phosphatase state; this would lead to increased phosphorylation of CpdR (and CtrA) and ultimately the G1-arrest phenotype characteristic of *divK* loss-of-function mutants. Further, *divK* mutants can be rescued if *cpdR* is replaced by a mutant allele that cannot be phosphorylated [41], and *divK* lethality was previously shown to be suppressed by other mutations that diminish

CtrA activity [3]. We thus favor a model in which DivK helps switch CckA, either directly or indirectly, from acting predominantly as a kinase to predominantly as a phosphatase, and that an inability to switch (in either direction) is lethal (Fig. 2.12). The switch in CckA from kinase to phosphatase likely depends on the phosphorylation of DivK by DivJ, its cognate kinase. DivJ is preferentially inherited by stalked cells and accumulates in stalked cells following the swarmer-to-stalked transition [32], presumably helping to temporally restrict the down-regulation of CckA kinase activity and the dephosphorylation of CtrA to stalked cells.

In sum, our results emphasize the critical role played by CckA in controlling cell cycle oscillations and cellular asymmetry in *Caulobacter*. Although CtrA is also regulated transcriptionally, constitutive expression of *ctrA* does not significantly disrupt or delay cell cycle progression, indicating that proteolysis and phosphorylation are likely the dominant modes of regulation. CckA controls both of these processes. In turn, a complex network of regulatory molecules, including DivJ, PleC, and DivK, appear to regulate CckA activity, helping to toggle it between kinase and phosphatase states at the appropriate stages of the cell cycle.

Materials and Methods

Strain construction and growth conditions

E. coli and *C. crescentus* strains were grown as described previously [1]. Strains, plasmids, and primers used in this study are listed in Table 4.1. All plasmids were introduced into *C. crescentus* by electroporation. PCR amplification of genes and promoters from CB15N genomic DNA was done with previously described conditions [1]. For Gateway-based cloning, PCR amplicons of CB15N genes (primer sequences listed in Table 1) were first cloned into the pENTR/D-TOPO vector according to manufacturer's protocol and sequence-verified with M13F and M13R primers or primers within the gene. All site-directed mutagenesis was performed using the following PCR conditions: 75 ng pENTR clone, 50 μM each dNTP, 100 nM each primer, 1X Pfu Turbo buffer, 1.25 U Pfu Turbo polymerase (Strategene), 2% DMSO, and 60 mM Betaine. For each reaction, 17 cycles of the following sequence were run: 94°C for 1 min, 55°C for 1 min, and 68°C for 15 minutes when using pENTR clones or 68°C for 45 minutes when using other plasmids as templates. pENTR clones were then recombined into destination vectors following the manufacturer's protocols (Invitrogen, Carlsbad, CA).

To construct strain ML1054, *chpT* was amplified from the chromosome using primers alt_ChpT_fw and ChpT_rev to create pENTR:*chpT*. This pENTR clone was recombined into the destination vector pLXM-DEST and then transformed into a strain harboring a markerless deletion of *chpT* [11].

To construct strains ML1491-1499, a pENTR clone of the *cckA* gene (pENTR:P_{cckA}-*cckA*), including 158 bp upstream of the translational start that presumably encompasses the *cckA* promoter, was amplified from CB15N genomic DNA using the primers PcckA-

cckA-fw and PcckA-cckA-rev. This pENTR clone was recombined into the destination vector pMR20-DEST to produce a low-copy plasmid harboring a full-length copy of *cckA* under the control of its native promoter (pMR20-P_{cckA}-*cckA*). The plasmid pMR20-P_{cckA}-*cckA* was then transformed into CB15N followed by ΦCr30-based transduction of a gentamycin-marked *cckA* deletion from strain LS3382. To generate *cckA* point mutants, site-directed mutagenesis was performed on pENTR:P_{cckA}-*cckA* using primers listed in Table S1. These pENTR plasmids were sequence-verified and then recombined into the pMR20 destination vector prior to transformation and transduction of the marked *cckA* deletion.

Strains expressing mutant or wild-type *cckA* and overexpressing mutant *ctrA* (ML1567, ML1571, ML1572, ML1576, ML1578, ML1583, ML1585, ML1587) were made by transforming ML1491 and ML1497 with the following plasmids: pJS14, pJS14-P_{xyl}-*ctrA*, pJS14-P_{xyl}-*ctrA(D51E)*, pJS14-P_{xyl}-*ctrAΔ3Ω*, or pJS14-P_{xyl}-*ctrA(D51E)Δ3Ω* (Domian et al., 1997).

To construct strain ML1073, full-length *cckA* was amplified from CB15N genomic DNA with forward primer CckA_full_fw, which adds an NdeI site at the 5' end of the gene and reverse primer CckA_full_rev, which adds a SalI site at the 3' end. Both pML83 and the PCR product containing *cckA* were digested with NdeI and SalI and ligated to form plasmid pML83-P_{xyl}-*cckA*, which was then electroporated into a *pleC::Tn5* strain [32]. ML1709 was constructed similarly, but pML83-P_{xyl}-*cckA* was modified by site-directed mutagenesis PCR with primers V366P_fw and V366P_rev before being electroporated into the *pleC::Tn5* strain.

To construct a strain overexpressing full-length *cckA* (ML1688), we first made pENTR:P_{xyl}-*cckA* by using primers Pxyl_fw and CckA_full_rev to amplify a fragment containing a xylose-inducible promoter and *cckA* from the plasmid pML83:P_{xyl}-cckA . This pENTR clone was then recombined into the destination vector pJS14-DEST. To construct a strain overexpressing full-length *cckA(H322A)* (ML1738), we used primers H322A_fw and H322A_rev for site-directed mutagenesis on the plasmid pJS14:P_{xyl}-*cckA* from ML1688.

To construct strains overexpressing pieces of *cckA* containing no transmembrane domain (ML1689) or only the receiver domain (ML1692), we generated PCR products from CB15N genomic DNA using the following primers: HK7_fw and RR53_rev (ML1689) or RR53_fw and RR53_rev (ML1692). pENTR clones containing these PCR fragments were then recombined into pHXM2-DEST using the Gateway cloning method. To construct ML1690 and ML1691, we performed site-directed mutagenesis on pENTR:*cckA-HK-RD* with primers D623A_fw and D623A_rev (ML1690) or V366P_fw and V366P_rev (ML1691) before recombining into pHXM2 -DEST.

To construct strain ML1681, the last 519 codons (without the stop codon) of *cckA* were amplified by PCR with primers CckA_GFP_fw and CckA_GFP_rev. The reverse primer removed the stop codon, added two nucleotides to keep it in frame with the downstream GFP fusion, and contains an EcoRI site. The forward primer contains a KpnI site. The *cckA* PCR product was cloned in-frame with the *egfp* gene in pGFP-c4 [42] using KpnI and EcoRI restriction sites. The coding region was sequence verified and the plasmid was recombined into CB15N by electroporation to generate chromosomally encoded CckA-GFP.

To create pJS14-DEST and pMR20-DEST for Gateway cloning, the RfA Gateway cassette was blunt cloned into an EcoRV site in pJS14 and pMR20. To create pHXM2-DEST, the SacI-KpnI fragment containing a xylose-inducible promoter and M2 tag (P_{xyl}-M2) was digested out of pHXM-DEST and then cloned into pJS14.

Differential interference contrast microscopy was performed on mid-exponential phase cells after fixing in PBS with 0.5% paraformaldehyde.

Table 2.1 - Strains, Plasmids, Primers

Organism or Category	Name	Genotype, Plasmid description, or Primer Sequence	Source
C. crescentus	CB15N	synchronizable derivative of wild-type CB15	Evinger et al (1977)
	LS3382	ΔcckA + pMR10-cckA (gent^K, kan^K)	Jacobs et al (1999)
	ML808	Δ*chpT* + pLXM-*chpT-ssrA* (tet^K)	Biondi et al (2006)
	ML1054	Δ*chpT* + pLXM-*chpT* (tet^K)	this study
	ML1073	*pleC::Tn5* + pML83:P_{xyl}-*cckA* (spec^K)	this study
	ML1491	Δ*cckA*::gent + pMR20-P_{cckA}-*cckA* (tet^K,gent^K)	this study
	ML1492	Δ*cckA*::gent + pMR20-P_{cckA}-*cckA(H322A)* (tet^K,gent^K)	this study
	ML1494	Δ*cckA*::gent + pMR20-P_{cckA}-*cckA(G318T)* (tet^K,gent^K)	this study
	ML1495	Δ*cckA*::gent + pMR20-P_{cckA}-*cckA(G319E)* (tet^K,gent^K)	this study
	ML1496	Δ*cckA*::gent + pMR20-P_{cckA}-*cckA(L327Q)* (tet^K,gent^K)	this study
	ML1497	Δ*cckA*::gent + pMR20-P_{cckA}-*cckA(V366P)* (tet^K,gent^K)	this study
	ML1499	Δ*cckA*::gent + pMR20-P_{cckA}-*cckA(F496L)* (tet^K,gent^K)	this study
	ML1567	Δ*cckA*::gent + pMR20-P_{cckA}-*cckA* + pJS14-P_{xyl}-*ctrA* (gent^R,tet^R,chlor^R)	this study
	ML1571	Δ*cckA*::gent + pMR20-P_{cckA}-*cckA(V366P)* + pJS14-P_{xyl}-*ctrA* (gent^R,tet^R,chlor^R)	this study
	ML1572	Δ*cckA*::gent + pMR20-P_{cckA}-*cckA* + pJS14-P_{xyl}-*ctrA(D51E)* (gent^R,tet^R,chlor^R)	this study
	ML1576	Δ*cckA*::gent + pMR20-P_{cckA}-*cckA(V366P)* + pJS14-P_{xyl}-*ctrA(D51E)* (gent^R,tet^R,chlor^R)	this study
	ML1578	Δ*cckA*::gent + pMR20-P_{cckA}-*cckA* + pJS14-P_{xyl}-*ctrAΔ3Ω* (gent^R,tet^R,chlor^R)	this study
	ML1583	Δ*cckA*::gent + pMR20-P_{cckA}-*cckA(V366P)* + pJS14-P_{xyl}-*ctrAΔ3Ω* (gent^R,tet^R,chlor^R)	this study
	ML1585	Δ*cckA*::gent + pMR20-P_{cckA}-*cckA* + pJS14-P_{xyl}-*ctrA(D51E)Δ3Ω* (gent^R,tet^R,chlor^R)	this study
	ML1587	Δ*cckA*::gent + pMR20-P_{cckA}-*cckA(V366P)* + pJS14-P_{xyl}-*ctrA(D51E)Δ3Ω* (gent^R,tet^R,chlor^R)	this study
	ML1681	P_{cckA}-*cckA-GFP* (gent^R)	this study
	ML1688	pJS14:P_{xyl}-*cckA* (chlor^R)	this study
	ML1689	pHXM2-*cckAΔTM* (chlor^K)	this study
	ML1690	pHXM2-*cckAΔTM(V366P)* (chlor^K)	this study
	ML1691	pHXM2-*cckAΔTM(D623A)* (chlor^K)	this study
	ML1692	pHXM2-*cckA-RD* (chlor^R)	this study
	ML1708	Δ*cckA*::gent + pMR20-P_{cckA}-*cckA-GFP* (gent^K,tet^K)	this study
	ML1709	*pleC::Tn5* + pML83:P_{xyl}-*cckA(V366P)* (spec^R)	this study
	ML1738	pJS14:P_{xyl}-*cckA(H322A)* (chlor^K)	this study
E. coli	DH5a	general cloning strain	Invitrogen
	BL21-Tuner	strain for protein expression and purification	Novagen
	TOP10	strain for constructing pENTR-TOPO clones	Invitrogen
General purpose vectors	pJS14	derivative of pBBR1MCS, high-copy replicon (chlor^R)	J. Skerker

Organism or Category	Name	Genotype, Plasmid description, or Primer Sequence	Source
	pJS71	derivative of pBBR1MCS, high-copy replicon (spec^R)	J. Skerker
	pML83	P_{xyl} oriented against Plac, inserted into EcoRI site of pJS71 (chlor^R)	M. Laub
	pMR10	broad host range, low copy vector (kan^R)	R. Roberts
	pMR20	broad host range, low copy vector (tet^R)	R. Roberts
	pENTR/D-TOPO	ENTRY vector for Gateway cloning system (kan^R)	Invitrogen
Overexpression plasmids	pJS14:P_{xyl}-*ctrA*	high-copy plasmid, xylose-inducible expression of *ctrA*	Domian et al (1997)
	pJS14:P_{xyl}-*ctrA(D51E)*	high-copy plasmid, xylose-inducible expression of *ctrA(D51E)*	Domian et al (1997)
	pJS14:P_{xyl}-*ctrAΔ3Ω*	high-copy plasmid, xylose-inducible expression of *ctrAΔ3Ω*	Domian et al (1997)
	pJS14:P_{xyl}-*ctrA(D51E)Δ3Ω*	high-copy plasmid, xylose-inducible expression of *ctrA(D51E)Δ3Ω*	Domian et al (1997)
	pML83:P_{xyl}-*cckA*	high-copy plasmid, xylose-inducible expression of full-length, untagged *cckA*	this study
	pJS14:P_{xyl}-*cckA*	high-copy plasmid, xylose-inducible expression of *cckA*	this study
Expression plasmid	pMR20:P_{cckA}-*cckA*	full-length *cckA* driven by its own promoter and expressed off pMR20	this study
ENTRY clones	pENTR:*chpT*	entry clone of *chpT* lacking the first 28 codons of the annotated CC3470 gene	this study
	pENTR:*chpTΔC*	entry clone of *chpT* lacking the last 126 codons of the annotated CC3470 gene	this study
	pENTR:P_{cckA}-*cckA*	entry clone of *cckA* and 158 bp upstream of the translational start site	this study
	pENTR:P_{xyl}-*cckA*	entry clone of full-length *cckA* behind the xylose promoter	this study
	pENTR:*cckA-HK-RD*	entry clone of *cckA* containing only the kinase and receiver domains	this study
	pENTR:*cckA-HK-RD(D623A)*	entry clone of *cckA* containing only the kinase and receiver domains with D623A mutation	Biondi et al (2006)
	pENTR:*cckA-RD*	entry clone of *cckA* containing only the receiver domain	Skerker et al (2005)
	pENTR:*ctrA*	entry clone of *ctrA*	Skerker et al (2005)
	pENTR:*cpdR*	entry clone of *cpdR*	Skerker et al (2005)
	pENTR:*phoR*	entry clone of *phoR* containing the last 415 codons of the annotated CC0289 gene	this study
	pENTR:*envZ*	entry clone of *envZ* containing the last 229 codons of the annotated b3404 gene	Skerker et al (2005)
	pENTR:*envZ(T247R)*	entry clone of the last 229 codons of *envZ* with a T247R mutation	this study
Destination vectors	pHIS-DEST	for producing His_6-tagged proteins	Skerker et al (2005)
	pTRX-HIS-DEST	for producing thioredoxin-His_6-tagged proteins	Skerker et al (2005)
	pHIS-MBP-DEST	for producing His_6-MBP-tagged proteins	Skerker et al (2005)
	pHXM-DEST	pJS71:P_{xyl}-M2 destination vector (spec^R, chlor^R)	Skerker et al (2005)
	pLXM-DEST	pMR20:P_{xyl}-M2 destination vector (tet^R, chlor^R)	Skerker et al (2005)
	pMR20-DEST	pMR20 destination vector (tet^R, chlor^R)	this study
	pJS14-DEST	pJS14 destination vector (chlor^R)	this study
	pHXM2-DEST	pJS14:P_{xyl}-M2 destination vector (chlor^R)	this study
Primers	PcckA-cckA-fw	CACCTCATCAGCTTCATCCTCAACGG	
	PcckA-cckA-rev	CAGCAGAAGCTTCTACGCCGCCTGCAGCTGCT	
	CckA_full_fw	GGCATATGGCCGACTTGCAGCTCCA	
	CckA_full_rev	GGGTCGACCTACGCCGCCTGCAGCTGCT	
	HK7_fw	CACCTCAGCGCTTTCCGGCGGCGA	
	HK9_rev	TCAGATGCGGCCGGCGCCCGACA	
	RR53_fw	CACCTGCCGCATCCTGTTCGTCGAGG	
	RR53_rev	CTACGCCGCCTGCAGCTGC	
	CC3470_HPT_for	CACCTTGCGTTATTTTCTCCAAG	
	ChpT_Hbox_rev	CAGCTTTTCCAGTTCGCGCGAG	
	CckA_GFP_fw	CAGCAGCAGGGTACCGCAGAGCGACGGCTGGAT	
	CckA_GFP_rev	CAGCAGCAGGAATTCTCCGCCGCCTGCAGCTGCTG	
	V366P_fw	CGCCGCCGACCTCCCGCGCAAGCTCTTG	
	V366P_rev	CAAGAGCTTGCGCGGGAGGTCGGCGGCG	

Organism or Category	Name	Genotype, Plasmid description, or Primer Sequence	Source
	A321D_fw	GGCCGGCGGCGTCGATCACGACTTCAACAAC	
	A321D_rev	GTTGTTGAAGTCGTGATCGACGCCGCCGGCC	
	V320G_fw	GCCGGCGGCGGCGCGCACGAC	
	V320G_rev	GTCGTGCGCGCCGCCGCCGGC	
	L327Q_fw	CACGACTTCAACAACCAGTTGACCGCCATCCAGC	
	L327Q_rev	GCTGGATGGCGGTCAACTGGTTGTTGAAGTCGTG	
	R361P_fw	ACGGGCGTGCCCGCCGCCGAC	
	R361P_rev	CGCGCCGCCGACGACGTGCGCAAGCT	
	N326R_fw	GCGCACGACTTCAACAGGCTCTTGACCGCCATCC	
	N326R_rev	GGATGGCGGTCAAGAGCCTGTTGAAGTCGTGCGC	
	F496L_fw	AGATCTTCGACCCGTTATTCACCACCAAGCCG	
	F496L_rev	CGGCTTGGTGGTGAATAACGGGTCGAAGATCT	
	G318T_fw	GCCAGCTGGCCACCGGCGTCGCGC	
	G318T_rev	GCGCGACGCCGGTGGCCAGCTGGC	
	G319E_fw	AGCTGGCCGGCGAGGTCGCGCACGAC	
	G319E_rev	GTCGTGCGCGACCTCGCCGGCCAGCT	
	N430K_fw	AGACGGCGGTCATGAAGCTGGCCGTC	
	N430K_rev	GACGGCCAGCTTCATGACCGCCGTCT	
	L365D_fw	CGCGCCGCCGACGACGTGCGCAAGCT	
	L365D_rev	AGCTTGCGCACGTCGTCGGCGGCGCG	
	D623A_fw	CCTCTTGATCAGCGCGGTGATCATGCCCG	
	D623A_rev	CGGGCATGATCACCGCGCTGATCAAGAGG	
	H322A_fw	CGGCGGCGTCGCGGCGGACTTCAACAACC	
	H322A_rev	GGTTGTTGAAGTCCGCCGCGACGCCGCCG	
	phoR_fw	CACCCTGAACCGGCGAAAGGCCGT	
	phoR_rev	TCAGGCGCTTCCCGCTTCCGCC	
	EnvZ_T247R_fw	AGTCACGACTTGCGCCGTCCGCTGACGCGTATT	
	EnvZ_T247R_rev	AATACGCGTCAGCGGACGGCGCAAGTCGTGACT	
	Pxyl_fw	CACCTCGAACAGGGCCGTCAGG	
	alt_ChpT_fw	caccTTGACCGAGACCGTCACC	
	ChpT_rev	GGTTAAGGAGCGGTTTGCTA	

Immunoblotting and synchronization

Mixed populations of wild-type cells grown in M2G were synchronized using Percoll density centrifugation as previously described [43]. Cell samples were taken every 20 minutes for 140 minutes, resolved on a 12% SDS polyacrylamide gel, transferred to PVDF transfer membrane (Pierce), and probed with anti-ChpT serum at a 1:10,000 dilution. Polyclonal rabbit antisera (Covance) was generated using His_6-ChpT.

Flow cytometry

Single colonies were inoculated into 5-10 mL liquid cultures from plates and grown overnight at 30°C under appropriate antibiotic selection, but were always maintained at

an OD_{600} less than 0.7. Cultures were then diluted to an OD_{600} of 0.005-0.01 and grown to OD_{600} ~ 0.2-0.4 before processing. All strains were grown in PYE except for strains overexpressing *ctrA* alleles (Fig. 2.8), which were grown in M2G. Strains overexpressing *cckA* or *ctrA* were induced by the addition of 0.3% xylose to culture media, or maintained in 0.2% glucose and processed after 4 or 8 hours. After 8 hours of induction, rifampicin (20 μg/ml) was added to strains overexpressing *ctrA*, which were grown for 3 more hours to allow for completion of DNA replication. Cells were fixed in 70% EtOH overnight at 4°C and stored at 4°C for up to a week. They were spun at 6000 rpm for 4 minutes, resuspended in 1 ml 50 mM sodium citrate, and incubated for 4 hours at 50°C with 2 ug/ml RNAse to allow complete RNA digestion. After digestion, cells were incubated in 2.5 μM SYTOX Green nucleic acid stain (Invitrogen) for 15 minutes at room temperature before analyzing by flow cytometry using an Epics C analyzer (Beckman-Coulter). For quantification of flow cytometry data in Figure 6, we gated 1N DNA content peaks, using the same gate for all samples. The percentages shown in the bar graph were obtained by dividing the gated number cells with 1N DNA content by the total number of cells, which were gated to exclude cellular debris on the far left of the flow cytometry profiles.

In vitro analysis of kinase, phosphatase, and phosphotransfer reactions

All protein purifications were done as reported previously [1]. Primers CC3470_HPT_for and ChpT_Hbox_rev were used to amplify the H-box-containing N-terminus of ChpT for constructing the plasmid pENTR:*chpTΔC*. Primers phoR_fw and phoR_rev were used to amplify the last 415 amino acids of PhoR (CC0289) for constructing the plasmid pENTR:*phoR*. Primers EnvZ_T247R_fw and EnvZ_T247R_rev were used for site-directed mutagenesis on the plasmid pENTR:*envZ* to create the

plasmid pENTR:*envZ(T247R)*. Creation of other pENTR clones for protein purification has been described previously [1].

Phosphatase reactions: First, 10 μM TRX-His_6-CtrA was incubated with 0.2 μM PhoR with 5 μC_i [γ^{32}P]ATP (~6000 Ci/mmol, Amersham Biosciences) in storage buffer supplemented with 2 mM DTT and 5 mM $MgCl_2$. Reactions were incubated at 30°C for 60 minutes and then depleted of any remaining ATP by the addition of 1.5 U hexokinase (Roche) and 5 mM D-glucose for 5 minutes at room temperature. Reactions were then washed in 10 kD Nanosep columns four times with 10X reaction volumes of HKEDG buffer (10 mM HEPES-KOH pH 8.0, 50 mM KCL, 10% glycerol, 0.1 mM EDTA, 1 mM DTT (added fresh)) with a final resuspension in the original reaction volume of HKEDG buffer. A similar procedure was used to prepare CpdR~P except that EnvZ(T247R) was used instead of PhoR. These preparations of CtrA~P or CpdR~P were then incubated with upstream components, as indicated in figure panels, each at a final concentration of 5 μM. Phosphatase reactions were supplemented with 5 mM $MgCl_2$ and incubated at 30°C before being stopped at indicated timepoints by the addition of 3.5 μL 4X sample buffer (500 mM Tris [pH 6.8], 8% SDS, 40% glycerol, 400 mM beta-mercaptoethanol). Samples were heated at 30°C for 2 minutes before loading onto 10% Tris-HCl gels (Bio-Rad) with electrophoresis at room temperature for 40 minutes at 150 V. Gels were exposed to phosphor screens overnight at -80°C and then scanned using a Storm 86 imaging system (Amersham Biosciences).

Autophosphorylation reactions: Histidine kinase constructs at 5 μM were incubated with 0.5 μM ATP and 5 μC_i [γ^{32}P]ATP in HKEDG buffer supplemented with 5 mM $MgCl_2$ at

30°C for 60 minutes. Reactions were stopped at indicated timepoints by the addition of 4X sample buffer and analyzed as with phosphatase reactions, described above.

Phosphotransfer reactions: To autophosphorylation reactions, His_6-ChpT or TRX-His_6-ChpT was added to a final concentration of 12.5 μM and reactions incubated at 30°C before being stopped at indicated timepoints and processed as above.

Acknowledgements

We thank members of the Laub lab for critical reading of the manuscript. This work was supported by an NIH grant (5R01GM082899) to MTL. MTL is an Early Career Scientist at the Howard Hughes Medical Institute.

References

1. Skerker, J.M., Prasol, M.S., Perchuk, B.S., Biondi, E.G., and Laub, M.T. (2005). Two-component signal transduction pathways regulating growth and cell cycle progression in a bacterium: a system-level analysis. PLoS Biol *3*, e334.

2. Jacobs, C., Domian, I.J., Maddock, J.R., and Shapiro, L. (1999). Cell cycle-dependent polar localization of an essential bacterial histidine kinase that controls DNA replication and cell division. Cell *97*, 111-120.

3. Wu, J., Ohta, N., and Newton, A. (1998). An essential, multicomponent signal transduction pathway required for cell cycle regulation in *Caulobacter*. Proc Natl Acad Sci U S A *95*, 1443-1448.

4. Quon, K.C., Marczynski, G.T., and Shapiro, L. (1996). Cell cycle control by an essential bacterial two-component signal transduction protein. Cell *84*, 83-93.

5. Hecht, G.B., and Newton, A. (1995). Identification of a novel response regulator required for the swarmer- to-stalked-cell transition in *Caulobacter crescentus*. J Bacteriol *177*, 6223-6229.

6. Hecht, G.B., Lane, T., Ohta, N., Sommer, J.M., and Newton, A. (1995). An essential single domain response regulator required for normal cell division and differentiation in *Caulobacter crescentus*. EMBO J *14*, 3915-3924.

7. Ohta, N., Lane, T., Ninfa, E.G., Sommer, J.M., and Newton, A. (1992). A histidine protein kinase homologue required for regulation of bacterial cell division and differentiation. Proc Natl Acad Sci U S A *89*, 10297-10301.

8. Sommer, J.M., and Newton, A. (1991). Pseudoreversion analysis indicates a direct role of cell division genes in polar morphogenesis and differentiation in *Caulobacter crescentus*. Genetics *129*, 623-630.

9. Stock, A.M., Robinson, V.L., and Goudreau, P.N. (2000). Two-component signal transduction. Annu Rev Biochem *69*, 183-215.

10. Burbulys, D., Trach, K.A., and Hoch, J.A. (1991). Initiation of sporulation in B. subtilis is controlled by a multicomponent phosphorelay. Cell *64*, 545-552.

11. Biondi, E.G., Reisinger, S.J., Skerker, J.M., Arif, M., Perchuk, B.S., Ryan, K.R., and Laub, M.T. (2006). Regulation of the bacterial cell cycle by an integrated genetic circuit. Nature *444*, 899-904.

12. Freeman, J.A., and Bassler, B.L. (1999). Sequence and function of LuxU: a two-component phosphorelay protein that regulates quorum sensing in Vibrio harveyi. J Bacteriol *181*, 899-906.

13. Laub, M.T., Chen, S.L., Shapiro, L., and McAdams, H.H. (2002). Genes directly controlled by CtrA, a master regulator of the Caulobacter cell cycle. Proc Natl Acad Sci U S A *99*, 4632-4637.

14. Quon, K.C., Yang, B., Domian, I.J., Shapiro, L., and Marczynski, G.T. (1998). Negative control of bacterial DNA replication by a cell cycle regulatory protein that binds at the chromosome origin. Proc Natl Acad Sci U S A *95*, 120-125.

15. Domian, I.J., Reisenauer, A., and Shapiro, L. (1999). Feedback control of a master bacterial cell-cycle regulator. Proc Natl Acad Sci U S A *96*, 6648-6653.

16. Domian, I.J., Quon, K.C., and Shapiro, L. (1997). Cell type-specific phosphorylation and proteolysis of a transcriptional regulator controls the G1-to-S transition in a bacterial cell cycle. Cell *90*, 415-424.

17. Iniesta, A.A., McGrath, P.T., Reisenauer, A., McAdams, H.H., and Shapiro, L. (2006). A phospho-signaling pathway controls the localization and activity of a protease complex critical for bacterial cell cycle progression. Proc Natl Acad Sci U S A *103*, 10935-10940.

18. Jacobs, C., Ausmees, N., Cordwell, S.J., Shapiro, L., and Laub, M.T. (2003). Functions of the CckA histidine kinase in Caulobacter cell cycle control. Mol Microbiol *47*, 1279-1290.

19. Freeman, J.A., and Bassler, B.L. (1999). A genetic analysis of the function of LuxO, a two-component response regulator involved in quorum sensing in Vibrio harveyi. Mol Microbiol *31*, 665-677.

20. Perego, M. (2001). A new family of aspartyl phosphate phosphatases targeting the sporulation transcription factor Spo0A of Bacillus subtilis. Mol Microbiol *42*, 133-143.

21. Perego, M., Hanstein, C., Welsh, K.M., Djavakhishvili, T., Glaser, P., and Hoch, J.A. (1994). Multiple protein-aspartate phosphatases provide a mechanism for the integration of diverse signals in the control of development in B. subtilis. Cell *79*, 1047-1055.

22. Ohlsen, K.L., Grimsley, J.K., and Hoch, J.A. (1994). Deactivation of the sporulation transcription factor Spo0A by the Spo0E protein phosphatase. Proc Natl Acad Sci U S A *91*, 1756-1760.

23. Nierman, W.C., Feldblyum, T.V., Laub, M.T., Paulsen, I.T., Nelson, K.E., Eisen, J., Heidelberg, J.F., Alley, M.R., Ohta, N., Maddock, J.R., et al. (2001). Complete genome sequence of Caulobacter crescentus. Proc Natl Acad Sci U S A *98*, 4136-4141.

24. Georgellis, D., Kwon, O., De Wulf, P., and Lin, E.C. (1998). Signal decay through a reverse phosphorelay in the Arc two-component signal transduction system. J Biol Chem *273*, 32864-32869.

25. Uhl, M.A., and Miller, J.F. (1996). Central role of the BvgS receiver as a phosphorylated intermediate in a complex two-component phosphorelay. J Biol Chem *271*, 33176-33180.

26. Brissette, R.E., Tsung, K.L., and Inouye, M. (1991). Suppression of a mutation in OmpR at the putative phosphorylation center by a mutant EnvZ protein in Escherichia coli. J Bacteriol *173*, 601-608.

27. Dutta, R., Yoshida, T., and Inouye, M. (2000). The critical role of the conserved Thr247 residue in the functioning of the osmosensor EnvZ, a histidine Kinase/Phosphatase, in Escherichia coli. J Biol Chem *275*, 38645-38653.

28. Hsing, W., Russo, F.D., Bernd, K.K., and Silhavy, T.J. (1998). Mutations that alter the kinase and phosphatase activities of the two-component sensor EnvZ. J Bacteriol *180*, 4538-4546.

29. Nagasawa, S., Tokishita, S., Aiba, H., and Mizuno, T. (1992). A novel sensor-regulator protein that belongs to the homologous family of signal-transduction proteins involved in adaptive responses in Escherichia coli. Mol Microbiol *6*, 799-807.

30. Russo, F.D., and Silhavy, T.J. (1991). EnvZ controls the concentration of phosphorylated OmpR to mediate osmoregulation of the porin genes. J Mol Biol *222*, 567-580.

31. Tokishita, S., Kojima, A., and Mizuno, T. (1992). Transmembrane signal transduction and osmoregulation in Escherichia coli: functional importance of the transmembrane regions of membrane-located protein kinase, EnvZ. J Biochem *111*, 707-713.

32. Wheeler, R.T., and Shapiro, L. (1999). Differential localization of two histidine kinases controlling bacterial cell differentiation. Mol Cell *4*, 683-694.

33. Judd, E.M., Ryan, K.R., Moerner, W.E., Shapiro, L., and McAdams, H.H. (2003). Fluorescence bleaching reveals asymmetric compartment formation prior to cell division in Caulobacter. Proc Natl Acad Sci U S A *100*, 8235-8240.

34. Szurmant, H., Muff, T.J., and Ordal, G.W. (2004). Bacillus subtilis CheC and FliY are members of a novel class of CheY-P-hydrolyzing proteins in the chemotactic signal transduction cascade. J Biol Chem *279*, 21787-21792.

35. Zhao, R., Collins, E.J., Bourret, R.B., and Silversmith, R.E. (2002). Structure and catalytic mechanism of the E. coli chemotaxis phosphatase CheZ. Nat Struct Biol *9*, 570-575.

36. Porter, S.L., and Armitage, J.P. (2002). Phosphotransfer in Rhodobacter sphaeroides chemotaxis. J Mol Biol *324*, 35-45.

37. Silversmith, R.E., Smith, J.G., Guanga, G.P., Les, J.T., and Bourret, R.B. (2001). Alteration of a nonconserved active site residue in the chemotaxis response regulator CheY affects phosphorylation and interaction with CheZ. J Biol Chem *276*, 18478-18484.

38. Thomas, S.A., Brewster, J.A., and Bourret, R.B. (2008). Two variable active site residues modulate response regulator phosphoryl group stability. Mol Microbiol *69*, 453-465.

39. Marina, A., Waldburger, C.D., and Hendrickson, W.A. (2005). Structure of the entire cytoplasmic portion of a sensor histidine-kinase protein. EMBO J *24*, 4247-4259.

40. Hung, D.Y., and Shapiro, L. (2002). A signal transduction protein cues proteolytic events critical to Caulobacter cell cycle progression. Proc Natl Acad Sci U S A *99*, 13160-13165.

41. Iniesta, A.A., and Shapiro, L. (2008). A bacterial control circuit integrates polar localization and proteolysis of key regulatory proteins with a phospho-signaling cascade. Proc Natl Acad Sci U S A *105*, 16602-16607.

42. Thanbichler, M., Iniesta, A.A., and Shapiro, L. (2007). A comprehensive set of plasmids for vanillate- and xylose-inducible gene expression in Caulobacter crescentus. Nucleic acids research *35*, e137.

43. Ohta, N., Grebe, T. W., and Newton, A. (2000). In Prokaryotic Development Y.V.a.S. Brun, L. J., ed. (Washington DC: ASM Press), pp. 341-359.

Chapter 3

A spatial gradient of protein phosphorylation underlies replicative asymmetry in a bacterium

This work was published as Y. Erin Chen*, Carolina Tropini*, Kristina Jonas, Christos G. Tsokos, Kerwyn Casey Huang, and Michael T. Laub. 2011 PNAS. Jan;108(3):1052-7.

Y.E.C., M.T.L., and K.C.H. designed the study and analyzed the data. Y.E.C. executed the experiments and produced all experimental figures. C.T. and K.C.H. designed and performed the mathematical modeling and produced all computational figures. K.J. and C.G.T. assisted with strain construction and experiments. Y.E.C., C.T., M.T.L., and K.C.H. wrote the manuscript. All authors discussed the results and commented on the manuscript.

*These authors contributed equally to this work.

Abstract

Spatial asymmetry is crucial to development. One mechanism for generating asymmetry involves the localized synthesis of a key regulatory protein that diffuses away from its source, forming a spatial gradient. While gradients are prevalent in eukaryotes, at both the tissue and intracellular levels, it is unclear whether gradients of freely diffusible proteins can form within bacterial cells given their small size and the speed of diffusion. Here, we show that the bacterium Caulobacter crescentus generates a gradient of the active, phosphorylated form of the master regulator CtrA, which directly regulates DNA replication. Employing a combination of mathematical modeling, single-cell microscopy, and genetic manipulation, we demonstrate that this gradient is produced by the polarly localized phosphorylation and dephosphorylation of CtrA. Our data indicate that cells robustly establish the asymmetric fates of daughter cells before cell division causes physical compartmentalization. More generally, our results demonstrate that uniform protein abundance may belie gradients and other sophisticated spatial patterns of protein activity in bacterial cells.

Introduction

Asymmetry plays a crucial role in generating complexity within biological systems, and the establishment of asymmetry often requires spatial heterogeneity of key regulatory proteins. Among the best-studied examples of this phenomenon are morphogen gradients in multicellular organisms that drive developmental patterning [1]. In such cases, signaling proteins form a concentration gradient across many cells via diffusion from a spatially localized source. Protein gradients have also been observed within individual eukaryotic cells (reviewed in [2]), such as the gradient of Ran-GTP that emanates from yeast chromosomes to help organize the mitotic spindle.

Consistent with their ability to establish protein gradients in the presence of diffusion, eukaryotic cells can sense gradients of small molecules by directly comparing concentrations across their cell bodies [3]. By contrast, due to their small size, bacterial detection of chemoattractant gradients relies on temporal comparisons during swimming [4]. It is thus unclear whether bacteria, typically smaller than eukaryotic cells by an order of magnitude or more, can establish spatial gradients of freely diffusible proteins. Indeed, most bacterial cytoplasmic proteins are uniformly distributed within the cell, and exceptions such as the gradient of MinC protein in *E. coli* are notable for their dependence on interaction with membrane-associated proteins [5].

The bacterium *Caulobacter crescentus* is a model bacterium for understanding the molecular basis of cellular asymmetry. Each cell division in this organism is asymmetric, producing a daughter stalked cell in S phase and a daughter swarmer cell in G1. This difference in cell fate is dictated by the cytoplasmic protein CtrA, an essential transcription factor that also binds to and directly silences the origin of replication [6].

Here, we present evidence for a spatial gradient of the active, phosphorylated form of CtrA. Before cell division occurs, phosphorylated CtrA (CtrA~P) is abundant and transcriptionally activates more than 70 target genes, many required for cell division [7]. Following cell division, CtrA~P continues to repress DNA replication in daughter swarmer cells, but is rapidly dephosphorylated and degraded in daughter stalked cells, permitting the immediate initiation of DNA replication. A prevailing model posits that cytokinesis is necessary for the establishment of cell fate asymmetry [8], implying that phosphorylated CtrA is homogeneously distributed prior to cell division. Our data challenge this model, indicating instead that the cell employs a sophisticated symmetry-breaking mechanism such that CtrA is differentially phosphorylated across the predivisional cell. Cytokinesis then serves to reinforce the existing asymmetry in daughter cells.

CtrA activity is regulated by CckA, which can act either as a kinase or as a phosphatase for CtrA via the phosphotransferase ChpT [9, 10]. In predivisional cells, when CtrA phosphorylation levels peak, CckA is usually bipolarly localized [10, 11]. Here, we demonstrate a critical role for the localization and bifunctional activity of CckA in which CckA is a kinase at the swarmer pole and a phosphatase at the stalked pole. This spatial asymmetry in opposing CckA activities produces a gradient of CtrA phosphorylation across the predivisional cell with dramatic consequences for the asymmetry of critical cellular processes such as DNA replication.

Results

Replication in predivisional cells has an intrinsic spatial asymmetry

Caulobacter cells normally replicate their DNA exactly once per cell cycle [12]. However, we found that blocking cell division with the antibiotic cephalexin allowed for additional rounds of replication in predivisional cells. Intriguingly, flow cytometry indicated that for most cephalexin-treated cells, only one of the two chromosomes replicated such that cells transitioned from having two to three chromosomes (Fig. 3.1A). By contrast, when *E. coli* cells harboring two chromosomes were treated with cephalexin, both chromosomes replicated to yield cells with four chromosomes (Fig. 3.1A). We thus asked whether the two chromosomes in *Caulobacter* predivisional cells have unequal likelihoods of initiating replication, even before cell division occurs.

To visualize DNA replication in individual living cells, we implemented a fluorescent repressor-operator system [13] in which cells produce TetR-YFP and harbor an array of *tet* operator (*tetO*) sites near the origin of replication [14]. Binding of TetR-YFP molecules to the *tetO* array produces a fluorescent focus that marks the origin and enables tracking of DNA replication (Fig. 3.1B). In a synchronous population of G1 swarmer cells, a single focus was visible at the older pole, which became the stalked pole after differentiation. Following the G1-S transition, DNA replication led to the appearance of a second focus that was rapidly tethered to the opposite, nascent swarmer, pole (Fig. 3.1C). In the presence of cephalexin, cells did not divide and 77% replicated again to produce a third TetR-YFP focus, on average 105 minutes after the appearance of the second focus (Fig. 3.1C). Strikingly, this third focus originated from the stalked pole in 82% of cells and from the swarmer pole in only 16% of cells, with 2% of cells replicating bipolarly

(defined as instances when origins at both poles fire within one 6 minute frame of each other) (Fig. 3.1D). Experiments using BrdU labeling also revealed a strong bias for replication of the stalked pole-proximal chromosome (Fig. 3.2A-B). To confirm that cephalexin inhibits compartmentalization in *Caulobacter*, we performed fluorescence recovery after photobleaching (FRAP) on cells expressing a YFP-CtrA fusion. After bleaching one of the poles, fluorescence in that area typically recovered rapidly, and levels within the two halves of the cell converged to similar values, indicating that YFP-CtrA diffuses freely throughout cephalexin-treated cells (Fig. 3.2C-D). Consistent with the cephalexin-treated cells, we also observed a strong asymmetry of DNA replication in cells depleted of *ftsZ* (Fig. 3.2E). Our data thus indicate that replicative capacity in predivisional cells is strongly asymmetrical, being heavily biased toward the stalked pole, and occurs without compartmentalization.

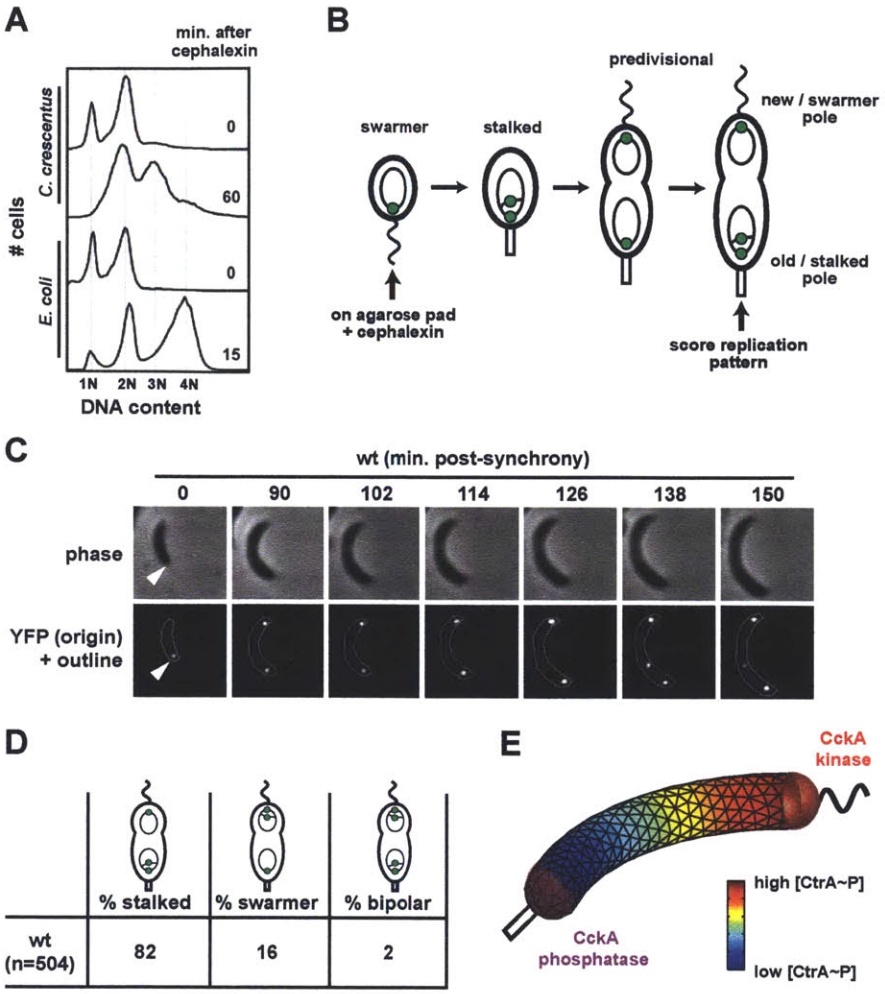

Figure 3.1. Chromosomal replication in wild-type predivisional cells exhibits spatial asymmetry. (A) Flow cytometry analysis of DNA content in mixed populations of Caulobacter crescentus and E. coli cells. Cephalexin was added to cultures at time t=0 to inhibit cell division. Samples were taken immediately or after 15 minutes (E. coli) or 60 minutes (Caulobacter) and chromosome content examined by flow cytometry. (B) Experimental design for using the tetO, TetR-YFP fluorescent reporter-operater system to examine DNA replication in individual cells. At time t=0, newly synchronized swarmer cells are placed on an agarose pad supplemented with cephalexin and imaged at various time points by phase and epifluorescence microscopy. Green dots represent fluorescent foci of TetR-EYFP, which label the origins of replication. (C) Representative time-lapse images from a wild type cell harboring the tet FROS. A single origin at the old/stalked pole (marked with arrowhead) replicates within the first 90 minutes to yield two polar origins. A third origin stemming from the stalked pole is visible following the 126-minute time point. (D) Quantification of the spatial patterns of DNA replication in division-inhibited wild-type cells. (E) Computational modeling of CtrA~P asymmetry when CckA functions as a kinase at the swarmer pole and as a phosphatase at the stalked pole (phosphorylation and dephosphorylation rates are sk = 100/sec and sp = 10/sec, respectively, and occur across the hemispherical surfaces indicated in red). The predivisional cell is represented as a three-dimensional curved cylinder with length 4 mm. Small triangles represent the surfaces of tetrahedral simulation grid points and the concentration of CtrA~P is shaded relative to total CtrA protein.

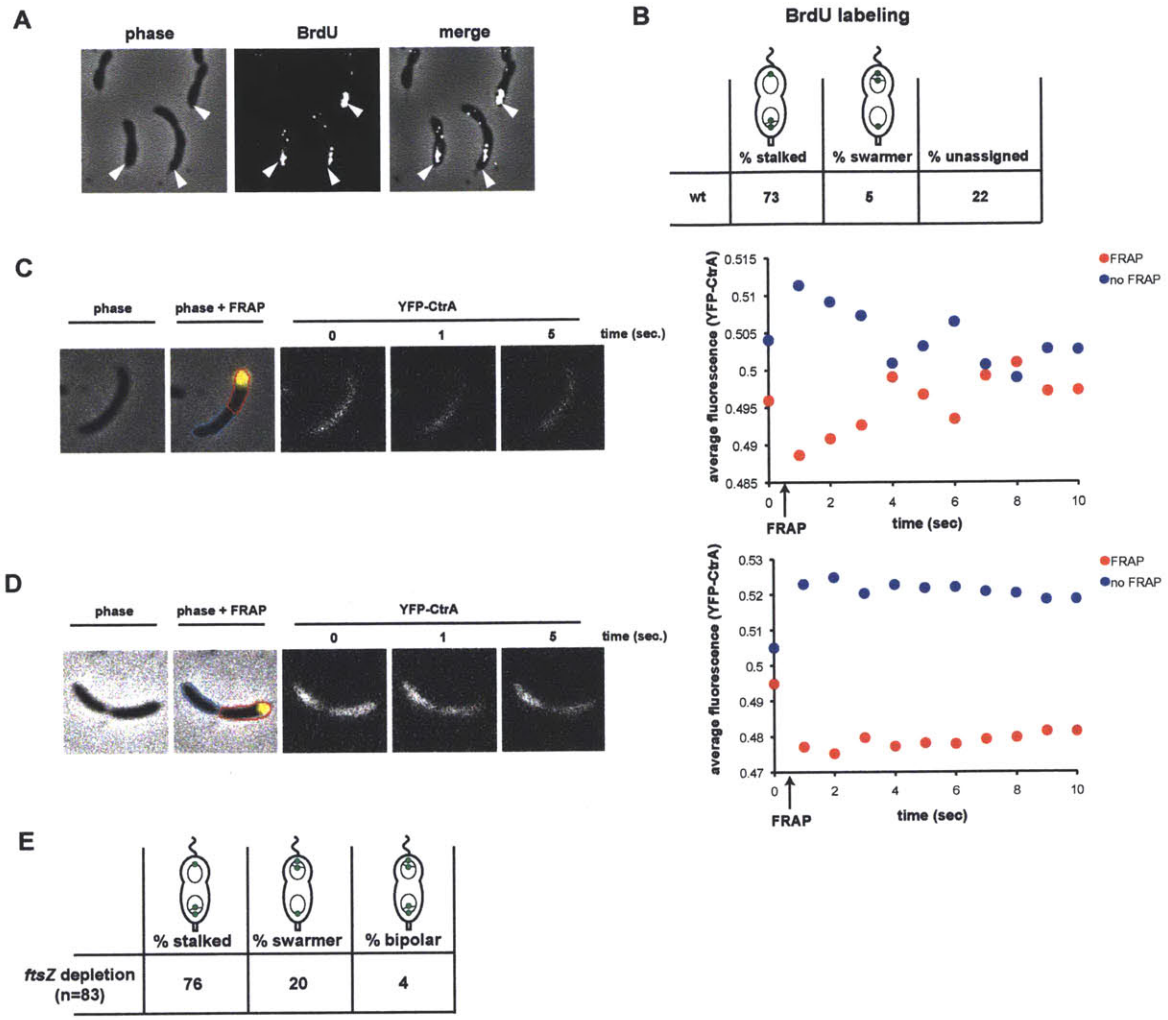

Figure 3.2. DNA replication occurs asymmetrically in cells treated with cephalexin or depleted of ftsZ. (A) Representative immunofluorescence images of asymmetrical bromodeoxyuridine (BrdU) incorporation in the stalked half of wild-type predivisional cells treated with cephalexin. White arrowheads indicate the stalked pole, as determined from the phase micrograph. (B) Quantification of BrdU incorporation in cells analyzed by microscopy. (C) Fluorescence recovery after photobleaching analysis of a cell expressing YFP-CtrA and growing on an agarose pad containing cephalexin. A phase image of the cell is shown alone and with a yellow dot representing the portion of the cell bleached, followed by fluorescence images taken immediately before and at 1 and 5 seconds after bleaching. The average fluorescence intensity within the two halves of the cell (indicated with red and blue outlines in the phase image) was measured before bleaching and every second after bleaching. These fluorescent intensities are plotted as a function of time (right panel). The arrow labeled "FRAP" shows the time of bleaching. A total of 47 cells were examined by FRAP with the majority (>75%) showing similar YFP-CtrA levels in the two halves of the cell within 1-8 seconds after bleaching, as in panel C. (D) Same as in panel C, but for a cell in which compartmentalization had already occurred prior to FRAP analysis and cephalexin addition. YFP-CtrA levels in the two halves of the cell do not converge after bleaching one pole. (E) Quantification of the spatial patterns of DNA replication in cells depleted of ftsZ.

A spatial gradient of CtrA phosphorylation generates replicative asymmetry in predivisional cells

The difference in DNA replication potential of *Caulobacter* daughter cells after cell division involves asymmetry in the levels of the master regulator CtrA. Whether CtrA dictated the replicative asymmetry we observed in predivisional cells (Fig. 3.1D) was initially unclear because a YFP-CtrA reporter was found uniformly distributed throughout the cytoplasm (Fig. 3.3A) [15]. However, we hypothesized that phosphorylated CtrA was asymmetrically distributed, forming a spatial gradient of CtrA *activity* that was responsible for the observed replicative asymmetry. The phosphorylation of CtrA is ultimately driven by CckA, which likely requires the essential factor DivL for kinase activity [16]. While CckA typically localizes to both poles of a predivisional cell, DivL usually localizes only to the swarmer pole [17]. These patterns are maintained in a large fraction of cephalexin-treated cells (Fig. 3.3B), suggesting that CckA functions as a kinase at the swarmer pole and perhaps as a phosphatase at the stalked pole, thereby acting as a source and a sink for CtrA~P, respectively.

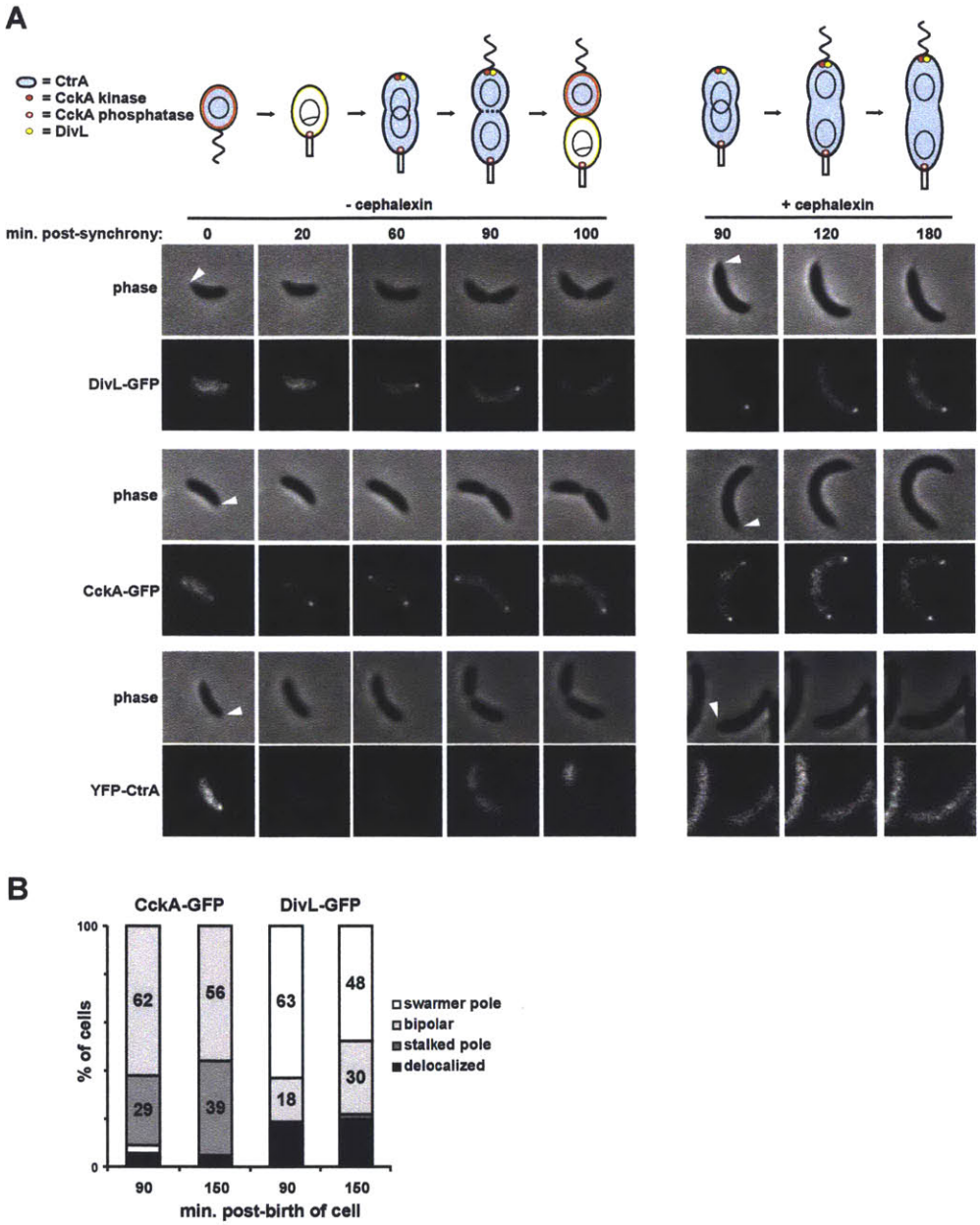

Figure 3.3. Cell-cycle dependent localization of DivL, CckA, and CtrA is not altered by cephalexin treatment. Schematics (top) illustrate progression through the cell cycle stages that correspond to the micrographs (below) and summarize the subcellular localization patterns of CtrA, DivL, and CckA. Synchronized swarmer cells were grown on agarose pads without cephalexin (left) or with cephalexin (right). DivL-GFP (top) is localized to the swarmer pole in late stalked and predivisional cells. DivL-GFP remains localized to the swarmer pole of most cells following cephalexin treatment (Fig. 2B). CckA-GFP (middle) is localized bipolarly in most predivisional cells. CckA-GFP remains localized to both poles in most cells following cephalexin treatment (Fig. 2B). YFP-CtrA (bottom) is abundant in swarmer cells, eliminated in stalked cells, and abundant again in predivisional cells. Following cell division, YFP-CtrA is cleared from the stalked daughter cell. In cells treated with cephalexin, CtrA remains homogenously distributed in predivisional cells. White arrowheads indicate the stalked poles.

To investigate whether this asymmetry in CckA activity could generate and maintain a steady-state gradient of CtrA~P prior to cell division, we developed a reaction-diffusion model of the *Caulobacter* predivisional cell (see Methods). In this model, we assumed that the phosphorylation state of CtrA is controlled predominantly by kinase and phosphatase activity localized at the swarmer and stalked poles, respectively, and that CtrA and CtrA~P freely diffuse within the cytoplasm. For a cell of length $L \sim 4$ μm and a CtrA diffusion constant of $D \sim$ 1-10 μm^2/sec (Fig. 3.4C and Methods), the time scale required to diffuse between the two poles is $\tau_D \sim L^2/2D \sim$ 1-10 sec. We then determined that if the rates of CtrA phosphorylation and dephosphorylation are fast compared with $1/\tau_D$, a gradient of CtrA~P can be produced while maintaining a uniform distribution of CtrA protein (Fig. 3.1E, 3.4A). We measured the half-life of the phosphoryl group on CtrA~P in predivisional cells to be on the order of tens of seconds or less, suggesting that there are indeed high rates of both phosphorylation and dephosphorylation (Fig. 3.5), which could produce a gradient. Incorporating ChpT into our model did not disrupt the spatial asymmetry of CtrA~P, even if ChpT is free to diffuse (Fig. 3.6A). This gradient was also insensitive to whether CckA activity was assumed to be spread across the entire pole or concentrated in a region as small as 50nm (Fig. 3.6B).

Because the direct observation of a protein phosphorylation gradient is currently intractable, we used our model to systematically alter the gradient via perturbation of CckA localization and function and then verified these predictions using a variety of mutations. Our model predicts that a gradient of CtrA~P would be substantially reduced or eliminated by removing (i) the kinase activity of CckA alone, (ii) both the kinase and phosphatase activity, or (iii) the phosphatase activity alone (Fig. 3.4A). In each case, the

absence of a source and/or sink of CtrA~P would lead to a near-uniform distribution of CtrA~P, which should reduce or eliminate the stalked pole bias in replicative asymmetry of predivisional cells and lead to an increase in the fraction of cells replicating bipolarly (Fig. 3.4A).

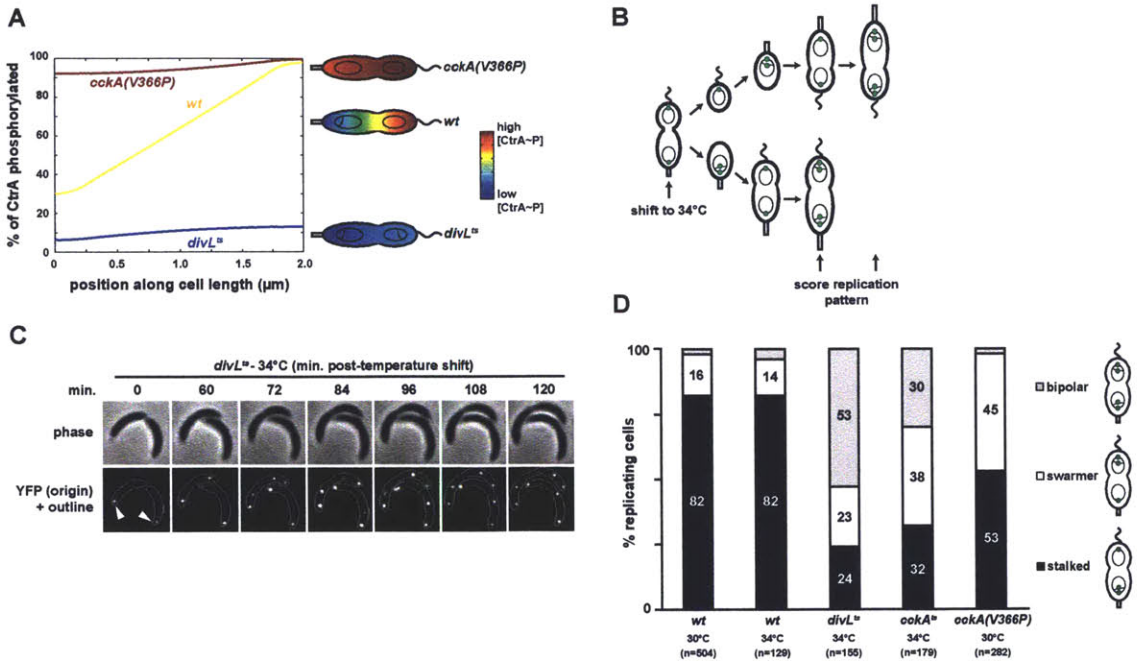

Figure 3.4. CtrA activity is required for replication asymmetry in predivisional cells. (A) Mathematical modeling of the spatial distribution of CtrA phosphorylation in wild type and mutant strains disrupted for CckA kinase activity (*divL*^{ts}) or CckA phosphatase activity (*cckA(V366P)*). For wild type the phosphorylation and dephosphorylation rates, σ_k and σ_p, respectively, are 100/sec and 10/sec. For *divL*^{ts}, $\sigma_k = 0$; for *cckA(V366P)*, $\sigma_p = 0$. The predicted patterns of CtrA~P as a percentage of the total CtrA concentration are shown as a function of position along a 1D, 2 μm cell and in the predivisional cell schematics. (B) Experimental design for examining DNA replication in *cckA*^{ts} and *divL*^{ts} cells. At time t=0, a mixed population of cells harboring the tet FROS and grown at 28°C (*cckA*^{ts}) or 30°C (*divL*^{ts}) was placed on an agarose pad for microscopy at 34°C. Phase contrast and epifluorescence microscopy were used to follow late predivisional cells that divided immediately after beginning a time-lapse movie. Both daughter cells inherit a single chromosome that replicates, leading to two origin foci. At the restrictive temperature of 34°C, cckAts and divLts cells do not divide; we then examined the spatial pattern of subsequent DNA replication events. (C) Frames from a representative time-lapse movie of divLts cells showing bipolar replication (left cell) and unipolar replication from the stalked pole (right cell). (D) Quantification of the spatial patterns of DNA replication in wild type, *cckA*^{ts}, *divL*^{ts}, and *cckA(V366P)* cells. Temperatures and numbers of replicating cells examined are indicated.

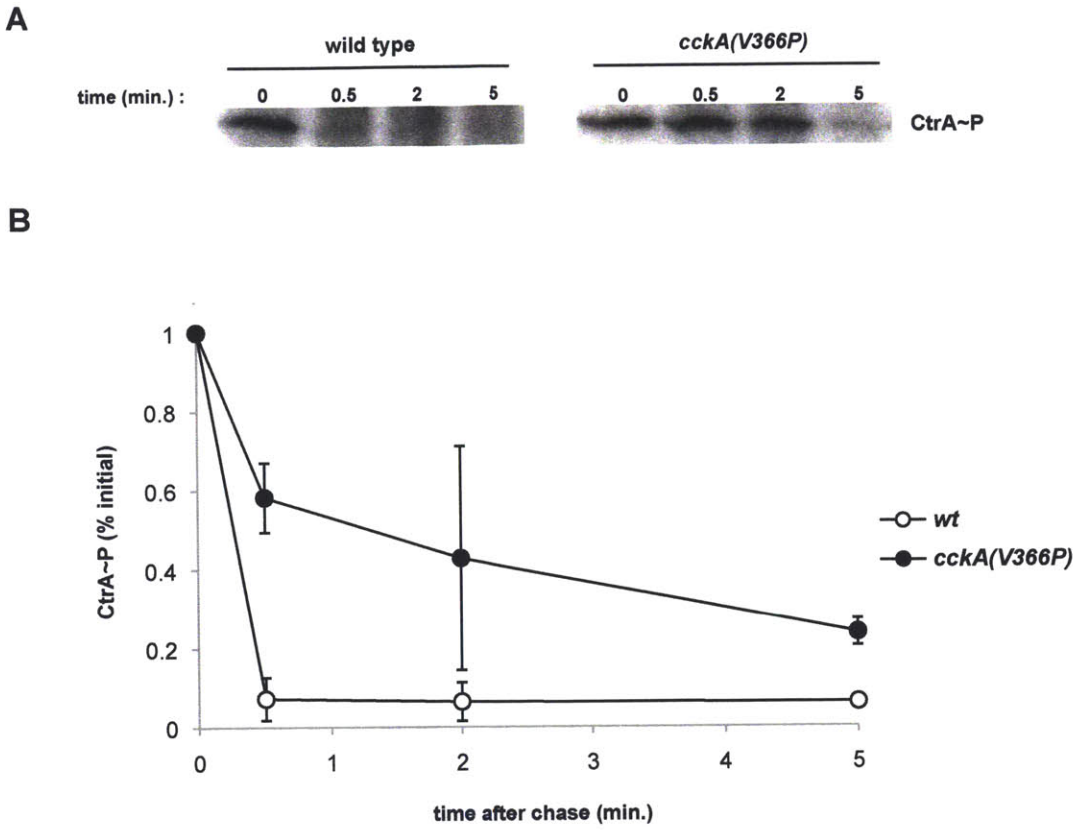

Figure 3.5. Kinetics of CtrA~P dephosphorylation in vivo. (A) In vivo phosphorylation pulse-chase showing 32P-labeled CtrA (CtrA~P) levels in synchronized predivisional cells from the wild-type strain or from cells expressing *cckA(V366P)*, each grown in M5G. Time 0 is after labeling and immediately before adding the chase solution. All other time points are taken after adding the chase solution. (B) Quantification of the CtrA~P bands. Error bars represent standard deviations calculated from two experiments done on separate days using independent cultures.

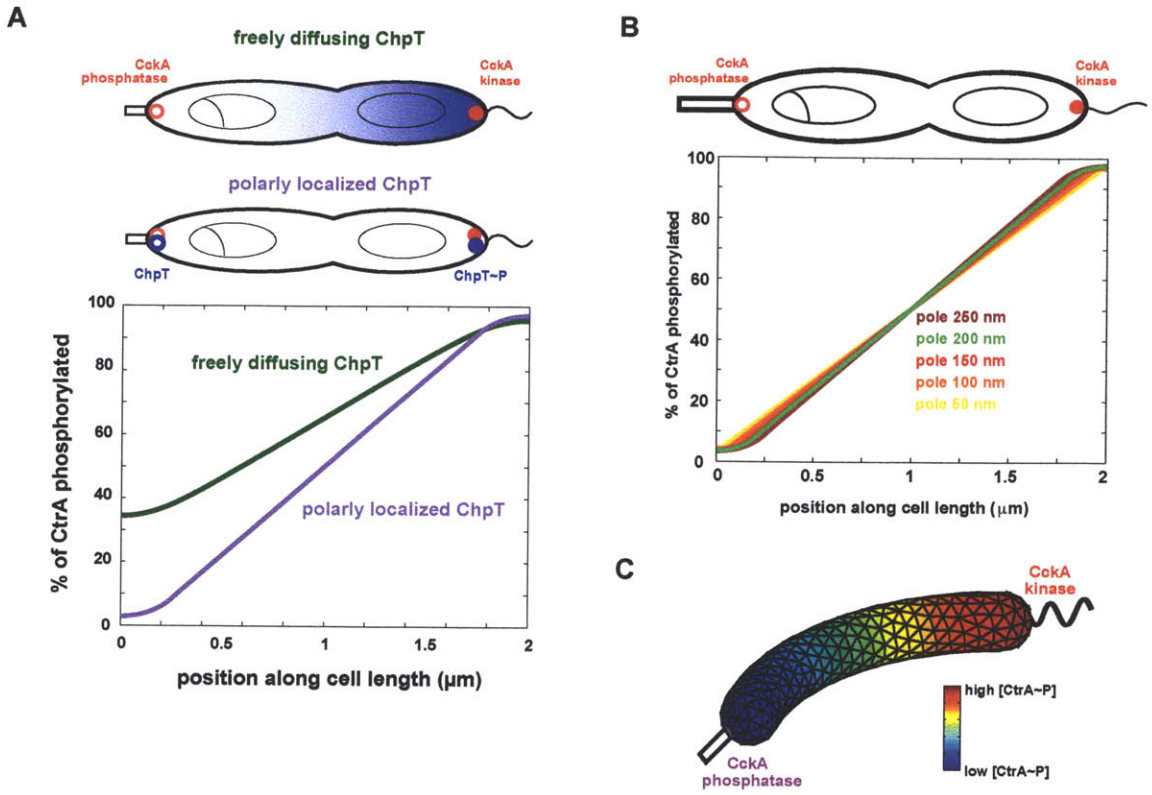

Figure 3.6. CtrA~P asymmetry is insensitive to ChpT diffusion and to the size of polar CckA activity. (A) Simulations of CtrA phosphorylation gradient when ChpT is included as a freely diffusible species (green line) or polarly localized during phosphotransfer via binding to CckA (purple line). The rates of ChpT phosphorylation and dephosphorylation by CckA are 100/sec and 10/sec, respectively, and levels of ChpT are chosen so that the rates of CtrA phosphorylation and dephosphorylation at the poles are 100/sec. If polarly localized, ChpT-mediated phosphorylation produces an identical CtrA~P gradient to that in Fig. 4A. If ChpT diffuses freely, CtrA~P has similar polar concentrations and has a concave distribution. Diagrams on the right indicate the distribution of ChpT and ChpT~P (blue) engaged in phosphotransfer to CtrA in the two models. (B) 1D simulations of the CtrA phosphorylation gradient when the area of CckA activity at the poles was varied between 50-250 nm. (C) 3D simulation of the CtrA phosphorylation gradient when the area of CckA activity at the poles is restricted to a width of 50 nm.

To test our predictions regarding the relationship between CtrA activity and replicative asymmetry, we first examined DNA replication in cells harboring the TetR-*tetO* system and either a *divL*^{ts} or *cckA*^{ts} mutation. Both strains exhibit a decrease in CtrA activity when shifted from a permissive to restrictive temperature [18, 19]. For *divL*^{ts}, CckA kinase activity is likely reduced at the restrictive temperature [16], while the *cckA*^{ts} mutation probably affects both kinase and phosphatase activities. We placed a mixed population of cells (for both *cckA*^{ts} and *divL*^{ts}) on agarose pads at 34°C and followed late predivisional cells, which divided once but not again due to the loss of CtrA activity, even without adding cephalexin (Fig. 3.4B-C). We then examined the spatial pattern of new rounds of DNA replication in these cells, assessing whether replication occurred at the old/stalked pole, the new/swarmer pole, or both.

In the *divL*^{ts} and *cckA*^{ts} strains, the loss of CckA kinase activity and consequent reduction in CtrA~P at 34°C completely eliminated the asymmetry of replication (Fig. 3.4D). For *divL*^{ts} cells that replicated unipolarly, 51% initiated at the stalked pole and 49% at the swarmer pole. For *cckA*^{ts} cells that replicated unipolarly, 46% of cells initiated at the stalked pole and 54% at the swarmer pole. By contrast, for wild-type cells at 34°C that replicated unipolarly, 85% initiated at the stalked pole. In agreement with our prediction of uniform CtrA~P levels, the *divL*^{ts} and *cckA*^{ts} strains also exhibited increases in bipolar firings; 50% of *divL*^{ts} cells and 30% of *cckA*^{ts} cells at 34°C replicated bipolarly, compared to just 4% in wild type (Fig. 3.4D). As a control, we verified that these losses in asymmetry were not attributable to differences in cell length in the mutant strains (Fig. 3.7). The timing of replication was also substantially faster in the mutant strains, with replication at the stalked pole in *divL*^{ts} and *cckA*^{ts} cells occurring an average of 45 and 43

minutes, respectively, earlier than in wild-type predivisional cells at 34°C. Earlier replication likely reflects a loss of CtrA-mediated inhibition of the origin of replication. In sum, our data indicate that replicative asymmetry is eliminated in *divL*^{ts} and *cckA*^{ts} cells at 34°C due to a loss in CckA kinase activity.

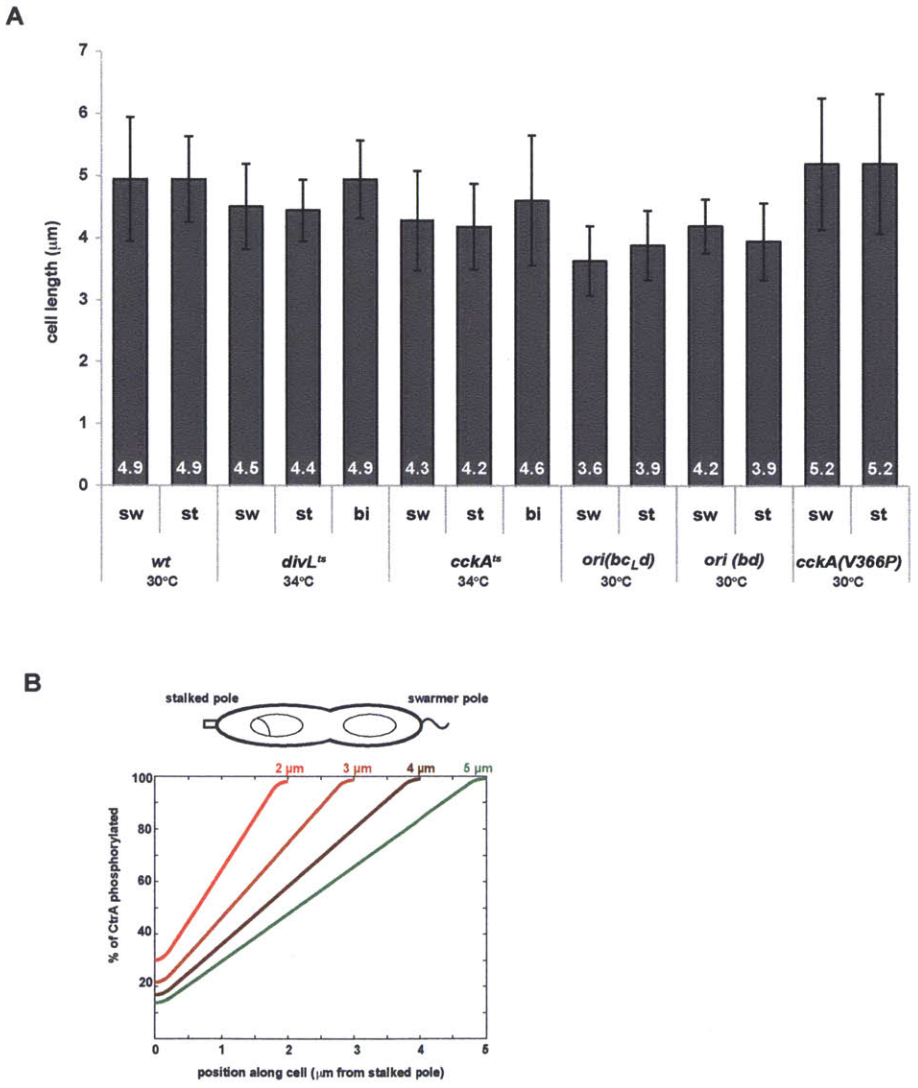

Figure 3.7. Cell length at the time of replication does not affect the extent of replicative asymmetry. (A) Cell length was measured at the time of replication initiation in predivisional cells in each of the strains indicated. Cells were classified according to whether replication initiated from the swarmer pole (sw), stalked pole (st), or from both poles (bi). The average cell length (mm) is listed at the bottom of each bar. (B) Mathematical modeling showing that the spatial asymmetry in CtrA~P concentration is insensitive to cell length, using the wild-type localization and kinetic parameters from Fig. 2A.

CckA phosphatase activity is important for generating a CtrA activity gradient

To test the importance of CckA phosphatase activity in forming a CtrA~P gradient, we replaced the chromosomal copy of *cckA* with *cckA(V366P)*. CckA(V366P) retains kinase activity, but has significantly diminished phosphatase activity *in vitro* [10] and leads to a significantly longer half-life of the phosphoryl group on CtrA~P *in vivo* (Fig. 3.5). Using the TetR-*tetO* system, we confirmed our prediction that predivisional cells of the *cckA(V366P)* strain also exhibited a dramatically decreased spatial replication bias, with 53% of origins coming from the stalked pole and 45% from the swarmer pole (Fig. 3.4D). Additionally, *cckA(V366P)* predivisional cells took an average of ~10 minutes longer before initiating DNA replication than wild type cells ($p = 0.0003$, two-sided t-test). This delay is likely due to an increase in the overall levels of CtrA~P, resulting from a loss of CckA phosphatase activity. If the V366P mutation had simply increased kinase activity rather than eliminating phosphatase activity, our model predicts that CtrA~P asymmetry would be retained. Thus, the combination of decreased asymmetry and slower replication implies that CckA at the stalked pole is not inert [11], but is actively dephosphorylating CtrA to help form a CtrA~P gradient.

Replicative asymmetry depends on direct repression of the origin by CtrA

CtrA has two distinct functions: direct repression of the origin and transcriptional regulation of cell-cycle genes [6, 7]. To show that replicative asymmetry depends on CtrA~P binding to the origin rather than indirectly on CtrA-dependent transcription, we used strains in which either two or three of the five CtrA~P binding sites at the origin were mutated to severely disrupt CtrA~P binding [20] (Fig. 3.8A). These strains still

harbor wild type copies of *ctrA*, *cckA*, and *divL*, and exhibit relatively normal cellular morphology and doubling times, suggesting CtrA transcriptional activity is not significantly affected. For the strain with two mutated binding sites, we observed a weaker spatial bias, with 58% of cells replicating from the stalked pole and 31% from the swarmer pole (Fig. 3.8B). The strain in which three of the five CtrA binding sites were mutated exhibited a further reduction in replicative asymmetry, with 51% of cells replicating from the stalked pole and 31% from the swarmer pole (Fig. 3.8B). We predict that mutating all five CtrA binding sites would completely eliminate spatial bias, but such strains could not be examined because they are extremely sick, likely because removing all CtrA binding sites eliminates other critical, overlapping elements of the origin.

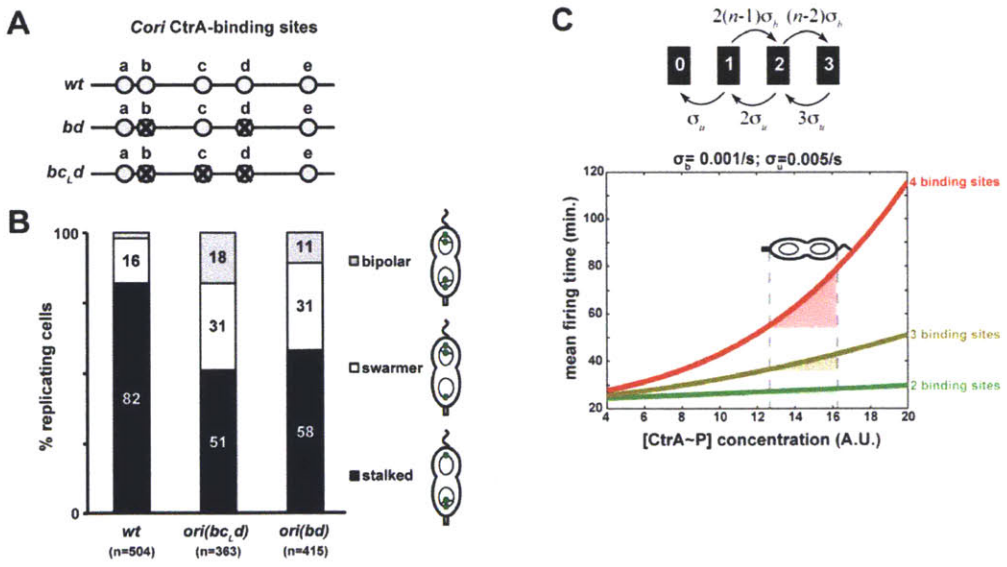

Figure 3.8. Asymmetry of replication depends on direct CtrA repression of the origin. (A) Schematic of CtrA binding sites in the origin of replication of wild type and the 'bd' and 'bcLd' mutants [20] which have mutations in two or three sites, respectively. (B) Quantification of spatial patterns of DNA replication in wild type and origin mutants. Cells were examined as in Fig. 2C at 30°C. (C) Markov model for concentration dependence of the average time before all CtrA~P binding sites are left unoccupied, thereby allowing for DNA replication initiation. Rates of binding (σ_b = 0.001/sec) and unbinding (σ_u = 0.005/sec) were selected to reproduce the average firing time in wild-type cells. Polar concentrations (dashed lines) were translated into approximate molecule counts using a DNA-interaction volume of 105 nm^3, and the heights of the shaded

triangles indicate the degree of asymmetry between the stalked pole (left) and swarmer pole (right). As the number of CtrA binding sites increases from 2 to 4 (green line to red line), the height of the shaded triangle increases, indicating an expected increase in the asymmetry of firing times between the stalked and swarmer poles.

The effects of mutating the origin on replicative asymmetry were captured in a Markov chain model in which CtrA~P molecules rapidly bind to and dissociate from the origin, with replication initiating only when all binding sites are unoccupied (Fig. 3.8C). This model predicts that the difference in firing times at opposite poles should decrease in the presence of fewer CtrA binding sites in a manner consistent with our experimental results (see Methods). Hence, our data collectively indicate that a spatial gradient of phosphorylation dictates CtrA's propensity to bind and repress the origins in different regions of predivisional cells, and that the dependence of origin firing on CtrA~P concentration can be altered by perturbing the regulation of CtrA~P *in trans* or the binding of CtrA~P *in cis*.

Fundamental criteria for generating phosphorylation asymmetry

Our experimental readout provides information on CtrA activity only near the poles where the origins of replication are anchored. While there are not yet tools to measure the complete spatial distribution of phosphorylated CtrA, our mathematical modelling predicts that a sufficiently fast-acting source and sink for phosphorylation localized at opposite poles would produce a linear gradient of CtrA~P. To test whether other mechanisms could explain our data, we used the model to investigate the range of kinetic parameters that produce robust gradients, whether gradient formation relies on localization of both the source and the sink, and the role of localized synthesis and proteolysis in gradient formation.

We first exhaustively explored the ranges of possible phosphorylation and dephosphorylation rates that would support a substantial steady-state gradient of CtrA~P, and uncovered a general rule that a robust gradient requires both rates to be faster than the inverse diffusive time scale $1/\tau_D \sim 1$/sec (Fig. 3.9A). The phosphorylation and dephosphorylation rates for CtrA *in vivo* are likely 50-100/sec (see Methods), suggesting that cells operate well above the threshold necessary to produce a substantial gradient of CtrA~P. We then used the model to assess whether a gradient can be produced if either the CckA kinase or phosphatase activity is delocalized. We also considered a scenario where CckA phosphatase activity at the pole is slow, but an additional delocalized phosphatase for CtrA exists [10]. Our simulations indicated that, provided the overall rates of phosphorylation and dephosphorylation remained faster than $1/\tau_D$, the formation of a gradient was robust to delocalization of one, but not both activities (Fig. 3.10).

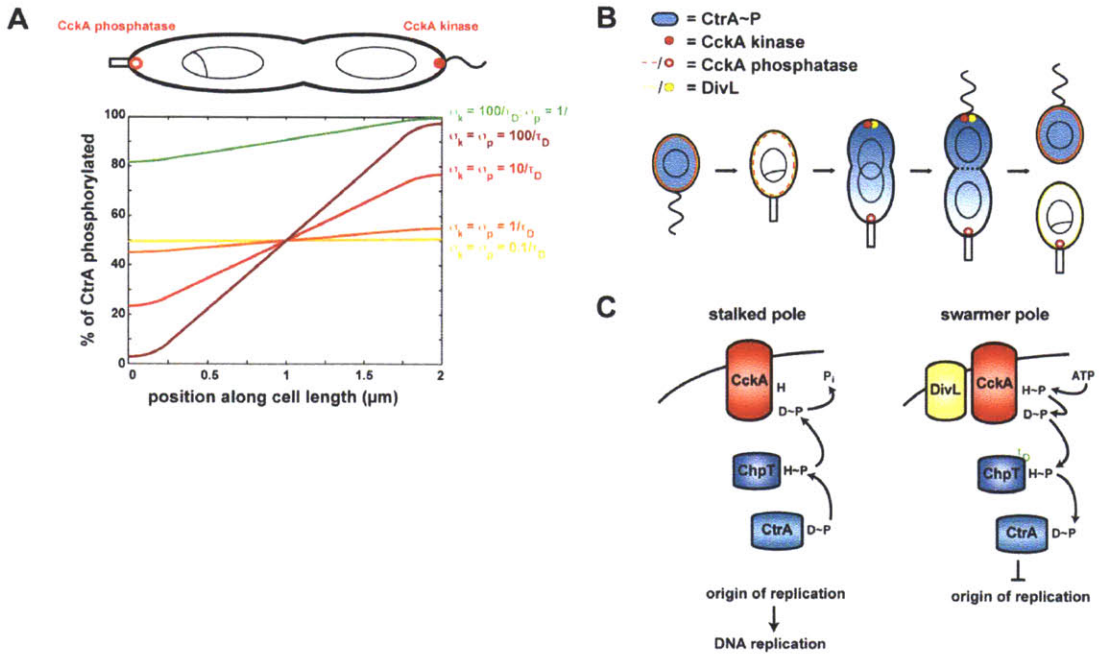

Figure 3.9. Both kinase and phosphatase activities of CckA must be fast to produce a CtrA~P gradient. (A) Mathematical modeling of the spatial asymmetry in CtrA~P across a 1D cell for varying kinase and phosphatase rates. A substantial gradient is obtained only when CtrA phosphorylation and dephosphorylation are faster than the inverse of the time scale required for diffusion across the cell, $1/\tau_D = 2D/L^2$. Degradation and synthesis are not included in these simulations as they have little effect on the gradient unless the half-life is shorter than τ_D. (B) Schematic of protein localization patterns in Caulobacter resulting in formation of a gradient of CtrA~P in predivisional cells. Cell division reinforces the asymmetric distribution of CtrA~P, resulting in daughter cells with different replicative capacities and fates. (C) Schematic of the CckA/ChpT/CtrA phosphorelay. When stimulated by DivL at the swarmer pole, CckA operates as a kinase, resulting in phosphorylation of ChpT and, ultimately, CtrA. When unstimulated at the stalked pole, CckA operates as a phosphatase, driving dephosphorylation of CtrA~P.

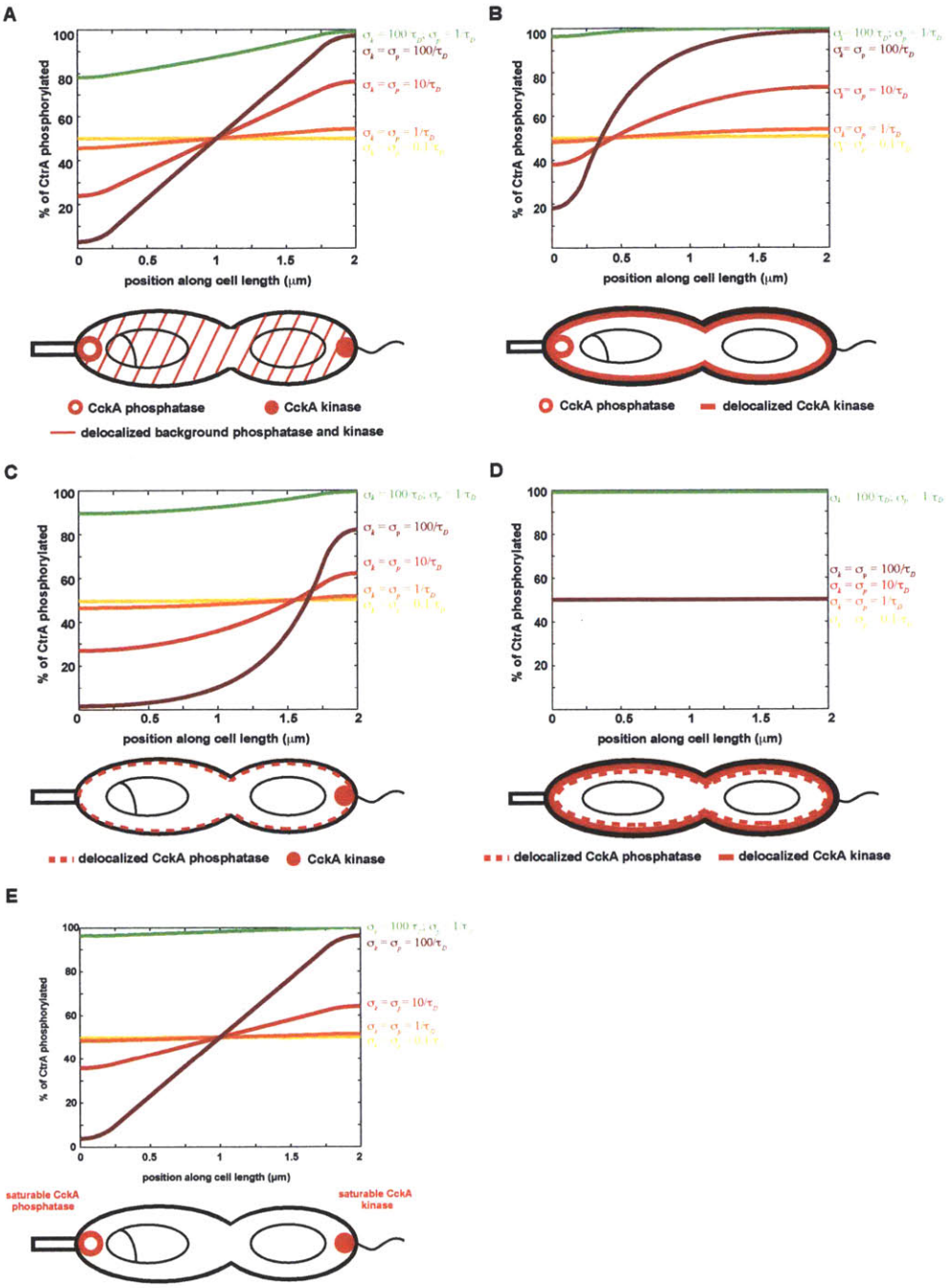

Figure 3.10. CtrA~P asymmetry can be established if either phosphorylation or dephosphorylation, but not both, is delocalized. (A) Low levels of delocalized background phosphotransfer activity with rate $0.1/\tau_D$ have little effect on the gradients shown in Fig. 4A. (B, C) A delocalized exogenous kinase (B) or phosphatase (C) will also generate spatial gradients in CtrA~P if the phosphorylation and dephosphorylation rates are fast compared with $1/\tau_D$ and the opposing activity remains localized. (D) The spatial gradient is completely eliminated when both kinase and phosphatase activity is delocalized. (E) Modeling predicts that saturation of the phosphorylation and dephosphorylation of CtrA at 10% of its average cellular concentration (see Methods) does not abolish the spatial asymmetry in CtrA~P when the phosphorylation and dephosphorylation rates, σ_k and σ_p, are large compared with $1/\tau_D$.

Finally, we used our model to address the potential roles of localized CtrA synthesis or proteolysis in gradient formation. We assumed that synthesis produces unphosphorylated CtrA while degradation does not distinguish between CtrA and CtrA~P. Although the absolute levels of CtrA activity will depend on total CtrA protein levels, our model predicts that the shape of the gradient (and hence the relative asymmetry) is insensitive to the location or amount of CtrA synthesis, because diffusion between the poles is fast relative to the rate of CtrA synthesis. Because the protease for CtrA is often polarly localized in stalked cells [21], we also considered a model in which CtrA proteolysis is concentrated at the stalked pole. Such asymmetry in proteolysis also did not significantly affect a gradient of CtrA~P unless the half-life of CtrA protein was comparable to, or shorter than, τ_D (on the order of seconds or faster) (Fig. 3.11A). However, we measured a half-life for CtrA in predivisional cells of ~60 minutes (Fig. 3.11B-C), several orders of magnitude too slow to impact a phosphorylation gradient. Moreover, if the rate of proteolysis at the stalked pole were comparable to $1/\tau_D$, a clear signature would be a gradient of CtrA protein, which we do not observe with YFP-CtrA. Finally, we note that while the protease for CtrA is often localized in stalked cells, it is usually dispersed in predivisional cells [21], and our model predicts that dispersed proteolysis at a rate that is slow compared with $1/\tau_D$ would also not significantly impact a phosphorylation gradient. We conclude that replicative asymmetry depends primarily on the phosphorylation and dephosphorylation of CtrA and not on proteolysis or synthesis, specifically because phosphorylation state can be modified on time scales faster than diffusion.

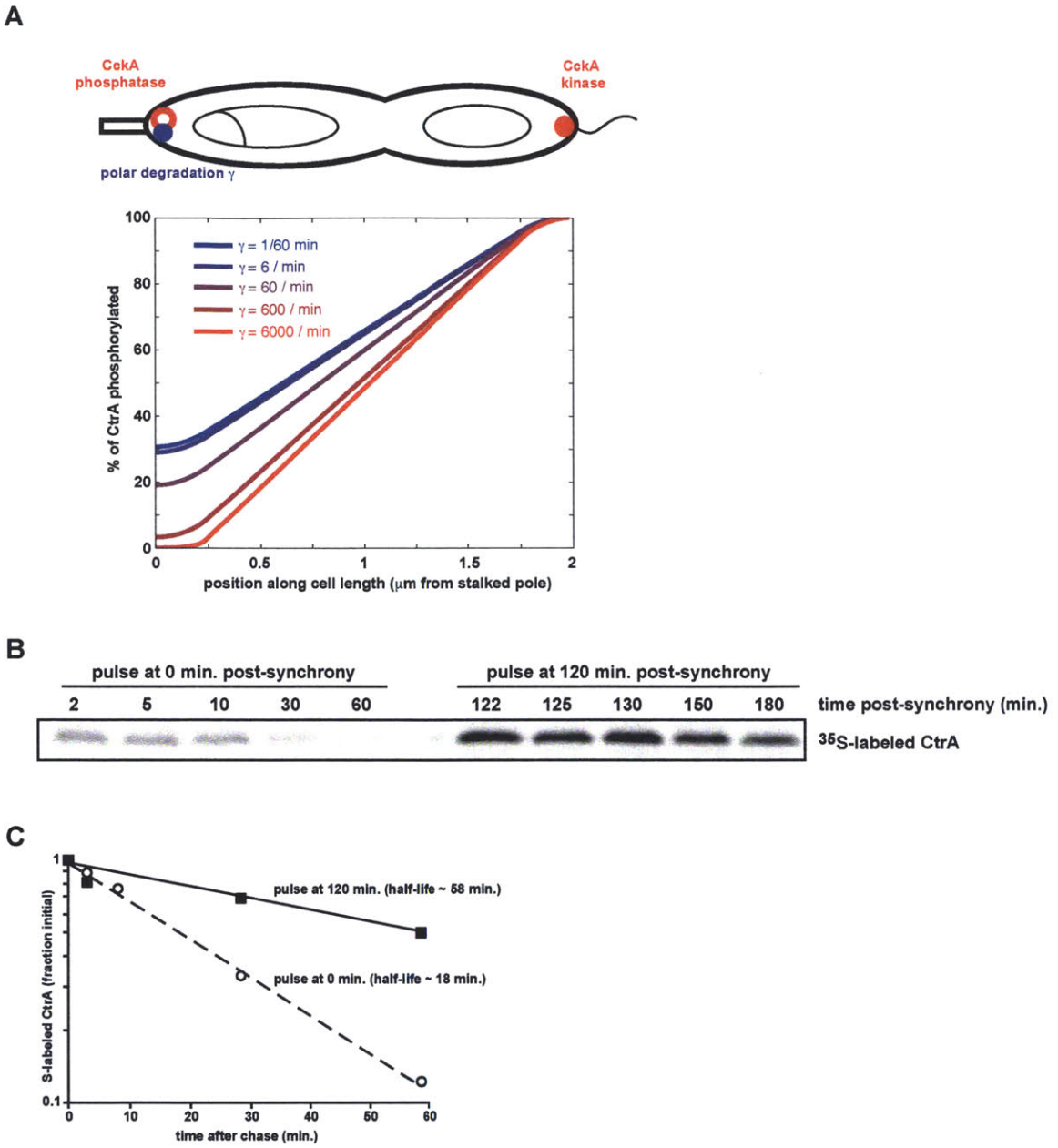

Figure 3.11. CtrA proteolysis does not significantly contribute to the CtrA~P gradient. (A) Mathematical modeling of the effects of CtrA proteolysis on the distributions of CtrA~P using a 1D reaction-diffusion model; proteolysis (represented by the blue circle) is assumed to be concentrated at the stalked pole (see Methods for details). For the experimentally measured CtrA half-life of 60 min (rate ~0.0003/sec), the spatial gradient generated by CckA-mediated phosphorylation with rate σ_k=100/sec and dephosphorylation with rate σ_p=10/sec is almost completely unaffected (purple curve). (B) Pulse-chase analysis of CtrA protein stability in synchronized cultures of wild type CB15N. Swarmer cells were synchronized, released into fresh M2G, and CtrA stability measured either immediately or after 120 minutes. (C) Exponential fit to pulse-chase data from panel A. The half-lives of CtrA in cells pulsed immediately or 120 minutes after release into M2G were calculated to be 18 and 58 minutes, respectively.

Discussion

Spatial homogeneity of a protein's *abundance* throughout the cell does not necessitate spatial homogeneity of the protein's *activity*. Here, we provided evidence that although YFP-CtrA is uniformly distributed in a *Caulobacter* predivisional cell, CtrA~P forms a gradient. We observed a remarkable spatial bias for DNA replication in predivisional cells with initiation occurring much more frequently at the stalked pole. Because chromosomal origins are tethered to opposite poles in *Caulobacter* predivisional cells and are silenced by CtrA~P, this replication bias reflects an underlying asymmetry in CtrA phosphorylation at the poles. This asymmetry in CtrA phosphorylation depends on the bifunctional enzyme CckA. Although localized to both poles, our data suggest a difference in activity state of polar CckA in predivisional cells, with a strong bias toward the kinase state at the swarmer pole and toward the phosphatase state at the stalked pole (Fig. 3.9B). The gradient of phosphorylated CtrA identified here thus establishes replicative asymmetry before cytokinesis, which then locks in the existing spatial bias in CtrA activity.

Although it is often assumed that diffusion eliminates spatial variations in protein concentrations at this short length scale and on time scales relevant to cell division, our data indicate that phosphorylated CtrA, a freely diffusible protein, forms a robust gradient. Given the prevalence of two-component signaling systems in bacteria, there may be other regulators that have uniform protein distribution but spatially heterogeneous activity. Our work reveals a pressing need for phosphorylation state-specific reporters of bacterial proteins. There may also be other enzyme pairs with opposing, spatially segregated activities that can produce gradients, such as the diguanylate cyclases and

phosphodiesterases that produce and degrade, respectively, the bacterial second messenger c-di-GMP [22]. In sum, while the advent and application of GFP technology has clearly demonstrated that bacterial proteins can be targeted to specific cellular locations, our results suggest yet another level of spatial organization operating on protein activity.

Materials and Methods

Growth conditions

Escherichia coli and *C. crescentus* strains were grown as described previously [23]. Strains, plasmids, and primers used in this study are listed in Table S1. All plasmids were introduced into *C. crescentus* by electroporation or by conjugation with *E. coli* S17 cells as described previously [24]. PCR amplification of genes and promoters from CB15N genomic DNA was performed under previously described conditions [23].

For analysis of synchronized populations, mixed populations were grown in PYE and induced and synchronized using Percoll density centrifugation as previously described [25]. Synchronized swarmer cells were resuspended in PYE to an OD_{600} of 0.2-0.3. For movies of mixed populations, cells were grown in PYE to an OD_{600} of 0.2-0.3. Synchronized swarmer or mixed population cells were spotted onto 1.2%-1.5% agarose (UltraPure Agarose, Invitrogen) PYE pads containing 0.3% xylose. Cephalexin (36 μg/ml) was added to the pads when indicated.

Strain construction

All strains and plasmids are listed in Table 3.1. To construct *C. crescentus* strain ML1753, ϕCr30-based transduction of a chloramphenicol-marked, temperature sensitive *divL(A288V)* allele ($divL^{ts}$) [19] from ML1798 was used to replace wild-type chromosomal *divL* in the FROS strain (MT16) [14]. To construct strain ML1798, a C-terminal fragment of *divL(A288V)* was amplified from PC4403 with primers divLfulllengthrev and divLfwd1788 [19]. The PCR product was digested with EcoRI and KpnI and ligated into those sites in pMCS6, a chloramphenicol-marked integration

vector [26]. The resulting plasmid (pMCS6:*divL(A288V)*) was electroporated into CB15N.

To construct strain ML1754, 1261 bp of *cckA(V366P)* were amplified from pML83:P_{xyl}-*cckA(V366P)* with primers CckA_EcoRI_Fw and CckA_HindIII_Rev, which added a 5' EcoRI site and 3' HindIII site. This fragment of *cckA(V366P)* was then TOPO cloned into pCR2.1-TOPO (Invitrogen), sequenced, and then digested with EcoRI and HindIII, and ligated into the integration vector pNPTS138, also digested with EcoRI and HindIII. The resulting plasmid pNPTS138-*cckA(V366P)* was electroporated into the FROS strain (MT16). Clones in which the plasmid had recombined were counterselected on sucrose and screened by sequencing of the *cckA* gene for the correct markerless replacement of wild type *cckA* with the mutant allele.

To construct strain ML1756, a C-terminal fragment of *divL* without the stop codon was amplified by PCR with primers divLfulllengthrev and divLfwd1788. The *divL* PCR product was cloned in frame with the *egfp* gene in pGFPC-4 using KpnI and EcoRI restriction sites. The plasmid was recombined into CB15N by electroporation to generate chromosomally encoded *divL-egfp*.

To construct strains ML1793 and ML1794, the *tetO* cassette in MT16 was first PCR amplified using primers CC0006_HindIII_fw and M13R_EcoRI. This PCR product was digested with HindIII and EcoRI and ligated into the *Caulobacter* integration vector pNPTS138, also digested with HindIII and EcoRI. The resulting plasmid pNPTS138:*cc0006-tetO* was electroporated into the origin mutant 'bc_Ld' strain GM3193 and 'bd' strain GM3103 [20]. A ϕCr30-based transduction with phage lysate from MT16

and selection on spectinomycin was then used to insert *lacI-ECFP-tetR-EYFP* at the *xylX* locus.

To construct strain ML1876, P_{xyl}-*ftsZ*::kan was transduced from YB1585 [27] into a strain containing the *tetO* cassette at the origin and P_{van}-*tetR-YFP* at the *vanA/B* locus.

Table 3.1 - Strains, Plasmids, Primers

Organism or Category	Name	Genotype, Plasmid description, or Primer Sequence	Source
C. crescentus	CB15N	synchronizable derivative of wild-type CB15	[28]
	GM3193	*ori(bc$_L$d)*	[20]
	GM3103	*ori(bd)*	[20]
	LS4259	pKR173 (pMR20:Pxyl-*YFP-ctrA*) (gent^R)	[29]
	MT16	*cc0006*::*(tetO)$_n$* (gent^R) + *xylX*::*lacI-ECFP, tetR-EYFP* (spec^R) (gent^R, spec^R)	[14]
	PC4403	*divL346 (divL^{ts})*	[19]
	ML1506	pJS14:Pxyl-ctrA (chlor^R)	[30]
	ML1681	*cckA-EGFP*::gent (gent^R)	[10]
	ML1753	*divL^{ts}*::chlor in MT16 (chlor^R, spec^R, gent^R)	this study
	ML1754	*cckA(V366P)* in MT16 (spec^R, gent^R)	this study
	ML1755	*ΔpleC*::tet in MT16 (tet^R,spec^R,gent^R)	this study
	ML1756	*divL-EGFP*::gent (gent^R)	this study
	ML1793	*ori(bc$_L$d) + cc0006::(tetO)$_n$ (gent^R, kan^R) + xylX::lacI-CFP, tetR-YFP (spec^R)* (kan^R, gent^R, spec^R)	this study
	ML1794	*ori(bd) + cc0006::(tetO)$_n$ (gent^R, kan^R) + xylX::lacI-CFP, tetR-YFP (spec^R)* (kan^R, gent^R, spec^R)	this study
	ML1795	*cckA^{ts}* in MT16 (spec^R, gent^R)	this study
	ML1798	*divL^{ts}::chlor* (chlor^R)	this study
	ML1876	*Pxyl-ftsZ (kan^R) + cc0006::(tetO)$_n$ (gent^R) + vanA::tetR-YFP* (kan^R, gent^R)	this study
E. coli	DH5a	general cloning strain	Invitrogen
	TOP10	strain for constructing pENTR-TOPO clones	Invitrogen
General purpose vectors	pJS14	derivative of pBBR1MCS, high-copy replicon (chlor^R)	Lab collection
	pJS71	derivative of pBBR1MCS, high-copy replicon (spec^R)	Lab collection
	pML83	P_{xyl} oriented against P_{lac}, inserted into EcoRI site of pJS71 (chlor^R)	Lab collection
	pMR10	broad host range, low copy vector (kan^R)	Lab collection
	pMR20	broad host range, low copy vector (tet^R)	Lab collection
	pNPTS138	Integration vector (kan^R)	Lab collection
	pGFPC-4	Integration vector for c-terminal tagging of desired protein with EGFP (gent^R)	[26]
	pMCS-6	Integration vector (chlor^R)	[26]
Integration plasmids	pNPTS138:*cckA(V366P)*	for markerless allelic replacement of *cckA*	this study
	pNPTS138:*cc0006-tetO*	for integration of *tetO* cassette at *cc0006*, near the origin	this study
	pGFPC-4:*cckA-GFP*	for replacing *cckA* with *cckA-EGFP* on the chromosome	this study
	pGFPC-4:*divL-GFP*	for replacing *divL* with *divL-EGFP* on the chromosome	this study
	pMCS-6: *divL(A288V)*	for integration of *divL^{ts}* at the native locus	this study
Overexpression plasmids	pJS14:P_{xyl}-*ctrA*	high-copy plasmid, xylose-inducible expression of *ctrA* (pID42)	[30]
	pML83:P_{xyl}-*cckA(V366P)*	high-copy plasmid, xylose-inducible expression of *cckA(V366P)*	[10]
Primers	CckA_497_EcoRI_Fw	GAATTCtgcgggcggacggctgatga	this study
	CckA_1717_HindIII_Rev	AAGCTTtcgtcctcgacgaacaggat	this study
	CC0006_HindIII_fw	cagcagcagaagcttATGGCCCAGTTCCAGACCCT	this study
	M13R_EcoRI	cagcagcaggaattcCACAGGAAACAGCTATGA	this study
	divLfulllengthrev	cagcagcaggaattctcGAAGCCGAGTTCGGGCTGC	this study
	divLfwd1788	cagcagcagggtaccCGTGCTGGACATGGCCCA	this study

Flow cytometry

Wild type CB15N were grown in PYE and wild type *E. coli* K12 were grown in LB. At time 0, cephalexin (36 μg/ml) was added to both *Caulobacter* and *E. coli* cultures to stop cell division. Rifampicin (60 μg/ml for *Caulobacter*, 300 mg/ml for *E. coli*) was then added to cultures at either t=0 to prevent new rounds of DNA replication or at a later time to allow for one additional round of replication in division-inhibited cells (60 minutes for *Caulobacter* and 15 minutes for *E. coli*). After rifampicin addition, cells were incubated at 30°C for 4 hours (*Caulobacter*) or at 37°C for 3 hours (*E. coli*) to allow for completion of ongoing rounds of replication before sample collection. Processing and flow cytometry of samples was performed as previously described for *Caulobacter* [10] and *E. coli* [31].

Pulse-chase analyses

For determining CtrA half-life, cultures of ML1506, which contains *ctrA* driven by a xylose-inducible promoter on a medium-copy plasmid, were grown in M2G at 30°C until OD_{600} reached ~0.3. Expression of plasmid-encoded *ctrA* was then induced with 0.03% xylose for 1.5 hours before synchronization. For measurement of CtrA half-life, a synchronized culture was either pulse-labeled immediately after release into M2G or grown for 120 minutes in M2G supplemented with cephalexin (36 μg/ml) before pulse-labeling. Cells were pulsed for 2 minutes with 10 μCi ml^{-1} [^{35}S]-methionine and then chased with excess cold methionine and casamino acids. 1 ml of culture was collected at each time point indicated and flash-frozen in liquid nitrogen. After resuspending cell pellets in 50 ml SDS buffer and boiling for 2 min, the cell lysate was resuspended in 800 ml IP wash buffer (50 mM Tris-HCl pH 8, 150 mM NaCl, 1 mM EDTA, 0.5% Triton X-

100) and pre-cleared with 25 µl Staph A cells (Calbiochem) for 10 minutes on ice. Each sample was then spun down and the pre-cleared supernatant transferred to a new tube. CtrA antiserum (Covance) was added at a dilution of 1:550 and rocked gently at 4°C overnight; 30 µl protein A-agarose (Invitrogen) was then added for 1 h. The immunoprecipitate was collected by centrifugation, washed three times with IP wash buffer, resuspended in 15 µl of SDS sample buffer, and boiled for 4 min. The resulting samples were resolved by SDS-PAGE. The gel was dried and exposed against a Phosphor Screen (Molecular Dynamics) for at least 5 days. Labeled protein bands were scanned and quantified using a PhosphorImager with ImageQuant software (Molecular Dynamics).

Determination of the phosphoryl group half-life of CtrA~P was done as previously described [32] with the following modifications. A synchronized culture of the wild-type FROS strain (MT16) was grown in M5G for 80 minutes until they had reached the predivisional stage. The cells were then labelled for 5 minutes with 90 µCi [γ^{32}P]-ATP per ml culture and the first sample collected. After labeling, the cells were chased with an excess of cold ATP (1 mM). Samples were then immunoprecipitated using CtrA antiserum (Covance).

Fluorescence recovery after photobleaching analyses

FRAP experiments were performed on a Nikon Eclipse Ti inverted microscope with a Nikon Plan Apo 100x objective (numerical aperture of 1.4) and a Haison plexiglass chamber heated with an Air-Therm Atx heater to maintain cells at 30°C. Images were recorded with an Andor DU-885 camera. A 405 nm solid state Ixon laser passed through a Chroma CFP filter cube was used for illumination. The laser formed a Gaussian spot

with a full-width-half-maximum size of ~3 μm. Cells constitutively expressing YFP-CtrA were grown on agarose pads containing cephalexin for 90 minutes and then imaged. YFP-CtrA levels in each cell was measured with a 1 second exposure, followed by bleaching of a polar region with the laser for 200 msec. YFP-CtrA levels were then measured every second (with one second exposures) for nine seconds to assess recovery. Forty-seven cells were analyzed and a representative cell is shown in Fig. S1C. For comparison, a cell in which compartmentalization had already occurred is shown in Fig. S1D. All imaging and FRAP was done with an ND8 filter. Image analysis was done in Excel and Matlab using a modified version of PSICIC (http://www.molbio1.princeton.edu/labs/gitai/psicic/psicic.html).

Determination of cell length

To measure cell lengths, a freehand line in ImageJ (http://rsbweb.nih.gov/ij/) was drawn through the middle of the cell running from the pole to pole. The pixel length of this line was then converted to mm based on the magnification used.

Reaction-diffusion model of CtrA~P dynamics

Our reaction-diffusion model of the CckA/DivL/CtrA system is described in the main Methods section. Additional details are provided here.

To model the effects of ChpT on CtrA~P asymmetry, we treat σ_k=100/sec and σ_p=10/sec as the phosphotransfer rates between CckA and ChpT, and assume that phosphotransfer between ChpT and CtrA occurs at the poles at the rate 100/sec. We assume that the concentration of ChpT is significantly higher than CckA, such that ChpT is not a bottleneck for CtrA phosphorylation. When ChpT spends a significant fraction of the

time bound to CckA, the phosphorylation and dephosphorylation of CtrA again occurs predominantly at the poles and there is a linear gradient of CtrA~P with higher levels of CtrA~P at the swarmer pole. If ChpT is free to diffuse, CckA produces opposing linear gradients of ChpT and ChpT~P, identical to the gradients of CtrA and CtrA~P in Fig. 2A. These gradients of CtrA phosphorylation and dephosphorylation are still able to maintain an asymmetric distribution of CtrA~P (Fig. S4A), with similar effects to delocalizing the kinase activity of CckA (Fig. S6B).

If the population of CtrA is very large, the CckA population could saturate, reducing the kinase and phosphatase rates in a CtrA and CtrA~P concentration-dependent manner, respectively. In Fig. S6E, we incorporate saturation of CckA at high CtrA concentration by multiplying σ_k and σ_p by $(1+[\text{CtrA}]/K)^{-1}$ and $(1+[\text{CtrA~P}]/K)^{-1}$, respectively, where K is 10% of the total amount of CtrA. We verified that saturation has little effect on a gradient (Fig. S6E), since the concentrations of CtrA and CtrA~P are kept low at the swarmer and stalked poles, respectively, by the activities of CckA.

Markov model of CtrA~P replication inhibition

If CtrA~P is the only determinant of the timing of origin firing, the average duration before firing events is determined by the steady-state densities at the poles. To determine the dependence of replication asymmetry on the number of CtrA~P binding sites, we varied the number of independent binding sites n_b between 2 and 4 binding sites (sites a and b are cooperative and hence treated as a single site [33]), and assumed that binding of CtrA~P to any one site is sufficient to inhibit replication initiation. Given a CtrA population of 10,000 molecules, the number of CtrA~P molecules available to bind to the origin within a volume of $(50\text{ nm})^3$ is between 0 and 20, depending on the gradient of

concentration in Fig. 2A. We selected rates of CtrA~P binding (σ_b) and unbinding (σ_u) to match the average time of initiation in wild-type cells. We assumed that replication initiates rapidly as soon as all binding sites are empty. This selection of DNA-binding volume and rate constants illustrates the qualitative dependence of firing time on the number of binding sites, although other pairs of values (σ_b, σ_u) and numbers of CtrA~P also produce the same initiation time. We ignored diffusion within this volume given that comparatively slow time scales of binding are required to reproduce measured firing times. The number of sites bound by CtrA~P was varied stochastically using a Monte Carlo algorithm, and we calculated the probabilities P_i of i=1,2,...,n_b sites being occupied. The average time before firing in 1000 simulations (Fig. 3C) was determined as $\langle T \rangle = (P_1 \sigma_u)^{-1}$, where we have assumed that multiple simultaneous unbinding events is extremely unlikely.

Microscopy

Imaging was performed on a Zeiss Axiovert 200 microscope with a 63x phase objective fitted with an objective heater (Bioptechs). The stage was fitted with a culture dish heater (Warner Instruments). Imaging was performed at 30°C or 34°C. We examined *divL*^{ts} and *cckA*^{ts} strains at 34°C because at 37°C, under our movie conditions, many cells failed to segregate their chromosomes; individual origin foci increased in intensity indicating rereplication had occurred, but segregation of the new origins was impaired.

For analysis of synchronized cells, the stalked pole was determined as the pole proximal to the initial, single origin. For analysis of unsynchronized cells, we followed the two daughter cells of each mother cell that was in the late predivisional stage at the beginning of the movie. The poles of the mother cell become the stalked poles of each daughter cell

while the two poles formed upon cytokinesis of the mother cell become the nascent swarmer poles of each daughter cell in the predivisional stage. Fluorescence images were taken every 6 minutes, and origin firing was designated as bipolar if the two origins in a predivisional cell fired within one frame of each other. Replication patterns were counted in cells that replicated; some cells did not grow or lysed, presumably due to the effects of growth on cephalexin or on an agarose pad. To confirm the quantification of replication patterns, a member of the lab who did not collect the microscopy data performed a blind quantification of two strains (wild type and *cckA(V366P)*). The results fit within the error bars shown in Fig. 3.12

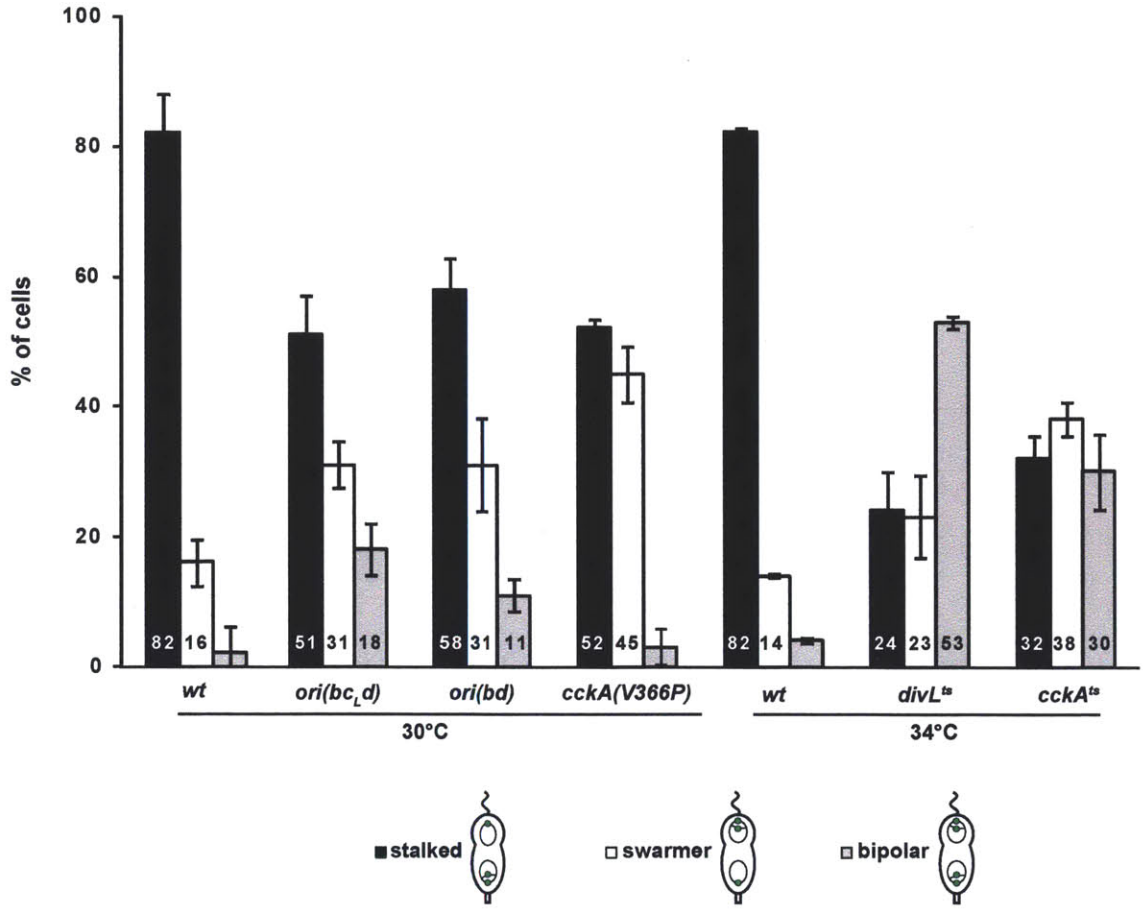

Figure 3.12. Summary of spatial patterns of DNA replication. Quantification of DNA replication patterns in predivisional cells of the strains indicated. Error bars represent standard deviations for quantifications from three independent cultures, processed on three different days.

Reaction-diffusion model of CtrA~P dynamics

We developed a reaction-diffusion model of the CckA/DivL/CtrA system consisting of two equations describing the spatial and temporal evolution of the [CtrA] and [CtrA~P] densities:

$$\frac{\partial[\mathrm{CtrA}]}{\partial t} = \overbrace{D\frac{\partial^2[\mathrm{CtrA}]}{\partial x^2}}^{\text{Diffusion}} - \overbrace{\left(\sigma_k Sw(x)+\sigma_k^0\right)[\mathrm{CtrA}]}^{\text{Phosphorylation}} + \overbrace{\left(\sigma_p St(x)+\sigma_p^0\right)[\mathrm{CtrA}\sim\mathrm{P}]}^{\text{Dephosphorylation}} + \overbrace{\tilde{\alpha}}^{\text{Synthesis}} - \overbrace{\gamma(x)[\mathrm{CtrA}]}^{\text{Degradation}}$$

$$\frac{\partial[\mathrm{CtrA}\sim P]}{\partial t} = D\frac{\partial^2[\mathrm{CtrA}\sim\mathrm{P}]}{\partial x^2} + \left(\sigma_k Sw(x)+\sigma_k^0\right)[\mathrm{CtrA}] - \left(\sigma_p St(x)+\sigma_p^0\right)[\mathrm{CtrA}\sim\mathrm{P}] - \gamma(x)[\mathrm{CtrA}\sim\mathrm{P}]$$

We used the Einstein relation ($D = k_BT/6\pi\eta R$) and the 23 kDa molecular weight of CtrA to estimate an upper bound on the CtrA diffusion constant $D \sim 8$ μm^2/sec. Our FRAP studies demonstrated full recovery of photobleaching at the poles within 1-8 seconds in the majority of cells examined (Fig. B.S1C, Appendix B), indicating that D ~ 1-10 μm^2/sec. For all calculations, we assume D = 2 μm^2/sec and is independent of phosphorylation state. Any reduction in D caused by factors such as DNA binding only enhances the gradient of CtrA~P. The functions $Sw(x)$ and $St(x)$ are 1 at the swarmer and stalk poles, respectively, and zero elsewhere. The poles occupy 1/8 of the cell length, except in Fig. B.S4B, Appendix B where they range from 1/8 to 1/40 of the cell length. The uniform appearance of YFP-CtrA indicates that CtrA does not spend a significant amount of time in an immobile bound state, hence the rate constants σ_k and σ_p representing the phosphorylation and dephosphorylation of CtrA, respectively, are assumed to be linearly dependent on the concentration of CckA. Unless otherwise stated, we set these rates at 100/sec and 10/sec, respectively, which are conservative, lower-bound estimates. For predivisional cells with CtrA and stalked pole-localized CckA

numbering 10,000 [15] and 50 molecules, respectively, a half-life of the phosphoryl group on CtrA~P on the order of seconds (Fig. B.S3, Appendix B) implies a rate of CtrA dephosphorylation by each CckA molecule on the order of 100/sec. The rate of CtrA phosphorylation must be even faster as there is a net accumulation of phosphorylated CtrA in predivisional cells. We assume that other cytoplasmic sources of phosphorylation and dephosphorylation are uniformly distributed and, except for Fig. B.S6, are slow enough (0.1/sec) to only define the overall levels of CtrA~P in the absence of CckA.

To analyze CtrA~P asymmetry in mutants, we set $\sigma_k = 0$ for $divL^{ts}$ and $\sigma_p = 0$ for *cckAV366P*. For $divL^{ts}$, we assume that CckA remains as a phosphatase at the swarmer pole. In Figs. 1E and 2A, we ignore CtrA synthesis ($\alpha = 0$) and proteolysis ($\gamma = 0$). In Fig. B.S8, we investigate the effects of stalk pole-localized proteolysis using the function $\gamma(x) = \gamma_0 St(x)$. The phosphorylated fraction of CtrA determined by Eqs. 1-2 is independent of the amount of CtrA protein.

Acknowledgements. We thank Z. Gitai, N. Wingreen, R. Phillips, T. Ursell, and J. Modell for comments on the manuscript, and C. Aakre for constructing strain ML1876. M.T.L. is an Early Career Scientist at the Howard Hughes Medical Institute. This work was supported by a NIH grant (5R01GM082899) to M.T.L. and an NIH Director's New Innovator award (DP2OD006466) to K.C.H. K.J. is supported by a research fellowship from the German Research Foundation.

References

1. Lander, A.D. (2007). Morpheus unbound: reimagining the morphogen gradient. Cell *128*, 245-256.

2. Dehmelt, L., and Bastiaens, P.I. (2010). Spatial organization of intracellular communication: insights from imaging. Nat Rev Mol Cell Biol *11*, 440-452.

3. Parent, C.A., Blacklock, B.J., Froehlich, W.M., Murphy, D.B., and Devreotes, P.N. (1998). G protein signaling events are activated at the leading edge of chemotactic cells. Cell *95*, 81-91.

4. Berg, H.C., and Purcell, E.M. (1977). Physics of chemoreception. Biophys J *20*, 193-219.

5. Raskin, D.M., and de Boer, P.A. (1999). MinDE-dependent pole-to-pole oscillation of division inhibitor MinC in Escherichia coli. J Bacteriol *181*, 6419-6424.

6. Quon, K.C., Yang, B., Domian, I.J., Shapiro, L., and Marczynski, G.T. (1998). Negative control of bacterial DNA replication by a cell cycle regulatory protein that binds at the chromosome origin. Proc Natl Acad Sci U S A *95*, 120-125.

7. Laub, M.T., Chen, S.L., Shapiro, L., and McAdams, H.H. (2002). Genes directly controlled by CtrA, a master regulator of the Caulobacter cell cycle. Proc Natl Acad Sci U S A *99*, 4632-4637.

8. Matroule, J.Y., Lam, H., Burnette, D.T., and Jacobs-Wagner, C. (2004). Cytokinesis monitoring during development; rapid pole-to-pole shuttling of a signaling protein by localized kinase and phosphatase in Caulobacter. Cell *118*, 579-590.

9. Biondi, E.G., Reisinger, S.J., Skerker, J.M., Arif, M., Perchuk, B.S., Ryan, K.R., and Laub, M.T. (2006). Regulation of the bacterial cell cycle by an integrated genetic circuit. Nature *444*, 899-904.

10. Chen, Y.E., Tsokos, C.G., Biondi, E.G., Perchuk, B.S., and Laub, M.T. (2009). Dynamics of two Phosphorelays controlling cell cycle progression in Caulobacter crescentus. J Bacteriol *191*, 7417-7429.

11. Angelastro, P.S., Sliusarenko, O., and Jacobs-Wagner, C. (2009). Polar localization of the CckA histidine kinase and cell cycle periodicity of the essential master regulator CtrA in Caulobacter crescentus. J Bacteriol *192*, 539-552.

12. Marczynski, G.T. (1999). Chromosome methylation and measurement of faithful, once and only once per cell cycle chromosome replication in Caulobacter crescentus. J Bacteriol *181*, 1984-1993.

13. Robinett, C.C., Straight, A., Li, G., Willhelm, C., Sudlow, G., Murray, A., and Belmont, A.S. (1996). In vivo localization of DNA sequences and visualization of large-scale chromatin organization using lac operator/repressor recognition. J Cell Biol *135*, 1685-1700.

14. Viollier, P.H., Thanbichler, M., McGrath, P.T., West, L., Meewan, M., McAdams, H.H., and Shapiro, L. (2004). Rapid and sequential movement of individual chromosomal loci to specific subcellular locations during bacterial DNA replication. Proc Natl Acad Sci U S A *101*, 9257-9262.

15. Judd, E.M., Ryan, K.R., Moerner, W.E., Shapiro, L., and McAdams, H.H. (2003). Fluorescence bleaching reveals asymmetric compartment formation prior to cell division in Caulobacter. Proc Natl Acad Sci U S A *100*, 8235-8240.

16. Iniesta, A.A., Hillson, N.J., and Shapiro, L. (2010). Cell pole-specific activation of a critical bacterial cell cycle kinase. Proc Natl Acad Sci U S A *107*, 7012-7017.

17. Sciochetti, S.A., Ohta, N., and Newton, A. (2005). The role of polar localization in the function of an essential Caulobacter crescentus tyrosine kinase. Mol Microbiol *56*, 1467-1480.

18. Jacobs, C., Domian, I.J., Maddock, J.R., and Shapiro, L. (1999). Cell cycle-dependent polar localization of an essential bacterial histidine kinase that controls DNA replication and cell division. Cell *97*, 111-120.

19. Wu, J., Ohta, N., Zhao, J.L., and Newton, A. (1999). A novel bacterial tyrosine kinase essential for cell division and differentiation. Proc Natl Acad Sci U S A *96*, 13068-13073.

20. Bastedo, D.P., and Marczynski, G.T. (2009). CtrA response regulator binding to the Caulobacter chromosome replication origin is required during nutrient and antibiotic stress as well as during cell cycle progression. Mol Microbiol *72*, 139-154.

21. McGrath, P.T., Iniesta, A.A., Ryan, K.R., Shapiro, L., and McAdams, H.H. (2006). A dynamically localized protease complex and a polar specificity factor control a cell cycle master regulator. Cell *124*, 535-547.

22. Christen, M., Kulasekara, H.D., Christen, B., Kulasekara, B.R., Hoffman, L.R., and Miller, S.I. Asymmetrical distribution of the second messenger c-di-GMP upon bacterial cell division. Science *328*, 1295-1297.

23. Skerker, J.M., Prasol, M.S., Perchuk, B.S., Biondi, E.G., and Laub, M.T. (2005). Two-component signal transduction pathways regulating growth and cell cycle progression in a bacterium: a system-level analysis. PLoS Biol *3*, e334.

24. Ely, B. (1991). Genetics of Caulobacter crescentus. Methods Enzymol *204*, 372-384.

25. Jones, M.W., Peckham, H.M., Errington, M.L., Bliss, T.V., and Routtenberg, A. (2001). Synaptic plasticity in the hippocampus of awake C57BL/6 and DBA/2 mice: interstrain differences and parallels with behavior. Hippocampus *11*, 391-396.

26. Thanbichler, M., Iniesta, A.A., and Shapiro, L. (2007). A comprehensive set of plasmids for vanillate- and xylose-inducible gene expression in Caulobacter crescentus. Nucleic Acids Res *35*, e137.

27. Wang, Y., Jones, B.D., and Brun, Y.V. (2001). A set of ftsZ mutants blocked at different stages of cell division in Caulobacter. Mol Microbiol *40*, 347-360.

28. Evinger, M., and Agabian, N. (1977). Envelope-associated nucleoid from Caulobacter crescentus stalked and swarmer cells. J Bacteriol *132*, 294-301.

29. Iniesta, A.A., McGrath, P.T., Reisenauer, A., McAdams, H.H., and Shapiro, L. (2006). A phospho-signaling pathway controls the localization and activity of a protease complex critical for bacterial cell cycle progression. Proc Natl Acad Sci U S A *103*, 10935-10940.

30. Domian, I.J., Quon, K.C., and Shapiro, L. (1997). Cell type-specific phosphorylation and proteolysis of a transcriptional regulator controls the G1-to-S transition in a bacterial cell cycle. Cell *90*, 415-424.

31. Riber, L., and Lobner-Olesen, A. (2005). Coordinated replication and sequestration of oriC and dnaA are required for maintaining controlled once-per-cell-cycle initiation in Escherichia coli. J Bacteriol *187*, 5605-5613.

32. Jacobs, C., Hung, D., and Shapiro, L. (2001). Dynamic localization of a cytoplasmic signal transduction response regulator controls morphogenesis during the Caulobacter cell cycle. Proc Natl Acad Sci U S A *98*, 4095-4100.

33. Siam, R., and Marczynski, G.T. (2000). Cell cycle regulator phosphorylation stimulates two distinct modes of binding at a chromosome replication origin. EMBO J *19*, 1138-1147.

Chapter 4

Modularity of the bacterial cell cycle enables independent spatial and temporal control of DNA replication

This work is in press as Kristina Jonas*, Y. Erin Chen*, and Michael T. Laub. 2011 Curr Biol.

K.J., Y.E.C., and M.T.L. designed the study, analyzed the data, and wrote the manuscript. Y.E.C. executed the experiments for figures 4.2 and 4.3 and collaborated with K.J. to produce figures 4.11 and 4.12.

*These authors contributed equally to this work.

Abstract

Background: Complex regulatory circuits in biology are often built of simpler sub-circuits, or modules. In most cases, the functional consequences and evolutionary origins of modularity remain poorly defined.

Results: Here, by combining single-cell microscopy with genetic approaches, we demonstrate that two separable modules independently govern the temporal and spatial control of DNA replication in the asymmetrically dividing bacterium Caulobacter crescentus. DNA replication control involves DnaA, which promotes initiation, and CtrA, which silences initiation. We show that oscillations in DnaA activity dictate the periodicity of replication while CtrA governs the asymmetric replicative fates of daughter cells. Importantly, we demonstrate that DnaA activity oscillates independently of CtrA.

Conclusions: The genetic separability of spatial and temporal control modules in Caulobacter reflects their evolutionary history. DnaA is the central component of an ancient and phylogenetically widespread circuit that governs replication periodicity in *Caulobacter* and most other bacteria. By contrast, CtrA, which is found only in the asymmetrically dividing α-proteobacteria, was integrated later in evolution to enforce replicative asymmetry on daughter cells.

Introduction

Important cellular processes are often orchestrated by regulatory circuits involving numerous genes and proteins. These complex circuits are often comprised of simpler parts, or modules, that are interconnected but perform separable functions [1, 2]. A modular architecture of biological systems may enhance evolvability as it allows the generation of new functions or network properties by altering the connections between modules, rather than by creating new networks from scratch. Defining the modularity and evolutionary history of regulatory circuits remains a major challenge. Here, we demonstrate an intrinsic modularity to the *Caulobacter crescentus* cell cycle with two interlinked, but genetically separable circuits governing the temporal and spatial control of DNA replication. *Caulobacter* is an ideal model for investigating the regulation of DNA replication as cells replicate a single chromosome once-and-only-once per cell cycle [3] (Fig. 4.1A). The absence of multi-fork replication facilitates the analysis of DNA replication in individual cells using time-lapse fluorescence microscopy [4].

Table 4.1. Summary of DNA replication periodicity measurements

Strain	Temp.	Replication period[a]	n*
wt	30 °C	69 ± 10 (81 ± 13)	90 (46)
wt	34 °C	67 ± 13 (80 ± 14)	337 (319)
divL^{ts}	34 °C	66 ± 19[b]	243
cckA^{ts}	34 °C	65 ± 21[b]	117
Δ*pleC*	34 °C	73 ± 14 (73 ± 14)	178 (175)
Cori bc$_L$d	34 °C	64 ± 17 (72 ± 17)	395 (331)
FtsZ depletion	34 °C	80 ± 16	113
FtsZ depletion, *divL*^{ts}	34 °C	61 ± 13[b]	232
FtsZ depletion, *Cori bc$_L$d*	34 °C	68 ± 12	50
wt + P$_{xyl}$-*M2-dnaA*[&] (high copy)	30 °C	47 ± 35[b]	228
wt + P$_{xyl}$-*M2-dnaA*[&] (low copy)	30 °C	77 ± 15	77
wt + P$_{xyl}$-*M2-dnaA(R357A)*[&] (low copy)	30 °C	50 ± 33[b]	280
wt + P$_{van}$-*hdaA*[&]	30 °C	95 ± 20 (110 ± 20)	132 (89)
wt + P$_{van}$-*hdaA(Q4A)*[&]	30 °C	78 ± 13 (94 ± 15)	172 (101)
HdaA depletion	30 °C	30 ± 11 / 78 ± 12[c]	26 / 113

[a] The mean values with standard deviations are shown for stalked and swarmer (in parenthesis) replication periods.

[b] For strains that have lost replicative asymmetry due to a loss of CtrA activity (*divL*^{ts} or *cckA*^{ts}) or that initiate significantly earlier than wild type, we did not distinguish between stalked and swarmer replication cycles.

[c] Because the distribution for the HdaA depletion strain appeared bimodal, the periods listed are for those cells with replication periods less than or greater than 48 minutes.

* Number of replication cycles counted.

[&] For strains harboring plasmids with a xylose- or vanillate-inducible promoter, cells were grown in the presence of 0.3% xylose or 2.5 mM vanillate, respectively.

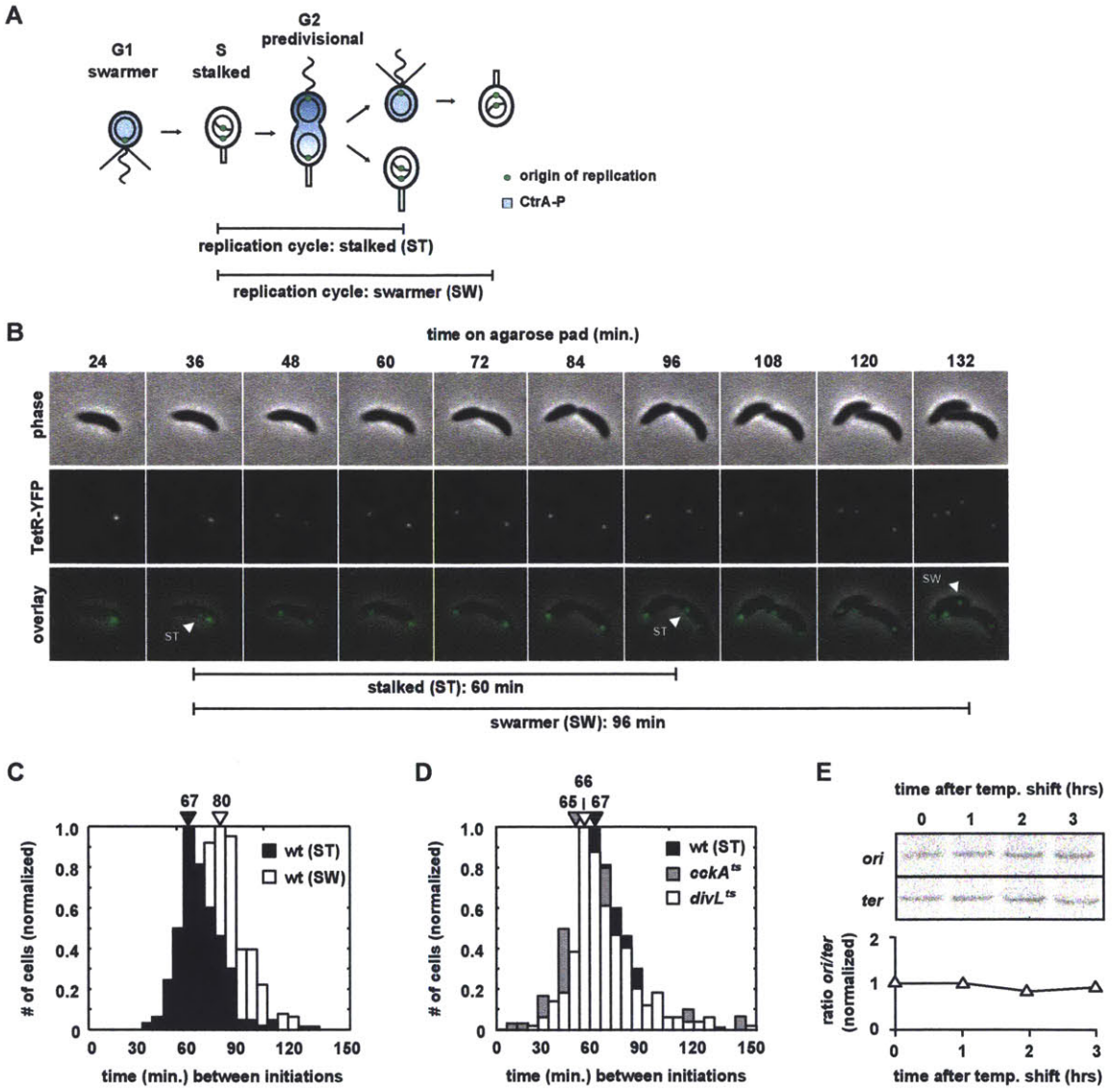

Figure 4.1. A loss of CtrA activity does not perturb DNA replication periodicity. (A) Schematic of the Caulobacter cell cycle showing the stalked (ST) and swarmer (SW) replication cycles. (B) Representative time-lapse images of wild-type cells with TetR-YFP-labeled origins of replication. Arrowheads depict the appearance of a new origin in either stalked (ST) or swarmer (SW) daughter cell. (C) Histograms of wild-type stalked (ST) and swarmer (SW) replication cycles for cells grown at 34°C. Mean values for each population are noted. The number of cells (see Table 4.1) are normalized to 1.0 for visualization. (D) Histograms showing replication cycle periodicity in *divL*^{ts} and *cckA*^{ts} cells compared to wild-type stalked cells at 34°C. (E) Southern blots of DNA near the origin (ori) and terminus (ter) in *divL*^{ts} cells shifted to the restrictive temperature of 37°C at time 0. Band intensities were quantified and ratios normalized to the 0-hr time point.

DNA replication initiation in *Caulobacter* requires DnaA [5], which binds and helps melt the origin of replication to promote initiation. DnaA is a member of the AAA^+ family of ATPases, with DnaA-ATP but not DnaA-ADP active for replication initiation [6-8]. DnaA is highly-conserved and present in all bacteria, with the exception of some obligate endosymbionts [9]. In *E. coli*, DnaA activity is tightly regulated, peaking immediately before replication initiation and then dropping rapidly after initiation [8]. Inactivation depends largely on Hda, which stimulates ATP hydrolysis by DnaA [10].

In *Caulobacter*, every cell division is asymmetric, resulting in daughter cells with different cell fates [11]. The daughter stalked cell immediately initiates replication, whereas the daughter swarmer cell must first differentiate into a stalked cell before replicating. This cell-fate asymmetry and cellular differentiation process depend on CtrA, an essential transcription factor that activates ~100 genes and that also binds to and silences the origin of replication [12-14]. A complex circuit of two-component signaling proteins ensures that swarmer cells phosphorylate and stabilize CtrA to repress replication while stalked cells dephosphorylate and degrade CtrA to permit DNA replication [15-18]. CtrA is again phosphorylated and stabilized in predivisional cells so that it can activate target genes. CtrA is often assumed to also prevent the reinitiation of replication, but mutating CtrA binding sites in the origin does not severely perturb replication control [19].

Although both CtrA and DnaA have been previously studied in *Caulobacter*, the precise roles played by each and the interdependencies of the two regulators remain surprisingly

ill-defined. One current model suggests that CtrA and DnaA are connected through a transcriptional circuit, in which *dnaA* transcription is indirectly activated by CtrA and *ctrA* transcription is indirectly activated by DnaA [20, 21]. This circuit, proposed to drive cell cycle progression, implies that the accumulation of DnaA depends on CtrA activity. However, cells lacking active CtrA accumulate multiple chromosomes [12], indicating that DnaA is likely not limiting in these cells. Moreover, cells constitutively transcribing *dnaA* or *ctrA* do not exhibit a severe replication phenotype [16, 22].

It thus remains unresolved how the task of regulating DNA replication in *Caulobacter* is distributed between CtrA and DnaA and how these two regulators are wired together. To address these issues, we have investigated DNA replication in individual living cells using time-lapse fluorescence microscopy. We provide evidence that periodic changes in DnaA activity determine the periodicity of DNA replication and, importantly, that DnaA activity cycles independently of CtrA. By contrast, CtrA establishes replicative asymmetry by silencing replication in daughter swarmer cells, with no major effect on the periodicity of replication in stalked cells. These findings suggest that DnaA lies at the heart of a primordial cell cycle oscillator that continues to dictate replication timing in *Caulobacter*, as it does in most bacteria, while CtrA was recruited later in evolution to coordinate asymmetric replication with cellular differentiation. The modularity of replication control in *Caulobacter* thus reflects its evolution and reveals its relationship to the cell cycles of other bacteria.

Results

CtrA dictates replication asymmetry but does not influence the periodicity of initiation

To probe the temporal regulation of DNA replication in *Caulobacter*, we monitored replication initiation in individual living cells. We used a fluorescent repressor-operator system in which origins of replication are fluorescently marked by TetR-YFP proteins bound to an array of *tet* operator (*tetO*) sites inserted near the origin [4]. Using time-lapse microscopy, we observed that wild-type stalked cells initially harbor a single, polarly localized origin of replication, represented by a single fluorescent focus (Fig. 1A, B). Shortly after replication initiation, one origin remains at the stalked pole while the other rapidly translocates to the opposite pole [23]. The time at which two separate foci are first visible in an individual cell was used as a proxy for the time of initiation. We then tracked each cell through its cell cycle and measured the time at which each daughter cell initiated replication. Daughter stalked cells typically initiated shortly after cell division whereas the daugther swarmer cells had to first differentiate into stalked cells. We refer to the intervals between replication initiation in a stalked cell and its daughter stalked and swarmer cells as the stalked and swarmer replication cycles, respectively (Fig. 4.1A). For wild type, we observed a stalked replication cycle of ~67 minutes and a swarmer cycle of ~80 minutes (Fig. 4.1B-C), consistent with the known replicative asymmetry of daughter cells.

To investigate whether CtrA influences the periodicity of replication, we analyzed replication in cells harboring either a $divL^{ts}$ or $cckA^{ts}$ mutation, such that CtrA activity decreases after shifting cells to a restrictive growth temperature of 34°C [24-26]. Surprisingly, despite the loss of CtrA activity, and consequently cell division, the $divL^{ts}$

and *cckA*^{ts} mutants accumulated chromosomes with an average time between rounds of DNA replication of 65-66 minutes, nearly identical to that measured in wild-type stalked cells (Fig. 4.1D, 4.2A).

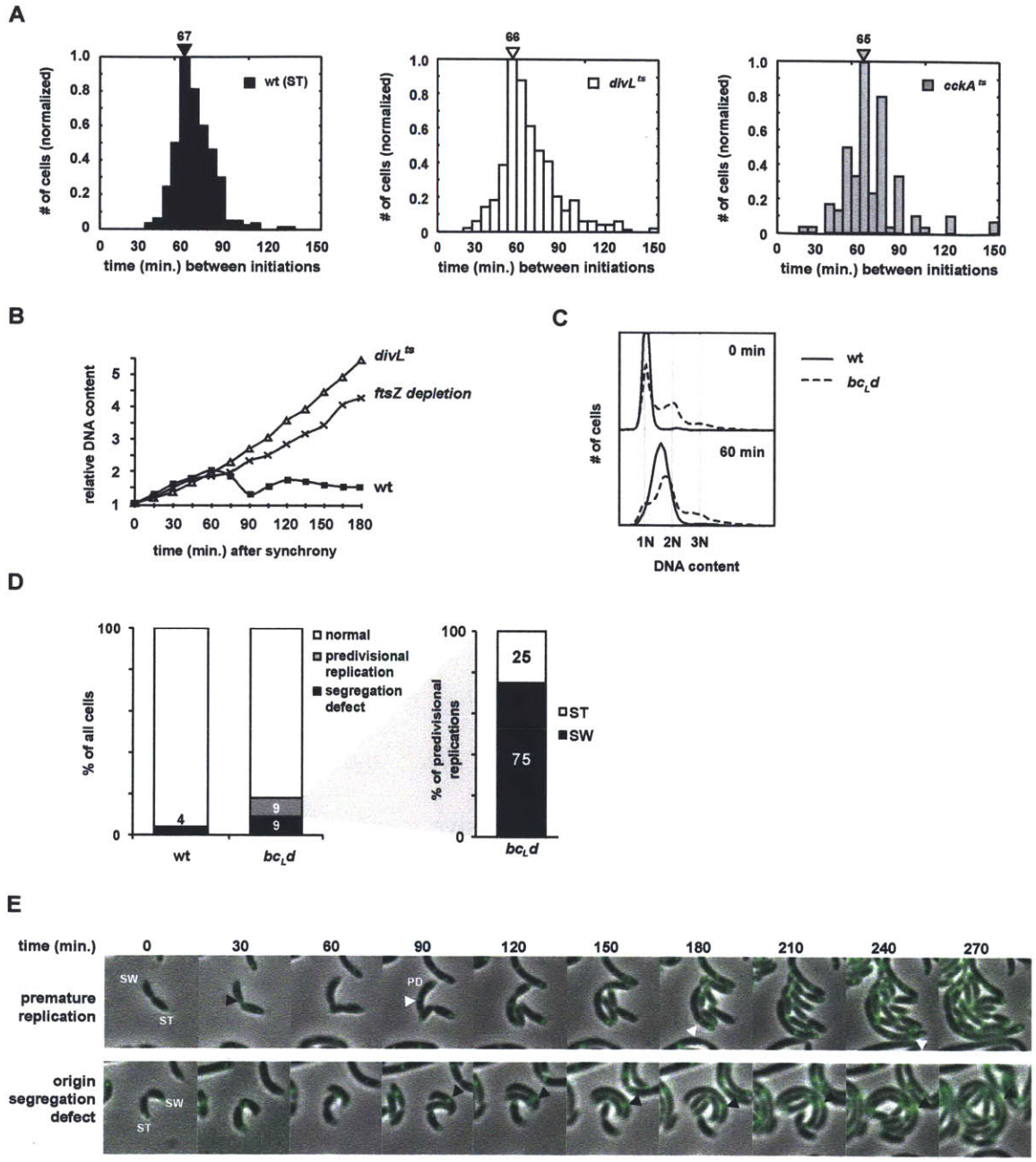

Figure 4.2. CtrA silences replication in swarmer cells. (A) Histograms showing replication cycle periodicity in wild-type stalked cells and in *divL*^{ts} and *cckA*^{ts} cells when grown at 34 °C. These same histograms are overlaid in Figure 1D. (B) Time course of flow cytometry data showing normalized DNA content per cell in synchronized populations of wild-type, *divL*^{ts} and FtsZ-depleted cells. Synchronized swarmer cells were diluted in plain PYE media and shifted to 37oC at time 0. (C) Flow cytometry profiles of synchronized populations of wild-type (solid line) and bc_Ld (dashed line) cells after 0 or 60 minutes of growth. At 0 minutes, a significant population of newly synchronized bcLd swarmer cells has 2N DNA content. At 60 minutes, a significant population of bcLd predivisional cells has 3N DNA content.

(D) Quantification of filamentous cells in wild-type or bc_Ld strains. In wild type, 4% of cells became filamentous, all due to an inability to segregate newly replicated origins (black bar). In bc_Ld mutants, 18% of cells became filamentous; 9% had an apparent origin segregation defect (black bar) and 9% initiated replication inappropriately in predivisional cells (gray bar), an event that never occurred in wild-type cells. Of the predivisional cells that inappropriately replicated, 75% arose from swarmer cells that had replicated prematurely (inset, black bar) while 25% arose from stalked cells (inset, white bar). (E) Time-lapse images of bc_Ld mutant cells with TetR-YFP-marked origins in green overlaid onto phase contrast images. The top panel shows a swarmer cell that prematurely replicated at time 30 (black arrowhead) and developed into a predivisional cell that replicated inappropriately at time 90, 180, and 240 (white arrowheads). The bottom panel shows a swarmer cell that cannot segregate its newly replicated origins (black arrowheads). SW = swarmer cell, ST = stalked cell, PD = predivisional cell. In both cases, the cell is delayed for cell division or unable to divide.

This unexpected result suggests that CtrA is not required to maintain the periodicity of DNA replication nor does CtrA prevent reinitiation during an ongoing round of replication. Using Southern blotting, we verified that the copy-number ratio of origin- and terminus-proximal DNA (*ori/ter* ratio) was unchanged in the $divL^{ts}$ strain after a shift to the restrictive temperature (Fig. 4.1E). An increase in the *ori/ter* ratio would have indicated that extra rounds of replication initiated before prior rounds had completed (hereafter referred to as overinitiation). Thus, $divL^{ts}$ and $cckA^{ts}$ mutants accumulate multiple chromosomes because cells fire successive rounds of DNA replication without intervening cell divisions and not because of overinitiation. These data are consistent with a recent study showing that mutations in the CtrA binding sites in the origin do not lead to significant overreplication [19].

CtrA delays the reinitiation of DNA replication in division-inhibited cells

Because $divL^{ts}$ and $cckA^{ts}$ cannot divide at the restrictive temperature, we wanted to compare replication in these strains to an FtsZ depletion strain, which also cannot divide but maintains CtrA activity. Using flow cytometry to measure total DNA as a function of time, we observed that DNA accumulated in the $divL^{ts}$ mutant faster than in cells depleted of *ftsZ* (Fig. 4.2B). The retention of active CtrA in FtsZ-depleted cells could explain their

slower chromosome accumulation relative to *divL*^{ts} cells. To test this hypothesis, we measured DNA replication in the FtsZ depletion strain using fluorescence microscopy. Consistent with our flow cytometry data, the intervals between replication events stemming from the stalked pole averaged 80 minutes, longer than that of *divL*^{ts} and *cckA*^{ts} cells (Fig. 4.3A). When the FtsZ depletion was combined with the *divL*^{ts} mutation, replication intervals decreased to 61 minutes at the restrictive temperature. Thus, the presence of active CtrA in division-inhibited cells delays replication initiation.

Previously, we found that division-inhibited cells maintain a gradient of phosphorylated CtrA that preferentially inhibits replication at the swarmer pole [24]. Although replication therefore occurs preferentially at the stalked pole in FtsZ-depleted cells, it was still delayed compared to cells without active CtrA, including *divL*^{ts}, *cckA*^{ts}, and wild-type stalked cells (Fig. 4.1D, 4.3A). If this delay depends on the direct binding of residual CtrA to the origin at the stalked pole, it should be possible to shorten the replication period in an FtsZ depletion strain by disrupting CtrA binding sites in the origin. We therefore analyzed replication timing in a strain with mutations in three (bc_Ld) of the five CtrA binding sites in the origin (Fig. 4.3A) [19]. In cells depleted of FtsZ and harboring the bc_Ld mutations, stalked replication cycles were shortened from 80 to 68 minutes. Thus, disrupting CtrA binding to the origin largely restored the normal timing of replication cycles. We conclude that the compartmentalization of cells during cytokinesis is necessary to completely clear CtrA from the stalked cell and to prevent a delay in replication that results from residual CtrA binding to the origin.

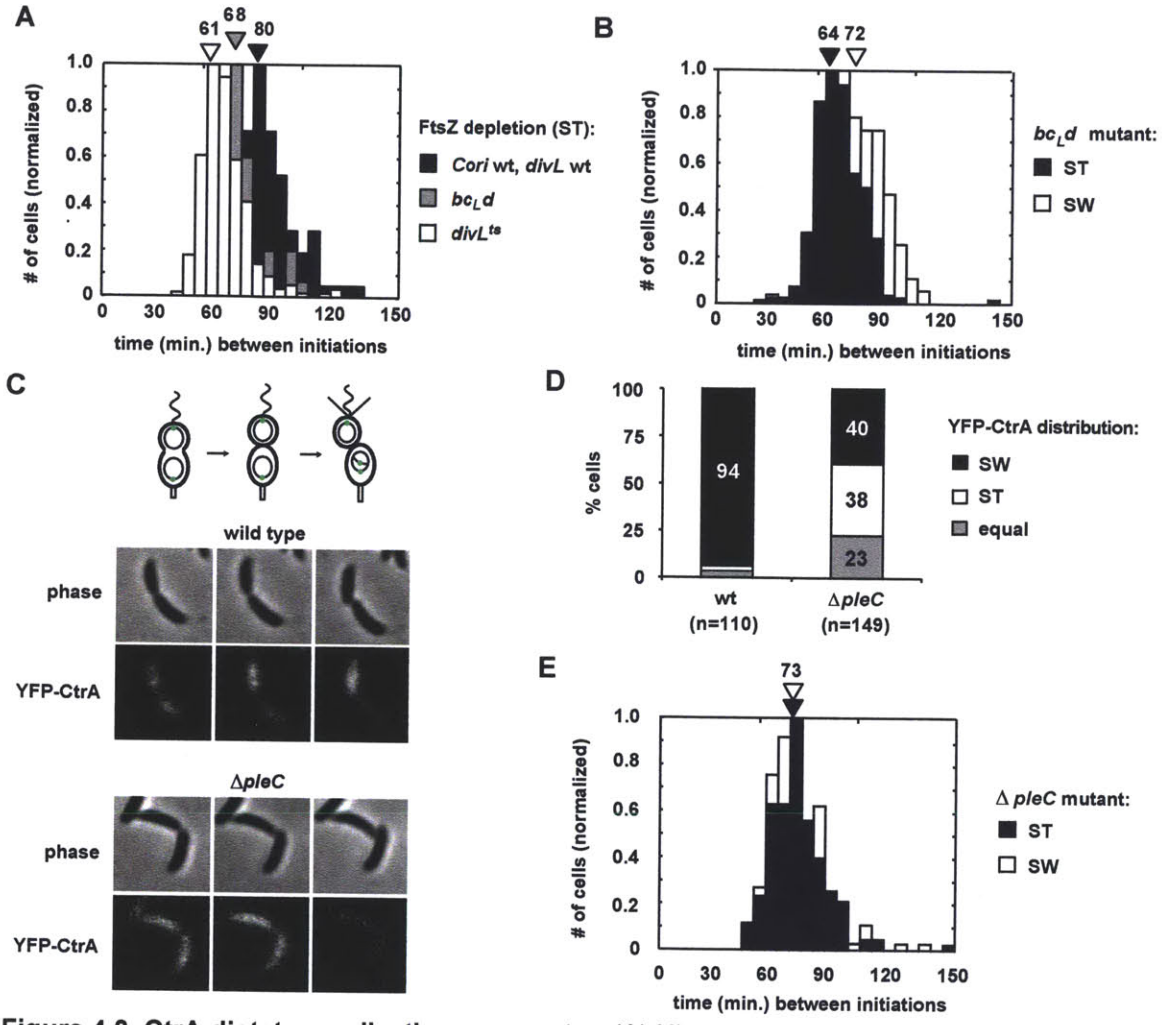

Figure 4.3. CtrA dictates replicative asymmetry. (A) Histograms of replication intervals in FtsZ-depleted cells with or without the divLts or ori(bc_Ld) mutations grown at 34°C. Mean values for each population are indicated. (B) Histograms showing the periodicity of stalked (ST) and swarmer (SW) replication cycles in the ori(bc_Ld) strain. (C) Representative time-lapse images at 10-minute intervals with phase-contrast and epifluorescence images of wild-type or Δ*pleC* cells expressing YFP-CtrA. The schematic shows the wild-type cell-cycle stage for each column. (D) Quantification of YFP-CtrA partitioning ~10 minutes after division in wild-type and Δ*pleC* cells. Pairs of daughter cells were scored for preferentially retaining YFP-CtrA in the swarmer cell, the stalked cell, or neither. (E) Histograms of replication cycle times for Δ*pleC* daughter cells. Daughter cells were designated "stalked" (ST) or "swarmer" (SW) by following inheritance of the old (stalked) or new (swarmer) poles over two consecutive cell cycles.

We also examined DNA replication in cells harboring the bc_Ld origin mutations while maintaining native *ftsZ* expression. In this strain, the stalked replication cycle was 64 minutes, similar to wild type (Fig. 4.3B). However, the swarmer replication cycle averaged 72 minutes, 8 minutes shorter than wild-type swarmer replication cycles (Fig. 4.3B), as bc_Ld swarmer cells often initiated DNA replication prematurely (defined as an initiation event occurring within one frame of initiation in the sister stalked cell). For swarmer cells that initiated prematurely, DNA replication still continued periodically; consequently, the next round of DNA replication sometimes occurred before cell division, leading to predivisional cells with three origins (Fig. 4.2C-E). These cells frequently failed to divide and subsequently became filamentous. Such premature replication, resulting in three origins and cellular filamentation, was never observed in wild-type cells (Fig. 4.2D). Although wild-type swarmer cells occasionally initiated prematurely, these cells did not replicate again before cell division, likely because CtrA can block new rounds of replication, thereby resynchronizing DNA replication with cell division. Taken together, our results suggest that CtrA is important for coordinating DNA replication with cellular differentiation and for enforcing the asymmetric replicative fates of daughter cells, but does not significantly affect the intrinsic periodicity of DNA replication.

As an additional test of CtrA's role in replication control, we examined a Δ*pleC* mutant, which produces morphologically symmetric daughter cells [27]. We found that a YFP-CtrA reporter partitions symmetrically in Δ*pleC*, in contrast to the wild-type (Fig. 3C-D). Consistently, DNA replication in both Δ*pleC* daughter cells occurred with a period of ~73 minutes, a value intermediate to that of wild-type swarmer (~80 minutes) and stalked

(~67 minutes) cells (Fig. 4.3E). This finding further supports the notion that the asymmetric accumulation of CtrA in wild-type daughter cells accounts for their differential replication capacities.

Replication periodicity is governed by DnaA

If CtrA does not impact the fundamental periodicity of stalked cell replication cycles, another oscillatory control module must exist. We hypothesized that such a module centers on DnaA, an essential, widely-conserved positive regulator of replication initiation [8]. To test if changes in DnaA perturb replication timing, we first examined strains expressing *dnaA* from a xylose-inducible promoter on a high-copy vector. Flow cytometry revealed a substantial accumulation of extra chromosomes per cell within 3 hours of xylose addition (Fig. 4.4A, 4.5A). Moreover, the *ori*/*ter* ratio increased ~3.6-fold in this strain within one hour after inducing *dnaA*, indicating that new rounds of replication initiated before prior rounds had completed (Fig. 4.4B). Thus, overexpressing *dnaA* in *Caulobacter* causes an overinitiation of DNA replication, as in *E. coli* [28], but in contrast to *divL*^{ts} cells (Fig. 4.1D).

We then examined replication timing in a high-copy *dnaA* overexpression strain harboring the TetR-YFP/*tetO* system. Strikingly, DNA replication periodicity was completely lost upon induction (Fig. 4.4C). Many cells initiated multiple rounds of replication within 30 minutes of a previous initiation without an intervening cell division, resulting in the accumulation of 5-6 origins per cell and cellular filamentation (Fig. 4.4D, 4.5B). In contrast to the high-copy vector, expressing *dnaA* from a xylose-inducible promoter on a low-copy vector did not lead to significant overinitiation (Fig. 4.4A,C).

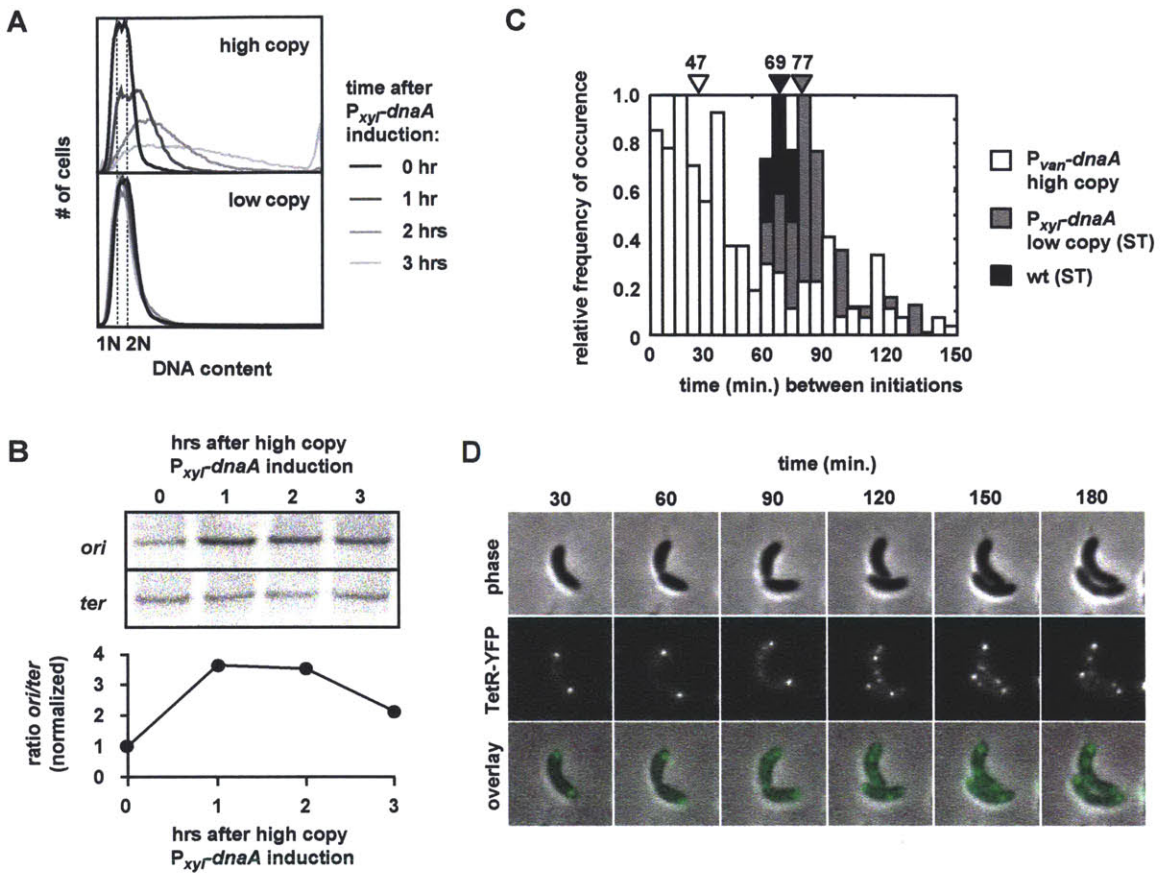

Figure 4.4. Overproducing DnaA disrupts replication periodicity. (A) Flow cytometry analysis of DNA content in a mixed population of cells overexpressing dnaA with a xylose-inducible promoter on a high- or low-copy vector for the times indicated. (B) Southern blots of DNA near the origin (ori) and terminus (ter) in cells overexpressing *dnaA* for 0-3 hrs. Band intensities were quantified and ori/ter ratios normalized to the 0-hr time point. (C) Histograms of replication cycle times in the high-copy *dnaA* overexpression strain compared to wild-type and low-copy *dnaA* overexpression stalked cells at 30°C. Mean values of each population are indicated above. (D) Representative time-lapse images showing accumulation of origins over time in high-copy *dnaA* overexpression cells grown on agarose pads containing 500 μM vanillate at 30°C.

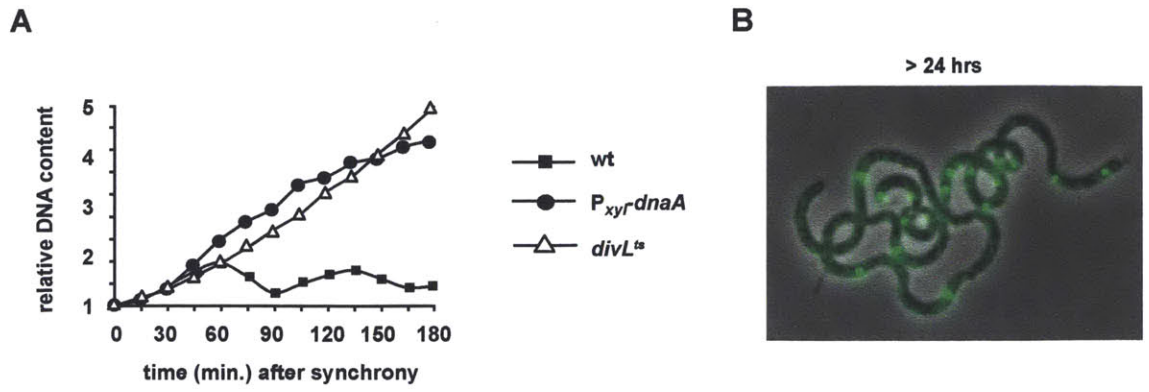

Figure 4.5. Overexpressing *dnaA* causes overinitiation. (A) Time course of flow cytometry data showing normalized DNA content per cell in synchronized populations of wild-type and high copy *dnaA* overexpressing cells at 30 °C. dnaA overexpression was induced with xylose after synchrony at time 0. For comparison, the graph displaying the increase of DNA content in *divL*^{ts} cells was duplicated from Fig. 4.2B. (B) A representative image of cells overexpressing *dnaA* from a high-copy plasmid after >24 hours of induction.

Cell cycle-dependent regulation of DnaA is independent of CtrA

Our finding that *dnaA* overexpression severely disrupted replication periodicity suggests that changes in DnaA activity are critical to temporally regulating replication initiation. A previous model proposed that regulated changes in DnaA transcription and abundance drive cell cycle progression and depend on CtrA; in this model CtrA promotes DnaA synthesis by driving expression of *ccrM*, a DNA methyltransferase, which methylates the *dnaA* promoter to promote *dnaA* transcription [21]. However, given our observation that replication periodicty is unchanged in cells lacking active CtrA, we expected that the synthesis and hence abundance of DnaA would be independent of CtrA.

To test whether the abundance of DnaA is affected via promoter methylation in *divL*^{ts} cells, we first measured the methylation status of the chromosome in synchronized populations of cells using Southern blotting. For wild type, the chromosome alternated between hemi- and fully-methylated states as the chromosome was replicated and then

subsequently methylated *de novo* (Fig. 4.6A). In *divL*^{ts} cells, fully-methylated DNA disappeared while hemi- and unmethylated DNA accumulated, confirming that CcrM activity depends on CtrA activity [13] (Fig. 4.6A). However, in contrast to CcrM, DnaA protein levels did not seem to depend strongly on CtrA. Using immunoblotting and quantitative phosphorimaging, we found that DnaA was present at a relatively constant level throughout the cell cycle in *divL*^{ts} and wild-type cells grown synchronously in rich media at the restrictive temperature of 37°C (Fig. 4.6B). Further, we found that in mixed populations of cells, DnaA levels were comparable in *divL*^{ts} and wild type at both the permissive and restrictive temperatures (Fig. 4.6C). The finding that DnaA levels do not depend strongly on CtrA or CcrM is also consistent with a recent study in which the mutation of a putative methylation site in the *dnaA* promoter did not significantly affect expression of a P_{dnaA}-*lacZ* reporter [29]. Collectively, these data are also consistent with our studies showing that DNA replication continues periodically in cells lacking CtrA activity (Fig. 4.1D).

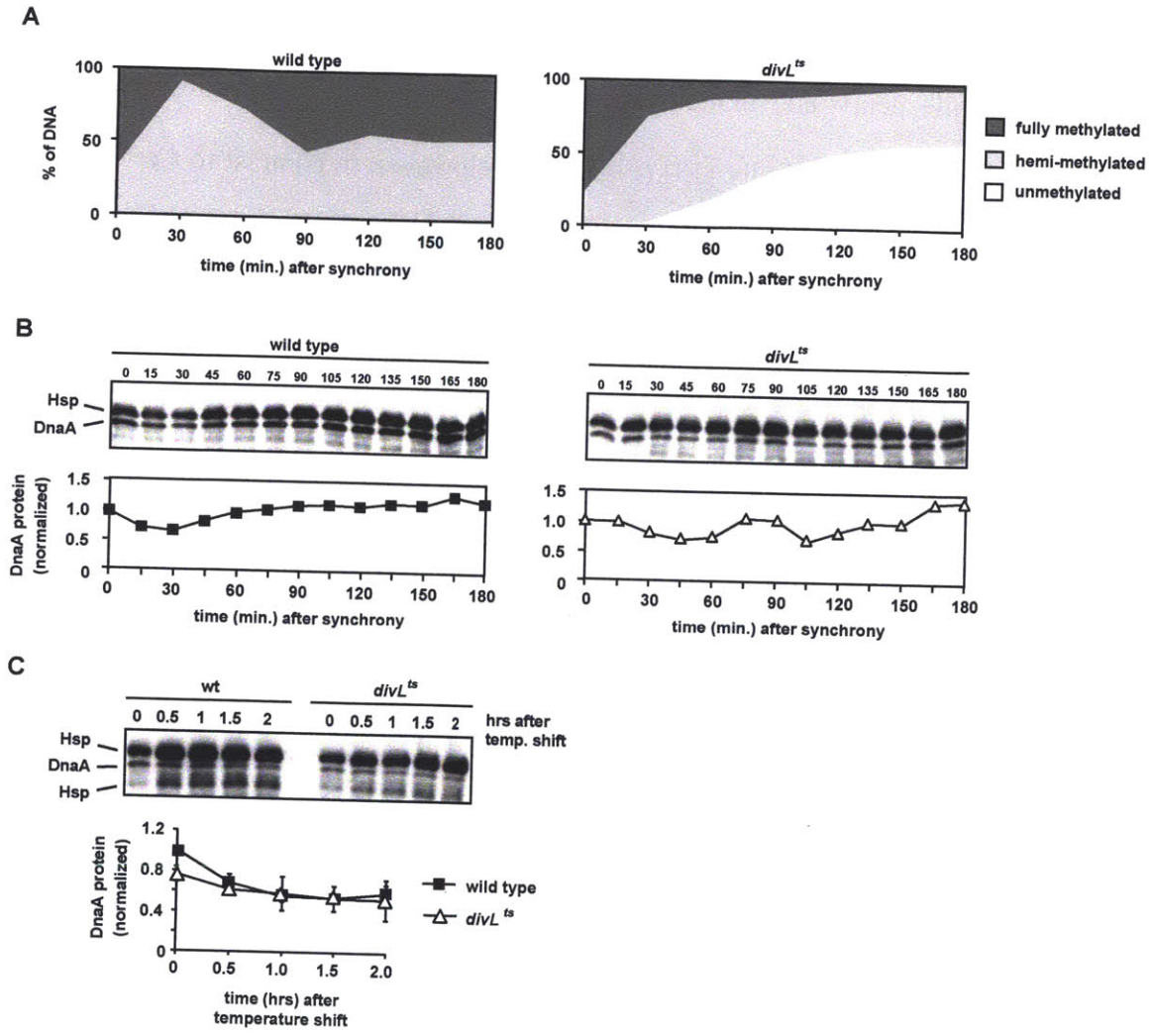

Figure 4.6. CtrA and chromosome methylation state do not significantly affect DnaA abundance. (A) Percentages of fully (dark gray), hemi- (light gray) and unmethylated (white) DNA in wild-type and *divL*^{ts} cells over two consecutive cell cycles starting with synchronized swarmer cells. *divL*^{ts} was shifted to the restrictive temperature of 37 °C at time 0. The percentages were determined by quantifying the band intensity of Southern blots in which fully, hemi- and unmethylated DNA can be distinguished. (B) Western blots showing DnaA protein levels in wild-type and *divL*^{ts} swarmer cells released into fresh media and followed for 180 minutes, or approximately two consecutive cell cycles. The upper band corresponds to a heat shock protein (Hsp), also previously shown to cross-react with DnaA antisera [1]. *divL*^{ts} cells were shifted to the restrictive temperature of 37 °C at t=0. The band intensities from the blots, relative to t=0, are plotted over time for wild type (squares) and *divL*^{ts} (triangles). (C) Western blot of DnaA protein in mixed populations of wild-type and *divL*^{ts} cells that were shifted to the restrictive temperature of 37 °C at t=0. The means of band intensities, relative to t=0 in wild type, with standard deviations from independent repetitions of the experiment were plotted as a function of time.

Changes in DnaA activity govern the periodicity of DNA replication

Because DnaA levels do not vary significantly during the cell cycle in rich media (Fig. 4.6B) and because cells constitutively expressing *dnaA* do not overreplicate (Fig. 4.4A,C), we hypothesized that oscillations in DnaA activity ultimately determine replication periodicity. In *E. coli* DnaA switches between an active ATP-bound and an inactive ADP-bound state [6-8]. ATP hydrolysis by DnaA thus prevents replication reinitiation and a highly-conserved arginine residue, R334, is critical for this hydrolysis [30]. We substituted the corresponding residue, R357, with alanine in *C. crescentus* DnaA (Fig. 4.7) and expressed the resulting mutant from a xylose-inducible promoter on a low-copy plasmid. Unlike cells expressing wild-type *dnaA*, the induction of *dnaA(R357A)* led to an increase in chromosome content per cell and replication overinitiation (Fig. 4.8A-B), as in cells overexpressing *dnaA* from a high-copy plasmid. Western blotting indicated that DnaA(R357A) accumulated to similar levels as the wild-type DnaA control after 2 hours of induction (Fig. 4.8C). Quantitative analysis of individual cells confirmed that inducing *dnaA(R357A)* drastically disrupted the periodicity of replication (Fig. 4.8D) with intervals between replication rounds often less than 30 minutes. These data suggest that the R357A substitution hyperactivates DnaA and that regulated changes in DnaA activity, which are CtrA-independent, are important in determining the periodicity of DNA replication.

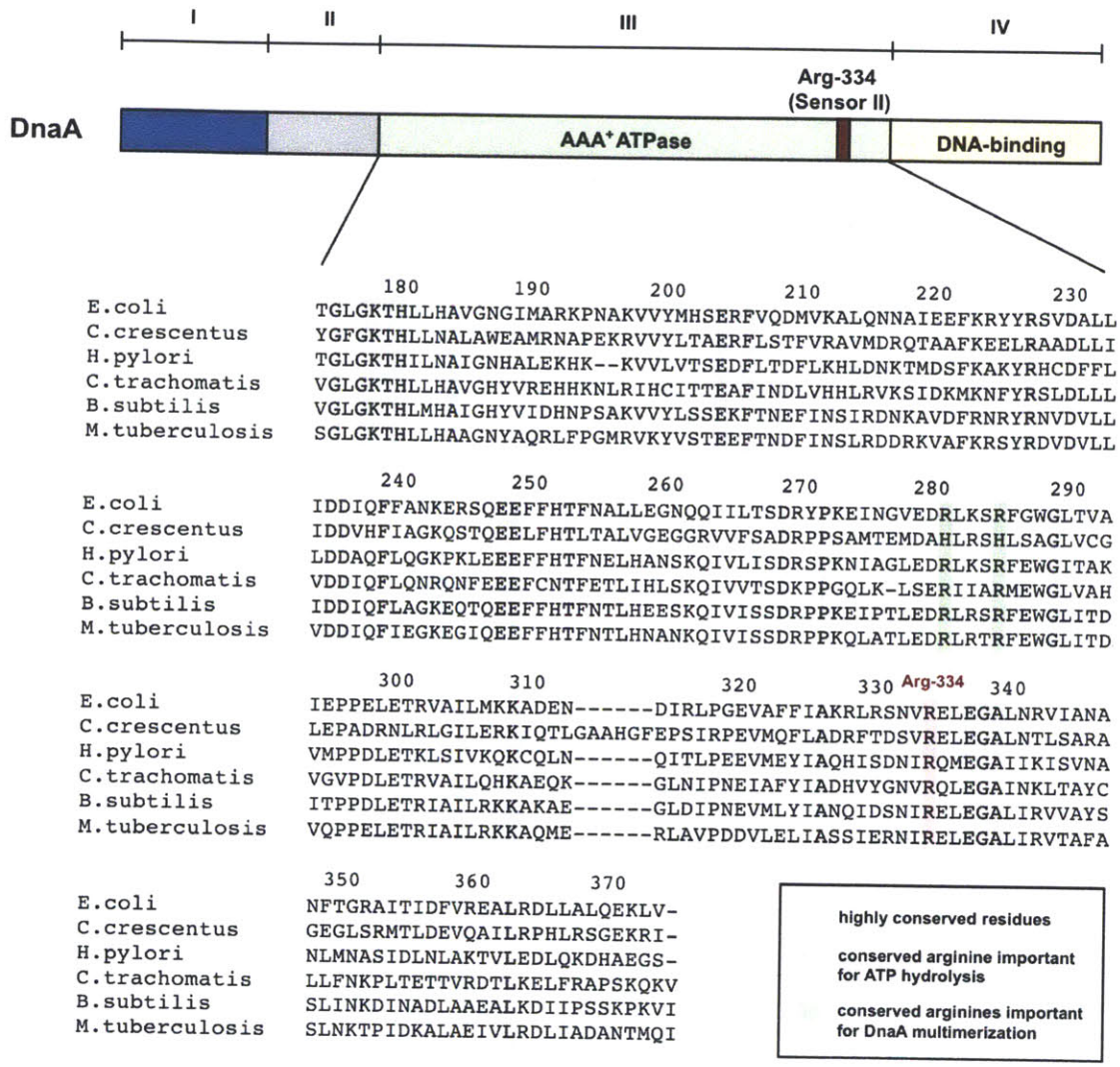

Figure 4.7. Domain structure and amino acid alignment of DnaA. *E. coli* DnaA consists of four functional domains, of which domain III harbors AAA+ ATPase activity. The amino acid sequence of domain III of *E. coli* DnaA was aligned with the corresponding sequences of *C. crescentus*, *Helicobacter pylori*, *Chlamydia trachomatis*, *Bacillus subtilis* and *Mycobacterium tuberculosis*. Residues identical in all six organisms are highlighted in gray. Arg-334 (Arg-357 in *Caulobacter*) important for ATP hydrolysis is highlighted in red. Arg-281 and Arg-285, both of which are important for the stabilization of DnaA multimers upon replication initiation, but correspond to histidines in *Caulobacter*, are marked in green.

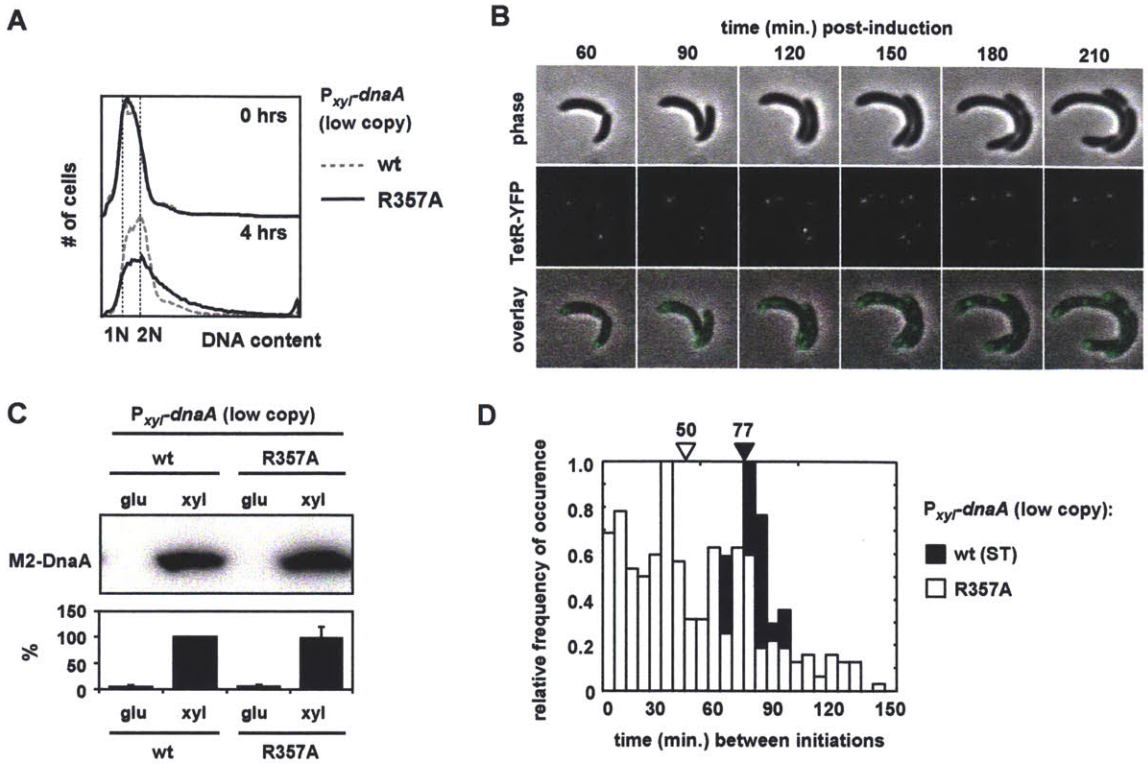

Figure 4.8. DnaA(R357A) is hyperactive and leads to the overinitiation of replication. (A) Flow cytometry profiles showing DNA content in cells expressing wild-type *dnaA* or *dnaA(R357A)* from a xylose-inducible promoter a low-copy vector for 0 or 4 hours. (B) Representative time-lapse images of cells expressing *dnaA(R357A)* with TetR-YFP-marked origins in green overlaid onto phase contrast images. (C) Western blot (top) and quantification (bottom) showing wild-type M2-DnaA and M2-DnaA(R357A) protein levels after induction with xylose for four hours. (D) Histograms of replication intervals in cells expressing either *dnaA* or *dnaA(R357A)* from a low-copy plasmid in cells grown at 30°C.

HdaA influences replication periodicity, not asymmetry, by interacting directly with DnaA

ATP hydrolysis by *E. coli* DnaA is stimulated by Hda, a DnaA homolog that also interacts with DnaN, the beta-subunit of DNA polymerase [10, 31, 32]. Hda has a homolog in *Caulobacter*, called HdaA, and cells depleted of this protein exhibit a mild accumulation of chromosome content and an increased *ori/ter* ratio [22]. Consistently, when we examined replication in HdaA-depleted cells using fluorescence microscopy, we found that a subpopulation of cells overinitiated, with replication periods less than 48 minutes (Fig. 4.9A). Taken together, our data suggest that increasing DnaA activity,

either by depleting HdaA or synthesizing DnaA(R357A), leads to shorter intervals between rounds of DNA replication.

To test whether decreasing DnaA activity extends replication intervals, we overexpressed *hdaA* from a vanillate-inducible promoter on a high-copy plasmid. At a vanillate concentration of 2.5 μM, HdaA protein levels were moderately elevated (Fig. 4.10A) and replication intervals were extended to ~95 min in stalked cells and ~110 min in swarmer cells (Fig. 4.9B). These data indicate that overproducing HdaA changes replication periodicity, but, importantly, not asymmetry. We verified that this mild overexpression of *hdaA* did not substantially change DnaA protein levels (Fig. 4.10B), suggesting that the elevated levels of HdaA impact DnaA activity.

To test whether HdaA's effect on replication depends on a direct interaction with DnaA, we searched for a mutation in HdaA that specifically disrupts interaction with DnaA. In *E. coli*, Hda(Q6A) is deficient in binding DnaA and in stimulating ATP hydrolysis, the latter likely stemming from a failure to also interact with DnaN [32, 33]. We engineered a mutant variant of *Caulobacter* HdaA harboring the corresponding substitution, Q4A (Fig. 4.10C). Yeast two-hybrid analysis indicated that HdaA(Q4A), but not wild-type HdaA, was indeed impaired in binding *Caulobacter* DnaA and DnaN (Fig. 4.9C). We then measured the timing of DNA replication initiations in a strain mildly overexpressing HdaA(Q4A) and observed significantly shorter inter-replication times compared to isogenic cells overexpressing wild-type HdaA (Fig. 4.9B). Immunoblots indicated that HdaA(Q4A) accumulated with a similar rate and to similar levels as the wild-type HdaA protein (Fig. 4.10A). We conclude that excess HdaA slows down replication cycles by

directly modulating DnaA activity, but without affecting the replicative asymmetry of daughter cells.

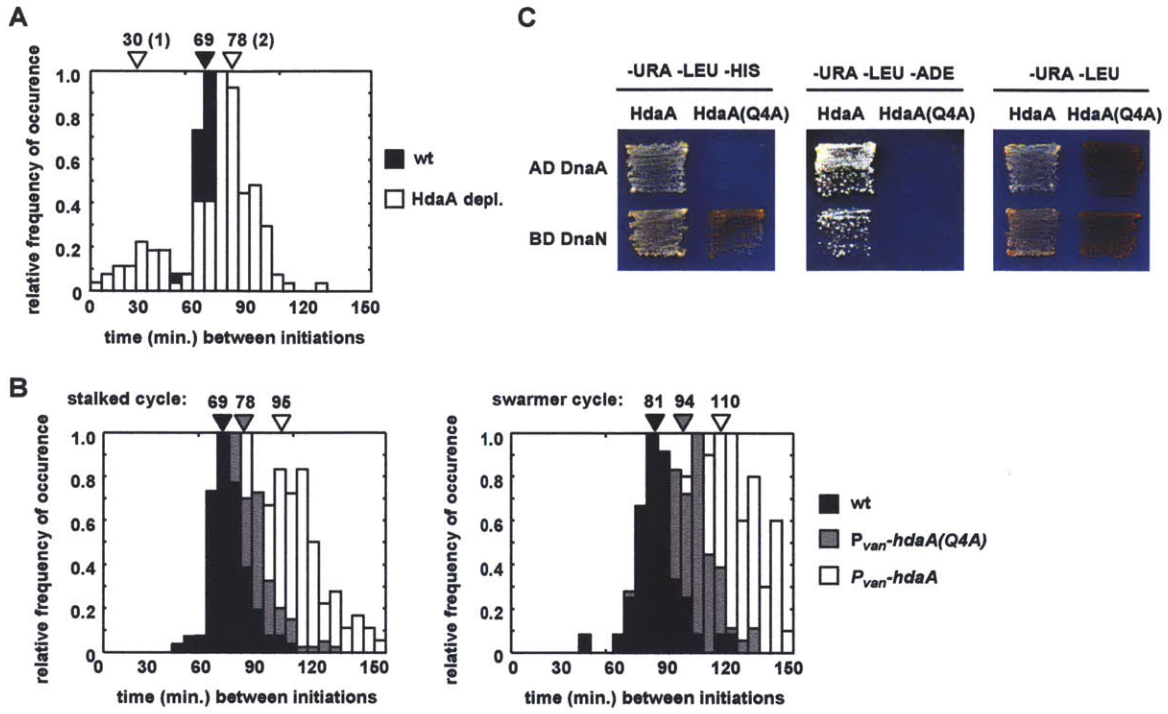

Figure 4.9. Overproducing HdaA leads to slower replication cycles. (A) Histograms of stalked replication cycles in the HdaA depletion strain compared to wild type at 30°C. For the HdaA depletion, replication timing appeared bimodal, so means were calculated separately for cells with replication times shorter or longer than 48 min. (B) Histograms depicting stalked (left) and swarmer (right) replication cycles in wild type (black) and in cells in which *hdaA* (white) or *hdaA(Q4A)* (gray) driven by a vanillate-inducible promoter were induced with 2.5 mM vanillate at 30°C. (C) Yeast two-hybrid assay showing interactions between wild-type and mutant variants of DnaA, HdaA and DnaN. Yeast containing plasmids encoding the proteins indicated fused to either the activation (AD) or DNA-binding domain (BD) of Gal4 were restreaked on media lacking histidine (-HIS) or adenine (-ADE). Media lacking uracil and leucine (-URA-LEU) selects for plasmid maintenance. Growth and light colony color indicate strong protein interactions, whereas no growth or dark color indicate no or weak interactions.

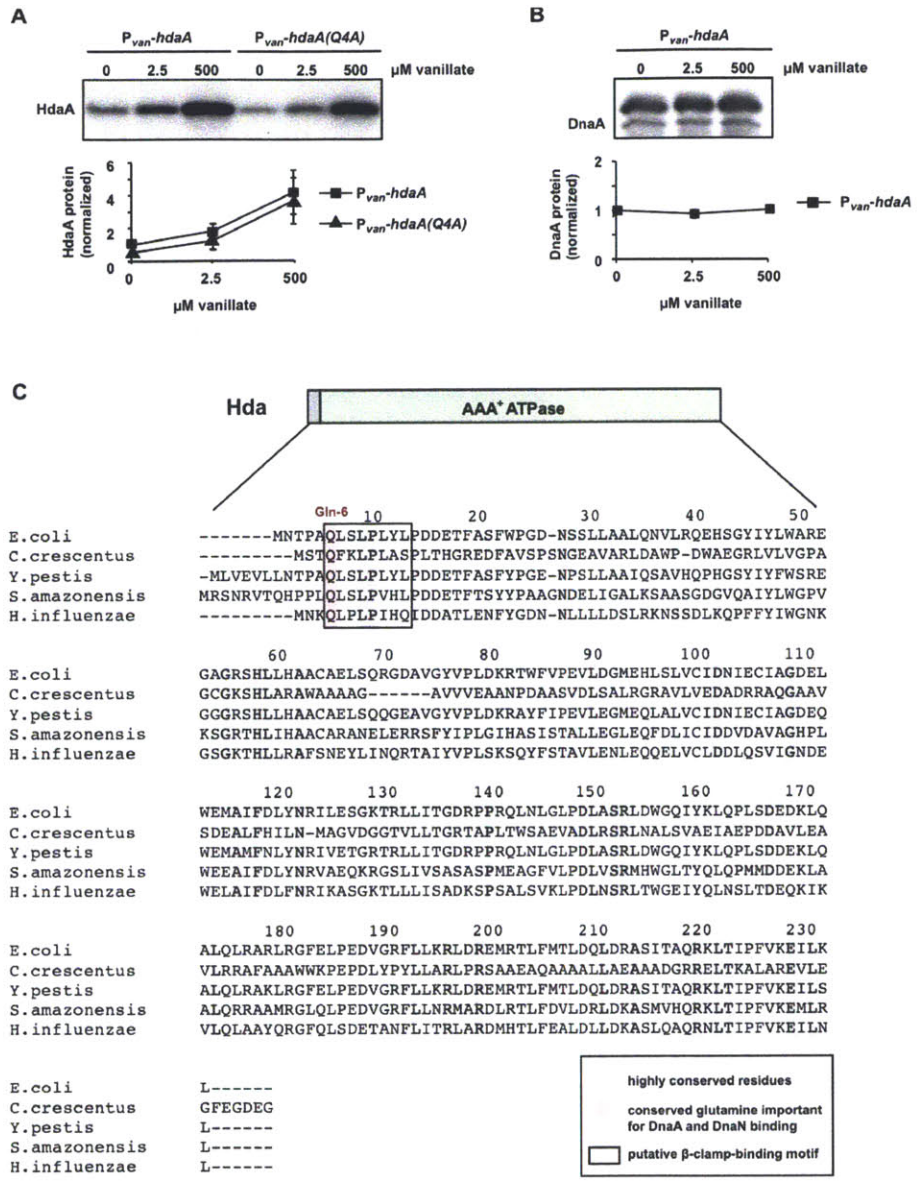

Figure 4.10. HdaA acts as a repressor of DnaA-mediated replication. (A) Western blot and quantification of the Western blot showing comparable HdaA and HdaA(Q4A) protein levels expressed from a high copy vector after 2 hrs induction with 0, 2.5, or 500 mM vanillate. (B) Western blot (top) and quantification of the Western blot (bottom) showing that DnaA protein levels remain unchanged when *hdaA* is overexpressed. (C) Domain structure and amino acid sequence alignment of Hda. Hda consists of a short N-terminal region (gray) and an AAA+ domain (green) that shares homology with the AAA+ ATPase domain of DnaA proteins. The amino acid sequence of *E. coli* Hda was aligned with the sequences of Hda homologs from *C. crescentus*, *Yersinia pestis*, *Shewanella amazonensis* and *Haemophilus influenzae*. Residues identical in all five organisms are highlighted in gray. The N-terminal region of Hda proteins contains a putative β-clamp-binding motif (box) [2]. Residue Gln-6 within this motif is required for the interaction and negative regulation of DnaA and is highlighted in red.

Discussion

We found that DNA replication initiation in *Caulobacter* is regulated by two genetically separable modules. One module centers on the essential initiation factor DnaA, which promotes replication initiation. Mutations affecting DnaA activity severely perturbed the timing of replication initiation, with increases and decreases in activity leading to shorter and longer intervals between rounds of replication. The other module involves the essential response regulator CtrA, which silences DNA replication in a cell type-specific manner, ensuring that swarmer cells cannot initiate replication until after differentiating into stalked cells. In stark contrast to DnaA, mutations that reduced or eliminated CtrA activity had almost no effect on the periodicity of DNA replication during the stalked cell cycle of *Caulobacter* (for a summary of all replication periods measured, see Table 4.1). We conclude that CtrA's role in replication control is mainly to enforce the asymmetry of daughter cells while DnaA serves as the fundamental pacemaker of DNA replication.

The functional separability of these two modules was revealed by examining DNA replication in individual cells lacking active CtrA. In $divL^{ts}$ and $cckA^{ts}$ strains, which harbor very little phosphorylated CtrA [24-26], the periodicity of replication was virtually indistinguishable from that of wild-type stalked cells indicating that DnaA activity oscillates independent of CtrA. However, CtrA activity does not oscillate completely independent of DnaA. Cells depleted of DnaA stop replicating and also fail to activate CtrA through an unknown mechanism [5, 34]. Thus, the DnaA module entrains the CtrA module, but not *vice versa*. This coupling of DnaA and CtrA presumably helps cells coordinate DNA replication with the cellular functions controlled transcriptionally by CtrA, such as polar morphogenesis and cell division. Indeed, our results suggest that a

failure to coordinate replication initiation with other cell cycle events can have lethal consequences. Mutations that disrupted CtrA binding to the origin often resulted in replication occurring out of phase with other cell-cycle events (Fig. 4.2C-E, 4.3B), leading to cell division defects, chromosome accumulation, and a failure to proliferate. Under stressful conditions, the failure to coordinate replication control with cellular development might result in a particularly severe fitness disadvantage [19].

In sum, our data lead to a new model for DNA replication control during the *Caulobacter* cell cycle in rich media (Fig. 4.11, 4.12). In a swarmer cell, CtrA is abundant and phosphorylated such that it can inhibit the initiation of DNA replication. Upon differentiating into a stalked cell, CtrA activity is eliminated, thereby enabling active DnaA-ATP to drive the initiation of DNA replication and promote the activation of newly synthesized CtrA. DnaA is inactivated immediately after replication initiation, likely by the combined action of HdaA and other factors that promote ATP hydrolysis. DnaA activity then reaccumulates approximately 60 minutes later, through new synthesis and the reloading of DnaA with ATP. If DnaA activity accumulates to high levels before cell division, the abundance of CtrA at this stage will prevent premature initiation, thereby ensuring that replication occurs once-and-only-once per cell cycle. Following cell division, both daughter cells likely inherit active DnaA. In stalked cells, CtrA is rapidly eliminated, enabling DnaA to immediately drive a new round of replication. By contrast, swarmer cells maintain active CtrA, thereby delaying DNA replication until after they differentiate into stalked cells and eliminate CtrA activity.

Regulated changes in DnaA activity are important for replication periodicity

Our results indicate that changes in DnaA activity are the primary means by which DNA replication timing is controlled during the *Caulobacter* cell cycle. Although the transcription of *dnaA* peaks in G1 [35, 36], and *de novo* synthesis is probably required to replenish DnaA-ATP levels after initiation occurs, cells constitutively expressing *dnaA* initiated replication with a periodicity similar to wild type (Fig. 4.8A,C). Thus, while the transcription of *dnaA* is necessary for replication, it appears that regulated transcription alone cannot account for the periodicity of initiation. By contrast, mutations that affect the regulation of DnaA activity, but not its abundance, significantly disrupted the timing of replication initiation (Table 4.1). In *E. coli*, the primary mechanism for inhibiting DnaA, termed RIDA (regulatory inactivation of DnaA), involves direct stimulation of DnaA ATPase activity by Hda [10]. In *B. subtilis*, DnaA activity is regulated by direct interactions with the Soj (ParA), SirA and YabA [37-40]. Thus, it appears that, like these other bacteria, *Caulobacter* primarily regulates the timing of replication by modulating DnaA activity, at least in rich medium, the growth condition used here. Regulated changes in DnaA abundance may, however, be important in stressful and nutrient-limited conditions [41].

Modularity of the bacterial cell cycle

Recognizing the intrinsically modular design of replication control during the *Caulobacter* cell cycle has important implications for understanding the evolution of the bacterial cell cycle. We propose that DnaA lies at the heart of a primordial cell cycle oscillator that has been conserved in virtually all bacteria and that sets the fundamental periodicity of DNA replication in each (Fig. 4.11B, Fig. 4.12B), whereas CtrA was

recruited later, in a subset of α-proteobacteria, to establish replicative asymmetry in daughter cells (Fig. 4.11B). CtrA is highly-conserved throughout the α-proteobacteria (Fig. 4.12B) where it transcriptionally regulates a range of genes, often involved in polar morphogenesis and cell division [14, 42, 43]. Many, and perhaps most, α-proteobacteria divide asymmetrically and there is evidence that CtrA is often differentially regulated in daughter cells [43-45]. Hence, the evolution of replicative asymmetry in *Caulobacter* and closely related species likely required only the evolution of CtrA binding sites within the origin. The plausibility of this parsimonious scenario is supported by the fact that CtrA binding sites within an origin are thought to have evolved independently at least twice within the lineage leading to the *Caulobacterales* [46]. Also, in the more distantly related α-proteobacteria *Rickettsia*, functional binding sites for the CtrA homolog CzcR were identified in the chromosomal origin of replication [47]. However, whether the binding of CzcR to these sites silences replication is difficult to address as *Rickettsia* grow slowly and only as intracellular parasites of eukaryotic cells.

In sum, we propose that CtrA and the regulatory circuit that controls it arose early within the α-proteobacteria lineage; this CtrA module was subsequently recruited to spatially control DNA replication, without significantly impacting the DnaA-based temporal control of replication (Fig. 4.11B). The net result is a system with two genetically separable modules, as observed here. Our results thus help to provide a unifying view of cell cycle regulation in bacteria with a conserved cell cycle engine built around DnaA. Other modules and components, such as CtrA, have then been integrated with, and are often entrained by, DnaA, but are otherwise autonomous and hence genetically separable. Notably, a modular circuit was also recently proposed to control the cell cycle in *S.*

cerevisiae, where multiple regulatory modules, each capable of oscillating on their own, were phase-locked to a central pacemaker [48]. More generally, our findings emphasize the notion that regulatory circuits are not monolithic entities of irreducible complexity, but instead are built over time by the relatively straightforward, sequential integration of discrete modules [1, 2, 48].

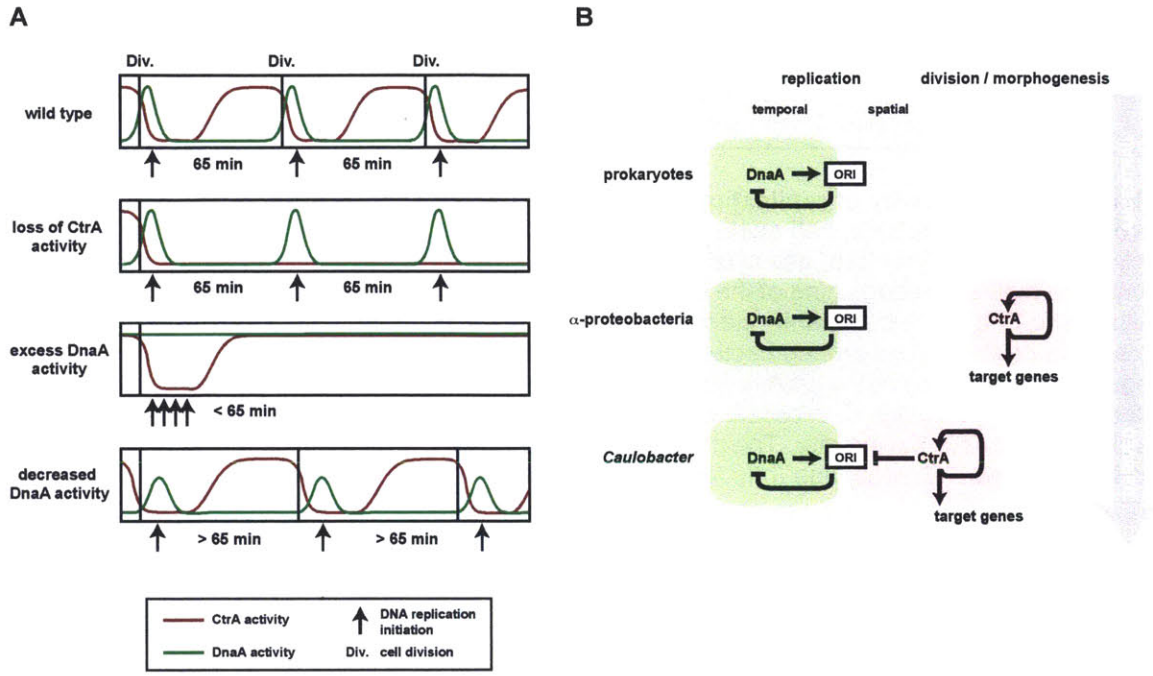

Figure 4.11. Modularity of replication control in *Caulobacter crescentus* reflects the evolution of the bacterial cell cycle. (A) Schematic summary of CtrA and DnaA activities during the stalked cell cycle in various strains. For a comparison to the swarmer cell cycle, see Fig. S6A. (B) Evolution of replication control in *Caulobacter*. DnaA is part of an ancestral control module that sets the periodicity of replication in nearly all bacteria. In α-proteobacteria the CtrA module arose to transcriptionally regulate division and polar morphogenesis. In a sub-group of α-proteobacteria including *Caulobacter*, CtrA evolved to bind to the origin, thereby enforcing replicative asymmetry of daughter cells. Although DnaA and CtrA each influence the origin (ORI), each factor is regulated largely independently.

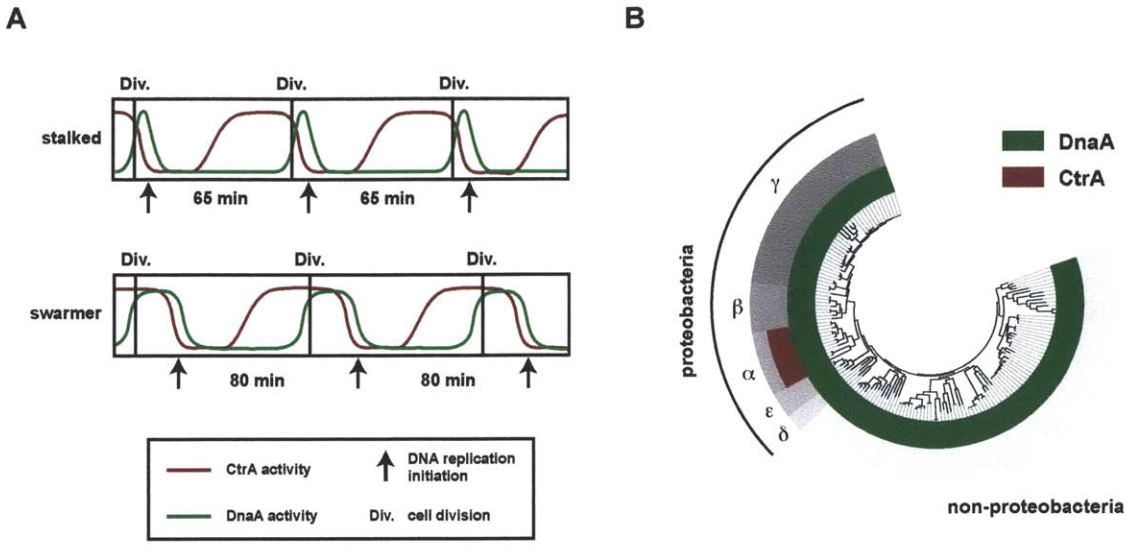

Figure 4.12. Modularity of replication control in Caulobacter crescentus reflects the evolution of the bacterial cell cycle. (A) Schematic model of CtrA (red) and DnaA (green) activities during stalked (top) and swarmer (bottom) replication cycles. In swarmer cells, CtrA and DnaA are high at the beginning of the cell cycle. First after clearance of CtrA, replication can initiate and DnaA is subsequently inactivated (B) Phylogenetic tree showing the distribution of *dnaA* and *ctrA* orthologs among bacteria. *dnaA* is nearly universal and represents an ancient regulator of DNA replication. ctrA is only present in α-proteobacteria. A subset of α-proteobacteria, including *C. crescentus*, subsequently evolved CtrA binding sites at the origin to facilitate replicative asymmetry. The phylogenetic tree was built using the default species tree provided on the iTOL webpage (http://itol.embl.de/) [3].

Experimental Procedures

Strains, plasmids, and growth conditions

All strains and plasmids used in this chapter are listed in Table 4.2. Primers are listed in Table 4.3. Cultures of *C. crescentus* and *E. coli* were grown in PYE or LB, respectively, as described previously [4]. PYE was supplemented with 0.2% glucose, 0.3% xylose, and 2.5 or 500 μM vanillate, as indicated. Synchronizations were performed on mid-log phase cells using Percoll (GE Healthcare) density gradient centrifugation [5]. Transductions were performed using ϕCr30 as described previously [6].

ML1878 was constructed by transducing a chloramphenicol-marked temperature sensitive *divL*(A288V) allele ($divL^{ts}$) into GM1251 [7]. To construct ML1879,

pNPTS138::*Pvan-tetR-YFP* from ML1876 [8] was integrated at the *vanAB* locus by selection on kanamycin followed by counterselection on sucrose to generate a markerless strain containing *vanAB::tetR-YFP* in the HdaA depletion strain JC353 [9]. The *tetO* array on pNPTS138::*cc0006-tetO* [8] was then integrated at locus CC0006. To construct ML1881, $divL^{ts}$*::chlor* was introduced by transduction into ML1876 [8]. To construct ML1882, pNPTS138::*cc0006-tetO* was digested with *XhoI* and *ClaI* and then blunt-end ligated to drop out the kanamycin resistance gene. This modified integration vector was integrated into GM3193 [10] harboring the mutant chromosomal origin, *ori(bc1d)*. This mutant origin, as well as *cc0006::(tetO)n* (*gentR*), were then moved into a markerless strain containing *vanAB::tetR-YFP* by transduction. Finally, P_{xyl}*-ftsZ::kan* from YB1585 was introduced by transduction and selection on both kanamycin and gentamycin. ML1883 was constructed by transduction of Δ*pleC::*tet from ML1755 into LS4259 [11].

All expression vectors were constructed using the Gateway cloning system (Invitrogen) and are listed in Table S1. PCR products were cloned into the pENTR/D-TOPO vector and subsequently recombined into destination vectors following the manufacturer's protocol. To construct pENTR clones for *dnaA*, *hdaA*, and *dnaN*, PCR was performed using primer pairs DnaA_For/DnaA_Rev, HdaA_For/HdaA_Rev, and DnaN_For/DnaN_Rev, respectively. To construct pENTR-*vanR*-P_{van}-*dnaA* and pENTR-*vanR*-P_{van}-*hdaA*, each of which contains the entire *vanR* gene followed by the P_{van} promoter driving *dnaA* or *hdaA*, respectively, fusion PCR was used. First, the coding region for the VanR repressor and the promoter P_{van}, was amplified using primers Pvan_F2 and Pvan_R. In a separate reaction, *dnaA* or *hdaA* was amplified using the primer pairs DnaA_Pvan_F/DnaA_Rev and HdaA_Pvan_F/HdaA_Rev, respectively. The

vanR-P_{van} construct was then fused, using fusion PCR, to the construct containing *dnaA* or *hdaA*, using primers Pvan_F2 and DnaA_Rev, or Pvan_F2 and HdaA_Rev, respectively. All entry vectors were sequence verified and recombined with the destination vectors pML1716, pML498, pML375, pCT155, pAD or pBD to generate pML1716-*dnaA*, pML498-*dnaA*, pML375-*dnaA*, pCT155-*vanR*-P*van-dnaA*, pCT155-*vanR*-P*van-hdaA*, pAD-*dnaA*, pAD-*hdaA*, pBD-*hdaA* and pBD-*dnaN*. The resulting plasmids were transformed into *Caulobacter*, *E. coli*, or *S. cerevisiae*, as appropriate.

Table 4.2 - Strains and Plasmids

Name	Description	Source
***C. crescentus* strains**		
CB15N	Synchronizable derivative of wild-type CB15	[16]
GM1251	*purA*::Tn*5*Ω-MP	[7]
GM3193	*ori(bc$_L$d)*	[10]
JC353	Δ*hdaA* + pMR20-*hdaA* (*tet^R*)	[9]
LS4259	pKR173 (pMR20:P$_{xyl}$-*yfp-ctrA*) (*tet^R*)	[11]
MT16	*cc0006*::(*tetO*)$_n$ (*gent^R*), P$_{xyl}$:*lacI-ecfp:tetR-eyfp* (*spec^R*)	[17]
ML1852	*divL^{ts}* (*kan^R*)	[18]
YB1585	P$_{xyl}$-*ftsZ* (*kan^R*)	[19]
ML1753	*divL^{ts}* (*chlor^R*), *cc0006*::(*tetO*)$_n$ (*gent^R*), P$_{xyl}$:*lacI-ecfp:tetR-eyfp* (*spec^R*)	[8]
ML1754	*cckA(V366P), cc0006*::(*tetO*)$_n$ (*gent^R*), P$_{xyl}$:*lacI-ecfp:tetR-eyfp* (*spec^R*)	[8]
ML1755	Δ*pleC* (*tet^R*), *cc0006*::(*tetO*)$_n$ (*gent^R*), P$_{xyl}$:*lacI-ecfp:tetR-eyfp* (*spec^R*)	[8]
ML1793	*ori(bc$_L$d), cc0006*::(*tetO*)$_n$ (*gent^R*), P$_{xyl}$:*lacI-ecfp:tetR-eyfp* (*spec^R*)	[8]
ML1876	YB1585 (*kan^R*), *cc0006*::(*tetO*)$_n$ (*gent^R*), P$_{van}$:*tetR-eyfp*	this study
ML1878	GM1251, *divL^{ts}* (*chlor^R*)	this study
ML1879	JC353, *cc0006*::(*tetO*)$_n$ (*gent^R*), P$_{van}$:*tetR-eyfp*	this study
ML1881	ML1876, *divL^{ts}* (*chlor^R*)	this study
ML1882	ML1876, *ori(bc$_L$d)*	this study
ML1883	LS4259, Δ*pleC* (*tet^R*)	this study
***E. coli* strains**		
BL21-Tuner	Strain for protein expression and purification	Novagen
DH5a	General cloning strain	Invitrogen
TOP10	General cloning strain for pENTR/D-TOPO clones	Invitrogen
***S. cerevisiae* strain**		
PJ69-4A	Strain for yeast two-hybrid with *GAL1-HIS3*, *GAL2-ADE2*, *GAL7-lacZ*	[20]
General purpose vectors		
pAD-DEST	Destination vector of pGAD-C1, Gal4-AD (activating domain) fusion plasmid (*carb^R*, *LEU2*)	[15]
pBD-DEST	Destination vector of pGBDU-C3, Gal4-BD (DNA-binding domain) fusion plasmid (*carb^R*, *URA3*)	[15]
pENTR/D-TOPO	ENTRY vector for Gateway cloning system (*kan^R*)	Invitrogen
pCT155	Destination vector of high-copy plasmid pJS14 (*chlor^R*)	lab collection
pML375 (pTRX-HIS-DEST)	Destination vector of pET-His$_6$ (*amp^R*)	[12]
pML498 (pLXM-DEST)	Destination vector of pMR20, low copy vector (*tet^R*)	[12]
pML1716	Destination vector of pJS14; high-copy, *P$_{xyl}$*, M2 tag (*chlor^R*)	lab collection
Plasmids		
pENTR-*dnaA*	pENTR containing the *dnaA* open reading frame	this study
pENTR-*dnaN*	pENTR containing the *dnaN* open reading frame	this study
pENTR-*hdaA*	pENTR containing the *hdaA* open reading frame	this study
pENTR-*vanR*-P$_{van}$-*dnaA*	pENTR containing *vanR* and P$_{van}$ fused to *dnaA*	this study
pENTR-*vanR*-P$_{van}$-*hdaA*	pENTR containing *vanR* and P$_{van}$ fused to *hdaA*	this study
pCT155-*vanR*-P$_{van}$-*dnaA*	pCT155 containing *vanR* and P$_{van}$ fused to *dnaA*	this study
pCT155-*vanR*-P$_{van}$-*hdaA*	pCT155 containing *vanR* and P$_{van}$ fused to *hdaA*	this study

pCT155-*vanR*-P_{van}-*hdaA(Q4A)*	pCT155 containing *vanR* and P_{van} fused to *hdaA(Q4A)*	this study
pML375-*dnaA*	pML375 containing *His_6-dnaA*	this study
pML498-*dnaA*	pML498 containing *P_{xyl}-M2-dnaA*	this study
pML498-*dnaA(R357A)*	pML498 containing *P_{xyl}-M2-dnaA(R357A)*	this study
pML1716-*dnaA*	pML1716 containing *P_{xyl}-M2-dnaA*	this study
pAD-*dnaA*	*dnaA* fused to Gal4-AD	this study
pAD-*dnaA(R357A)*	*dnaA(R357)* fused to Gal4-AD	this study
pAD-*hdaA*	*hdaA* fused to Gal4-AD	this study
pAD-*hdaA(Q4A)*	*hdaA(Q4A)* fused to Gal4-AD	this study
pBD-*hdaA*	*hdaA* fused to Gal4-BD	this study
pBD-*hdaA(Q4A)*	*hdaA(Q4A)* fused to Gal4-BD	this study
pBD-*dnaN*	*dnaN* fused to Gal4-BD	this study
pNPTS138::*cc0006-tetO*	for integration of $(tetO)_n$ at *cc0006*, near the origin	[8]

Table 4.3 - Primers

Primers	**Sequence (5' → 3')**	**Purpose**
DnaA_For	CACCTTGACCATGAAGGGCGGGGTTGC	pENTR cloning
DnaA_Rev	CAATCCTACGATACGGTTTCG	pENTR cloning
DnaAR334A_F	CACCGACAGCGTCGCCGAGCTGGAAGGCGC	Site-directed mutagenesis
DnaAR334A_R	GCGCCTTCCAGCTCGGCGACGCTGTCGGTG	Site-directed mutagenesis
HdaA_For	CACCTTGTCCACCCAGTTCAAACTGCCG	pENTR cloning
HdaA_Rev	GGAGAAGGAGCGTCACGGC	pENTR cloning
pCT155hdaAQ6A_F	CGACGTTGTCCACCGCGTTCAAACTGCCGCTG	Site-directed mutagenesis
pCT155hdaAQ6A_R	CAGCGGCAGTTTGAACGCGGTGGACAACGTCG	Site-directed mutagenesis
pENTRhdaAQ6A_F	CTTCACCTTGTCCACCGCGTTCAAACTGCCGCTG	Site-directed mutagenesis
pENTRhdaAQ6A_R	CAGCGGCAGTTTGAACGCGGTGGACAAGGTGAAG	Site-directed mutagenesis
DnaN_For	CACCATGAAGCTTACGATCGAACGG	pENTR cloning
DnaN_Rev	TCCGATGACCCGGCTGCG	pENTR cloning
Pvan_F2	GACTGGTTCACACCTAAAGCG	Fusion PCR for pENTR cloning
Pvan_R	CGTCGTTTCCTCGCATCGTG	Fusion PCR for pENTR cloning
DnaA_Pvan_F	CACGATGCGAGGAAACGACGATGACCATGAAGG GCGGGGTTGC	Fusion PCR for pENTR cloning
HdaA_Pvan_F	CACGATGCGAGGAAACGACGTGTCCACCCAGTTC AAACTGCCG	Fusion PCR for pENTR cloning
Tn5MPprobe_For	CTAGAATCGATACCGACTCG	Southern blot probe
Tn5MPprobe_Rev	ATCGAATCGATGAGCCTGAC	Southern blot probe
Ter_For	ACCCAGGTCCTCGCCAAGCTG	Southern blot probe
Ter_Rev	CTCAACATGCTTGACCGCCAGATC	Southern blot probe
Cori_For	GAAGCCCTGGACTACGCCATCG	Southern blot probe
Cori_Rev	CAGAGGCAGGCCCAGGATGG	Southern blot probe

PCR conditions

DNA was amplified from CB15N genomic DNA as described previously [12]. Fusion PCR was performed similarly, but in the presence of 1 mM $MgCl_2$ and with the template

concentration of 50 ng of the larger template PCR fragment and equimolar amounts of the smaller PCR fragment. Site-directed mutagenesis was performed as previously described [13].

Time-lapse microscopy

Time-lapse movies were performed as previously described [24]. Briefly, cells were immobilized on agarose pads, containing 1-1.5% agarose in PYE. Imaging was performed at 30°C or 34°C using a Zeiss Axiovert 200 microscope with a 63x phase objective fitted with an objective heater (Bioptechs) and a culture dish heater (Warner Instruments). Images were acquired using the phase and YFP emission/excitation filters in 6 min intervals over at least 4 hrs. ImageJ software was used to analyze and process the images (http://rsbweb.nih.gov/ij/). To analyze DNA replication timing, we measured the interval between consecutive DNA replication initiations using the TetR-YFP/*tetO* system as diagrammed in Fig. 1A. The time between replication initiation in a stalked cell and its daughter stalked and swarmer cells are referred to as the stalked and swarmer replication cycles, respectively. In division-inhibited cells, stalked and swarmer cycles were examined by measuring the time interval between replication in a stalked cell and at the stalked and swarmer poles, respectively, of the filamenting cell. For all timing measurements, Matlab (Mathworks) was used to generate histograms of replication times and to calculate the mean values of replication periods.

Isolation of genomic DNA

Genomic DNA was isolated using the Qia kit, according to the manufacturer's protocol (Qiagen). DNA concentration and quality were assessed using the NanoDrop ND-1000

UV-Vis Spectrophotometer (NanoDrop Technologies) and on ethidium-bromide stained TAE agarose gels.

Southern Blotting

To determine the copy number ratio of *ori* to *ter* DNA, genomic DNA from mixed cultures grown to mid-log phase, was digested with *BamHI*. For each sample, approximately 3 μg of digested DNA was run on a TAE agarose gel and then blotted onto Amersham Hybond-N+ membrane (GE Healthcare) according to the manufacturer's manual. Two Southern probes, one complementary to a 1010 bp region near the origin and the other to a 720 bp region at the terminus, were obtained by PCR using primer pairs Cori_For/Cori_Rev and Ter_For/Ter_Rev. Labeling of the probes, hybridization to membranes, and detection were performed using the Amersham Gene Images AlkPhos Direct Labeling and Detection system (GE Healthcare) according to the manufacturer's instructions. Blots were scanned with a Typhoon scanner (GE Healthcare), images were processed with Photoshop (Adobe), and the relative band intensities quantified using ImageJ.

To analyze the methylation status of the chromosome, Southern Blot analysis was performed as described earlier [7], using GM1251 which contains Tn*5*Ω-MP at the *purA* locus, ~120 kb from *Cori*. Tn*5*Ω-MP contains two sets of GANTC sites overlapping *ClaI* sites, which are blocked by methylation, and two additional *PstI* sites, which are methylation insensitive and flank Tn*5*Ω-MP. Digestion with *ClaI* and *PstI* results in DNA fragments that are characteristic in their length of fully, hemi- or unmethylated DNA. Chromosomal DNA was sampled every 30 min for 3 h from synchronized cultures of GM1251 and its isogenic $divL^{ts}$ mutant, ML1878, and digested with *ClaI* and *PstI*.

Blotting, hybridization and detection were performed as described above using a probe that was generated with the primers Tn5MPprobe_For and Tn5MPprobe_Rev. Relative band intensities were quantified using ImageJ and the percentages of fully, hemi- and unmethylated DNA were plotted as a function of time.

Flow Cytometry

Flow Cytometry was performed as previously described [13]. For time-course experiments, samples were taken every 15 min after synchronization and the median value of fluorescence for each time point determined using Flowjo software (http://www.flowjo.com/) and plotted as a function of time. Each experiment was repeated independently and representative results are presented.

Protein purification and antibody production

His_6-*dnaA* was expressed from pML375-*dnaA* in *E. coli* BL21 for 4 hrs at 30°C. Purification of His_6-DnaA was performed as described previously [14]. To avoid protein precipitation at high concentrations, DnaA was denatured with 5 M Urea, and then used as antigen in the production of polyclonal rabbit antisera (Covance).

Immunoblotting

Pelleted cells, normalized to the optical density of the culture, were resuspended in 1X SDS sample buffer and heated to 95°C for 10 min. Equal amounts of total protein were then subject to SDS-PAGE for 60 or 80 min (for HdaA or DnaA blots, respectively) at 150 V at room temperature on 12%, 10% or 7.5% Tris-HCl gels (Bio-Rad) and transferred to PVDF membranes (Bio-Rad). Proteins were detected using a 1:1500 or 1:1000 dilution of primary antibody against DnaA, HdaA, or the M2-tag, respectively, and a 1:5000 dilution of secondary HRP-conjugated antibody. Blots were scanned with a

Typhoon scanner (GE Healthcare), images processed with Adobe Photoshop, and the relative band intensities quantified with ImageJ.

Yeast two-hybrid assay

Protein-protein interactions were assayed in the yeast two-hybrid system as described previously [15].

Acknowledgements

We thank A. Murray, A. Grossman, J. Modell, C. Tsokos, and C. Aakre for comments on the manuscript. We acknowledge Justine Collier for providing the anti-HdaA serum and the HdaA depletion strain JC353. M.T.L. is an Early Career Scientist at the Howard Hughes Medical Institute. This work was supported by a National Institutes of Health grant (5R01GM082899) to M.T.L and a research fellowship (JO 925/1-1) from the German Research Foundation (DFG) to K.J.

References

1. Bhattacharyya, R.P., Remenyi, A., Yeh, B.J., and Lim, W.A. (2006). Domains, motifs, and scaffolds: the role of modular interactions in the evolution and wiring of cell signaling circuits. Annu Rev Biochem *75*, 655-680.

2. Hartwell, L.H., Hopfield, J.J., Leibler, S., and Murray, A.W. (1999). From molecular to modular cell biology. Nature *402*, C47-52.

3. Marczynski, G.T. (1999). Chromosome methylation and measurement of faithful, once and only once per cell cycle chromosome replication in Caulobacter crescentus. J Bacteriol *181*, 1984-1993.

4. Viollier, P.H., Thanbichler, M., McGrath, P.T., West, L., Meewan, M., McAdams, H.H., and Shapiro, L. (2004). Rapid and sequential movement of individual chromosomal loci to specific subcellular locations during bacterial DNA replication. Proc Natl Acad Sci U S A *101*, 9257-9262.

5. Gorbatyuk, B., and Marczynski, G.T. (2001). Physiological consequences of blocked Caulobacter crescentus dnaA expression, an essential DNA replication gene. Mol Microbiol *40*, 485-497.

6. Mott, M.L., and Berger, J.M. (2007). DNA replication initiation: mechanisms and regulation in bacteria. Nat Rev Microbiol *5*, 343-354.

7. Kaguni, J.M. (2006). DnaA: controlling the initiation of bacterial DNA replication and more. Annu Rev Microbiol *60*, 351-375.

8. Katayama, T., Ozaki, S., Keyamura, K., and Fujimitsu, K. (2010). Regulation of the replication cycle: conserved and diverse regulatory systems for DnaA and oriC. Nat Rev Microbiol *8*, 163-170.

9. Klasson, L., and Andersson, S.G. (2004). Evolution of minimal-gene-sets in host-dependent bacteria. Trends Microbiol *12*, 37-43.

10. Kato, J., and Katayama, T. (2001). Hda, a novel DnaA-related protein, regulates the replication cycle in Escherichia coli. EMBO J *20*, 4253-4262.

11. Curtis, P.D., and Brun, Y.V. (2010). Getting in the loop: regulation of development in Caulobacter crescentus. Microbiol Mol Biol Rev *74*, 13-41.

12. Quon, K.C., Yang, B., Domian, I.J., Shapiro, L., and Marczynski, G.T. (1998). Negative control of bacterial DNA replication by a cell cycle regulatory protein that binds at the chromosome origin. Proc Natl Acad Sci U S A *95*, 120-125.

13. Quon, K.C., Marczynski, G.T., and Shapiro, L. (1996). Cell cycle control by an essential bacterial two-component signal transduction protein. Cell *84*, 83-93.

14. Laub, M.T., Chen, S.L., Shapiro, L., and McAdams, H.H. (2002). Genes directly controlled by CtrA, a master regulator of the Caulobacter cell cycle. Proc Natl Acad Sci U S A *99*, 4632-4637.

15. Biondi, E.G., Reisinger, S.J., Skerker, J.M., Arif, M., Perchuk, B.S., Ryan, K.R., and Laub, M.T. (2006). Regulation of the bacterial cell cycle by an integrated genetic circuit. Nature *444*, 899-904.

16. Domian, I.J., Quon, K.C., and Shapiro, L. (1997). Cell type-specific phosphorylation and proteolysis of a transcriptional regulator controls the G1-to-S transition in a bacterial cell cycle. Cell *90*, 415-424.

17. Iniesta, A.A., McGrath, P.T., Reisenauer, A., McAdams, H.H., and Shapiro, L. (2006). A phospho-signaling pathway controls the localization and activity of a protease complex critical for bacterial cell cycle progression. Proc Natl Acad Sci U S A *103*, 10935-10940.

18. Tsokos, C.G., Perchuk, B.S., and Laub, M.T. (2011). A Dynamic Complex of Signaling Proteins Uses Polar Localization to Regulate Cell-Fate Asymmetry in Caulobacter crescentus. Dev Cell *20*, 329-341.

19. Bastedo, D.P., and Marczynski, G.T. (2009). CtrA response regulator binding to the Caulobacter chromosome replication origin is required during nutrient and antibiotic stress as well as during cell cycle progression. Mol Microbiol *72*, 139-154.

20. Shen, X., Collier, J., Dill, D., Shapiro, L., Horowitz, M., and McAdams, H.H. (2008). Architecture and inherent robustness of a bacterial cell-cycle control system. Proc Natl Acad Sci U S A *105*, 11340-11345.

21. Collier, J., McAdams, H.H., and Shapiro, L. (2007). A DNA methylation ratchet governs progression through a bacterial cell cycle. Proc Natl Acad Sci U S A *104*, 17111-17116.

22. Collier, J., and Shapiro, L. (2009). Feedback control of DnaA-mediated replication initiation by replisome-associated HdaA protein in Caulobacter. J Bacteriol *191*, 5706-5716.

23. Jensen, R.B., and Shapiro, L. (1999). The Caulobacter crescentus smc gene is required for cell cycle progression and chromosome segregation. Proc Natl Acad Sci U S A *96*, 10661-10666.

24. Chen, Y.E., Tropini, C., Jonas, K., Tsokos, C.G., Huang, K.C., and Laub, M.T. (2011). Spatial gradient of protein phosphorylation underlies replicative asymmetry in a bacterium. Proc Natl Acad Sci U S A.

25. Jacobs, C., Domian, I.J., Maddock, J.R., and Shapiro, L. (1999). Cell cycle-dependent polar localization of an essential bacterial histidine kinase that controls DNA replication and cell division. Cell *97*, 111-120.

26. Wu, J., Ohta, N., Zhao, J.L., and Newton, A. (1999). A novel bacterial tyrosine kinase essential for cell division and differentiation. Proc Natl Acad Sci U S A *96*, 13068-13073.

27. Sommer, J.M., and Newton, A. (1989). Turning off flagellum rotation requires the pleiotropic gene pleD: pleA, pleC, and pleD define two morphogenic pathways in Caulobacter crescentus. J Bacteriol *171*, 392-401.

28. Atlung, T., Lobner-Olesen, A., and Hansen, F.G. (1987). Overproduction of DnaA protein stimulates initiation of chromosome and minichromosome replication in Escherichia coli. Mol Gen Genet *206*, 51-59.

29. Cheng, L., and Keiler, K.C. (2009). Correct timing of dnaA transcription and initiation of DNA replication requires trans translation. J Bacteriol *191*, 4268-4275.

30. Nishida, S., Fujimitsu, K., Sekimizu, K., Ohmura, T., Ueda, T., and Katayama, T. (2002). A nucleotide switch in the Escherichia coli DnaA protein initiates chromosomal replication: evidnece from a mutant DnaA protein defective in regulatory ATP hydrolysis in vitro and in vivo. J Biol Chem *277*, 14986-14995.

31. Katayama, T., Kubota, T., Kurokawa, K., Crooke, E., and Sekimizu, K. (1998). The initiator function of DnaA protein is negatively regulated by the sliding clamp of the E. coli chromosomal replicase. Cell *94*, 61-71.

32. Nakamura, K., and Katayama, T. (2010). Novel essential residues of Hda for interaction with DnaA in the regulatory inactivation of DnaA: unique roles for Hda AAA Box VI and VII motifs. Mol Microbiol *76*, 302-317.

33. Su'etsugu, M., Shimuta, T.R., Ishida, T., Kawakami, H., and Katayama, T. (2005). Protein associations in DnaA-ATP hydrolysis mediated by the Hda-replicase clamp complex. J Biol Chem *280*, 6528-6536.

34. Iniesta, A.A., Hillson, N.J., and Shapiro, L. (2010). Polar remodeling and histidine kinase activation, which is essential for Caulobacter cell cycle progression, are dependent on DNA replication initiation. J Bacteriol *192*, 3893-3902.

35. Laub, M.T., McAdams, H.H., Feldblyum, T., Fraser, C.M., and Shapiro, L. (2000). Global analysis of the genetic network controlling a bacterial cell cycle. Science *290*, 2144-2148.

36. Zweiger, G., and Shapiro, L. (1994). Expression of Caulobacter dnaA as a function of the cell cycle. J Bacteriol *176*, 401-408.

37. Murray, H., and Errington, J. (2008). Dynamic control of the DNA replication initiation protein DnaA by Soj/ParA. Cell *135*, 74-84.

38. Wagner, J.K., Marquis, K.A., and Rudner, D.Z. (2009). SirA enforces diploidy by inhibiting the replication initiator DnaA during spore formation in Bacillus subtilis. Mol Microbiol *73*, 963-974.

39. Noirot-Gros, M.F., Dervyn, E., Wu, L.J., Mervelet, P., Errington, J., Ehrlich, S.D., and Noirot, P. (2002). An expanded view of bacterial DNA replication. Proc Natl Acad Sci U S A *99*, 8342-8347.

40. Rahn-Lee, L., Merrikh, H., Grossman, A.D., and Losick, R. (2010). The Sporulation Protein SirA Inhibits the Binding of DnaA to the Origin of Replication by Contacting a Patch of Clustered Amino Acids. J Bacteriol.

41. Gorbatyuk, B., and Marczynski, G.T. (2005). Regulated degradation of chromosome replication proteins DnaA and CtrA in Caulobacter crescentus. Mol Microbiol *55*, 1233-1245.

42. Brilli, M., Fondi, M., Fani, R., Mengoni, A., Ferri, L., Bazzicalupo, M., and Biondi, E.G. (2011). The diversity and evolution of cell cycle regulation in alpha-proteobacteria: a comparative genomic analysis. BMC Syst Biol *4*, 52.

43. Hallez, R., Bellefontaine, A.F., Letesson, J.J., and De Bolle, X. (2004). Morphological and functional asymmetry in alpha-proteobacteria. Trends Microbiol *12*, 361-365.

44. Hallez, R., Mignolet, J., Van Mullem, V., Wery, M., Vandenhaute, J., Letesson, J.J., Jacobs-Wagner, C., and De Bolle, X. (2007). The asymmetric distribution of the essential histidine kinase PdhS indicates a differentiation event in Brucella abortus. EMBO J *26*, 1444-1455.

45. Lam, H., Matroule, J.Y., and Jacobs-Wagner, C. (2003). The asymmetric spatial distribution of bacterial signal transduction proteins coordinates cell cycle events. Dev Cell *5*, 149-159.

46. Shaheen, S.M., Ouimet, M.C., and Marczynski, G.T. (2009). Comparative analysis of Caulobacter chromosome replication origins. Microbiology *155*, 1215-1225.

47. Brassinga, A.K., Siam, R., McSween, W., Winkler, H., Wood, D., and Marczynski, G.T. (2002). Conserved response regulator CtrA and IHF binding sites in the alpha-proteobacteria Caulobacter crescentus and Rickettsia prowazekii chromosomal replication origins. J Bacteriol *184*, 5789-5799.

48. Lu, Y., and Cross, F.R. (2010). Periodic cyclin-Cdk activity entrains an autonomous Cdc14 release oscillator. Cell *141*, 268-279.

Chapter 5

Conclusions and future directions

Conclusions

In this work, I used *Caulobacter crescentus* as a model organism to investigate how regulatory proteins drive the establishment of daughter cells with different replicative fates. Specifically, I showed that the essential histidine kinase CckA has both kinase and phosphatase activities *in vitro* and *in vivo* (Chapter 2). CckA is bipolarly localized in predivisional cells and other studies from our lab recently demonstrated that CckA likely adopts the kinase state at the swarmer pole and phosphatase state at the stalked pole [1]. Using a variety of genetic manipulations corroborated by computational modeling, I showed that this spatial separation of kinase and phosphatase activities at opposite poles generates a spatial gradient of CtrA phosphorylation across the cell before cytokinesis. This spatial gradient is responsible for asymmetrically repressing the origin of replication at the swarmer pole of a predivisional cell (Chapter 3). These results thus uncover a previously unappreciated method for producing spatial asymmetry in bacteria. Although a protein may be spatially homogeneous within a cell, its activity can be spatially heterogeneous due to asymmetric posttranslational modifications. Given the prevalence of two-component systems in bacteria, spatially asymmetric phosphorylation and dephosphorylation of response regulators may be a general mechanism for establishing asymmetric cell fates. Other enzyme pairs, such as diguanylate cyclases and phosphodiesterases, with opposing, spatially segregated activities may also be able to produce such gradients.

In Chapter 4, I investigated how CtrA activity might be linked to DnaA activity and replication timing. In agreement with previous reports, we showed that asymmetric

inheritance of CtrA activity in daughter cells enforces replicative asymmetry. Surprisingly, and in contrast to previous models, I found that in the absence of CtrA activity, replication continues with wild-type periodicity. By contrast, increasing DnaA activity abolished replicative periodicity and caused overinitiation while decreasing DnaA activity slowed down replication cycles but did not change the asymmetry in replication timing between swarmer and stalked daughter cells.

From these data, we concluded that DnaA activity oscillates independently of CtrA activity and developed a model for the modular evolution of the bacterial cell cycle. In our model, a primordial oscillator drives periodic changes in DnaA activity and subsequent replicative cycling in *Caulobacter* as it likely does in almost all bacteria. CtrA and the phosphorelay controlling it represents a later development required to drive asymmetric cell divisions and morphogenesis. The CtrA circuitry was then recruited in some species, such as *Caulobacter*, to couple asymmetry in replicative fates to asymmetry in morphogenesis; this recruitment step likely only required the evolution of CtrA-binding sites at the origin of replication.

Visualizing the spatial gradient in CtrA phosphorylation

Our results in Chapter 3 demonstrate that although the levels of a freely diffusible protein, such as CtrA, may be homogenous throughout a prokaryotic cell, its activity may be spatially heterogeneous. In this work, I did not directly visualize the spatial gradient of CtrA phosphorylation. Instead, I took advantage of CtrA's phosphorylation-dependent function as a repressor of replication initiation. By examining the probability of initiation events at the stalked and swarmer poles, I indirectly assayed the level of CtrA phosphorylation at each pole. To better understand how CtrA phosphorylation might look

between the two poles, we made a reaction-diffusion model with CckA kinase activity at the swarmer pole and CckA phosphatase activity at the stalked pole (Fig. 3.1E, see Chapter 3 Methods). CtrA was assumed to diffuse freely and degraded throughout the cell. When CckA kinase and phosphatase activities were within physiological range, CtrA phosphorylation levels varied linearly across the cell length (Fig. 3.4A). If an additional delocalized phosphatase for CtrA exists, then the CtrA phosphorylation gradient is exponential, dropping off more quickly with distance from the swarmer pole (Fig. 3.10C). The existence of an additional phosphatase for CtrA is likely given that a kinase-only allele of CckA (CckA(V366P)) complements a deletion of *cckA* with no significant cell cycle or morphologic defects (Fig. 2.7). Alternatively, CckA(V366P) could be an imperfect allele with some phosphatase activity *in vivo* although it had no detectable phosphatase activity *in vitro*. Thus, knowing the precise shape of the CtrA phosphorylation gradient would yield more insight into understanding what controls CtrA activity. From our modeling data, we can predict what the shape of CtrA phosphorylation across the cell might look like in various scenarios. However, we could not directly visualize CtrA phosphorylation *in vivo* because there are multiple challenges to monitoring the spatial distribution of a phosphorylated response regulator in individual cells. Below, I outline these challenges and potential methods that could be developed to visualize a phosphorylated response regulator on a single cell level.

In eukaryotes, one method that is widely used to detect a specific phosphorylated protein involves generating an antibody specific to the phosphorylated form of this protein. This antibody can then be used to visualize the spatial distribution of this phosphorylated protein in individual cells by immunofluorescence. However, it has been difficult to

apply this approach in prokaryotes [2]. In contrast to the phosphorylated serine, threonine, and tyrosine residues generally found in eukaryotic kinases and substrates, phosphorylated histidine and aspartate residues found in bacterial two-component systems have high-energy bonds that undergo hydrolysis easily under acidic conditions. This property makes phosphorylated histidine kinases and response regulators difficult to isolate from cells. This also makes it difficult to generate specific antibodies against proteins containing phosphohistidine or phosphoaspartate since these residues are easily dephosphorylated in the serum.

To address this problem of phosphohistidine instability, a nonhydrolyzable phosphohistidine analogue using phosphoryltriazolylalanine (pTza) was recently developed [3]. Using solid-phase peptide synthesis, the authors synthesized the N-terminal tail of histone H4 with the phosphorylatable histidine replaced by pTza. Using this synthetic peptide as an immunogen, the authors obtained the first antibody that specifically recognizes a phosphorylated histidine. This work might be generally applicable to histidine kinases and phosphotransferases. Although this work suggests that a similar approach might be used to generate antibodies specific to proteins containing a phosphorylated aspartate, currently, there are no stable analogs for phosphoaspartates, precluding the use of an antibody specific to any phosphorylated response regulator, such as CtrA.

To circumvent the difficulty of making antibodies to two-component system proteins, *in vivo* fluorescence resonance energy transfer (FRET) was used to monitor phosphate flow through the chemotaxis two-component system in *E. coli* [4-7]. In chemotaxis, bacteria move toward higher concentrations of attractants while avoiding higher concentrations of

repellents. Swimming control is mediated by the directionality of flagellar motor rotation, which is in turn controlled by signaling from chemoreceptors through two-component systems [8, 9]. Specifically, in *E. coli*, binding of chemoreceptors to attractant inhibits autophosphorylation of the histidine kinase CheA while binding to repellent stimulates CheA autophosphorylation. When autophosphorylated, CheA phosphorylates the response regulator CheY, which binds the flagellar motor and increases tumbling. CheY can also be dephosphorylated by the phosphatase CheZ. Therefore, the concentration of phosphorylated CheY is determined by a balance between phosphorylation by CheA and dephosphorylation by CheZ. The concentration of the enzyme-substrate complex, CheZ with CheY~P, represents the rate of CheY~P dephosphorylation and can then be used as an indirect marker of net CheY phosphorylation [6]. By fusing CheY and CheZ to YFP and CFP, respectively, interactions between CheY and CheZ can be determined by FRET in individual living cells [4, 6]. This FRET signal can be mapped with high spatial resolution within the cell, demonstrated as follows. The phosphatase CheZ is generally localized to the chemoreceptor clusters, resulting in a high FRET signal near the cluster that drops off quickly outside the cluster. However, expression of an allele of CheZ ($CheZ^{F98S}$) that cannot be localized caused a quantifiable spatial gradient of FRET signal over the length of the cell, corresponding to diffusion of CheZ and the response regulator CheY away from the cluster [7]. The fine spatial resolution of this FRET approach makes it ideal for observing any spatial heterogeneities in phosphorylation or dephosphorylation reactions within individual cells.

Despite the advantages of having both temporal and spatial information of phosphorylation events in living cells, there are significant challenges to applying *in vivo*

FRET to the CtrA phosphorelay. Unlike CheY, CtrA does not have a separate kinase and phosphatase; CckA functions as the kinase at the swarmer pole and as the phosphatase at the stalked pole. Therefore, detecting an interaction between ChpT and CckA or between ChpT and CtrA does not distinguish between phosphorylation and dephosphorylation. Instead of simply detecting an interaction between the phosphorelay components, we must find an interaction or conformational change that is specifically phosphorylation-dependent or dephosphorylation-dependent. One candidate is a phosphorylation-dependent conformational change in CtrA that allows for increased DNA binding affinity. Upon phosphorylation, response regulators are thought to undergo allosteric activation of effector domains, dimerization, oligomerization, or increased interaction with heterologous target proteins [10, 11]. It is not known mechanistically how phosphorylation alters CtrA structurally. If homodimerization increases upon phosphorylation, then simultaneous expression of YFP-tagged CtrA and CFP-tagged CtrA might show increased FRET signal near the swarmer pole and decreased signal near the stalked pole of a predivisional cell. If the receiver and DNA-binding domains of CtrA change conformation upon phosphorylation, then tagging CtrA with CFP at the N-terminus and YFP at the C-terminus might yield a phosphorylation-dependent FRET signal. Alternatively, one could tag CtrA with YFP and RNA polymerase with CFP to look for a FRET signal upon CtrA-mediated recruitment of RNA polymerase to target promoters [12]. However, these methods require that YFP-tagged CtrA is still phosphorylatable, which has not yet been published.

Another method to examine the spatial gradient of CtrA phosphorylation could take advantage of CtrA's function as a transcription factor. Using quantitative fluorescence *in*

situ hybridization to mRNAs (RNA FISH), chromosomally expressed mRNAs were shown to stay near their site of transcription in *Caulobacter* and *E. coli* [13]. Given this information, it might be possible to visualize the expression of genes that are positively regulated by CtrA by using RNA FISH. We would predict that the same origin-proximal genes would be highly expressed in the swarmer half of the cell but repressed in the stalked half of the cell, while terminus-proximal genes should not show a difference in expression between the swarmer and stalked halves. Unlike FRET, RNA FISH would be a less direct measure of CtrA phosphorylation. On the other hand, RNA FISH does not require any proteins to be fluorescently tagged and could give additional information about whether mRNAs are inherited asymmetrically by daughter cells.

How does DnaA affect CtrA activity?

In Chapter 4, I showed that disrupting CtrA activity does not change the periodicity of DnaA activity and DNA replication. However, replication does somehow affect CtrA activity. Previously, it was reported that replication is required for CckA and DivL localization to the swarmer pole, which is necessary to activate CckA kinase activity in late stalked and predivisional cells [14]. In a DnaA depletion strain, a strain producing stable, constitutively active CtrA, or wild type treated with novobiocin, DNA replication does not initiate and neither CckA nor DivL localizes to the swarmer pole [14]. In Chapter 4, we showed that overproducing HdaA, a negative regulator of DnaA activity, lengthened replication periods and cell division cycles. Interestingly, Western blot data showed that CtrA accumulation in stalked and predivisional cells is delayed in a strain that moderately overexpresses *hdaA* and replicates more slowly (Fig. 5.1). In a strain that highly overexpresses *hdaA*, CtrA accumulation is delayed and never reaches the same

level as in G1; this is consistent with the observation that cells highly overexpressing *hdaA* arrest in G2 (Chapter 4). Collectively, these data indicate that DNA replication or some associated event is required to trigger DivL and CckA swarmer pole localization, which are required for the reaccumulation of CtrA activity.

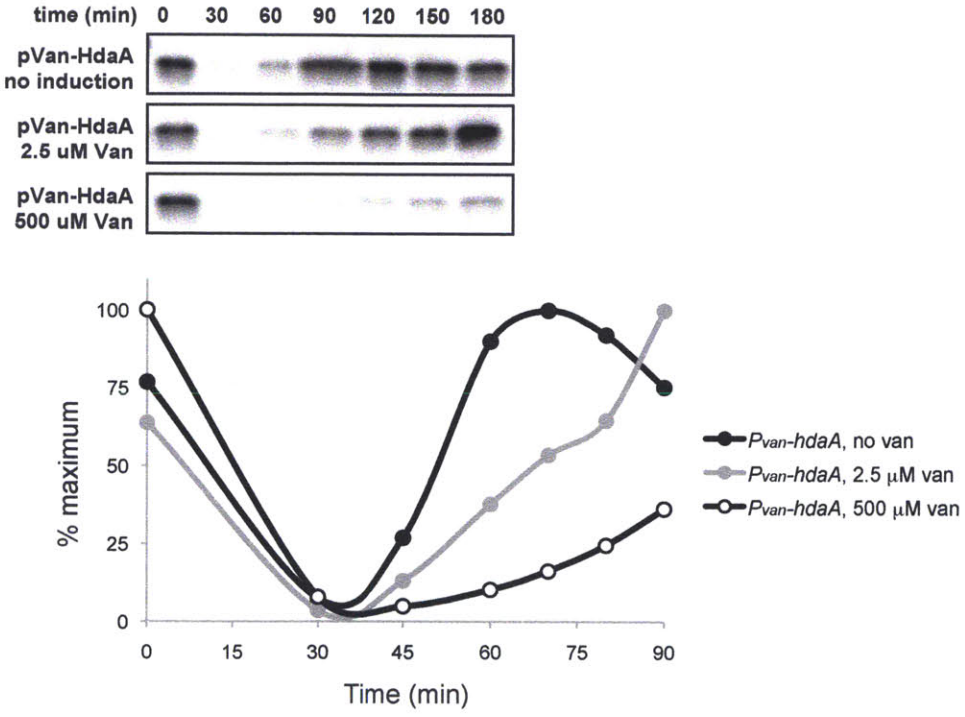

Figure 5.1. HdaA overproduction delays CtrA accumulation in late stalked cells. CtrA Western blot (top) and quantification (bottom) in synchronized populations that begin overexpressing *hdaA* moderately (2.5 uM van) or highly (5 uM van) at time 0.

What is the mechanism by which DNA replication impacts the localization of CckA and DivL, and consequently CtrA activity? There are several possibilities: (1) the act of DNA replication initiation might send a diffusible signal that prepares the swarmer pole for localization of DivL and/or CckA, (2) a gene required for the localization of DivL or

CckA could be induced or up-regulated following DNA replication, or (3) successful chromosome segregation which leads to a newly replicated origin arriving at the swarmer pole may permit the localization of DivL and/or CckA to that pole (Fig. 5.2). Any of these general scenarios could couple replication to the activation of CtrA, such that if DNA replication did not initiate, then the swarmer pole would not properly mature, thereby preventing the activation of CtrA. Below I discuss each possibility and experiments that could be done to test them or rule them out. Note that I have ruled out successful completion of DNA replication being involved in activating CtrA because replication takes about 40-50 minutes and CtrA activity begins to accumulate ~15 minutes after replication initiates, in rich medium. Additionally, replication does not terminate properly in a strain overexpressing *dnaA* due to overinitiation (Chapter 3, Fig. 4.4-4.5), and yet the rate of CtrA accumulation is unaffected in this strain (Fig. 5.1). Also for this reason, a change in DnaA activity is not likely to directly affect CtrA activity through DnaA-mediated transcription.

The first possibility is that replication initiation at the stalked pole leads to the release of a diffusible signal that allows for or triggers DivL and CckA localization to the swarmer pole. This diffusible signal could be some factor that is released from the replication initiation complex or regulated by another factor involved in replication initiation. This possibility is unlikely because cells initiate replication when mildly overexpression HdaA but CtrA accumulation is still significantly delayed in comparison to cells without HdaA overexpression (Fig. 5.1). A more rigorous test of this hypothesis would be to examine by timelapse microscopy if CckA and DivL localizes in cells overexpressing HdaA and harboring the TetR-YFP fluorescent repressor operator system, where origins are marked

by YFP foci (Chapter 3, Fig. 3.1). In these cells, one can observe the event of replication initiation and ask whether CckA and DivL successfully localize to the swarmer pole or not. If not, then replication initiation is not sufficient to release a factor necessary for swarmer pole maturation and some later necessary event is being disrupted by HdaA overexpression.

A second possibility is that replication results in a doubling of copy number in origin-proximal genes, which could double the amount of a gene product that controls swarmer pole maturation. This idea has been demonstrated in the process of *B. subtilis* sporulation, where transient exclusion of the terminal-proximal *spoIIAB* gene from the forespore contributes to forespore-specific activation of σ^F (Chapter 1, Fig. 1.7). In the case of *B. subtilis*, the copy number of *spoIIAB* undergoes a large fold change from one to zero upon forespore formation. By contrast, in the case of replication initiation, the gene copy-number would only increase by two-fold; therefore, this change is unlikely to be a robust mechanism for regulating an essential cell cycle event. Additionally, microarray studies have shown that few genes are cell cycle regulated by replication-induced change in chromosome copy number [15].

Chromosome segregation and polar maturation

The third possibility is the successful segregation of newly replicated origins to opposite poles. This is a good candidate for an event that regulates swarmer pole maturation and the activation of CtrA. During cell cycle progression, the cell poles undergo remodeling and dynamically associate with different proteins at different cell cycle stages. In the swarmer cell, the origin is tethered to the swarmer pole by a complex of proteins. ParB directly binds to the *parS* sequence approximately 8 kb to the left of the origin of

replication. ParB also binds MipZ and tethers the origin to an oligomeric network of PopZ at the swarmer pole (Fig. 5.2) [16, 17]. During the G1-S transition, the swarmer pole sheds its external structures and grows a stalk, becoming the stalked pole. Internally, the tether between PopZ and the *parS*/ParB/MipZ complex is broken; this can be seen on live-cell microscopy as a loosening of a CFP-tagged ParB focus from the pole [18]. During this process of stalked pole maturation, PopZ also recruits regulatory factors, such as SpmX and DivJ [18], which are instrumental in driving further cell cycle progression. Then, replication initiates and the *parS*/ParB/MipZ complex moves rapidly to the new pole [19-21]. This movement is driven by an interaction between ParB and ParA that stimulates ATP hydrolysis by ParA and ensuing retraction of the ParA filament. TipN at the new pole anchors ParA [22, 23]. Concomitant with chromosome segregation, PopZ accumulates at the new pole, where it captures the segregating *parS*/ParB/MipZ complex [16, 17]. CckA, DivL, and PleC also accumulate at the new pole around this time. CckA arrives at the new pole after arrival of the origin and likely interacts with PopZ [14], and PleC requires PodJ localization at the new pole [24], but the nature of these localizing interactions is unclear. The colocalization of CckA and DivL at the new pole upregulates CckA kinase activity [1, 25], which is required for the reaccumulation and reactivation of CtrA. Given the complexity of cell cycle-dependent polar remodeling and its importance for proper cell cycle progression, it makes sense that a simple signal such as the arrival of the origin at the new pole might serve as a "checkpoint" to set off further recruitment of proteins to the new pole.

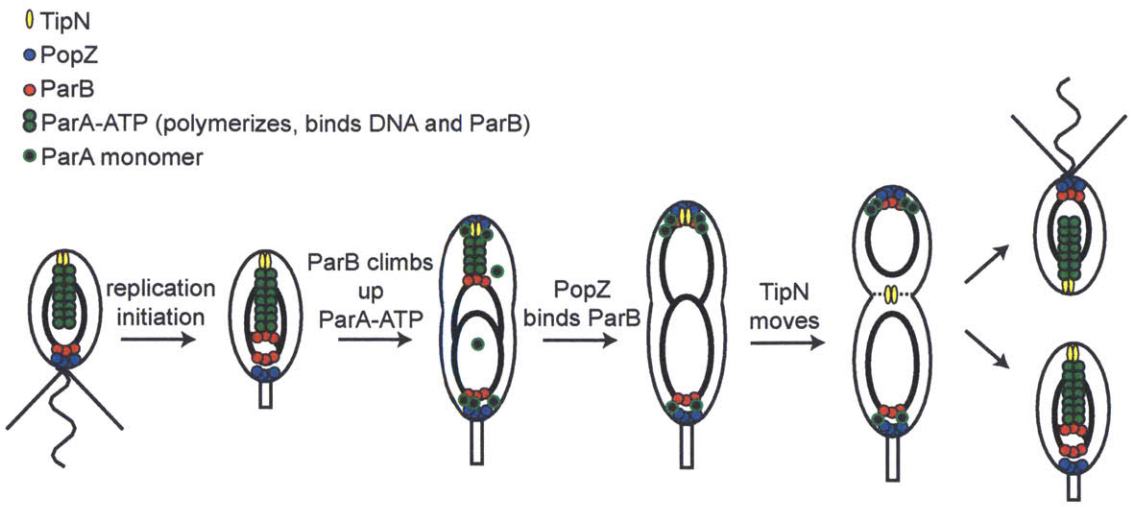

Figure 5.2. Mechanics of chromosome segregation in *Caulobacter*. In G1, ParA (green) associates with TipN (yellow) at the new pole while ParB (red) tethers the origin-proximal region to PopZ (blue) at the old pole. In S phase, replication initiates. In complex with newly replicate *parS*, ParB latches onto ParA-ATP and stimulates ParA ATP hydrolysis. Upon hydrolysis, ParA becomes a monomer, allowing ParB to pull the chromosome up the shortening ParA filament, toward the new pole. At the new pole, ParB is tethered to PopZ. TipN then moves to the division site in preparation to mark the new pole upon cell division. Figure adapted from [16, 17, 22, 23]

Previous data showed that a dominant negative allele of ParA (ParA(K20R)) delays the arrival of the origin to the new pole but does not delay CckA localization to the swarmer pole; this prompted the authors to discount chromosome segregation as a regulatory step for new pole maturation [14]. However, these experiments were done in populations of cells, where origin movement was not correlated to CckA localization timing within the same cell. Additionally, the authors used MipZ-YFP as a marker for the segregating origin. MipZ interacts with the origin through ParB, which also interacts with ParA; therefore, it is possible that ParB binding to *parS* or MipZ might be disturbed when ParA(K20R) is produced at high levels. To improve upon these experiments and more carefully examine the relationship between chromosome segregation and swarmer pole maturation, we could use the TetR-YFP fluorescent repressor-operator system to mark the origin. This heterologous system should not interact with any native proteins. Additionally, we can observe CckA and DivL localization and origin segregation within

the same cell, to better characterize the timing of origin segregation with that of CckA and DivL localization.

Another tool for investigating the connection between chromosome segregation and polar maturation is the *hdaA* overexpression strain. When HdaA is overproduced at high levels, some cells replicate and segregate their chromosomes partially such that an origin does not reach the new pole while other cells replicate and segregate both origins to the pole for a short while before the two origins collapse back together (Chapter 4) (Fig. 5.3). If successful segregation of the origin to the new pole triggers some polar maturation event, CckA localization should occur in only that population of cells, but should not occur in those cells that replicate but do not segregate properly. If cells that replicate and never segregate their chromosomes to the poles also exhibit timely CckA localization to the new pole, then segregation most likely does not contribute to new pole maturation. In addition to investigating DivL and CckA localization, it will be informative to examine the localization of TipN, PodJ, and PopZ at the new pole to better understand what step of polar maturation is affected in cells that cannot replicate.

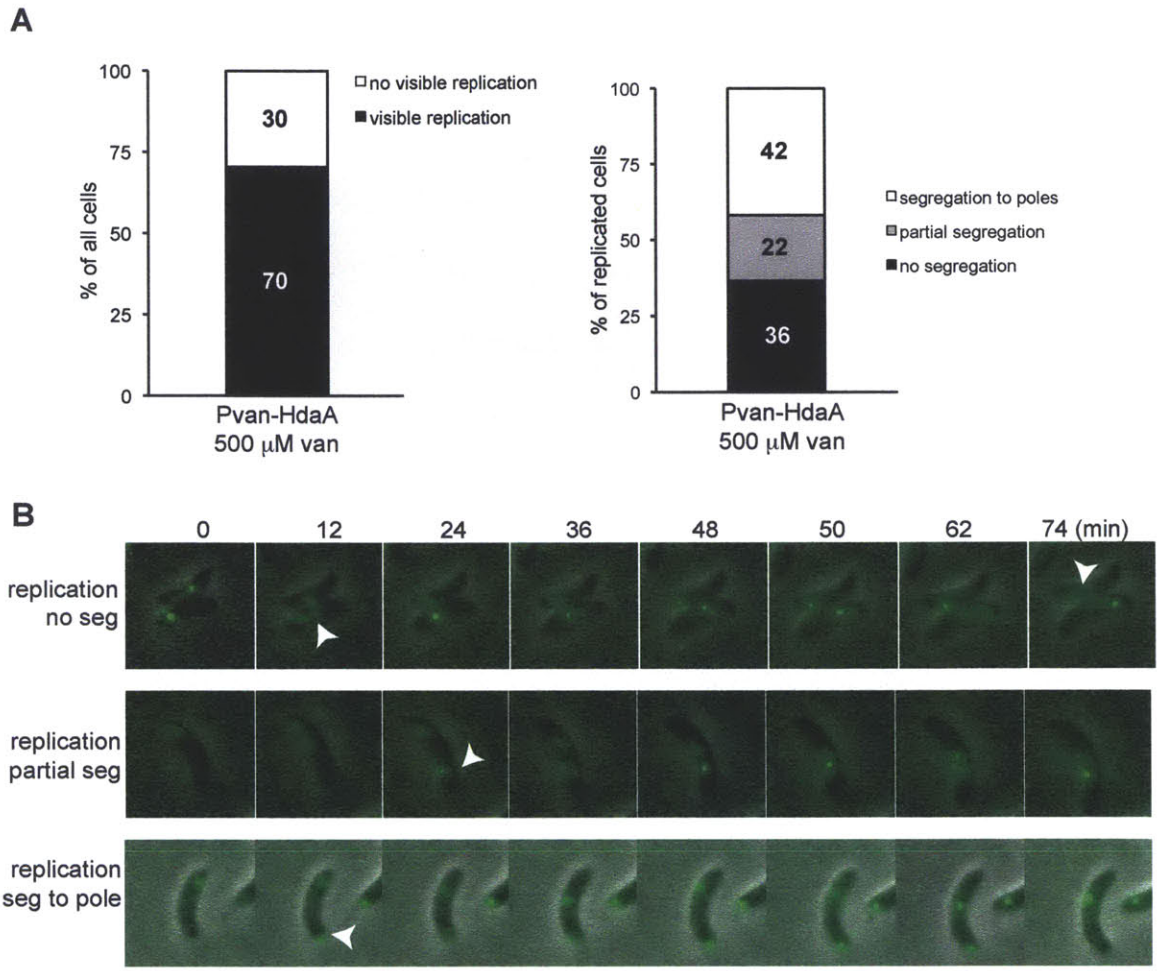

Figure 5.3. Segregation defect in cells that overexpress *hdaA*. (A) Bar graphs quantifying replication (left) and segregation (right) events in cells that harbor the fluorescent repressor-operator system and overexpress *hdaA*. All cells had a single chromosome when *hdaA* overexpression was induced. An initiation event was counted if two fluorescent foci could be detected at any point during a 6-hour timelapse movie. Partial segregation was counted if the two origins remained separated for more than 12 minutes. Segregation to the poles was counted if one of the two origins reached the new pole. (B) Representative timelapse images of the segregation patterns observed in cells quantified in part A. Top row, arrowheads indicate observable initiation events. Middle row, arrowhead indicates partial segregation of the two origins. Bottom row, arrowhead indicates segregation of the origin to the new pole.

A chromosome segregation checkpoint

The idea of a checkpoint that links a replication-associated event with downstream cell cycle and division events has been validated in other systems, particularly in yeast. The spindle assembly checkpoint, which is conserved from yeast to mammals, ensures the

fidelity of chromosome segregation in both mitosis and meiosis (reviewed in [26, 27]). If spindle assembly is defective, then a mitotic checkpoint complex containing Mad2, Mad3, Bub3, and Cdc20 directly binds to and inhibits the anaphase-promoting complex, a ubiquitin ligase that is required for chromosome segregation and cytokinesis [27]. This checkpoint is thought to monitor the attachment of chromosomes to the mitotic spindle as well as the tension across sister chromatids generated by the microtubules. This tension is generated when sister chromatids properly attach to microtubules emanating from opposite poles of the mitotic spindle [28, 29]. Only after all sister chromatids have achieved this bi-orientation, can the anaphase-promoting complex in concert with Cdc20 polyubiquitinate the securin protein, ultimately resulting in securin degradation, activation of the separase, proteolytic cleavage of cohesins, and separation of the sister chromatids [28, 30]. If the sister chromatids are not properly lined up and bi-oriented and the spindle checkpoint fails to be activated, as in a MAD3-deletion strain, chromosome segregation will not occur properly, resulting in cells that exhibit polyploidy or aneuploidy, and ultimately cell death.

Many of the spindle checkpoint genes were identified in screens looking for mutants that bypassed the mitotic arrest of wild-type budding yeast cells in the presence of spindle poisons [31, 32]. In *Caulobacter*, high overexpression of *hdaA* causes a segregation defect and an arrest in the cell cycle with an inability to reactivate CtrA, suggesting the presence of a checkpoint. Therefore, screening for mutants that bypass this checkpoint and regain motility should yield information about which proteins participate in this checkpoint.

References

1. Tsokos, C.G., Perchuk, B.S., and Laub, M.T. (2011). A Dynamic Complex of Signaling Proteins Uses Polar Localization to Regulate Cell-Fate Asymmetry in Caulobacter crescentus. Dev Cell *20*, 329-341.

2. Scharf, B.E. (2010). Summary of useful methods for two-component system research. Curr Opin Microbiol *13*, 246-252.

3. Kee, J.M., Villani, B., Carpenter, L.R., and Muir, T.W. (2010). Development of stable phosphohistidine analogues. J Am Chem Soc *132*, 14327-14329.

4. Sourjik, V., and Berg, H.C. (2000). Localization of components of the chemotaxis machinery of Escherichia coli using fluorescent protein fusions. Molecular microbiology *37*, 740-751.

5. Sourjik, V., and Berg, H.C. (2002). Binding of the Escherichia coli response regulator CheY to its target measured in vivo by fluorescence resonance energy transfer. Proceedings of the National Academy of Sciences of the United States of America *99*, 12669-12674.

6. Sourjik, V., Vaknin, A., Shimizu, T.S., and Berg, H.C. (2007). In vivo measurement by FRET of pathway activity in bacterial chemotaxis. Methods Enzymol *423*, 365-391.

7. Vaknin, A., and Berg, H.C. (2004). Single-cell FRET imaging of phosphatase activity in the Escherichia coli chemotaxis system. Proceedings of the National Academy of Sciences of the United States of America *101*, 17072-17077.

8. Baker, M.D., Wolanin, P.M., and Stock, J.B. (2006). Signal transduction in bacterial chemotaxis. Bioessays *28*, 9-22.

9. Wadhams, G.H., and Armitage, J.P. (2004). Making sense of it all: bacterial chemotaxis. Nat Rev Mol Cell Biol *5*, 1024-1037.

10. West, A.H., and Stock, A.M. (2001). Histidine kinases and response regulator proteins in two-component signaling systems. Trends Biochem Sci *26*, 369-376.

11. Gao, R., and Stock, A.M. (2009). Biological insights from structures of two-component proteins. Annual review of microbiology *63*, 133-154.

12. Wu, J., Ohta, N., and Newton, A. (1998). An essential, multicomponent signal transduction pathway required for cell cycle regulation in Caulobacter. Proceedings of the National Academy of Sciences of the United States of America *95*, 1443-1448.

13. Montero Llopis, P., Jackson, A.F., Sliusarenko, O., Surovtsev, I., Heinritz, J., Emonet, T., and Jacobs-Wagner, C. (2010). Spatial organization of the flow of genetic information in bacteria. Nature *466*, 77-81.

14. Iniesta, A.A., Hillson, N.J., and Shapiro, L. (2010). Polar remodeling and histidine kinase activation, which is essential for Caulobacter cell cycle progression, are dependent on DNA replication initiation. Journal of bacteriology *192*, 3893-3902.

15. Laub, M.T., McAdams, H.H., Feldblyum, T., Fraser, C.M., and Shapiro, L. (2000). Global analysis of the genetic network controlling a bacterial cell cycle. Science *290*, 2144-2148.

16. Bowman, G.R., Comolli, L.R., Zhu, J., Eckart, M., Koenig, M., Downing, K.H., Moerner, W.E., Earnest, T., and Shapiro, L. (2008). A polymeric protein anchors the chromosomal origin/ParB complex at a bacterial cell pole. Cell *134*, 945-955.

17. Ebersbach, G., Briegel, A., Jensen, G.J., and Jacobs-Wagner, C. (2008). A self-associating protein critical for chromosome attachment, division, and polar organization in caulobacter. Cell *134*, 956-968.

18. Bowman, G.R., Comolli, L.R., Gaietta, G.M., Fero, M., Hong, S.H., Jones, Y., Lee, J.H., Downing, K.H., Ellisman, M.H., McAdams, H.H., et al. (2010). Caulobacter PopZ forms a polar subdomain dictating sequential changes in pole composition and function. Molecular microbiology *76*, 173-189.

19. Thanbichler, M., and Shapiro, L. (2006). MipZ, a spatial regulator coordinating chromosome segregation with cell division in Caulobacter. Cell *126*, 147-162.

20. Toro, E., Hong, S.H., McAdams, H.H., and Shapiro, L. (2008). Caulobacter requires a dedicated mechanism to initiate chromosome segregation. Proceedings of the National Academy of Sciences of the United States of America *105*, 15435-15440.

21. Viollier, P.H., Thanbichler, M., McGrath, P.T., West, L., Meewan, M., McAdams, H.H., and Shapiro, L. (2004). Rapid and sequential movement of individual chromosomal loci to specific subcellular locations during bacterial DNA replication. Proceedings of the National Academy of Sciences of the United States of America *101*, 9257-9262.

22. Schofield, W.B., Lim, H.C., and Jacobs-Wagner, C. (2010). Cell cycle coordination and regulation of bacterial chromosome segregation dynamics by polarly localized proteins. Embo J *29*, 3068-3081.

23. Ptacin, J.L., Lee, S.F., Garner, E.C., Toro, E., Eckart, M., Comolli, L.R., Moerner, W.E., and Shapiro, L. (2010). A spindle-like apparatus guides bacterial chromosome segregation. Nat Cell Biol *12*, 791-798.

24. Hinz, A.J., Larson, D.E., Smith, C.S., and Brun, Y.V. (2003). The Caulobacter crescentus polar organelle development protein PodJ is differentially localized and is required for polar targeting of the PleC development regulator. Molecular microbiology *47*, 929-941.

25. Iniesta, A.A., Hillson, N.J., and Shapiro, L. (2010). Cell pole-specific activation of a critical bacterial cell cycle kinase. Proceedings of the National Academy of Sciences of the United States of America *107*, 7012-7017.

26. Yu, H. (2002). Regulation of APC-Cdc20 by the spindle checkpoint. Curr Opin Cell Biol *14*, 706-714.

27. Musacchio, A., and Salmon, E.D. (2007). The spindle-assembly checkpoint in space and time. Nat Rev Mol Cell Biol *8*, 379-393.

28. Nasmyth, K., Peters, J.M., and Uhlmann, F. (2000). Splitting the chromosome: cutting the ties that bind sister chromatids. Science *288*, 1379-1385.

29. Tanaka, T.U. (2002). Bi-orienting chromosomes on the mitotic spindle. Curr Opin Cell Biol *14*, 365-371.

30. Peters, J.M. (2002). The anaphase-promoting complex: proteolysis in mitosis and beyond. Mol Cell *9*, 931-943.

31. Hoyt, M.A., Totis, L., and Roberts, B.T. (1991). S. cerevisiae genes required for cell cycle arrest in response to loss of microtubule function. Cell *66*, 507-517.

32. Li, R., and Murray, A.W. (1991). Feedback control of mitosis in budding yeast. Cell *66*, 519-531.